Crosstalk between DNA Methylation and Histone Modifications

GARWIN PICHLER

Dissertation
an der Fakultät fur Biologie
der Ludwig-Maximilians-Universität München

vorgelegt von
Garwin Pichler
aus Oberhausen
München, den 5. März 2012

Erstgutachter:	Prof. Dr. Heinrich Leonhardt
Zweitgutachter:	Prof. Dr. Peter Becker

Tag der mündlichen Prüfung: 22.05.2012

Contents

Summary **1**

1 Introduction **2**
1.1 Epigenetic Gene Regulation . . . 2
1.1.1 DNA Methylation . . . 3
1.1.2 Histone Modifications . . . 6
1.1.3 Nucleosome Positioning . . . 9
1.1.4 Crosstalk between Epigenetic Modifications . . . 10
1.2 DNA Methyltransferases . . . 12
1.2.1 Structure and Function Dnmt1 . . . 14
1.2.2 Regulation of Dnmt1 by Interactions . . . 16
1.2.3 Regulation of Dnmt1 by Post-translational Modifications . . . 19
1.3 The Uhrf Family of Proteins . . . 21
1.3.1 Phylogenetic Tree of Evolution . . . 21
1.3.2 Structure and Function of Uhrf Proteins . . . 23
1.3.3 Regulation of Uhrf Proteins . . . 25

2 Aims of this work **26**

3 Results **27**
3.1 Fluorescent protein specific Nanotraps to study protein-protein interactions and histone tail peptide binding . . . 27
3.2 Versatile Toolbox for High-Throughput Biochemical and Functional Studies with Fluorescent Fusion Proteins . . . 43
3.3 The multi-domain protein Np95 connects DNA methylation and histone modification . . . 56
3.4 Cooperative DNA and histone binding by Uhrf2 links the two major repressive epigenetic pathways . . . 75
3.5 DNMT1 regulation by interactions and modifications . . . 93
3.6 Cell Cycle-dependent Interactions of Dnmt1 . . . 105

4 Discussion **117**
4.1 Versatile Toolbox for High-Throughput Biochemical and Functional Studies with Fluorescent Proteins . . . 117
4.2 Uhrf proteins connect different pathways . . . 120
4.2.1 Uhrf1 coordinates repressive epigenetic pathways . . . 120
4.2.2 Uhrf2 coordinates repressive epigenetic pathways . . . 121
4.2.3 Diverse function of Uhrf proteins . . . 123
4.3 Dynamic interactions of Dnmt1 . . . 129

5 Annex **130**
5.1 References 130
5.2 Abbreviations 157
5.3 Contributions 160
5.4 Declaration 162
5.5 Acknowledgement 163
5.6 Publications 165

List of Figures

1 Three levels of epigenetic regulation . . . 3
2 Overview of DNA modifications . . . 5
3 Histone post-translational modifications and their binding partners . . . 8
4 Schematic outline of DNA Methyltransferases . . . 12
5 Structural insights into the DNA methyltransferases 1 . . . 15
6 Interactom of Dnmt1. . . . 16
7 Regulation of Dnmt1 by post-translational modifications . . . 20
8 Phylogenetic Tree of Life for Dnmts and Uhrf proteins . . . 22
9 Multi-domain proteins Uhrf1 and Uhrf2 . . . 23

10 Workflow of SILAC-based quantification of cell cycle-dependent interactions of Dnmt1 . . . 108
11 Initial testing of different Dnmt1 binder . . . 110
12 Immunoprecipitation of Dnmt1 with the Dnmt1 binder . . . 111
13 Cell cycle synchronization of HeLa cells using mimosine . . . 112
14 Dynamic Dnmt1 interactome visualized by a heat map and one-way hierarchical clustering . . . 115
15 SILAC ratios for Dnmt1, PCNA and H2A . . . 116

16 Schematic drawing of the GFP-multiTrap . . . 118
17 Radioactive *in vitro* DNA methyltransferase assay . . . 124
18 Diverse functions of Uhrf proteins . . . 128

List of Tables

1 Interaction partners of Dnmt1 . . . 113

2 Interaction partners of Uhrf1-GFP and Uhrf2-GFP . . . 125
3 Uhrf proteins associate with a broad range of proteins . . . 126

Summary

DNA methylation and histone modifications play a central role in the epigenetic regulation of gene expression and cell differentiation. DNA methyltransferase 1 (Dnmt1) is the most ubiquitously expressed DNA methyltransferase and is essential for maintaining DNA methylation patterns during semi-conservative DNA replication and DNA repair. The fidelity and processivity of this process is crucial for genome stability and is based on the specific recognition of hemimethylated CpG sites emerging at the replication forks. Remarkably, a variety of proteins have been reported to interact with Dnmt1, regulating the activation, stabilization and recruitment of Dnmt1 to specific sites and regions. Recently, Uhrf1 has been found to interact with Dnmt1, indicating together with genetic studies a central role in the maintenance of DNA methylation. However, the exact mechanism how Uhrf1 plays a role in DNA methylation remains elusive.

Uhrf1 is a multi-domain protein harbouring distinct functional domains, which specifically recognize epigenetic marks such as DNA methylation and histone modifications. To investigate the histone-tail binding specificities of Uhrf1, we developed an *in vitro* histone-tail peptide binding assay using GFP-fusion proteins. Moreover, we expanded this assay to 96-well micro plates, allowing high-throughput screening for histone-tail peptide binding, DNA binding, protein-protein interactions, detection of endogenous binding partners and quantification of post-translational modifications. Using this assay, we demonstrated that Uhrf1 preferentially binds to H3K9me3 via a tandem Tudor domain. The binding is mediated by three highly conserved aromatic amino acids that form an aromatic cage similar to the chromodomain of HP1 .

Furthermore, we characterized the second member of the Uhrf family, Uhrf2. Binding assays demonstrate a cooperative interplay of Uhrf2 domains that induces preference for hemimethylated DNA and enhances binding to H3K9me3 heterochromatin marks. Localization and binding dynamics of Uhrf2 *in vivo* require an intact tandem Tudor domain and depend on H3K9 trimethylation but not on DNA methylation. Remarkably, both genes showed an opposite expression pattern and ectopic expression of Uhrf2 in *uhrf1*$^{-/-}$ ESCs did not restore DNA methylation at major satellites indicating functional differences.

Finally, we used a combination of SILAC and mass spectrometry to quantify protein interactions of Dnmt1 over the cell cycle. Therefore, we immunoprecipitated endogenous Dnmt1 from HeLa cells cultured in "light" or "heavy" media synchronized in either G_1, early S or late S phase of the cell cycle. With this approach, we could accurately identify interactions of endogenous Dnmt1 and characterize the cell cycle-dependent dynamics.

In conclusion, this work contributes to the further elucidation of the complex and dynamic mechanisms of Dnmt1 regulation by interacting factors and demonstrates the role of Uhrf proteins in mediating epigenetic crosstalk.

1 Introduction

1.1 Epigenetic Gene Regulation

Multicellular organisms comprise a variety of highly specialized cells that contain the same genetic information, the DNA sequence, but differ dramatically in morphology and function. In simple terms, large ranges of different phenotypes arise from the same genotype. The formation of organs and tissues of morphological and functional distinct cell types throughout development are controlled by spatial and temporal changes of gene activation and repression. One of the most important control mechanisms to ensure proper development is transcriptional regulation by a complex protein network that results in gene transcription by the RNA polymerase II. Basically, the regulation of transcription initiation is accomplished by three different mechanisms: (i) Architecture of the core promoter including regulatory elements, multiple start sites and alternative promoter usage (ii) control of DNA accessibility by altering the chromatin structure (Berger, 2007) and (iii) general and sequence-specific transcription factors (Malik and Roeder, 2005).
Transcription factors are crucial determinants for the regulation of gene expression that activate or repress specific genes through sequence-specific interactions with their promoters. Interaction of transcription factors with their cognate DNA sequence triggers a chain of events, often involving changes in the structure of chromatin, leading to the assembly of an active transcription complex. However, due to the complexity of genomic functions in eukaryotes, transcription factors are not sufficient for full establishment and long-term stability of transcriptional states. This probably accounts for the very low efficiency of cloning animals from the nuclei of differentiated cells and that cloned animals generated from the same donor DNA are not identical to their donor. Even more drastically, cloned animals by nuclear transfer often develop diseases with various defects (Rideout et al., 2001). It became clear that stable cell-type specific gene expression pattern are established and maintained by a complex interplay between transcription factors and epigenetic regulators. In particular, epigenetic processes like DNA methylation, post-translational histone modifications and nucleosome positioning play an essential role in the regulation of gene expression (Figure 1). These modifications are by definition epigenetic, since epigenetics in its classic definitions describes heritable modifications of DNA or chromatin that do not alter the primary nucleotide sequence (Bird, 2002; Jaenisch and Bird, 2003). These epigenetic processes control the composition, structure and dynamics of chromatin and thereby regulate gene expression by regulating the condensation and accessibility of genomic DNA (Bird, 2002; Kouzarides, 2007; Reik, 2007).

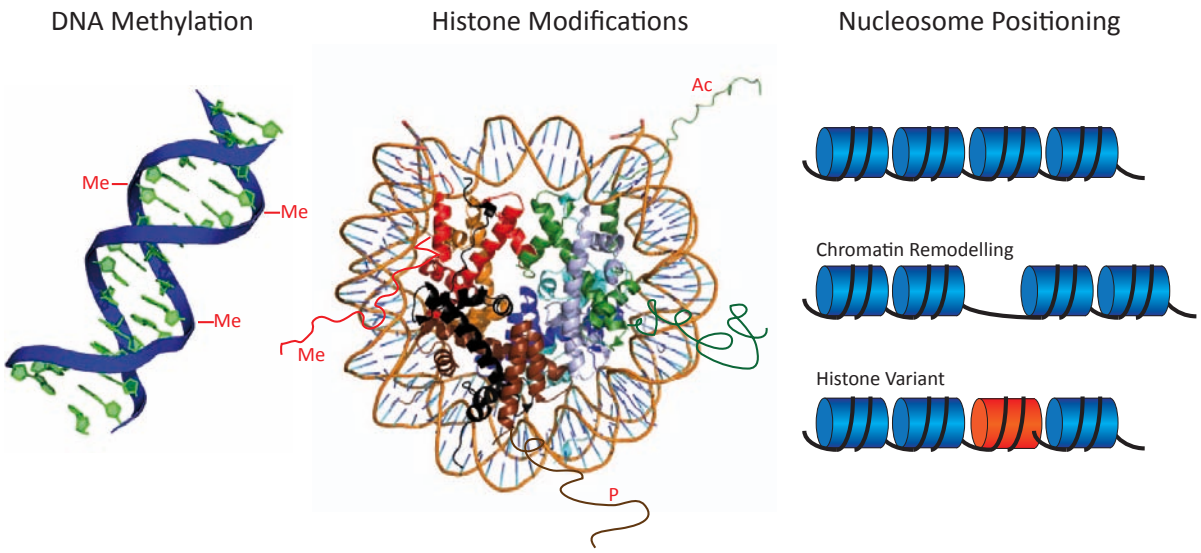

Figure 1: Three levels of epigenetic regulation

Epigenetic regulation depends on the interplay of DNA methylation (PDB ID code: 3BSE), histone modifications (PDB ID code: 1AOI) and nucleosome positioning. Figure is adapted from (Portela and Esteller, 2010)

1.1.1 DNA Methylation

DNA methylation was the first epigenetic modification to be identified and has been intensively studied for half a century. DNA methylation is the post-replicative addition of methyl groups to the C5 position of cytosines catalysed by a family of DNA methyltransferases (Dnmt). Methylation of cytosines within DNA is found in most eukaryotes, including plants, animals and fungi (Goll and Bestor, 2005; Chan et al., 2005; Klose and Bird, 2006), but, it has been lost from some species including budding yeast *Saccharomyces cerevisae* and *Caenorhabditis elegans* (Feng et al., 2010). DNA methylation occurs almost exclusively in the context of CpG dinucleotides that tend to cluster in regions called CpG islands, which constitute about 1 %-2 % of the genome. In general, CpG islands are DNA stretches of more than 200 base pairs in length (0.2-3 kb) characterized by an elevated C/G content (at least 50 %) and a ratio of observed to statistically expected CpG frequencies of a least 0.6 (Illingworth and Bird, 2009). About the half of CpG islands are associated with transcription start sites (Deaton and Bird, 2011) and many are linked to housekeeping genes and developmental regulators (Meissner, 2011). Studies estimated that about 60 % of human genes are associated with CpG islands that are usually unmethylated at all stages of development and in all tissue types (Antequera and Bird, 1993), although some of them (~6 %) become methylated in a

tissue-specific manner during early development or in differentiated tissues (Straussman et al., 2009). Comprehensive microarray analyses showed that unmethylated regions seem to be established during early embryogenesis, not as a result of CpG-ness, but rather through the recognition of specific sequence motifs closely associated with transcription start sites (TSS) (Straussman et al., 2009). In general, CpG island methylation is associated with transcriptional silencing and genomic imprinting, resulting in monoallelic, parent-of-origin-specific expression (Kacem and Feil, 2009), and X-chromosome inactivation in females (Reik and Lewis, 2005). However, DNA methylation does not exclusively correlate with transcriptional silencing. A recent publication reported that gene body methylation positively correlates with active transcription of genes on the active X chromosome while their promoter remains unmethylated (Hellman and Chess, 2007). Also, DNA methylation does not occur exclusively in CpG islands but also in so-called CpG island shores, that are closely associated with transcriptional repression (Irizarry et al., 2009). A comprehensive DNA methylation map of haematopoietic progenitors revealed that differential DNA methylation correlates with gene expression more strongly at CpG shores than CpG islands and ~70 % of the differentially methylated regions in reprogramming are associated with CpG shores (Doi et al., 2009; Ji et al., 2010).

Although DNA methylation occurs mainly in the context of CpG sites, non-CG methylation, which is well characterized in plants, has recently been described in humans at CHG and CHH sites (where H is A, C or T) (Lister et al., 2009). In plant cells non-CG sites are methylated *de novo* by the Chromomethylase *CMT3* responsible for maintaining epigenetic gene silencing (Lindroth et al., 2001). Genome-wide, single-base-resolution maps of methylated cytosines in mammalian genome (human embryonic stem cells as well as fetal fibroblasts) revealed that nearly one-quarter of all methylation identified in embryonic stem cells (ESCs) was in a non-CG context (Lister et al., 2009). Methylation in non-CG context is enriched in gene bodies and depleted in protein binding sites and enhancers. The level of non-CpG methylation decreases upon differentiation and is restored in induced pluripotent stem cells, suggesting that ESCs may use a different methylation mechanism to affect gene regulation (Lister et al., 2009; Laurent et al., 2010). However, the role and origin of non-CpG methylation remains unclear (Laurent et al., 2010).

It has become clear that the regulation of DNA methylation is crucial for normal development. For example, knockout mutations of any of the three mouse genes encoding DNA methyltransferases (Dnmt1, Dnmt3a and Dnmt3b) are lethal (Okano et al., 1999; Lei et al., 1996), demonstrating that aberrant DNA methylation impair normal development. Loss-of-function mutations in *MET1*, the homolog of Dnmt1 in *Arabidopsis thaliana*, and *CMT3* impair the normal development of Arabidopsis embryos, displaying altered planes and numbers of cell divisions and reduced cell viability (Xiao et al.,

2006). Knockdown of dnmt1 in zebra fish embryos caused defects in terminal differentiation of the intestine, exocrine pancreas, and retina (Rai et al., 2006).
Recently, additional DNA modifications have been identified. Besides the fifth base 5-methylcytosine (5mC), 5-hydroxymethylcytosine (5hmC), 5-formylcytosine (5fC) and 5-carboxylcytosine (5caC) have been identified (Ito et al., 2011) (Figure 2). 5hmC is abundant 5fC and 5caC are detectable in genomic DNA of mouse ESCs and organs and can be increased or decreased by overexpression or depletion of Tet proteins (Ito et al., 2011). In tumour cells, the DNA methylation pattern is altered, resulting in global hypomethylation of the genome and hypermethylation at CpG sites of tumor-suppressor genes (Esteller, 2008). Interestingly, hemizygous deletions and mutations of TET2 were found in a wide range of myeloid malignancies, including myelodysplastic syndrome (MDS) and myeloproliferative disorders (Langemeijer et al., 2009; Delhommeau et al., 2009). Furthermore, genomic 5hmC levels correlate with TET2 mutations and with a distinct global gene expression pattern in secondary acute myeloid leukemia (Konstandin et al., 2011). The presence of 5hmC (or 5fc and 5caC) may contribute to both passive and active demethylation in the genome. The maintenance of DNA methylation during DNA replication by Dnmt1 may be inhibited by the inability of Dnmt1 to recognize 5hmC (Lao et al., 2010), leading to the passive loss of DNA methylation during cell division. However, the rapid loss of DNA methylation during mammalian development shortly after fertilization (Hajkova et al., 2010; Mayer et al., 2000; Oswald et al., 2000) and again in primordial germ cells (Hajkova et al., 2002; Lee et al., 2002) within one single cell cycle, suggest the presence of enzymes that can actively remove 5mC independently of DNA replication. In plants, methylated cytosines are excised by the DNA glycosylase DEMETER and replaced with C leading to active genomic demethylation (Kinoshita et al., 2004). However, DNA glycosylases that recognize 5mC have not been identified in mammals until now (Cimmino et al., 2011).

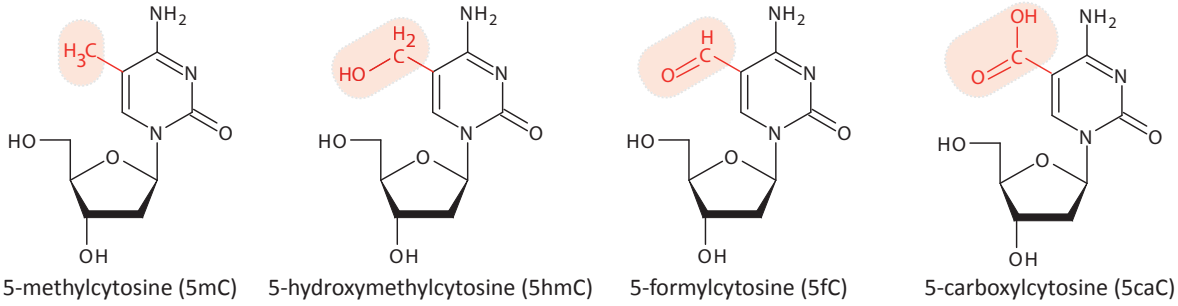

Figure 2: Overview of DNA modifications

Stepwise oxidation starting from 5-methylcytosine (5mC) results in 5-hydroxymethylcytosine (5hmC), 5-formylcytosine (5fC) and finally in 5-carboxylcytosine (5caC).

Instead, the mammalian DNA glycosylase TDG, analogous to plant demethylases, has been shown to possess weak 5mC glycosylase activity, although it is unclear whether TDG is indeed responsible for the active DNA demethylation observed *in vivo* (Zhu et al., 2000; Hardeland et al., 2003). Other studies have shown that active TET hydroxylases may catalyse active DNA demethylation by oxidizing 5mC followed by subsequent deamination and replacement via BER pathway (Guo et al., 2011).

1.1.2 Histone Modifications

The straightened DNA from a single human cell would have a length of ~2 metres and taken into account that the average diameter of a human cell nuclei is ~6 micrometres, eukaryotic organisms are faced with an information storage and packaging problem (Radman-Livaja and Rando, 2010). To overcome these problems, DNA has to be folded in a hierarchy of different levels into higher order chromatin consisting of DNA, histone proteins and non-histone proteins in a way that permits the transcriptional machinery access to enable gene expression. The first level is accomplished by wrapping 147 base pairs (bp) of DNA in 1.65 turns around an histone octamer, consisting of two H2A/H2B and H3/H4 heterodimers (Luger et al., 1997). A DNA linker, with a length of ~50 bp on average, connects these core units of chromatin and thousand of nucleosomes end up looking like "beads on a string" in electron microscopy. Nucleosomes are then further condensed into a shorter, thicker filament, the so-called 30-nm fibre. Finally, nucleosomes are folded into various higher order structures that can be unwrapped as needed (Luger and Hansen, 2005). Importantly, the core histones are predominantly globular except for their N-terminal tails that are unstructured. These histone-tails protrude out of the histone octamer and are mostly subjected to a large variety of post-translational modifications with different impact on chromatin accessibility and stability (Kouzarides, 2007). Histones are modified at about 150 different sites and several different types of post-translational modifications have been reported. It was proposed that distinct histone modifications, on one or more histone tails, act sequentially or in combination to form a "histone code" that is read by other proteins to bring about distinct downstream events (Strahl and Allis, 2000).
In the last 20 years a large variety of enzymes has been identified for acetylation (Sterner and Berger, 2000), methylation (Zhang and Reinberg, 2001), phosphorylation (Nowak and Corces, 2004), ubiquitination (Shilatifard, 2006), sumoylation (Nathan et al., 2003), ADP-ribosylation (Hassa et al., 2006), deimination (Cuthbert et al., 2004), proline isomerization (Nelson et al., 2006) and crotonylation (Tan et al., 2011). Some of the best-characterized histone modifying enzymes are the protein complexes of the polycomb (PcG) and trithorax (trxG) groups (Francis and Kingston, 2001; Campos and

Reinberg, 2009; Bernstein et al., 2007). PcG proteins catalyse two distinct histone modifications: H3K27me3 is catalysed by the polycomb repressive complex (Prc) 2 (Cao et al., 2002) and mono-ubiquitination of lysine 119 of H2A by Prc1 (Campos and Reinberg, 2009). Loss of any of the Prc2 subunits results in severe gastrulation defects, highlighting its essential role in normal development (Faust et al., 1998; O'Carroll et al., 2001; Pasini et al., 2004).

In general, post-translational histone modifications can function via two different mechanisms. Firstly, the disruption of contacts between nucleosomes can disturb the chromatin structure. Of all known modifications, acetylation of lysine residues has the highest potential to decondense chromatin since it neutralizes the basic charge of histones. Another striking example is the phosphorylation of histone residues. Phosphorylation has important consequences on chromatin compactness via charge change and has been shown to play an important role in mitosis, apoptosis and gametogenesis (Ahn et al., 2005; Fischle et al., 2005; Krishnamoorthy et al., 2006). Secondly, the composition of histone modifications can encourage or abolish the binding of non-histone proteins to chromatin. One example is the heterochromatin-associated protein HP1 that specifically binds to the predominant heterochromatin mark H3K9me3 (Jacobs and Khorasanizadeh, 2002; Jacobs et al., 2001) and is released upon phosphorylation of the adjacent serine 10 during M phase of the cell cycle (Fischle et al., 2005).

In the last years structural and functional studies revealed how chromatin effector modules target their respective covalent histone modification (reviewed by (Taverna et al., 2007) (Figure 3). Besides the already mentioned HP1 , which specifically recognizes H3K9me3 by its chromodomain, many other protein domains are known to recognize methylated lysine residues. The so-called Royal superfamily comprises chromodomains, double chromodomains, chromo barrels, Tudor domains, double/tandem Tudor domains and MBT (malignant brain tumor) domains, and readout higher lysine methylation. In contrast, members of the PHD-finger (Plant Homeo Domain) family can target both, methylated and unmodified lysine residues. On one hand, the BPTF PHD finger, the largest subunit of the nucleosomal remodelling factor (NURF) ATP-dependent chromatin remodelling complex, targets di- and trimethyllysine in H3K4 context (Wysocka et al., 2006). On the other hand, the PHD finger of BHC80, a part of the Lsd1 co-repressor complex, binds unmethylated H3K4 and discriminates strongly against its methylated counterparts (Lan et al., 2007). Interestingly, it has been shown that the ADD (ATRX-Dnmt-Dnmt3L) domain of Dnmt3L, that is structurally very similar to PHD finger, targets unmethylated lysine in H3K4 context (Ooi et al., 2007). The reader modules for acetylated histone residues are bromodomains. For example, the prototypical bromodomain of the transcriptional coactivator "p300/CBP-associated factor" (P/CAF, the homolog of *S. cerevisiae* Gcn5p) targets acetyllysine in H4K16 context (Dhalluin et al., 1999). Other reader modules are WD40 repeats (Ruthenburg et al.,

2006), 14-3-3 (Macdonald et al., 2005) and BRCT domains (Stucki et al., 2005) recognizing unmethylated arginine residues, phosphoserine marks and phosphoserine marks in H2A.X context, respectively. In addition, there are many examples of proteins carrying two or more putative histone-binding modules allowing for combinatorial readout of multivalent post-translational modifications at the histone or nucleosome level (Ruthenburg et al., 2007).

A

Reader Module		PTM Mark
Bromodomain		Many histone Kac
Royal	Chromodomain	H3K9me2/3, H3K27me2/3
	Chromo Barrel	H3K36me2/3
	Double Chromodomain	H3K4me1/2/3
	Tudor	H3K4me3, H4K20me2
	Tandem Tudor	H3R2, H3K9m2/3
	MBT	H3k4me1, H4K20me1/2, H1K26me1
PHD		H3K4, H3K4me3, H3K9me3, H3K36me3
14-3-3		H3S10ph
WD40		H3R2/H3K4/H3K9me/H3K27me
BRCT		H2A.XS139ph
ADD		H3K4

B

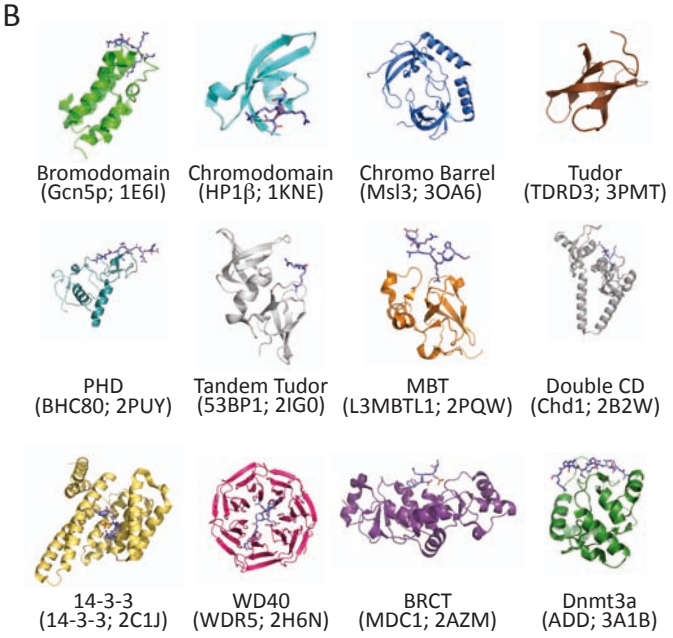

Figure 3: Histone post-translational modifications and their binding partners

A) Reading modules of histone post-translational modifications. Shown grouped by domain family are known chromatin-associated modules and the histone marks they have been reported to bind (Taverna et al., 2007). **B)** Solved structures of histone-binding modules. Protein names and PDB ID code are written in brackets. Figure is adapted from (Taverna et al., 2007).

One functional consequence of histone modifications is the establishment of global chromatin environments (Kouzarides, 2007). In relation to its transcriptional state, the human genome can be roughly divided into actively transcribed euchromatin and transcriptional inactive heterochromatin. Euchromatic regions are associated with acetylation of histone H3 and H4 and trimethylation of H3K4, H3K36 and H3K79. Modifications that are localized to heterochromatic regions are methylated H3K9, H3K27 and H4K20 (Li et al., 2007). In addition, bivalent domains have been found in mouse ESCs consisting of large regions of H3K27 methylation, implicated in silent chromatin. These domains harbour smaller regions of H3K4 methylation, an euchromatic mark, that tend to coincide with transcription factors at genes expressed at low levels (Bernstein et al., 2006). The bivalent domains allow ESCs to keep transcription factors in a poised, low-expressed level, which can be activated during differentiation.
Besides post-translational modifications, also histone H3 tail clipping regulates gene expression. An endopeptidase, which shows a preference for histone tail carrying repressive modifications, cleaves H3 after Ala21, generating a histone that lacks the first 21 residues (Santos-Rosa et al., 2009). Histones can also be modified at different sites simultaneously, leading to crosstalk between several different marks. The communication among histone modifications can occur within the same site (Wang et al., 2008), in the same histone tail (Duan et al., 2008) and among different histone tails (Nakanishi et al., 2009). Thus, a single histone mark does not determine the outcome alone. Instead, the cooperative interplay of several different histone marks or the combination of all modifications existing in nucleosomes specify the biological outcome (Portela and Esteller, 2010).

1.1.3 Nucleosome Positioning

In addition to DNA methylation and histone modifications, nucleosome positioning plays a role in the epigenetic regulation of gene expression. Nucleosomes are a barrier to transcription since they block the accession of the transcription machinery to DNA. The packaging of DNA into nucleosomes appears to affect all stages of transcription, thereby regulating gene expression (Portela and Esteller, 2010). In particular, the precise position of the nucleosome around the transcription start site (TSS) influences the initiation of transcription. Genome-wide studies provide a view of the nucleosome positions of a typical cell (Radman-Livaja and Rando, 2010). The promoter regions are overall depleted of nucleosomes relative to transcribed regions and the so-called nucleosome free regions (NFRs) are located just upstream of the TSS. In general, NFRs directly upstream of the TSS correlate with gene activation, whereas the occupancy of the TSS by a nucleosome correlates with gene repression (Schones et al., 2008; Cairns,

2009). The function and positioning of nucleosomes can also be influenced by histone variants. Histone variants differ in sequence and expression timing from the canonical counterparts and are enriched in chromatin of specific functional states, ranging from DNA repair and centromere determination to the regulation of gene expression (Wiedemann et al., 2010). For example, the incorporation of the histone variant H2A.Z changes the nucleosome positioning in comparison to canonical nucleosomes (Fan et al., 2002). Also, the incorporation of H2A.Z destabilizes the nucleosomes in comparison to canonical histones (Abbott et al., 2001).
The position of nucleosomes can also be changed by the sliding and eviction of nucleosomes by ATP-dependent chromatin remodelling machines (Clapier and Cairns, 2009). Chromatin modellers can be grouped into four families (SWI/SNF, ISWI, CHD and INO80) all containing a SWI2/SNF2-family ATPase subunit characterized by an ATPase domain and differ in their unique subunits (Clapier and Cairns, 2009; Korber and Becker, 2010).

1.1.4 Crosstalk between Epigenetic Modifications

Early studies have demonstrated a link between DNA methylation and histone modifications mediated by a group of proteins that specifically recognize methylated CpG sites (mCpG). The family of the methyl-CpG binding proteins (MBPs) consist of at least three protein families: the methyl-CpG binding domain (MBD), the Kaiso and the UHRF protein family (Rottach et al., 2009). These proteins bind to methylated DNA and recruit a protein complex that contains HDACs and histone methyltransferases, demonstrating a change of the chromatin structure induced by DNA methylation (Nan et al., 1998; Rottach et al., 2009; Hendrich and Tweedie, 2003; Bird, 2002). In addition, it is known that DNA methylation inhibits methylation of H3K4 and *vice versa* (Weber et al., 2007; Okitsu and Hsieh, 2007). On the one hand, H3K4 methylation is depleted from regions with DNA methylation (Okitsu and Hsieh, 2007), on the other hand early studies in *Neurospora crassa* demonstrate that mutations of histone H3K9 methyltransferase reduced DNA methylation, suggesting that DNA methylation depends on histone methylation (Tamaru and Selker, 2001). Moreover, genome-scale DNA methylation studies demonstrate a correlation between DNA methylation and histone modifications. In particular, DNA methylation correlates with the absence of H3K4 methylation and presence of H3K9 methylation (Meissner et al., 2008). This correlation may in part be caused by DNA methyltransferases specifically recognizing histone modifications. For instance, the *de novo* DNA methyltransferase Dnmt3a and its cofactor Dnmt3L specifically recognize unmethylated H3K4 via an ADD domain (Ooi et al., 2007; Otani et al., 2009). Also, a link between DNA methylation and nucleosome positioning has been shown in *A.*

thaliana (Zilberman et al., 2008). Exclusion of H2A.Z correlates with sites of DNA methylation in bodies of actively transcribed genes in methylated transposons. Interestingly, mutations in the *MET1*, which cause both loss and gain of DNA methylation leads to opposite changes (gains and losses) in H2A.Z deposition (Zilberman et al., 2008).

1.2 DNA Methyltransferases

DNA methylation is the post-replicative addition of methyl groups to the C5 position of cytosines catalysed by a family of DNA methyltransferases (Dnmt). All C5 cytosine Dnmts share the same conserved motifs involved in the complex molecular mechanism of methyl group transfer best studied in the prokaryotic DNA methyltransferases M. HhaI (Klimasauskas et al., 1994). This mechanism involves DNA methyltransferase binding to the DNA, flipping the target cytosine out of the DNA double helix, covalent bond formation between a conserved cysteine nucleophile and the cytosine C6, transfer of a methyl group from S-adenosyl-L-methionine to the activated cytosine C5 and DNA methyltransferase release by β-elimination (Klimasauskas et al., 1994; Cheng and Blumenthal, 2008).
In vertebrates, there are five known members of the Dnmt family that differ in structure and function and apart from Dnmt2, all Dnmts comprise an N-terminal regulatory domain in addition to the C-terminal catalytic domain (Figure 4)

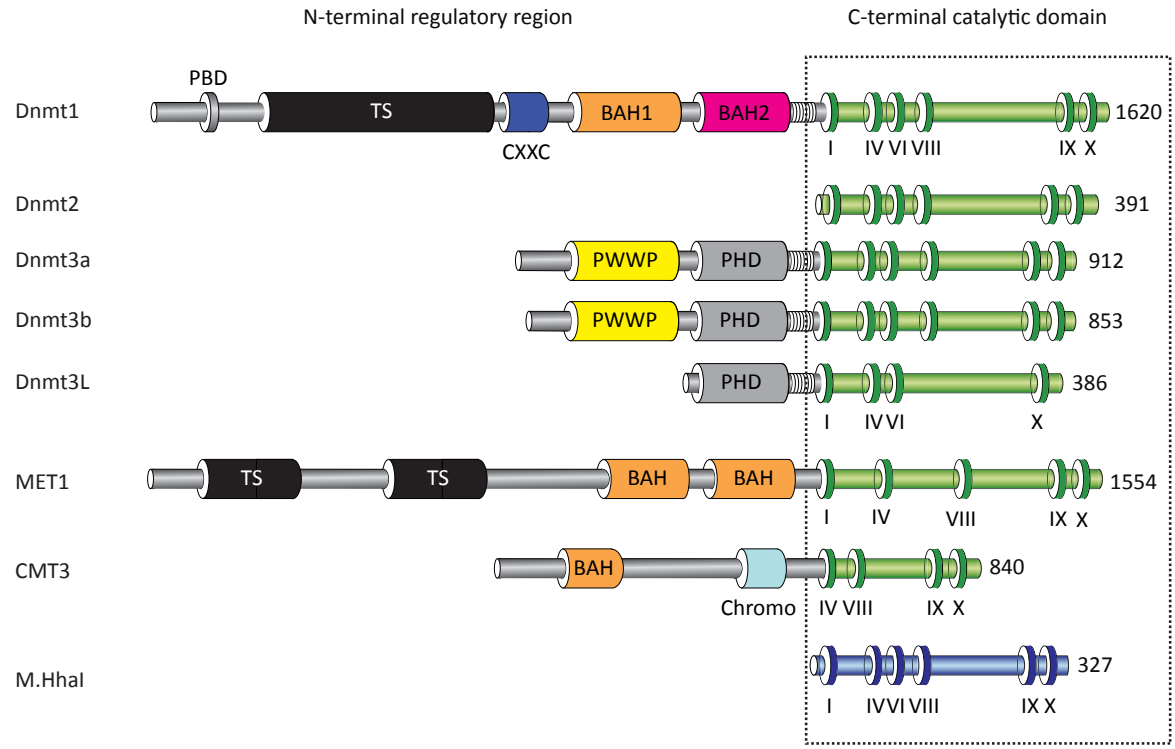

Figure 4: Schematic outline of DNA Methyltransferases

Schematic outline of the domain architecture of mammalian Dnmts and the *A. thaliana* Methyltransferase *MET3* and Chromomethylase3 *CMT3* in comparison to the prokaryotic DNA methyltransferases M.HhaI. All DNA methyltransferases harbour highly conserved motifs (I-X) in the C-terminal catalytic domain but differ in their N-terminal regulatory domain. Figure is adapted from (Qin et al., 2011b).

The Dnmt3 subfamily, comprising Dnmt3a and Dnmt3b, possesses activity towards unmethylated DNA and establishes *de novo* DNA methylation patterns during gametogenesis and embryogenesis (Kaneda et al., 2004; Okano et al., 1999; 1998). The *de novo* Dnmts are highly expressed in ESCs and down regulated in differentiated cells (Watanabe et al., 2002; Esteller, 2007). The Dnmt3 family contains a third member Dnmt3L, which is required for establishing maternal genomic imprinting (Bourc'his et al., 2001). The cofactor Dnmt3L (Aapola et al., 2000) specifically recognizes unmethylated histone H3K4 (Ooi et al., 2007; Otani et al., 2009) stimulates the activity of Dnmt3a and Dnmt3b (Suetake et al., 2004), but by itself lacks enzymatic activity (Hata et al., 2002). Established DNA methylation patterns are maintained during DNA replication and DNA repair by the ubiquitously expressed Dnmt1 (Leonhardt et al., 1992; Mortusewicz et al., 2005), which displays a strong preference for hemimethylated CpG sites, the substrate of maintenance DNA methylation (Bestor and Ingram, 1983). The fifth member of the Dnmt family, Dnmt2, shows very weak activity toward DNA and was instead shown to methylate cytoplasmic tRNAAsp (Goll et al., 2006; Hermann et al., 2004).

Despite their common catalytic mechanism, all three active eukaryotic Dnmts have distinct and non-redundant functions, which are likely mediated by their diverse regulatory domains (Figure 4). In contrast to prokaryotic Dnmts, the tissue-specific *de novo* Dnmts, Dnmt3a and Dnmt3b, are only active on a subset of target CpG sites (Hsieh, 1999), reflecting a selective control imposed by the N-terminal regulatory domain. The ubiquitously expressed Dnmt1 preferentially methylates hemimethylated CpG sites and thereby maintains DNA methylation patterns after DNA replication and DNA repair (Leonhardt et al., 1992; Mortusewicz et al., 2005; Bestor and Ingram, 1983). Remarkably, the catalytic domain of Dnmt1 -although possessing all conserved motifs- is not catalytically active by itself and requires allosteric activation by the N-terminal regulatory domain (Margot et al., 2000; Zimmermann et al., 1997; Fatemi et al., 2001).

However, none of the three catalytically active Dnmts shows a particular target preference that could explain cell-type-specific methylation patterns, suggesting that alternative mechanism must be in place to either direct or inhibit their recruitment (Meissner, 2011). A recent study investigated the role of the underlying genome sequence in guiding DNA methylation (Lienert et al., 2011). Small methylation-determining regions (MDRs) within gene promoters were identified which mediate both hypomethylation and *de novo* methylation in cis, and their activity depends on developmental state, motifs for DNA-binding factors and a critical CpG density (Lienert et al., 2011).

1.2.1 Structure and Function Dnmt1

Bioinformatics suggested that the mammalian Dnmt1 evolved by fusion of at least three ancestral genes (Margot et al., 2000). The N-terminal regulatory domain of Dnmt1 occupies 2/3 of the whole enzyme and harbours several functional distinct domains. It harbours a proliferating cell nuclear antigen (PCNA) binding domain (PBD), a targeting sequence (TS domain), a zinc finger domain (CXXC) and two bromo-adjacent homology domains (BAH1/2) and is connected to the C-terminal catalytic domain by seven lysyl-glycyl dipeptide repeats (Goll and Bestor, 2005; Rottach et al., 2009). The PBD domain has been shown to mediate the interaction with PCNA leading to the association of Dnmt1 with the replication machinery (Leonhardt et al., 1992; Chuang et al., 1997; Easwaran et al., 2004). The TS domain mediates association with heterochromatin and may lead to dimerization of Dnmt1 (Leonhardt et al., 1992; Easwaran et al., 2004; Fellinger et al., 2009). Recently, it has been shown that mutations in DNMT1 cause both central and peripheral neurodegeneration in one form of hereditary sensory and autonomic neuropathy with dementia and hearing loss (Klein et al., 2011). Exome sequencing revealed two mutations within the TS domain that cause premature degradation of mutant proteins, reduced methyltransferase activity and impaired heterochromatin binding during the G_2 cell cycle phase leading to global hypomethylation and site-specific hypermethylation (Klein et al., 2011). The CXXC domain of Dnmt1 binds to unmethylated DNA but its deletion does not alter the activity and specificity of Dnmt1 (Frauer et al., 2011). Interestingly, the isolated C-terminal catalytic domain of Dnmt1, although harbouring all conserved Dnmt motifs, requires an additional, large part of the N-terminal domain for enzymatic activity. Fusion of this N-terminal region of Dnmt1 to the prokaryotic Dnmt, M.HhaI, induced a preference for hemimethylated DNA (Pradhan and Roberts, 2000). Cleavage between the regulatory and the catalytic domain stimulated the initial velocity of methylation of unmethylated DNA without substantial change in the rate of methylation of hemimethylated DNA (Bestor, 1992). These findings illustrate the role of the N-terminal domain in the selective activation of the catalytic domain to ensure faithful maintenance of DNA methylation patterns.

First insights into the molecular mechanism of Dnmt1 regulation were provided by two recently published crystal structures comprising either a large fragment of mouse Dnmt1 (aa 291-1620) (PDB ID code 3AV4) or a shorter fragment (aa 650-1,602) in complex with unmethylated DNA (PDB ID code 3PT6) (Takeshita et al., 2011; Song et al., 2011b). Notably, the overall structure of the eukaryotic catalytic domain is highly similar to the prokaryotic M.HhaI (PDB ID code 5mht) (Figure 5). In addition, both structures showed an interaction of the N-terminal regulatory domain with the C-terminal catalytic domain, which is consistent with prior genetic and biochemical studies (Fatemi

et al., 2001; Margot et al., 2003). Remarkably, the TS domain was found deeply inserted into the catalytic pocket and would in this conformation prevent Dnmt1 binding to hemimethylated DNA, the substrate for maintenance DNA methylation (Takeshita et al., 2011).

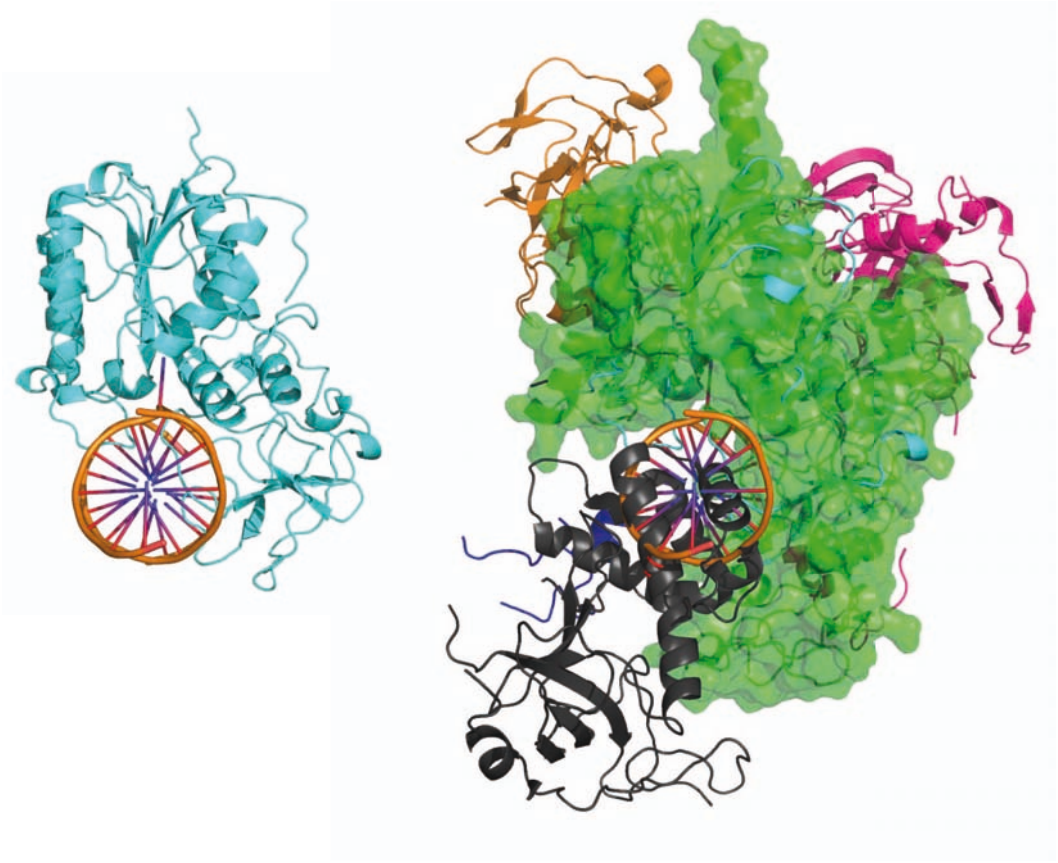

Figure 5: Structural insights into the DNA methyltransferases 1

Left: Crystal structure of the prokaryotic cytosine- (C5) methyltransferases M.HhaI in complex with hemimethylated DNA (PDB code 5MHT). **Right:** Crystal structure of the large fragment (291,Äì1620) of mouse Dnmt1 (PDB code 3AV4) in superimposition with the prokaryotic structure (left) showing the expected steric clash between the TS domain and DNA binding in the catalytic pocket. The single domains are color-coded: TS domain: black; Catalytic domain: green; BAH1: orange; BAH2: red; CXXC domain: blue. Figure is adapted from (Qin et al., 2011b).

These structural insights indicate that Dnmt1 most likely undergoes several conformational changes during the methylation reaction. Activation of Dnmt1 requires displacement of the TS domain from the DNA binding pocket to allow substrate binding. Indeed, deletion of the TS domain lowered the activation energy (O'Gara et al., 1996) and addition of purified TS domains inhibited Dnmt1 methylation activity *in vitro* (Syeda et al., 2011), clearly pointing to an auto-inhibitory function of the TS domain. These findings suggest that interacting proteins may modulate the interactions of the N-terminal

domain with the catalytic domain and thereby regulate the activity of Dnmt1 *in vivo*.

1.2.2 Regulation of Dnmt1 by Interactions

Over the last two decades, a large variety of proteins were reported to interact with Dnmt1, ranging from DNA methyltransferases, DNA binding proteins, chromatin modifiers and chromatin binding proteins to tumor suppressors, cell-cycle regulators and transcriptional regulators. Notably, many of these proteins also interact with each other, leading to a complex epigenetic network (Figure 6).

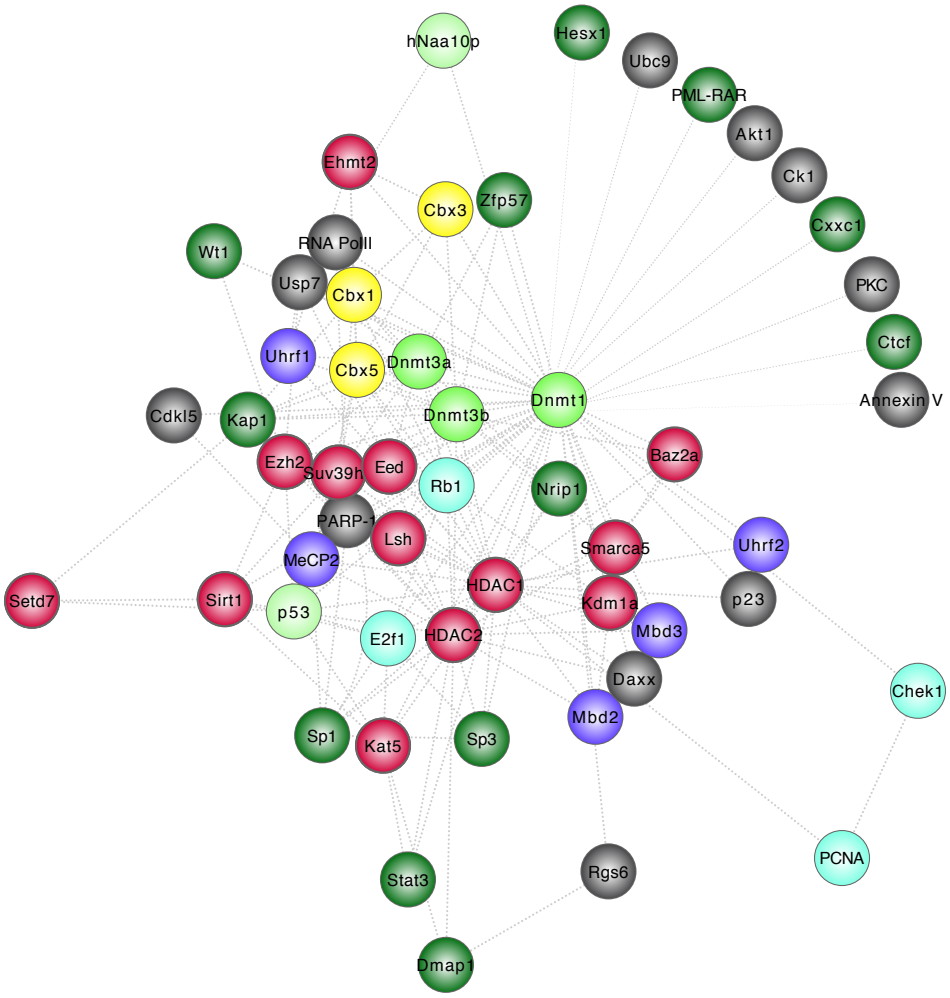

Figure 6: Interactom of Dnmt1.

Protein-Protein interactions were drawn in Cytoscape (Edge Weighted Spring Embedded Layout) and the proteins were grouped into the following functional classes: Light green: DNA methyltransferases; Blue: DNA binding proteins; Red: Chromatin modifiers; Yellow: Chromatin binding proteins; Green Yellow: Tumor suppressors; Blue: cell-cycle regulators; Dark green: Transcriptional regulators; Grey: Others

As mentioned before, Dnmt1 interacts with PCNA via its PBD domain and thereby locates to site of DNA replication during S phase. The transient association of Dnmt1 with PCNA (Chuang et al., 1997) could be an efficient mechanism to bridge the discrepancy between the high processivity of DNA replication (~0.035 seconds per nucleotide) (Jackson and Pombo, 1998) and the low turnover rates (70-450 seconds per methyl group) of recombinant Dnmt1 (Pradhan et al., 1999). Importantly, although being very transient and not strictly required for maintaining DNA methylation *in vivo*, the binding of Dnmt1 to PCNA enhances the methylation activity about twofold (Schermelleh et al., 2007; Spada et al., 2007). The reason for the enhancement of activity is still unclear and may result either from local enrichment of Dnmt1 concentration at the site of replication or from conformational changes induced by the Dnmt1-PNCA interaction and thus allosteric activation.
Although Dnmt1 can bind hemimethylated CpG sites by itself, it also interacts with methyl-CpG binding proteins like MeCP2 (Kimura and Shiota, 2003), Mbd2/3/4 (Tatematsu et al., 2000; Ruzov et al., 2009) and the Uhrf family of proteins (Bostick et al., 2007; Sharif et al., 2007; Arita et al., 2008; Avvakumov et al., 2008; Qian et al., 2008; Achour et al., 2009; Pichler et al., 2011; Meilinger et al., 2009). MeCP2 binds DNA, induces chromatin compaction (Brero, 2005; Georgel et al., 2003) and interacts with Dnmt1 via its transcription repressor domain (TRD) (Kimura and Shiota, 2003). MeCP2 and Mbd2, which specifically recognize fully methylated CpG sites and Mbd3 also form complexes with histone deacetylases HDAC1 and HDAC2, which in turn interact with Dnmt1 (Kimura and Shiota, 2003; Achour et al., 2007; Fuks et al., 2000; Robertson et al., 2000; Rountree et al., 2000). This set of interactions can explain the correlation between DNA hypermethylation and histone hypoacetylation at transcriptional inactive regions (Eden et al., 1998), suggesting a role in transcriptional repression (Wade, 2001). This complex may also comprise the Dnmt1 association protein (Dmap1) (Rountree et al., 2000; Mohan et al., 2011) and the transcriptional co-regulator Daxx (Muromoto et al., 2004) mediating repression in an HDAC-independent manner (Rountree et al., 2000; Mohan et al., 2011). In addition, the interaction with methyl-CpG binding proteins and HDACs may enrich Dnmt1 in highly methylated heterochromatic regions to increase local methylation efficiency and/or enhance heterochromatin formation at these highly methylated regions (Qin et al., 2011b). Dnmt1 also interacts with Mbd4, the only member of the MBD family of proteins that does not appear to be involved in transcriptional repression (Ruzov et al., 2009; Hendrich and Tweedie, 2003). Mbd4 directly interacts with Dnmt1 and Mlh1, leading to recruitment of Mlh1 to heterochromatic sites (Ruzov et al., 2009). Recently, Uhrf1 has emerged as an essential co-factor for maintenance DNA methylation. The genetic ablation of *uhrf1* in ESCs leads to genomic hypomethylation similar to *dnmt1*$^{-/-}$ ESCs (Bostick et al., 2007; Sharif et al., 2007). In addition Uhrf1 as well as Dnmt1 interacts with the *de novo* Dnmts, Dnmt3a and Dnmt3b (Fatemi et

al., 2002; Kim et al., 2002; Lehnertz et al., 2003; Meilinger et al., 2009; Rhee et al., 2002). These results demonstrate a complex interplay between methyl-CpG binding proteins and Dnmts in establishing genomic DNA methylation patterns.

Besides the interaction with methyl-CpG binding proteins, Dnmt1 also associates with a number of proteins involved in the establishment and maintenance of heterochromatin structure. Dnmt1 interacts with the major eukaryotic histone methyltransferases Suv39H1 (Fuks et al., 2003) and Ehmt2 (also known as G9a) (Estève et al., 2006; Kim et al., 2009; Peters et al., 2003; Tachibana et al., 2002), which are essential for H3K9 methylation (Lehnertz et al., 2003; Ikegami et al., 2007). Genetic ablation of *ehmt2* (Dong et al., 2008; Ikegami et al., 2007) and *suv39h* (Lehnertz et al., 2003) in mouse ESCs leads to DNA hypomethylation at specific loci in genomic DNA and altered DNA methylation of pericentric satellite repeats, respectively. Interestingly, also the H3K9me3 binding heterochromatin protein HP1 was shown to interact with Dnmt1 (Fuks et al., 2003), but localization of Dnmt1 at late replicating chromocenters seemed to be independent of Suv39h1/2 and HP1 (Easwaran et al., 2004). In addition, Dnmt1 interacts with Polycomb group (PcG) proteins Ezh2 (Vire et al., 2006; Xu et al., 2011) and Eed (Vire et al., 2006), which are subunits of the Prc2/Eed-Ezh2 complex that methylates H3K27. Ezh2 was shown to recruit Dnm1 to target genes and thereby mediate promoter methylation (Vire et al., 2006). A recent study showed that Dnmt1 inhibition decreased the expression levels of PcG proteins and induced cellular senescence, providing a possible link between DNA methylation, maintenance of stem cell self-renewal and multipotency (So et al., 2011).

In addition to the histone modifying enzymes, also chromatin remodelling ATPases like Lsh are required for maintaining DNA methylation in mammals. Lsh is related to the SNF2 family of chromatin-remodelling ATPases and forms a complex with Dnmt1, Dnmt3b and HDACs, suggesting a role in transcriptional repression (Jeddeloh et al., 1999; Myant and Stancheva, 2008). Similarly, Baz2a (also known as Tip5), the large subunit of the nucleolar remodelling complex (NoRC), forms a complex with Dnmt1, Dnmt3s, HDACs and hSNF2H, mediating recruitment to rDNA (Zhou and Grummt, 2005). One component of this complex, the chromatin remodelled hSNF2H, increases the binding affinity of Dnmt1 to mononucleosomes (Robertson et al., 2004). The interaction with these chromatin-remodelling factors may help Dnmt1 to access substrate sites in heterochromatic regions. Besides indirect connections to transcriptional regulation, also direct interactions of Dnmt1 with transcription regulators and factors have been described. Cxxc1 (Cfp1), a component of the SetD1A/B methyltransferase complex, binds to Dnmt1, and Cxxc1-deficient ESCs display reduced levels of global DNA methylation (Butler et al., 2008). Moreover, Dnmt1 was shown to interact with the transcription factors Sp1/3 (Estève et al., 2007) and Stat3 (Zhang et al., 2005). A Stat3-Dnmt1-HDAC1 complex binds to the promoter of *shp1*, encoding a negative regulator of cell sig-

nalling, inducing cell transformation (Zhang et al., 2005). Also Nrip1, a co-repressor for nuclear receptors, interacts with Dnmt1 and Dnmt3s in gene repression (Kiskinis et al., 2007). Additional Dnmt1 interactions have been reported with various tumor suppressor genes including Wt1 (Xu et al., 2011), Rb (Robertson et al., 2000; Pradhan and Kim, 2002), p53 (Estève et al., 2005) and hNaa10p (Lee et al., 2010). The Wilms tumor suppressor protein (Wt1) recruits Dnmt1 to the *pax2* promoter resulting in DNA hypermethylation (Xu et al., 2011). The retinoblastoma (Rb) tumor suppressor gene product associates with Dnmt1 and the transcription factor, E2f1, resulting in transcriptional repression of E2f1- responsive promoters (Robertson et al., 2000). The interaction with p53 stimulates Dnmt1 activity, leading to hypermethylation (Estève et al., 2005). Finally, the tumor suppressor, hNaa10p, recruits Dnmt1 to promoters of tumor suppressor genes and increases the DNA binding affinity of Dnmt1 (Lee et al., 2010). Besides a role in normal gene regulation, connections with deregulated gene expression in cancer were also reported. The leukemia-promoting PML-RAR fusion recruits Dnmt1 to target promoters, inducing gene hypermethylation, an early step of carcinogenesis (Di Croce et al., 2002).

1.2.3 Regulation of Dnmt1 by Post-translational Modifications

While most of the interacting factors regulate Dnmt1 activity by recruitment to specific DNA sequences and target genes, some of them have been described to modulate Dnmt1 activity by post-translational modifications (Figure 7). Recent publications have described several different post-translational modifications that influence the stability, abundance and activity of Dnmt1. Dnmt1 was shown to undergo cell cycle-dependent changes in acetylation and ubiquitination (Bronner, 2011; Du et al., 2010; Qin et al., 2011a). On the one hand, Dnmt1 is acetylated by Kat5 subsequently ubiquitinated by the E3 ubiquitin ligase, Uhrf1, marking Dnmt1 for proteolytic degradation. The abundance of Dnmt1 increases in early S phase and starts to decrease during late S or G phase, a pattern which inversely correlates with the abundance of Kat5, suggesting that Kat5-mediated Dnmt1 acetylation triggers Dnmt1 degradation (Du et al., 2010). On the other hand, Dnmt1 is deubiquitinated by Usp7 (also known as Herpes virus-associated ubiquitin-specific protease HAUSP) and deacetylated by HDAC1, protecting Dnmt1 from proteolytic degradation (Du et al., 2010; Qin et al., 2011a). The interaction between Dnmt1 and Usp7 is disrupted during mid-late S phase, showing that a physical interaction is required for the stabilization of Dnmt1. Furthermore, the interaction of Uhrf1 and Dnmt1 increases during late S phase leading to destabilization of Dnmt1 (Du et al., 2010)

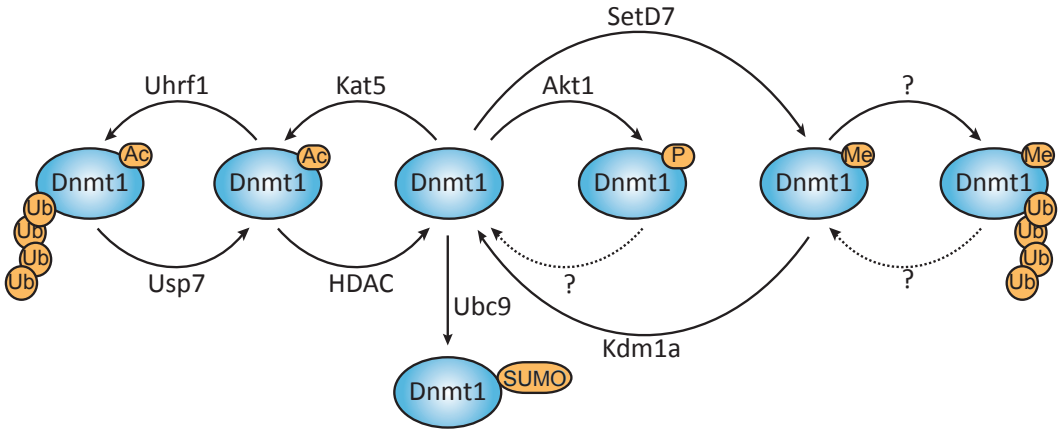

Figure 7: Regulation of Dnmt1 by post-translational modifications

Crosstalk between Dnmt1 and interacting proteins, leading to post-translational modifications of Dnmt1. The following abbreviations are used: Ac = Acetylation; Ub = Ubiquitination; SUMO = Sumoylation; p = Phosphorylation; Me = Methylation. The dotted line indicates a hypothetical dephosphorylation. Figure is adapted from (Qin et al., 2011b).

In fact, the first post-translational modification to be described was the phosphorylation of Dnmt1 at Ser515 (DNMT1 Ser509) (Glickman et al., 1997), which was suggested to modulate the interaction between the regulatory and catalytic domain (Goyal et al., 2007). In addition, Dnmt1 is phosphorylated at Ser146 (in mice only) by the casein kinase 1 / , decreasing the DNA binding affinity (Sugiyama et al., 2010), and at sites in the regulatory domain, which have yet to be mapped, by members of the PKC family (Lavoie et al., 2011). Notably, it has been reported that the phosphorylation of Dnmt1 disrupts the Dnmt1/PCNA/Uhrf1 interaction, promoting global DNA hypomethylation in human gliomas (Hervouet et al., 2010). Phosphorylation of Ser143 by Akt1 during early and mid-S phase has been described to stabilize Dnmt1 (Estève et al., 2011). S143 phosphorylation in turn blocks methylation of the adjacent Lys142 by Setd7, which marks Dnmt1 for proteolytic degradation during late S phase and G_2 (Estève et al., 2011; 2009) . Besides Lys142, Set7/9 can also methylate the Lys1096 residue of Dnmt1 (Lys1094 of DNMT1), which destabilizes the enzyme. The corresponding demethylation by Kdm1A (also known as lysine-specific demethylase Lsd1 and Aof2) in turn increases the stability of Dnmt1 (Wang et al., 2009). Consistently, the genetic ablation of *kdm1a* in ESCs led to a progressive loss of DNA methylation (Wang et al., 2009) and caused cellular differentiation (Adamo et al., 2011). Finally, Dnmt1 is also sumoylated by the ubiquitin-conjugating enzyme, Ubc9, leading to the increased catalytic activity of Dnmt1 on genomic DNA *in vitro* (Lee and Muller, 2009). In summary, post-translational modifications influence the abundance and activity of Dnmt1, and may thus play a role during normal development and disease.

1.3 The Uhrf Family of Proteins

As mentioned above, epigenetic memory of a cell involves DNA methylation, histone modifications and nucleosome positioning (Figure 1). There is a tight link between the histone code and DNA methylation, as modifications of histones contribute to the establishment of DNA methylation patterns and *vice versa* (Bronner et al., 2010). Interestingly, the family of Uhrf proteins has recently been identified to simultaneously read both methylated DNA and the histone code.

1.3.1 Phylogenetic Tree of Evolution

Uhrf1 (Ubiquitin-like-containing PHD and RING finger domains protein 1) also known as Np95 (nuclear protein of 95 kDa) or ICBP90 (inverted CCAAT box binding protein of 90 kDa) has initially been identified using a monoclonal antibody against murine thymic lymphoma, (Muto et al., 1995). The other member of the Uhrf family of proteins, Uhrf2, has been identified in a yeast two-hybrid screen for interacting factors for a novel PEST-containing nuclear protein (PCNP) (Mori et al., 2002). Uhrf1 and Uhrf2 are highly conserved in vertebrates ranging from humans to fish and are also found in invertebrates like ants and bees similar to the phylogenetic occurrence of Dnmts (Figure 8). Notably, the phylogenetic tree of the SRA superfamily (the SRA domain is unique for Uhrf proteins) (Figure 8) does not show any Uhrf1 or Uhrf2 equivalent in flies like *Drosophila melanogaster*, in worms like *Caenorhabditis elegans* or in the *Saccharomyces* genome. Dnmts show a similar pattern of evolution in the phylogenetic tree since they are also absent in *C. elegans* and *S. cerevisiae*. Notably, the Drosophila genome contains a single candidate DNA methyltransferases gene similar to Dnmt2 (Kunert et al., 2003) but no Dnmt1 or Dnmt3 equivalents. In contrast to *D. melanogaster*, other related insects such as the honeybee have functional Uhrf, Dnmt1 and Dnmt3 homologues (Honeybee Genome Sequencing Consortium, 2006). In general, the presence of Uhrf proteins correlates with DNA methylation. Although DNA methylation is conserved in most eukaryotic groups, including many plants, animals, and fungi, it has been lost from certain model organisms such as the mentioned budding yeast *S. cerevisae*, and *C. elegans* (Feng et al., 2010). The insect *D. melanogaster* is reported to contain low levels of 5mC (Lyko et al., 2000) although mostly in the CpT rather than in CpG context.

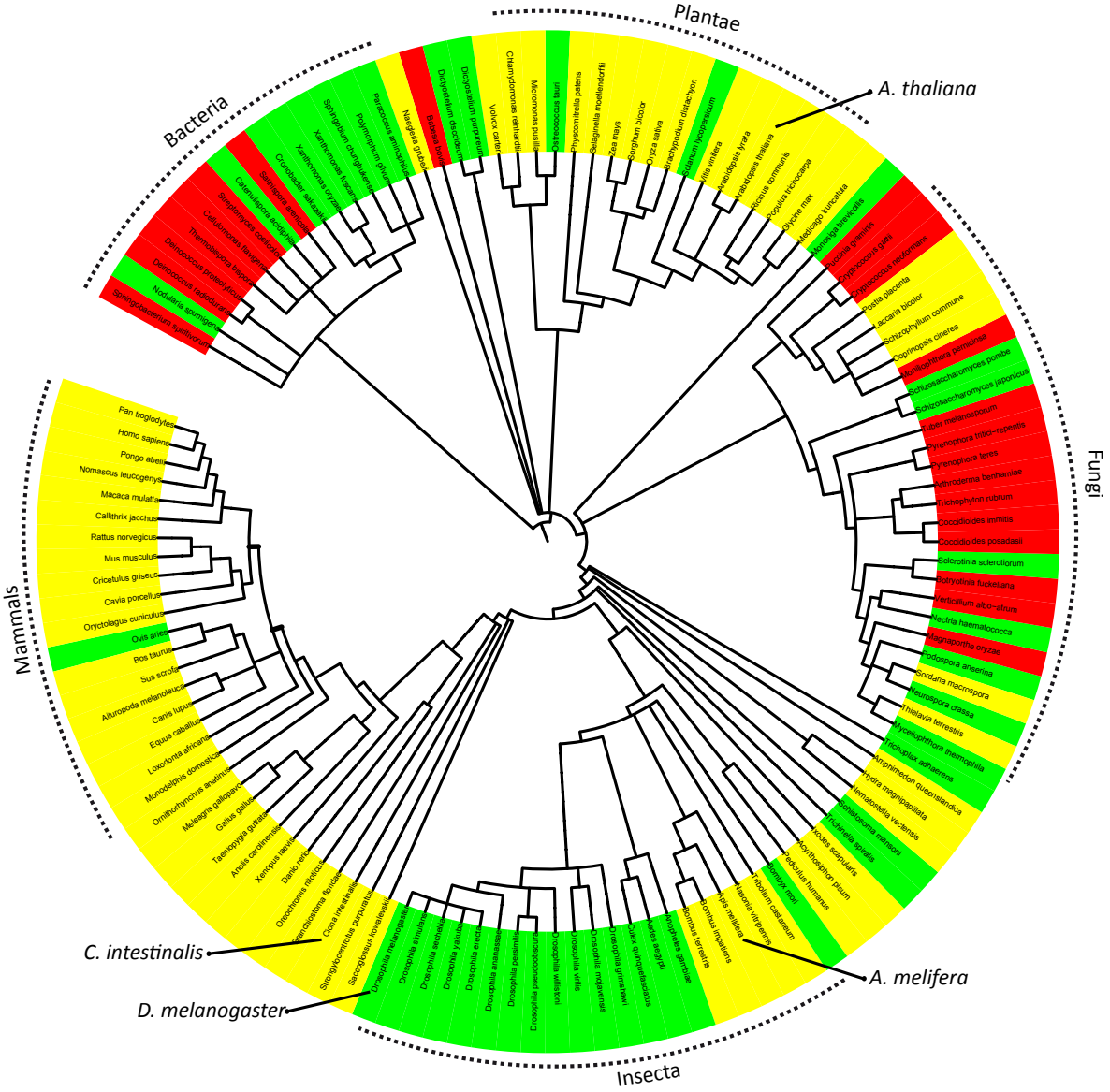

Figure 8: Phylogenetic Tree of Life for Dnmts and Uhrf proteins

Tree of life (Letunic and Bork, 2007; 2011) annotated with Dnmts (Dnmt1, Dnmt2, Dnmt3a and Dnmt3b) and the SRA superfamily. Note that the SRA domain is unique for Uhrf protein. Organism containing Dnmts are coloured in green, organism containing the SRA superfamily in red and those having both are coloured in yellow.

Recently, DNA methylation analyses revealed that the honeybee genome contains very low levels of CHG or CHH methylation and only ~1 % CG methylation (Feng et al., 2010). In addition to vertebrates, Uhrf and Dnmt homologues can also be found in *Ciona intestinalis*, a primitive chordate that is distantly related to vertebrates (Dehal et al., 2002). DNA methylation in *C. intestinalis* is nearly exclusively in CG context

and increases sharply in the body of protein-coding genes (Feng et al., 2010). Taken together, Uhrf homologues are mostly found in species with detectable DNA methylation and Dnmt homologues, suggesting a conserved role of UHRF proteins in eukaryotic methylation.

1.3.2 Structure and Function of Uhrf Proteins

The Uhrf family of proteins, comprising the multi-domain proteins Uhrf1 and Uhrf1, harbour an ubiquitin-like domain (Ubl), a tandem Tudor domain, a plant homeo domain (PHD), a SET-and-RING associated domain and a RING domain (Figure 9). In contrast, the Uhrf1 homologues in *Arabidopsis thaliana*, VIM1-3, are lacking the Ubl domain and carry a RING finger domain between the PHD and SRA domain (Bronner et al., 2007).

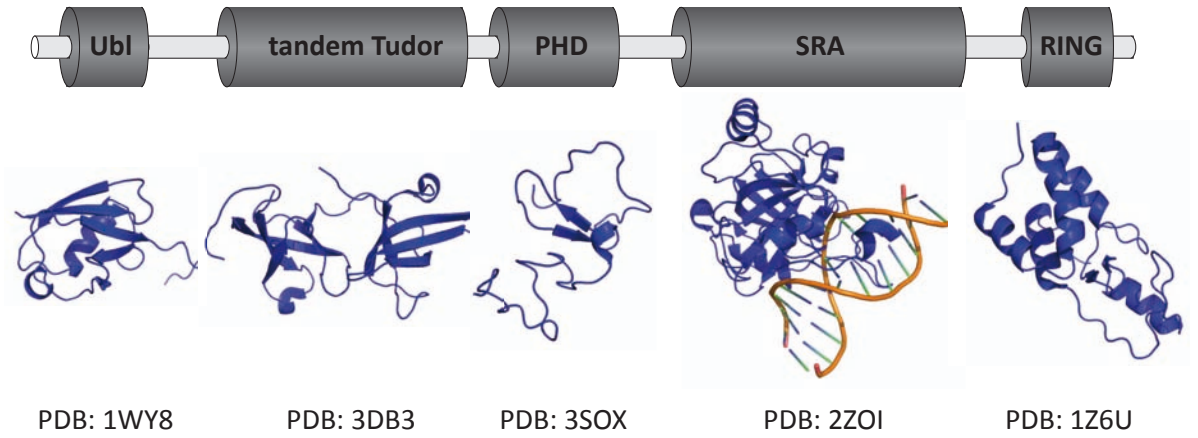

Figure 9: Multi-domain proteins Uhrf1 and Uhrf2

Schematic outline of the multi-domain architecture of Uhrf1 and Uhrf2. An N-terminal ubiquitin-like domain (Ubl; PDB code 1WY8) is followed by a tandem Tudor domain (TTD; PDB ID code 3DB3)), a plant homeo domain (PHD; PDB ID code: 3SOCX), a SET and RING associated (SRA; PDB ID code: 2ZKE) domain and a C-terminal really interesting new gene (RING; PDB ID code: 1Z6U) domain. The figure is adapted from (Hashimoto et al., 2009).

Studies revealed a co-localization of Uhrf1 with PCNA during S phase (Uemura et al., 2000), indicating a function of Uhrf1 in cell cycle progression, DNA replication (Fujimori et al., 1998) and DNA damage repair (Muto et al., 2002). The expression of Uhrf1 is essential for entry from G_1/G_0 phase into S phase in NIH-3T3 cells (Bonapace, 2002), but not in ESCs (Muto et al., 2002). Uhrf1 binds preferentially to histone H3 and displays E3 ubiquitin ligase activity for histone H3 (Citterio et al., 2004). Moreover, Uhrf1 has been shown to be involved in large scale reorganization of chromocenters (Papait et

al., 2007). It has been shown to bind to methylated DNA (Unoki et al., 2004) and to the methylated promoter of RB1 (Jeanblanc et al., 2005). In addition, Uhrf1 interacts with Dnmt3a and Dnmt3b and with histone modifying enzymes like HDAC1, G9a and Tip60 (Achour et al., 2009; Kim et al., 2009; Meilinger et al., 2009; Unoki et al., 2004). Uhrf1 binds hemimethylated DNA via a SET and RING associated (SRA) domain and likely targets Dnmt1 to its substrate of maintenance DNA methylation (Arita et al., 2008; Avvakumov et al., 2008; Bostick et al., 2007; Hashimoto et al., 2008; Sharif et al., 2007; Qian et al., 2008). In vertebrates, the SRA domain has only been observed in this family, demonstrating its unique function for the Uhrf family. However, the SRA domain is also present in histone methyltransferases in *A. thaliana* such as SUVH1 and SUVH2 (Bronner et al., 2007) and has been shown to be involved in directing DNA methylation to target sequences (Naumann et al., 2005). The second member of the Uhrf family, Uhrf2, harbours similar domains (Bronner et al., 2007). Until now, the only known function of Uhrf2 is a role in intranuclear degradation of polyglutamine aggregates (Iwata et al., 2009) and in cell cycle arrest (Mori et al., 2011).

Strikingly, genetic ablation of *uhrf1* leads to remarkable genomic hypomethylation, similar to the genetic ablation of *dnmt1* in ESCs (Bostick et al., 2007; Sharif et al., 2007) and *uhrf1*$^{-/-}$ null mice died in midgestation (Muto et al., 2002). Additional studies in tissue cultures cells demonstrate that Uhrf1 depletion causes cell cycle arrest (Bonapace, 2002; Jenkins et al., 2005; Tien et al., 2011), hypersensitivity to DNA damage and chemotherapeutic agents (Muto et al., 2002; Arima et al., 2004), or apoptosis (Abbady et al., 2003; Tien et al., 2011). Moreover, zebra fish mutants in *uhrf1*, and also *dnmt1*, have defects in lens development and maintenance and lens epithelial cells lacking *uhrf1* have altered gene expression and reduced proliferation (Tittle et al., 2011). Conversely, high levels of Uhrf1 are found in a number of human cancer cell lines (Mousli et al., 2003; Jenkins et al., 2005) and primary tumours (Hopfner et al., 2000; Crnogorac-Jurcevic et al., 2005). In some cells, overexpression of Uhrf1 increases cell-proliferation (Hopfner et al., 2002; Jenkins et al., 2005). The loss of the *UHRF2* gene was found at statistically significant levels in diverse tumours in the Oncomine database and a recurrent micro deletion at 9p24 targeting *UHRF2* was observed in small lung carcinoma (Mori et al., 2011). In contrast to Uhrf1, overexpression of Uhrf2 induced an increase in G_1 phase cells, cell cycle regulation by Uhrf2 appears to be executed through the mechanism regulating Cdk2 activity (Li et al., 2004).

1.3.3 Regulation of Uhrf Proteins

Despite the emerging understanding how and where Uhrf proteins function, little is known how they are regulated. Basically, Uhrf proteins can be regulated at the transcriptional level and recent studies revealed regulation by post-translational modifications (reviewed in Qin et al., 2011b).
The dynamic expression pattern of *uhrf1* mRNA during embryonic development (Sadler et al., 2007; Tittle et al., 2011) points to transcriptional control as a regulatory mechanism (Chu et al., 2011). Changes in *uhrf1* mRNA (Sadler et al., 2007), protein (Bonapace, 2002; Arima et al., 2004; Kim et al., 2009) and localization (Uemura et al., 2000; Miura et al., 2001; Kim et al., 2009) occur during different phases of the cell cycle. Also, both mRNA and protein levels of Uhrf1 are downregulated in response to DNA damage in human tumor cell lines controlled by p53/p21^{Cip1} (Arima et al., 2004). Notably, in cancer cells the level of Uhrf1 does not change dramatically during the cell cycle and the expression is continuously at a high level (Mousli et al., 2003; Arima et al., 2004; Bronner et al., 2007). In addition to regulation by p53/p21^{Cip1}, Uhrf1 expression is controlled by cell cycle regulators such as the Rb/E2f complex (Abbady et al., 2003) and the E1a transcription factor (Bonapace, 2002). As mentioned before, overexpression of Uhrf1 increases cell-proliferation (Hopfner et al., 2002; Jenkins et al., 2005) and the S and G_2/M phase cell fractions of serum-starved lung fibroblasts (Jeanblanc et al., 2005). Contrary to Uhrf1, overexpression of Uhrf2 induced an increase in G_1 phase cells and Uhrf2 is regulated by Cdk2 (Li et al., 2004), pointing to a role in G_1/S transition. Uhrf2 expression is growth dependent in normal fibroblasts, whereas in serum-starved cancerous cells the expression is consistently high (Mori et al., 2002). Notably, Uhrf2 was shown to interact with some cell cycle proteins including cyclins (A2, B1, D1 and E1), p53 and Rb and ubiquitinates cyclins D1 and E1 (Mori et al., 2011).
In addition to the regulation on the transcription level, recent studies demonstrated the regulation of Uhrf1 by post-translational modifications. Recently, the auto-ubiquitination of Uhrf1 has been demonstrated (Qin et al., 2011a) that is most likely mediated by the RING finder domain, which was also shown to ubiquitinate histone H3 (Citterio et al., 2004). Moreover, Uhrf1 interacts with the deubiquitinase Usp7 (Qin et al., 2011a; Felle et al., 2011). Usp7 was shown to interact and deubiquitinate Dnmt1, which leads to an increased protein stability of Dnmt1 and protects it from proteolytic degradation (Qin et al., 2011a; Du et al., 2010). In addition, Uhrf1 is phosphorylated in the region between the SRA and RING domain by Cdk2. Uhrf1 phosphorylation is required for gastrulation in zebra fish and phosphorylated Uhrf1 can be detected in human cancer cells and in non-transformed zebra fish cells (Chu et al., 2011). So far, these post-translational modifications have not been tested for Uhrf2.

2 Aims of this work

The role of Dnmt1 in maintenance DNA methylation and its role in the epigenetic network, controlling gene expression and genome stability during development, is well established. In the last decades, many protein interactions and post-translational modifications of Dnmt1 have been reported. These data clearly demonstrate that Dnmt1, and by extension also DNA methylation in general, are functionally linked with several other epigenetic pathways and cellular processes. General themes of these interactions and modifications include the activation, stabilization and recruitment of Dnmt1 at specific sites and heterochromatin regions. However, the molecular mechanisms that ultimately control DNA methylation still remain elusive.

During this thesis, I focus on the Dnmt1-interacting proteins Uhrf1 and Uhrf2 and develop methods to study the functional characteristics of these factors and their role in maintaining DNA methylation. At first I aimed at elucidating the histone-tail peptide binding specificities of Uhrf1, an essential co-factor for maintaining DNA methylation. Uhrf1 interacts with Dnmt1 and harbours several functional domains including DNA and putative histone binding domains. Although Uhrf1 has been reported to bind to histones, nothing is known about its histone-tail peptide binding specificities. To address this question, I developed an *in vitro* histone-tail peptide binding assay (Chapter 3.1) and I expanded the assay to 96-well micro plates (Chapter 3.2). This versatile high-throughput assay allows for determining the *in vitro* binding specificities of GFP-fusion proteins to histone-tail peptides, DNA substrates and RFP-fusions. Moreover, it allows for measuring DNA binding specificity in dependence on histone binding and *vice versa*. Using this assay, I measured the histone-tail binding specificities of Uhrf1 and identified highly conserved amino acid residues responsible for its specificity (Chapter 3.3).

Interestingly, a second member of the Uhrf family, Uhrf2, harbours similar domains. However, until now, the only known function of Uhrf2 is a role in intranuclear degradation of polyglutamine aggregates. To investigate the function of Uhrf2 in DNA methylation, I tested the *in vitro* binding specificities of Uhrf2, various single domains, hybrids and point mutants. Moreover, I tested the crosstalk between different repressive epigenetic marks such as methylated DNA and H3K9me3 (Chapter 3.4).

For a comprehensive understanding of the regulation of DNA methylation it is necessary to systematically quantify the interactions and modifications of Dnmt1, to elucidate their function at the molecular level and to integrate these data at the cellular level. To quantify the interactions of Dnmt1 over the cell cycle, I used a combination of SILAC and mass spectrometry. At the beginning of this project, I initially tested different Dnmt1 binding proteins and optimized the synchronization protocol (Chapter 3.6).

3 Results

3.1 Fluorescent protein specific Nanotraps to study protein-protein interactions and histone tail peptide binding

Fluorescent protein specific Nanotraps to study protein-protein interactions and histone-tail peptide binding

Garwin Pichler[1] , Heinrich Leonhardt[1], Ulrich Rothbauer[1,2]

[1] CIPS, Center for Integrated Protein Science at the Department of Biology II, Ludwig Maximilians University Munich, Grosshaderner Str 2, 82152 Planegg-Martinsried, Germany

[2] ChromoTek GmbH, Grosshaderner Str. 2, 82152 Planegg-Martinsried, Germany

pichler@bio.lmu.de

H.Leonhardt@lmu.de

U.Rothbauer@chromotek.com

Running title: Nanotraps: Connecting Cell Biology with Biochemistry

corresponding author:

Dr. Ulrich Rothbauer

LMU-Biocenter

Grosshaderner Str. 2

82152 Planegg-Martinsried

phone +49 89 2180 74 287

fax: +49 89 2180 74 236

u.rothbauer@chromotek.com

Summary

Fluorescent proteins are widely used to study protein localization and protein dynamics in living cells. Additional information on peptide binding, DNA binding, enzymatic activity and complex formation can be obtained with various methods including chromatin immunoprecipitation (ChIP) and affinity purification. Here we describe two specific GFP- and RFP binding proteins based on antibody fragments derived from llama single chain antibodies. The binding proteins can be produced in bacteria and coupled to monovalent matrixes generating so called Nanotraps. Both Traps allow a fast and efficient (one-step) isolation of fluorescent fusion proteins and their interacting factors for biochemical analyses including mass spectroscopy and enzyme activity measurements. Here we provide protocols for precipitation of fluorescent fusion proteins from crude cell extracts to identify and map protein-protein interactions as well as specific histone tail peptide binding in an easy and reliable manner.

Key words:

green fluorescent protein (GFP), red fluorescent protein (RFP), immunoprecipitation, mass spectrometry, peptide binding, protein-interactions

Introduction

Fluorescent proteins (FP) are widely used to study protein localization and dynamics in living cells (***1, 2***). The validation and interpretation of these data, however, require additional information on biochemical properties of the investigated fluorescent fusion proteins e.g. enzymatic activity, DNA binding and interaction with other cellular components. For these biochemical analyses proteins are mostly fused with a small epitope tag (e.g. Histidine-tag, c-Myc, FLAG or hemaglutinin). Monomeric derivates of the green fluorescent protein (GFP) and the red fluorescent protein (RFP) are the most widely used labelling tags in cell biology but are rarely used for biochemical analyses although various mono- and polyclonal antibodies are available (***3, 4***) (Abcam, Cambridge, UK; Sigma, St. Louis, USA.; Roche, Mannheim, Germany, ChromoTek, Martinsried, Germany).

We recently generated specific GFP- and RFP binding proteins (GFP-Trap, RFP-Trap) based on single domain antibodies derived from *Lama alpaca* (***5***). Those binding proteins are characterized by a small barrel shaped structure (~ 13 kDa, 2.5 nm X 4.5 nm) and very high stability (stable up to 70°C, functional in 2 M NaCl or 0.5% SDS). From detailed *in vitro* binding analysis we determined that one molecule of the GFP- or RFP-Trap binds one molecule GFP or RFP respectively in stable stoichiometric complexes. The dissociation constants (K_D) of both binding molecules are in the sub-nanomolar range comparable to conventional antibodies. Our binding analysis showed that the GFP-Trap exclusively binds to wtGFP, eGFP and GFP^{S65T} as well as to YFP and eYFP while no binding to red fluorescent proteins derived from DsRed was detectable. Those red fluorescent protein derivates including mRFP, mCherry or mOrange are recognized exclusively by the RFP-Trap without any crossreaction to GFP derivates.

Here we demonstrate the application of both FP-Traps to investigate interacting factors as well as histone-tail peptide binding of fluorescent fusion proteins. For immunoprecipitations of FP fusion proteins we coupled the GFP- or RFP-binding proteins covalently to monovalent matrices (e.g. agarose beads or magnetic particles).

A direct comparison of the FP-Trap with conventional antibodies for immunoprecipitation of FP from crude cell lysates reveal that the FP-Traps allow a very fast (~ 5 – 30 min) depletion of fluorescent fusion proteins from tested samples, which cannot be achieved with conventional antibodies even after 12 h of incubation. Moreover, after precipitation with the FP-Traps only the antigen (FP) was detectable on a coomassie gel whereas the typical antibody fragments (light chain, 25 kDa; heavy chain, 50 kDa) could be detected in the bound fraction after precipitation with conventional mono- and polyclonal antibodies (***5***).

The lack of unspecific binding or contaminating antibody fragments is one major advantage of the FP-Traps, because unspecific protein fragments in the bound fraction often interfere with subsequent mass spectrometry analysis of interacting complex partners. For the FP-Traps we demonstrated that they are versatile tools to purify FP-fusions and their interacting factors for biochemical studies including mass spectrometry and enzyme activity assays (***6-9***). Moreover, the FP-Traps are also suitable for chromatin immunoprecipitations (ChIPs) (***5, 10, 11***) in cells expressing fluorescent DNA binding proteins. In conclusion the protocol below can be used to perform immunoprecipitation of fluorescent fusion proteins from crude cell extracts to identify and map protein-protein interactions as well as specific peptide binding in an easy and reliable manner.

2. Materials

Prepare all solutions using ultrapure water (prepared by purifying deionized water to attain a resistance of 18 MΩ cm at 25°C) and analytical grade reagents. Prepare and store all reagents at room temperature (unless indicated otherwise). Ready to use buffers once prepared should be stored at 4°C. Diligently follow all applicable waste disposal regulations when disposing waste materials.

2.1. Immunoprecipiation of FP

Phosphate buffer saline (PBS): 137 mM NaCl, 2.7 mM KCl, 10 mM Na_2HPO_4, 2 mM KH_2PO_4, pH 7.4

Cell Lysis Buffer: 10 mM Tris-HCl pH 7.5, 150 mM NaCl, 0.5 mM EDTA, 0.5% Non-Ident 40 (NP 40), 1 mM PMSF, Protease Inhibitor cocktail (e.g. provided by Roche, Mannheim, Germany).

optional for nuclear proteins / chromatin proteins: DNaseI (f.c) 1 µg/ µl, 2.5 mM $MgCl_2$

RIPA Buffer: 10 mM Tris-HCl pH 7.5, 150 mM NaCl, 5 mM EDTA, 0.1 % SDS, 1% Triton X-100, 1% Deoxycholate, 1 mM PMSF, Protease Inhibitor cocktail (e.g. provided by Roche, Mannheim, Germany)

Dilution Buffer: 10 mM Tris-HCl pH 7.5, 150 mM NaCl, 0.5 mM EDTA, 1 mM PMSF, Protease Inhibitor cocktail (e.g. provided by Roche, Mannheim, Germany)

Wash Buffer 1: 10 mM Tris-HCl pH 7.5, 150 mM NaCl, 0.5 mM EDTA, 1 mM PMSF, Protease Inhibitor cocktail (e.g. provided by Roche, Mannheim, Germany)

Wash Buffer 2: 10 mM Tris-HCl pH 7.5, 0.5 M NaCl, 0.5 mM EDTA, 1 mM PMSF, Protease Inhibitor cocktail (e.g. provided by Roche, Mannheim, Germany)

Elution Buffer: 0.2 M glycine-HCl pH 2.5

Neutralization Buffer: 1 M Tris-base (pH 10.4)

SDS-PAGE Sample Buffer (3x): 150 mM Tris-HCl pH 6.8, 300 mM DTT, 6% SDS, 0.3% Bromphenol blue, 30% Glycerol

Coomassie Solution: 50% Methanol, 40% H_2O, 10% acetic acid, 0.25% Coomassie Blue R-250

FP-Trap

gta-20 (agarose coupled), gtm-20 (magnetic particles) (ChromoTek, Martinsried, Germany)

rta-20 (agarose coupled), rtm-20 (magnetic particles) (ChromoTek, Martinsried, Germany)

Nanotraps based on specific binding proteins as provided by ChromoTek are most consistently effective; however, Nanotraps can be generated and used from other sources.

2.2. Histone-tail peptide binding assay

Dilution Buffer: 10 mM Tris-HCl pH 7.5, 150 mM NaCl, 0.5 mM EDTA, 1 mM PMSF, Protease Inhibitor cocktail (e.g. provided by Roche, Mannheim, Germany)

Wash Buffer 3: 10 mM Tris-HCl pH 7.5, 300 mM NaCl, 0.5 mM EDTA, 1 mM PMSF, Protease Inhibitor cocktail (e.g. provided by Roche, Mannheim, Germany)

Histone-tail peptides

All histone-tail peptides are C-terminal labeled with fluorescent carboxytetramethylrhodamine succininmidyl ester (TAMRA) or Biotin. Absorptions- and emission wavelengths of TAMRA are 544 nm and 570 nm, respectively.

H3(1-20)K9me3-TAMRA, H3(1-20)K9me3-Biotin, H3(1-20)K9ac-Biotin were purchased from Peptide Specialty Laboratories (PSL, Heidelberg, Germany)

Microplate 96-well (e.g. Greiner Bio-One GmbH, Frickenhausen, Germany)

2.3. Evaluation of binding ratios

Microplate reader (e.g. Tecan Infinite M1000 (TECAN, Männedorf, Switzerland)

3. Methods

Carry out all procedures at 4°C unless otherwise specified.

3.1. Immunoprecipitation of FP

The following step by step immunoprecipitation protocol is based on about 1 x 10^7 cells (HEK293T or HeLa) transiently transfected with expression vectors coding for fluorescent fusion proteins of interest. The transfection efficiency should be in the range of 60-90% determined by fluorescence microscopy.

1. Wash the cells 2 times with 5 mL of PBS on ice. Scrape cells off. Transfer cells to a tube and centrifuge at 800 g and 4°C for 3 min.

2. Wash cells with 1 mL of PBS and centrifuge again (*see* **Subheading 3.1., item 1**).

3. Resuspend cell pellet in 200 µL of Cell Lysis Buffer (*see* **Note 1**).

4. For lysis incubate cells on ice for 30 min. Resuspend cells every 10 min by gently pipetting.

5. Clear lysate by centrifugation at 20,000 g and 4°C for 10 min (*see* **Note 2**).

6. Adjust volume to 500 µL with Dilution Buffer (*see* **Note 3**).

7. Take an aliquot which corresponds to 5% to 10% of your diluted sample (referred to as input fraction (IP)) and add SDS-PAGE sample buffer.

8. Add 20 µL to 40 µL of GFP-Trap or RFP-Trap (gta-20, gtm-20 or rta-20, rtm-20) and incubate for 10 min to 2 h at 4°C with constant mixing. Binding reaction can also be performed on a micro column (*see* **notes 4 and 5**).

9. Harvest immunocomplexes bound to the monovalent matrix by centrifugation for 2 min at 5,000 g and 4°C or magnetic separation using a specially designed rack (e.g. from Chemicell, Berlin, Germany).

10. Collect an aliquot of the supernatant or flow through (referred to as non-bound fraction (NB)) and add SDS-PAGE sample buffer.

11. Wash beads with 1 mL of Wash Buffer 1.

12. Repeat washing step with 1 mL of Wash Buffer 2 (see ***Note*** **6**).

13. Resuspend beads in 50 to 100 µL of SDS-PAGE sample buffer (referred to as bound (B)).

14. Elute proteins by boiling at 95°C for 10 min (*see* **Note 7**).

15. For immunoblot analysis subject 1% of input and e.g. 20% of bound fractions to SDS-PAGE. Transfer to a nitrocellulose or PVDF membrane.

16. Detect precipitated GFP- or RFP-fusion proteins with an anti-GFP or anti-RFP antibody (e.g. from Roche, Mannheim, Germany, ChromoTek, Martinsried, Germany) and interacting proteins with the respective antibodies.

3.2. Histone-tail peptide binding assay

The following step-by-step histone-tail peptide binding protocol for FP-fusions continues after the washing step of the immunoprecipitation with the FP-Traps (*see* **Subheading 3.1, item 11**).

1. Equilibrate beads with 1 ml of Dilution Buffer.

2. Add TAMRA-labeled histone-tail peptide to a final concentration of 0.15 µM (*see* **Note 8**).

3. Incubate for 15 min at room temperature with constant mixing (*see* **Note 9**).

4. Harvest beads by centrifugation for 2 min at 5,000g and 4°C.

5. Wash beads 2 times with 1 mL of Wash Buffer 3 (*see* **Note 9**).

6. Resuspend beads in 100 µL of Dilution Buffer.

7. Transfer beads in a 96-well plate.

3.3. Evaluation of binding ratios

For quantification, fluorescence intensity measurements are adjusted using standard curves from labelled probes with known concentrations. Fluorescence intensities (FI) were measured with a microplate reader Tecan Infinite M1000 (TECAN, Männedorf, Switzerland) (***12***). Following settings were used:

- GFP: 490±10 nm and 511±10 nm
- TAMRA: 560±5 nm and 586±5 nm

1. Measure fluorescence intensities (*see* **Note 10**).
2. Calculate GFP- and TAMRA concentration using standard curves (*see* **Note 10**).

3. Calculate relative binding ratio histone-tail peptide/protein.

4. Notes

1. The given example of buffer recipes can be modified according to the experimental needs. One can use different buffer recipes (e.g. phosphate buffered saline or HEPES) comprising higher salt concentrations or containing DNase I (AppliChem, Darmstadt, Germany) or MNase S7 (Roche, Mannheim, Germany) to release chromatin proteins or RIPA buffer to release chromatin or membrane bound fluorescent fusion proteins.

2. The centrifugation step to clarify the lysate can be shortened up the 2 to 5 min for highly soluble proteins. Such proteins will be transferred to the supernatant after 2 to 5 min of centrifugation.

3. If necessary the protein sample can be diluted in larger volumes. Accordingly, one should elongate the incubation time with the FP-Traps up to 12 h over night incubation at 4°C. Alternatively, one can increase the amount of GFP- or RFP-Trap in the pulldown reaction.

4. In some case it was observed that N-terminal GFP-tagged proteins were better recognized as C-terminal tagged ones. If that is the case you can achieve a comparable efficiency with a prolonged incubation time.

5. As an alternative to batch purification the pulldown reaction can be carried out on columns like micro columns (e.g. 1 mL column, MoBiTec GmbH, Göttingen, Germany).

6. Depending on the nature of the protein complexes one can increase the salt concentration (e.g. up to 500 mM NaCl to get rid of unspecific binding). Alternatively if transient interactoms characterized by hydrophilic interactions have to be analyzed one can lower the salt concentration in the Wash Buffer 2.

7. The interaction between the FP-Traps and the fluorescent epitope can be released by acidic elution. It is recommended to elute bound proteins by adding 100 µL of 0.2 M glycine-HCL pH 2.5 for 1 min. Acidic eluate should be immediately neutralized by adding

5 to 10 µL of 1 M Tris-base (pH 10.4).

8. As an alternative to TAMRA conjugates one can use every fluorescent label whose specific fluorescence characteristics do not interfere with GFP or RFP.

9. Depending on the nature of the protein and the histone-tail peptide one can vary the incubation time, temperature and salt concentrations for washing. In this case best results were observed at room temperature for 15 min and washing with 300 mM NaCl.

10. Calibration curves for the fluorescent DNA substrates and proteins were determined by measuring the fluorescence signal of known concentrations of the TAMRA-coupled histone-tail peptides and purified GFP and calculated by linear regression.

Acknowledgements

This work was supported by the GO-Bio Program of the BMBF (Federal Ministry of Science, Germany) and the Deutsche Forschungsgemeinschaft (SFB 646).

5. References

1. Baird, G. S., Zacharias, D. A., and Tsien, R. Y. (2000) Biochemistry, mutagenesis, and oligomerization of DsRed, a red fluorescent protein from coral, Proc Natl Acad Sci U S A 97, 11984-11989.

2. Campbell, R. E., Tour, O., Palmer, A. E., Steinbach, P. A., Baird, G. S., Zacharias, D. A., and Tsien, R. Y. (2002) A monomeric red fluorescent protein, Proc Natl Acad Sci U S A 99, 7877-7882.

3. Cristea, I. M., Williams, R., Chait, B. T., and Rout, M. P. (2005) Fluorescent proteins as proteomic probes, Mol Cell Proteomics 4, 1933-1941.

4. Rottach, A., Kremmer, E., Nowak, D., Leonhardt, H., and Cardoso, M. C. (2008) Generation and characterization of a rat monoclonal antibody specific for multiple red fluorescent proteins, Hybridoma (Larchmt) 27, 337-343.

5. Rothbauer, U., Zolghadr, K., Muyldermans, S., Schepers, A., Cardoso, M. C., and Leonhardt, H. (2008) A versatile nanotrap for biochemical and functional studies with fluorescent fusion proteins, Mol Cell Proteomics 7, 282-289.

6. Trinkle-Mulcahy, L., Boulon, S., Lam, Y. W., Urcia, R., Boisvert, F. M., Vandermoere, F., Morrice, N. A., Swift, S., Rothbauer, U., Leonhardt, H., and Lamond, A. (2008) Identifying specific protein interaction partners using quantitative mass spectrometry and bead proteomes, J Cell Biol 183, 223-239.

7. Agarwal, N., Hardt, T., Brero, A., Nowak, D., Rothbauer, U., Becker, A., Leonhardt, H., and Cardoso, M. C. (2007) MeCP2 interacts with HP1 and modulates its heterochromatin association during myogenic differentiation, Nucleic Acids Res 35, 5402-5408.

8. Schermelleh, L., Haemmer, A., Spada, F., Rosing, N., Meilinger, D., Rothbauer, U., Cristina Cardoso, M., and Leonhardt, H. (2007) Dynamics of Dnmt1 interaction with the replication machinery and its role in postreplicative maintenance of DNA methylation, Nucleic acids research.

9. Frauer, C., and Leonhardt, H. (2009) A versatile non-radioactive assay for DNA methyltransferase activity and DNA binding, Nucleic Acids Res.

10. Bergbauer, M., Kalla, M., Schmeinck, A., Gobel, C., Rothbauer, U., Eck, S., Benet-Pages, A., Strom, T. M., and Hammerschmidt, W. (2010) CpG-methylation regulates a class of Epstein-Barr virus promoters, PLoS Pathog 6.

11. Munoz, I. M., Hain, K., Declais, A. C., Gardiner, M., Toh, G. W., Sanchez-Pulido, L., Heuckmann, J. M., Toth, R., Macartney, T., Eppink, B., Kanaar, R., Ponting, C. P., Lilley, D. M., and Rouse, J. (2009) Coordination of structure-specific nucleases by human SLX4/BTBD12 is required for DNA repair, Mol Cell 35, 116-127.

12. Rottach, A., Frauer, C., Pichler, G., Bonapace, I. M., Spada, F., and Leonhardt, H. (2010) The multi-domain protein Np95 connects DNA methylation and histone modification, Nucleic Acids Res 38, 1796-1804.

Figure legends

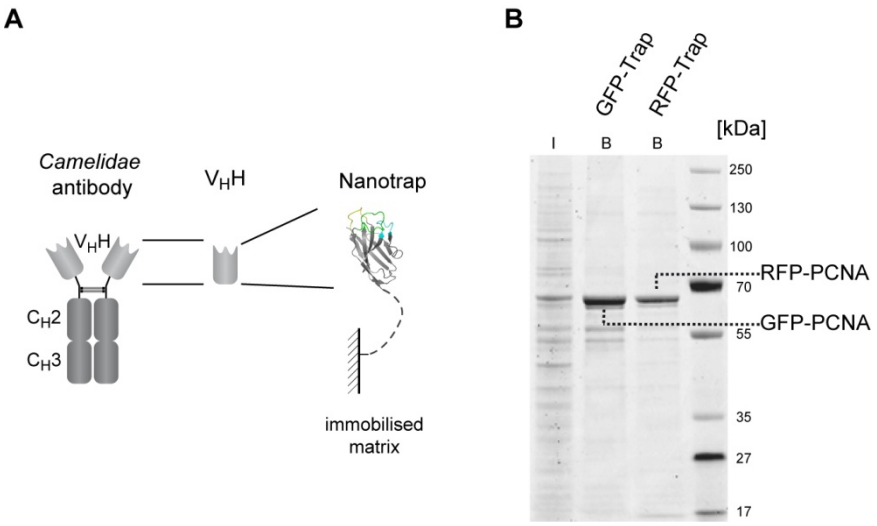

Figure 1 Immunoprecipiation of fluorescent fusion proteins (FP). (**A**) Schematic drawing of Nanotrap derived from *Camelidae* antibody. (**B**) Immunoprecipation of GFP- or RFP-PCNA with the GFP- or RFP-Trap. 1% of input and 20% of bound fractions were subjected to a SDS PAGE and detected by coomassie staining. The molecular size of the proteins (kDa) is indicated.

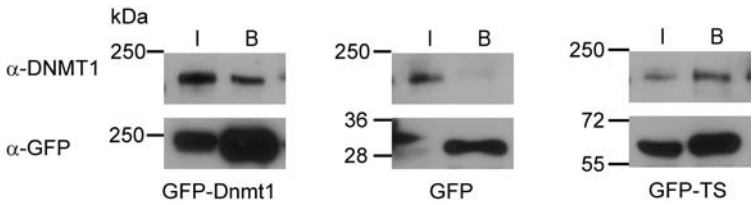

Figure 2 Immunoblots after co-immunoprecipitations illustrate the interaction between GFP-Dnmt1 and endogenous DNMT1, whereas precipitation of GFP alone was used as negative control. 1% of input and 30% of bound fractions were subjected to immunoblot analysis. The molecular size of the proteins (kDa) and the antibodies used are indicated. Mapping the Dnmt1 dimerization region to the TS domain of Dnmt1: Immunoblot after co-immunoprecipitation showing that the N-terminal TS domain of Dnmt1 can co-precipitate endogenous DNMT1 (Data taken from *Dimerization of DNA methyltransferase 1 is mediated by its regulatory domain, Fellinger et al., J. Cell. Biochem. Vol 106(4) p.521-28, Copyright 2009© Wiley-Blackwell*)

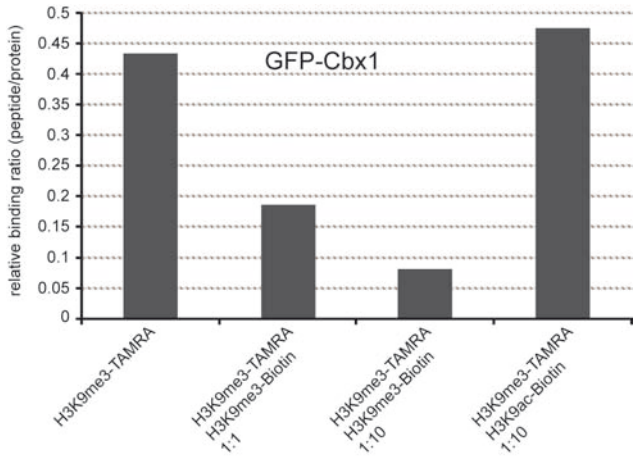

Figure 3. Histone-tail binding properties of mouse Cbx1 (Drosophila HP1 beta). GFP-Cbx1 was purified with the GFP-Trap and incubated with TAMRA-labeled H3(1-20)K9me3 histone-tail peptide in competition with either biotinylated H3K9me3 or H3K9ac in different molar ratios.

3.2 Versatile Toolbox for High-Throughput Biochemical and Functional Studies with Fluorescent Fusion Proteins

OPEN ACCESS Freely available online

PLoS one

Versatile Toolbox for High Throughput Biochemical and Functional Studies with Fluorescent Fusion Proteins

Garwin Pichler[1]*, Antonia Jack[2], Patricia Wolf[1], Sandra B. Hake[2]

1 Department of Biology II and Center for Integrated Protein Science Munich (CIPSM), Ludwig Maximilians University Munich, Planegg-Martinsried, Munich, Germany, **2** Center for Integrated Protein Science Munich at the Adolf-Butenandt Institute, Department of Molecular Biology, Ludwig Maximilians University of Munich, Munich, Germany

Abstract

Fluorescent fusion proteins are widely used to study protein localization and interaction dynamics in living cells. However, to fully characterize proteins and to understand their function it is crucial to determine biochemical characteristics such as enzymatic activity and binding specificity. Here we demonstrate an easy, reliable and versatile medium/high-throughput method to study biochemical and functional characteristics of fluorescent fusion proteins. Using a new system based on 96-well micro plates comprising an immobilized GFP-binding protein (GFP-mulitTrap), we performed fast and efficient one-step purification of different GFP- and YFP-fusion proteins from crude cell lysate. After immobilization we determined highly reproducible binding ratios of cellular expressed GFP-fusion proteins to histone-tail peptides, DNA or selected RFP-fusion proteins. In particular, we found Cbx1 preferentially binding to di-and trimethylated H3K9 that is abolished by phosphorylation of the adjacent serine. DNA binding assays showed, that the MBD domain of MeCP2 discriminates between fully methylated over unmethylated DNA and protein-protein interactions studies demonstrate, that the PBD domain of Dnmt1 is essential for binding to PCNA. Moreover, using an ELISA-based approach, we detected endogenous PCNA and histone H3 bound at GFP-fusions. In addition, we quantified the level of H3K4me2 on nucleosomes containing different histone variants. In summary, we present an innovative medium/high-throughput approach to analyse binding specificities of fluroescently labeled fusion proteins and to detect endogenous interacting factors in a fast and reliable manner *in vitro*.

Citation: Pichler G, Jack A, Wolf P, Hake SB (2012) Versatile Toolbox for High Throughput Biochemical and Functional Studies with Fluorescent Fusion Proteins. PLoS ONE 7(5): e36967. doi:10.1371/journal.pone.0036967

Editor: Pierre-Antoine Defossez, Université Paris-Diderot, France

Received January 12, 2012; **Accepted** April 10, 2012; **Published** May 11, 2012

Funding: GP was supported by the International Doctorate Program NanoBioTechnology (IDK-NBT, http://www.cens.de/doctorate-program/) and GP and AJ by the International Max Planck Research School for Molecular and Cellular Life Sciences (IMPRS-LS, https://www.imprs-ls.de/). PW is a fellow of the Graduate School Life Science Munich (LSM, http://www.lsm.bio.lmu.de/). SBH was supported by CIPSM (http://www.cipsm.de/en/index.html) and the DFG (http://www.dfg.de/index.jsp). The funders had no role in study design, data collection and analysis, decision to publish, or preparation of the manuscript.

Competing Interests: The authors have declared that no competing interests exist.

* E-mail: pichler@bio.lmu.de

Introduction

Over the past decade a variety of proteomic approaches have been used to identify cellular components in order to understand the mechanism and inner workings of cells [1]. For example, mass spectrometry-based proteomics uncovered the proteome of many different organisms as well as cell-type specific differences in protein expression. However, to understand and characterize the function of single proteins, as well as the interplay between different factors, it is essential to gain further insights into their abundance, localization, dynamic interactions and substrate specificities.

Fluorescent proteins like the green fluorescent proteins (GFP) [2] and spectral variants have become popular tools to study the localization and dynamic interactions of proteins *in vivo*. Despite, the availability of a variety of commercial mono- and polyclonal antibodies against GFP and other fluorescent proteins [3,4] (e.g. Abcam, UK; Sigma, USA; Roche, Germany, ChromoTek, Germany), proteins are mostly fused to a small epitope tag such as FLAG or c-Myc to analyze biochemical characteristics like enzymatic activities and/or binding specificities. Thus, integration of such *in vitro* data with *in vivo* data obtained with fluorescently labeled proteins has, in part, been impeded by the simple fact that different protein tags are used for different applications. The gold standard to examine binding affinities is surface plasmon resonance (SPR) [5]. One drawback of this method is the need of large amount of proteins. Such proteins have to be expressed and purified from bacterial systems (e.g. *E.coli*) or lower eukaryotes such as yeast (e.g. *S. cerevisiae*). Thus, the recombinant proteins lack essential post-translational modifications or are not folded properly possibly leading to different binding properties and inaccurate results. In addition with SPR measurements one can only determine the binding affinity to one substrate. This does not reflect the *in vivo* situation where most proteins have the choice between many different binding substrates in parallel.

Protein microarrays are an alternative to study protein-protein interactions in high-throughput manner [6]. Once more the drawback of this *in vitro* method is the laborative and time-consuming preparation of recombinant proteins or protein domains. Therefore protein microarrays are limited to domains that can be produced as soluble, well-folded proteins [6].

Recently, specific GFP binding proteins based on single domain antibodies derived from Lama alpaca have been described [7] (GFP-Trap ChromoTek, Germany). The GFP-Trap exclusively binds to wtGFP, eGFP and GFP^{S65T} as well as to YFP and eYFP. Coupling to matrices including agarose beads or magnetic

particles the GFP-Trap allows for one-step purification of GFP-fusion proteins. Previous studies made use of the GFP-Trap to perform a broad range of different methods including mass spectrometry analysis [8], DNA binding, DNA methyltransferase activity assays [9], as-well-as histone-tail peptide binding assays [10]. One mayor disadvantage of the GFP-Trap is, that batch purification of GFP-fusions is very laborious and time-consuming and one cannot test different GFP-fusion and/or assay conditions in parallel. Here, we present an innovative and versatile high-throughput method to quantitatively measure binding specificities and to detect endogenous interacting factors in a fast and reliable manner *in vitro*: 96-well micro plates coated with immobilized GFP-Trap (GFP-multiTrap). To demonstrate the general suitability of our assays, we choose already known binding partners and compared our results with previous publications. Using this method, we could confirm that Cbx1 preferentially binds to di- and trimethylated histone H3 lysine 9 and that this binding is abolished by phosphorylation of the adjacent serine 10 [11–13]. In addition, we determined a 4-fold preference of the MBD domain of MeCP2 for fully over unmethylated DNA in accordance to [14–16]. Furthermore, we performed protein-protein interaction assays and found that the Dnmt1 binds to PCNA in a PBD domain-dependent manner consistent to [17,18]. In contrast, LigaseIII binds Xrcc1 but does not interact with PCNA [19,20]. Using an ELISA-based assay, we were able to detect endogenous PCNA bound to immunoprecipiated Dnmt1, Fen1 and PCNA itself. In accordance with our protein-protein interaction data, Dnmt1 lacking the PBD domain (Dnmt1ΔPBD) could not co-immunoprecipate with PCNA. Consistent with our histone-tail peptide binding data, we could detect endogenous histone H3 bound to Cbx1. Finally, we quantified specific histone modifcations on nucleosomes comprising different histone variants. All of these data clearly demonstrate the versatility and easy handling of this high-troughput approach and its immense benefit to many researchers.

Results

One-step Purification of GFP-fusion Proteins

In a first step, we tested the efficiency of the GFP-multiTrap to purify GFP-fusion proteins from cellular extracts. First, we examined the pull-down efficiency of a GFP-tagged protein and chose GFP-Cbx1 as a model protein. Cbx1 is a chromodomain-containing protein related to the Drosophila HP1β, a well-studied heterochromatin-associated protein [11]. We used cell extracts from HEK293T cells transiently expressing GFP-Cbx1 or GFP, purified the GFP-fusions using the GFP-multiTrap, eluted the bound fractions, separated them by SDS-PAGE and visualized the bound proteins by coomassie staining. The bound fractions displayed mainly GFP as well as GFP-Cbx1 with only minor impurities (Figure 1A), providing therefore a reliable tool for downstream biochemical analyses. Notably, the washing conditions can be varied according to the downstream applications. In addition to these qualitative results, we performed experiments to quantify the pull-down efficiency. For this purpose we quantified the amount of bound GFP with varying concentrations of input GFP from cellular extracts. After binding, the single wells were subjected to several washing steps and bound GFP was analyzed by fluorescent read-out using a micro plate reader. Notably, the input amount of protein/substrate was measured in solution, whereas the bound fraction represents one value on the 96-well surface. We measured the fluorescence intensities of bound GFP and plotted the amount of bound GFP as a function of total GFP (Figure 1B). The amount of bound GFP increased linearly from 10 to 130 nM of total input and saturated between 130 and 400 nM. Next, we quantified the amount of bound GFP by immunoblotting. Therefore, we eluted the bound GFP fractions, separated them by SDS-PAGE, visualized the bound proteins by immunoblot analysis (Figure 1C) and quantified the GFP signal by measuring the mean intensity via Image J (Figure 1D). Similar to the quantifcation by fluorescent read out using a micro plate reader, the amount of bound GFP increases linearly from 10 to 130 nM of total input and saturates between 130 and 400 nM.

In summary, we demonstrated that the GFP-multiTrap allows for fast and efficient one-step purification of GFP-fusion proteins directly from crude cell lysates in a high-throughput manner. The method works well for both qualitative and quantitative measurements and the immunoprecipitated GFP-fusions can then be further tested in biochemical assays.

In vitro Histone-tail Peptide and DNA Binding Assay

In the next assay we determined whether this approach is also feasible to quantify binding affinities between GFP-proteins and peptides or DNA. First, we analyzed histone-tail peptide binding specificities of the chromobox homolog 1, Cbx1, fused with a N-terminal GFP-tag using the GFP-multiTrap. GFP-Cbx1 was purified from mammalian cell lysate, as described above, and the bound protein was incubated with TAMRA-labeled histone-tail peptides. A set of 20 different histone-tail peptides (Table 1) was used in technical triplicates in parallel and GFP served as negative control (GFP data is not shown). After removal of unbound substrate the amounts of protein and histone-tail peptide were determined by fluorescence intensity measurements using a micro plate reader. Binding ratios were calculated by dividing the concentration of bound histone-tail peptide by the concentration of GFP fusion (Figure 2A). GFP-Cbx1 preferentially binds H3K9me3 and H3K9me2 histone-tail peptides consistent with previous studies [11,12]. As expected, the phosphorylation of serine 10 (S10p) next to the trimethylated lysine 9 leads prevents binding of Cbx1, which is in accordance with previous reports [13]. In addition to fluorescent quantification via a micro plate reader, we scanned the TAMRA signals using a Typhoon scanner (Figure 2B). Here, we detected TAMRA signals in the wells corresponding to di- and trimethylated H3K9. Notably, we did not detect differences in binding towards di-and trimethylated H3K9 using a micro plate reader. However, we could detect a preference for tri- over dimethylated H3K9 using a fluorescence scanner. These differences could result from different sensitivities of both methods. Furthermore, we performed a competition assay to demonstrate the specificity of the histone-tail peptide-binding assay. We incubated GFP-Cbx1 with TAMRA-labeled H3K9me3 in parallel with either biotinylated H3K9me3 or H3K9ac histone-tail peptides. As expected, the addition of biotinylated H3K9me3 histone-tail peptide significantly decreased the binding of Cbx1 to TAMRA-labeled H3K9me3, whereas the addition of biotinylated H3K9ac did not alter the binding ratios (Figure 2C). In previous studies [11,12], the binding affinities of the HP1β chromo domain, the Drosophila homolog of mammalian Cbx1, for both di- and trimethylated H3K9 peptides have been found to be 7 and 2.5 μM, respectively. In contrast, we could not detect a significant difference in binding ratios between di- and trimethylated H3K9 histone tail peptides using a micro plate reader (Figure 2A). One explanation could be the use of different expression systems. While the binding ratios for the HP1β chromo domain were determined using bacterially expressed protein we used a fluorescent fusion protein derived from mammalian cells. In this context a recent study revealed that recombinant HP1α prepared from mammalian cultured cells exhibited a stronger binding affinity for K9-

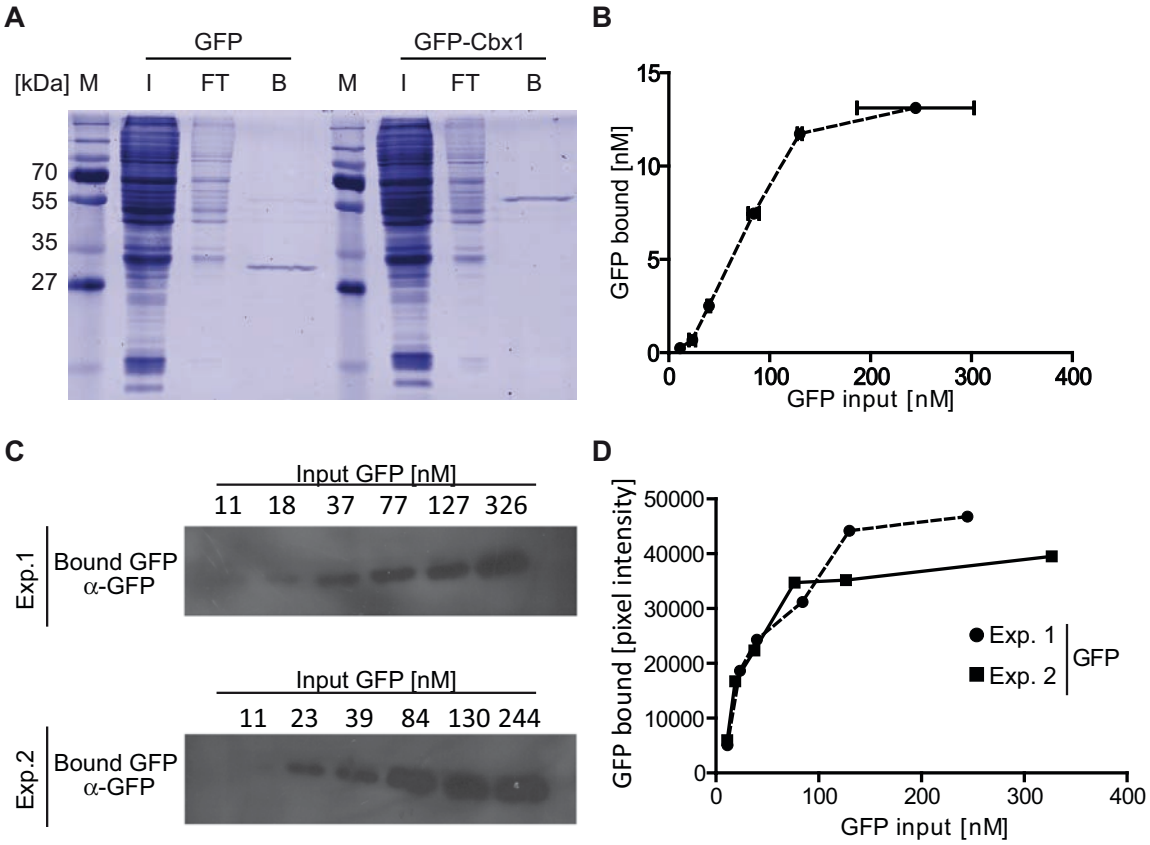

Figure 1. One-step purification of GFP and GFP-fusion proteins. Purification of GFP and GFP-Cbx1 expressed in HEK293T cells. All GFP concentrations were quantified via plate reader. (**A**) Purification of GFP and GFP-Cbx1 from HEK293T cell extracts, transciently transfected with the GFP-fusions. Input (I), flow-through (FT) and bound (B) fractions were separated by SDS-PAGE and visualized by coomassie staining. (**B**) Different amounts of GFP cell lysate were added into wells of a 96-well plate immobilized with the GFP-Trap (GFP-multiTrap).Shown are means ± SD from two independent experiments. (**C**) Bound GFP fractions from both independent experiments (B) were eluted, seperated by SDS-PAGE and visualized by immunoblot analysis using an anti-GFP mouse antibody (Roche, Germany). (**D**) Quantification of bound GFP fractions by immunoblotting. The mean intensities of the GFP signals were measured using Image J.
doi:10.1371/journal.pone.0036967.g001

methylated histone H3 (H3K9me) in comparison to protein produced in *Escherichia coli* [21]. Biochemical analyses revealed that HP1α was multiply phosphorylated at N-terminal serine residues (S11–14) in human and mouse cells and that this phosphorylation enhanced the affinity of HP1α for H3K9me, displaying the importance of post-translational modifications for binding affinities [21]. To determine the binding affinity of GFP-Cbx1 to H3K9me3, we varied the input amount of histone-tail peptide. We plotted the amount of bound histone-tail peptide as a function of total peptide and fitted the values using GraphPad Prism and nonlinear regression (Figure 2D). The amount of bound H3K9me3 histone-tail peptide increases linearly and saturates at approximately 500 nM of input peptide. In contrast to H3K9me3, we could not detect any binding of Cbx1 to H3 histone-tail peptides. Notably, the exact determination of binding affinities was not possible due to differences in the technical measurement of input versus bound fractions. Here, the input amount of protein/substrate was measured in solution, whereas the bound fraction represents one value on the 96-well surface.

In addition to histone-tail peptide binding assays, we performed DNA-binding assays. We purified the methyl-binding domain (MBD) of MeCP2, fused with a C-terminal YFP tag, from cell extracts as described and performed competition binding analysis by incubating immobilized MBD-YFP with fluorescently labeled un- and fully methylated DNA (Table 1). As a result we observed a five-fold preference of MBD for fully methylated DNA over unmethylated DNA (Figure 2E). In addition, we measured the amount of bound DNA to MBD-YFP by varying the input amount of DNA. We plotted the amount of bound un- and fully methylated DNA as a function of total un-and fully methylated DNA and fitted the values using GraphPad Prism and nonlinear regression (Figure 2F). Similar to the relative binding ratios, MBD binds preferentially to fully methylated DNA. These results are in accordance with previous studies describing that MeCP2 interacts specifically with methylated DNA mediated by the MBD domain. In these studies, electrophoretic mobility shift assays (EMSA) using the isolated MBD domain expressed in *E. coli* were performed and dissociation constants of 14,7 and 1000 nM were calculated for symmetrically methylated and unmethylated DNA, respectively [14–16].

To assess the suitability of the *in vitro* histone-tail peptide and DNA binding assay for high-throughput applications, the Z-factor was calculated. For histone-tail peptide binding assays, we calculated the Z-factor using the relative binding ratios of H3K9me3 to GFP-Cbx1 as positive state and of H3K9me0 to GFP-Cbx1 as negative state. For the DNA binding assay, we calculated the Z-factor using the relative binding ratios of fully methylated DNA to MBD-YFP as positive state and of

Table 1. Sequences of DNA oligonucleotides and histone-tail peptides.

DNA oligos

DNA substrate	DNA sequence	DNA labeling
CG-up	5′- CTCAACAACTAACTACCATCCGGACCAGAAGAGTCATCATGG -3′	No
MG-up	5′- CTCAACAACTAACTACCATCMGGACCAGAAGAGTCATCATGG -3′	No
um550	5′- CCATGATGACTCTTCTGGTCCGGATGGTAGTTAGTTGTTGAG -3′	ATTO550 at 5′end
um700	5′- CCATGATGACTCTTCTGGTCCGGATGGTAGTTAGTTGTTGAG -3′	ATTO700 at 5′end
mC700	5′- CCATGATGACTCTTCTGGTCMGGATGGTAGTTAGTTGTTGAG -3′	ATTO700 at 5′end

DNA substrates

DNA substrate	CpG site	Label	Oligo I	Oligo II
UMB-550	unmethylated	550	CG-up	um550
UMB-700	unmethylated	700	CG-up	um700
FMB-700	Fully methylated	700	MG-up	mC700

DNA sets

Binding set	Control set
UMB-550	UMB-550
FMB-700	UMB-700

Histone-tail peptides

H3 (1–20)	ART K QTARKSTGGKAPRKQLK	TAMRA at C-terminus
H3K4me1	ART X1 QTARKSTGGKAPRKQLK	
H3K4me2	ART X2 QTARKSTGGKAPRKQLK	
H3K4me3	ART X3 QTARKSTGGKAPRKQLK	
H3K4ac	ART Z QTARKSTGGKAPRKQLK	
H3K9me1	ARTKQTAR X1 S TGGKAPRKQLK	
H3K9me2	ARTKQTAR X2 S TGGKAPRKQLK	
H3K9me3	ARTKQTAR X3 S TGGKAPRKQLK	
H3K9me3S10p	ARTKQTAR X3 Z2 TGGKAPRKQLK	
H3K9ac	ARTKQTAR Z S TGGKAPRKQLK	
H3 (17–36)	RKQLATKAAR K SAPATGGVK	TAMRA at N-terminus
H3K27me1	RKQLATKAAR X1 SAPATGGVK	
H3K27me2	RKQLATKAAR X2 SAPATGGVK	
H3K27me3	RKQLATKAAR X3 SAPATGGVK	
H3K27ac	RKQLATKAAR Z SAPATGGVK	
H4 (10–29)	LGKGGAKRHR K VLRDNIQGI	
H4K20me1	LGKGGAKRHR X1 VLRDNIQGI	
H4K20me2	LGKGGAKRHR X2 VLRDNIQGI	
H4K20me3	LGKGGAKRHR X3 VLRDNIQGI	
H4K20ac	LGKGGAKRHR Z VLRDNIQGI	

X1: monomethylated Lysine; X2: dimethylated Lysine; X3: trimethylated Lysine; Z: acetylated Lysine; Z2: phosphorylated Serine.
doi:10.1371/journal.pone.0036967.t001

unmethylated DNA to MBD-YFP as negative state (Table 2). The Z-factors of 0.766 for the histone-tail peptide binding assay and 0.756 for the DNA binding assay strongly indicate that both assays are robust, reproducible and suitable for high-throughput applications.

In vitro Protein-protein Binding Assay

In addition to the detection of substrate specificity (e.g. histone-tail peptide) and DNA binding, analysis of the interaction with other cellular components and factors is essential to understand the function of proteins.

The use of fluorescence intensity read-out systems for the quantification of protein-protein interactions *in vitro* provides a new

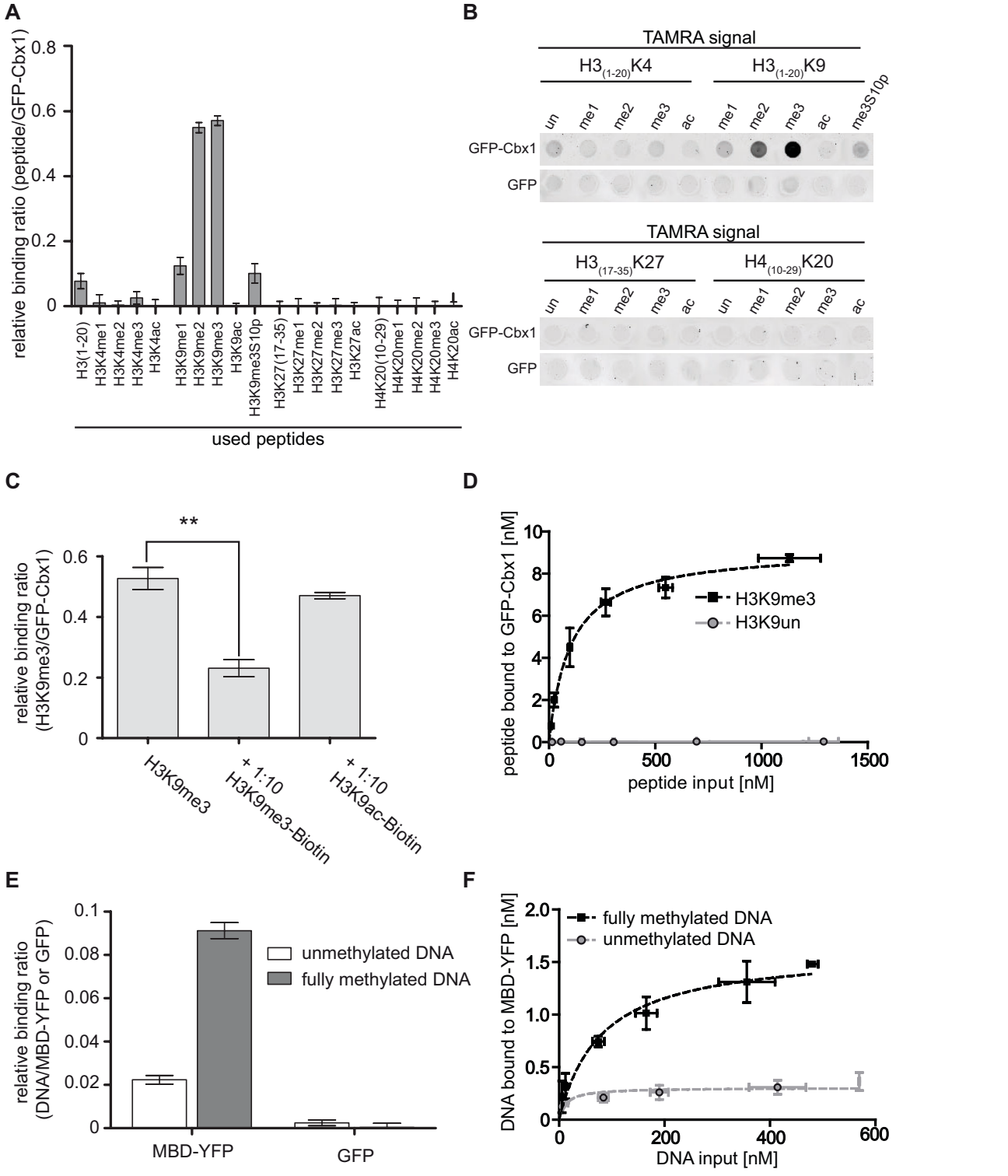

Figure 2. In vitro histone-tail peptide and DNA binding assay. *In vitro* binding ratios of fluorescently labeled substrates over bound GFP fusion proteins were determined. (A)–(D) *In vitro* histone-tail peptide binding assay with GFP-Cbx1. (**A**) Histone H3- and H4-tail binding specificities of Cbx1. A final concentration of 0.15 μM TAMRA-labeled histone-tail peptide was added per well. Fluorescent signals of bound TAMRA-labeled histone-tail peptides and GFP-fusion protein were quantified via plate reader. Shown are means ± SD from three independent experiments (**B**) Fluorescent signals of bound TAMRA-labeled histone-tail peptides visualized by fluorescent scanner. (**C**) Competition assay between TAMRA-labeled H3K9me3 and biotinylated histone-tail peptides with GFP-Cbx1. Shown are means ± SD from three independent experiments. Statistical significance between the binding ratios is indicated; **$P<0.003$. (**D**) Different amounts of TAMRA-labeled H3K9me3 and H3 histone-tail peptides were added to GFP-Cbx1. Three or two independent experiments for H3K9me3 or H3 histone-tail peptides were performed, respectively. Shown are means ± SD and the amount of bound histone-tail peptide was plotted as a function of total histone-tail peptide. The curve was fitted using GraphPad Prism and

nonlinear regression. All input and bound fractions were quantified via a plate reader. (**E**) DNA binding specificities of the MBD domain of MeCP2 to un- and fully methylated DNA in direct competition. Shown are means ± SD from three independent experiments. (**F**) Different amounts of Atto550-labeled unmethylated and Atto700-labeled fully methylated DNA in direct competition were added to purified MBD-YFP. Shown are means ± SD from three independent experiments. The amount of bound DNA peptide was plotted as a function of total DNA. The curve was fitted using GraphPad Prism and nonlinear regression. All input and bound fractions were quantified via a plate reader.
doi:10.1371/journal.pone.0036967.g002

and simple method avoiding laborious and inaccurate protein detection using conventional immunoblotting systems.

To address the question if such interaction analysis can be performed in a multi-well format we analyzed the interaction of single GFP-fusions with RFP-fusion proteins expressed in mammalian cells. More precisely, we determined quantitative binding ratios between nuclear located proteins involved in DNA-replication (PCNA) [17,18], DNA-methylation (Dnmt1) [22] as well as in DNA-repair (Xrcc1) [23]. As described, we immobilized GFP-fusions on the GFP-multiTrap and incubated them with cell lysate containing RFP-fusion proteins. After binding, we removed unbound material, measured the concentrations of RFP and GFP and calculated the molar binding ratios. Firstly, we determined the binding ratios of the green fluorescent PCNA-binding domain of Dnmt1 (GFP-PBD) to RFP-PCNA and used Dnmt1ΔPBD as a negative control. By measuring the fluorescent signal intensities we detected that RFP-PCNA binds to GFP-PBD in a molar ratio of 1.42±0.31 but not to Dnmt1ΔPBD (Figure 3A).

For a direct comparison we eluted the bound fractions, separated them by SDS-PAGE and visualized the proteins by immunoblotting (Figure 3B). Both, GFP-PBD and RFP-PCNA are detected in the input and bound fractions whereas RFP is not visible in the bound fraction of GFP-PBD (Figure 3B).

In addition, we measured the amount of bound RFP-fusion to GFP-PBD with varying the input amount of RFP-fusion. We plotted the amount of bound RFP-fusion as a function of total RFP-fusion and fitted the values using GraphPad Prism and nonlinear regression (Figure 3C). Similar to the relative binding ratios, GFP-PBD binds to RFP-PCNA but not to RFP.

These results are in accordance with previous findings that Dnmt1 associates with the replication machinery by directly binding to PCNA, a homotrimeric ring which serves as loading platform for replication factors, and that this binding depends on the PCNA-binding domain in the very N-terminus of Dnmt1 [17,18]. In addition by determining the quantitative binding ratio between both partner proteins our approach provides a more detailed insight in the binding events occurring at the central loading platform of the DNA replication.

Secondly, we determined the molar binding ratio of GFP-Ligase III to RFP-Xrcc1. Xrcc1 binds in a molar ratio of 0.61±0.14 to Ligase III but did not bind to other proteins such as GFP-PBD, GFP-Dnmt1ΔPBD or GFP. Previous studies demonstrated that DNA Ligase III was recruited to DNA repair sites via its BRCT domain mediated interaction with Xrcc1 [19,20].

For the protein-protein binding assays, we calculated the Z-factor using the molar binding ratios of RFP-PCNA to GFP-PBD as positive state and RFP to GFP-PBD as negative state (Table 2). The Z-factor of 0.56 indicated that the protein-protein binding assay is robust and reproducible.

In summary, we demonstrate a new quantitative and reliable high-throughput method to analyze protein-protein interactions using GFP- and RFP-fusion proteins.

Enzyme-linked Immunosorbent Assay (ELISA)

Next we examined endogenous protein-protein interactions using an ELISA assay. For this purpose, we precipitated GFP-fusion proteins in the 96 well format on the GFP-multiTrap and cross-linked bound fractions with formaldehyde (CH_2O) and/or treated the bound fractions with methanol (MeOH). Using specific antibodies against PCNA, we determined the binding of endogenous PCNA to GFP fusions of Dnmt1, Dnmt1ΔPBD, PCNA, Fen1, which is a flap endonuclease and an essential DNA replication protein [24]. We could detect endogenous PCNA binding to Dnmt1 but not to Dnmt1ΔPBD similar to the results obtained with the protein-protein interaction assay using RFP-PCNA (Figure 4A). In addition, we detected binding of endogenous PCNA to Fen1 but also to PCNA itself. These results fit well to former studies showing that Fen1 or maturation factor 1 associates with PCNA in a stoichiometric complex of three Fen1 molecules per PCNA trimer [25,26]. In addition to 100 described interacting partners, it is known that PCNA also interacts with itself and forms a trimeric ring, which is confirmed by our ELISA assay by giving a signal for endogenous PCNA binding to GFP-PCNA (Figure 4A).

Next, we determined the binding of Cbx1 to endogenous histone H3. Similar to PCNA, we precipitated GFP-Cbx1 and GFP and detected endogenous H3 via an H3-antibody coupled to HRP. In accordance with the experiments using TAMRA labeled histone 3 peptides, we observed an H3 ELISA signal for binding to Cbx1 but not to GFP. Using an H3K9me3-specific antibody, we could not detect an ELISA signal (data not shown), due to the fact that the tight binding of Cbx1 (Figure 2) to H3K9me3 most likely

Table 2. Overview of relative binding ratios and Z-factor values.

Relative binding ratios of Substrate/GFP- or YFP-fusion						
	Histone-tail peptide binding		**DNA binding**		**Protein-protein binding**	
Fusion protein	**GFP-Cbx1**		**MBD-YFP**		**GFP-PBD**	
Substrate	**H3K9me3**	**H3K9un**	**Fully methylated DNA**	**Unmethylated DNA**	**RFP-PCNA**	**RFP**
Average ratio	0,5715	0,0772	0,0912	0,0223	1,487	0,005
Standard deviation	0,0150	0,0236	0.0037	0.0019	0,2111	0,006
Z-factor	0,766		0.756		0.560	

Based on the average relative binding ratios and the standard deviations we calculated the Z-factor.
doi:10.1371/journal.pone.0036967.t002

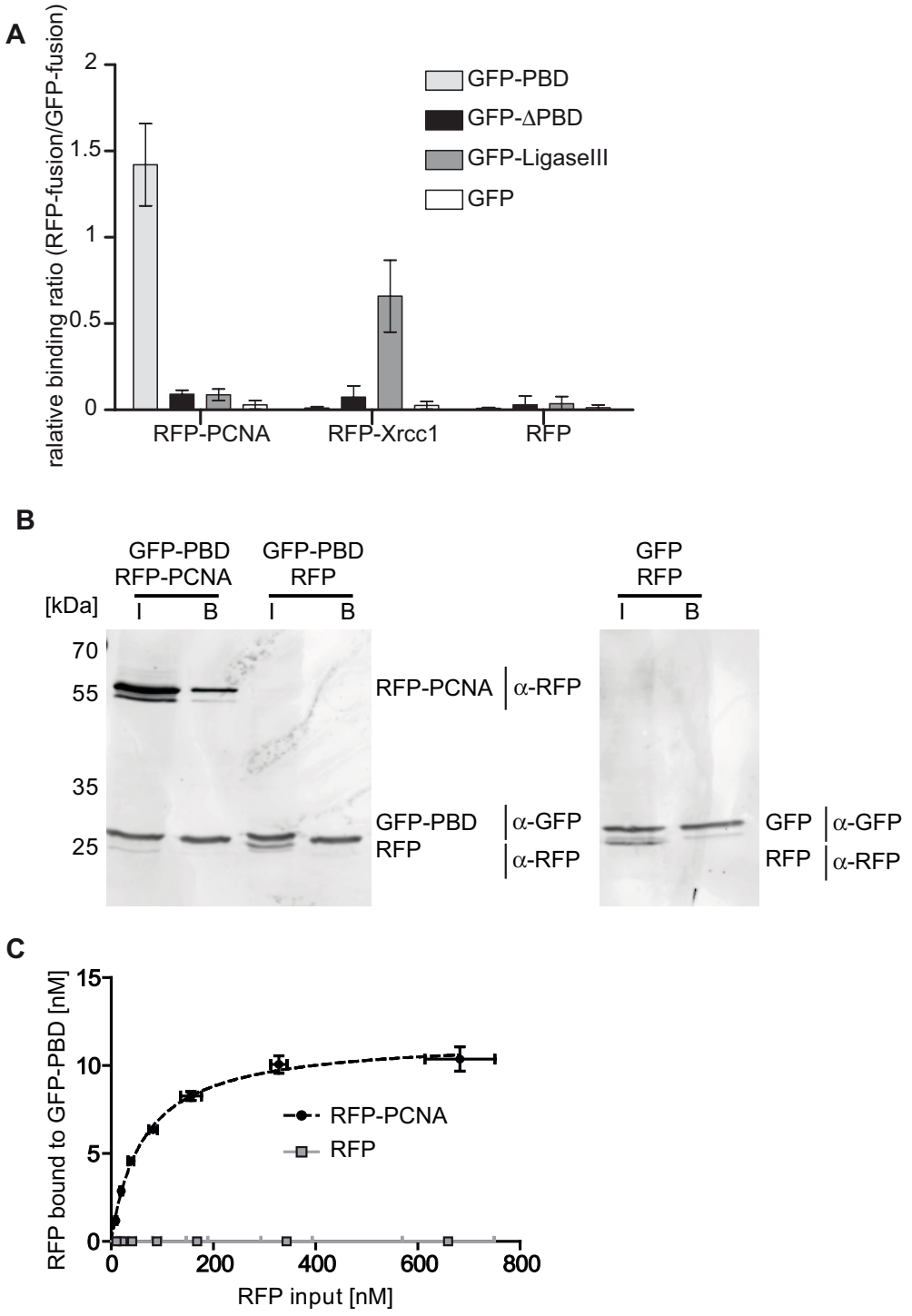

Figure 3. In vitro Protein-Protein binding assay. (**A**) *In vitro* binding ratios of RFP-fusion proteins over GFP-fusion proteins. Shown are means ± SD from six independent experiments. (**B**) After immunoprecipitation input (I) and bound (B) fractions were separated by SDS-PAGE and visualized by immunoblot analysis using the anti-GFP rat monoclonal antibody; 3H9, and the anti-RFP rat monoclonal antibody, 5F8 (both ChromoTek, Germany). GFP-PBD: 30 kDa; RFP-PCNA: 56 kDa; GFP: 28 kDa, RFP: 26 kDa. (**C**) Different amounts of RFP-fusion protein were added to purified GFP-PBD. Shown are means ± SD from two independent experiments. The amount of bound RFP was plotted as a function of total RFP. The curve was fitted using GraphPad Prism and nonlinear regression. All input and bound fractions were quantified via a plate reader.
doi:10.1371/journal.pone.0036967.g003

occludes the antibody epitope, as has been proposed for HP1 binding to H3K9me3. In this study, the histone H3 trimethyl-lysine epitope is embedded in an aromatic cage blocking thereby most likely the binding of any antibodies [27]. To further analyze the bound fractions, we eluted GFP-Cbx1 and GFP, separated them on an SDS-PAGE gel and visualized GFP and H3 by

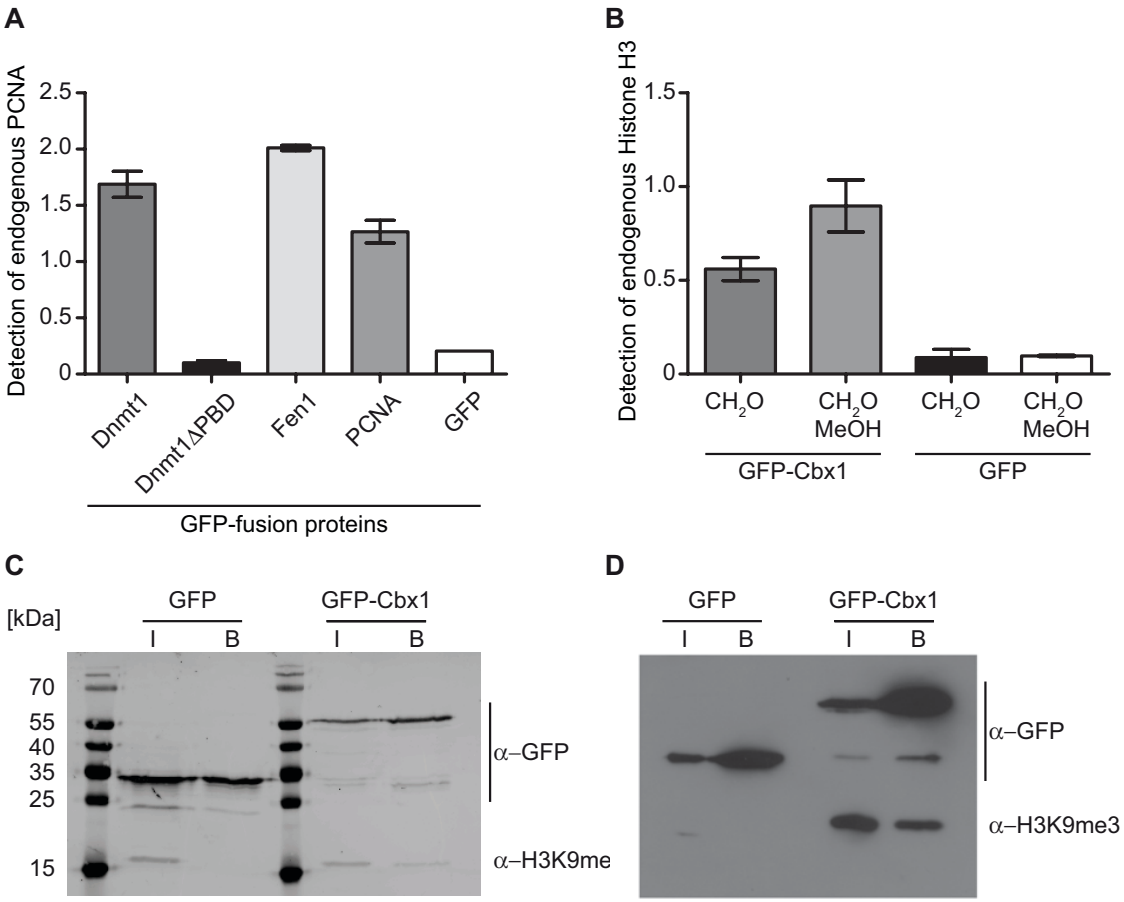

Figure 4. Pulldown of endogenous interaction partners. GFP-fusions were immunoprecipitated and endogenous interacting proteins were detected either by ELISA or immunoblot analysis. (**A**) ELISA signal (Absorbance at 450 nm) of bound endogenous PCNA detected by a PCNA antibody to purified GFP-fusion proteins. Shown are means ± SD from three independent experiments. (**B**) ELISA signal (Absorbance at 450 nm) of bound endogenous Histone H3 detected by an H3 antibody to purified GFP-fusion proteins. Bound fractions were either cross-linked with 2% formaldehyde (CH_2O) and/or additionally permeabilized with MeOH. Shown are means ± SD from two independent experiments. (C) and (**D**) After immunoprecipitation input (I) and bound (B) fractions were separated by SDS-PAGE and visualized by immunoblot analysis. (**C**) The total protein concentration of the input fractions were adjusted. (**D**) The GFP concentrations of the input fractions were adjusted.
doi:10.1371/journal.pone.0036967.g004

immunoblotting. Histone H3 was detectable in the input fractions of both GFP and GFP-Cbx1 but as expected, only in the bound fraction of GFP-Cbx1.

Comparative Analysis of Posttranslational Histone Modifications

Histone posttranslational modifications play an important role in the structural organization of chromatin and often correlate to transcriptional activation or repression depending on their type and location. Recently, it has been shown that nucleosomal incorporation of histone variants can lead to alterations in modification patterning and that such changes may complement the properties brought by the variant itself [28].

In order to investigate the suitability of the GFP-multiTrap in comparing such histone posttranslational modifications, we isolated nucleosomes from HeLa cells expressing either GFP-H2A or GFP-H2A.Z and precipitated them with the 96 well micro plate. GFP levels were then recorded (data not shown) to ensure equal loading of substrate per well. In addition, as a negative control, the cytoplasmic supernatant fraction was also incubated with the GFP-multiTrap. An ELISA approach was then used to quantify differences in histone H3K4me2 levels between the two different nucleosome compositions. Following cross-linking and permeablization, bound nucleosomes were incubated with either anti-H3, directly conjugated to HRP or anti-H3K4me2 (both antibodies Abcam, UK). Histone H3K4me2 levels were then normalized to the histone H3 signal. In accordance with published data, H2A containing nucleosomes were depleted in H3K4me2 where as those containing H2A.Z showed a large enrichment for this modification (Figure 5) [28].

Discussion

One challenge of the proteomic era is the effective integration of proteomic, cell biological and biochemical data. Ideally, proteomic data on tissue and cell cycle-specific expression of specific proteins should be combined with subcellular localization and binding dynamics of fluorescent proteins. Additionally, it is crucial to determine cell biological and biochemical characteristics such as interacting factors, enzymatic activity and substrate binding specificities. The integration of all these different data has, in part, been impeded by the simple fact that different protein tags

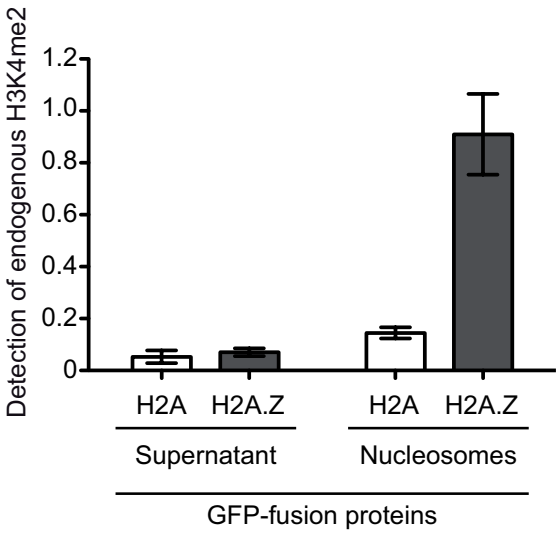

Figure 5. Comparative analysis of posttranslational histone modifications. Cytoplasmic supernatant (SN) or mononucleosome (MN) fractions prepared from HeLa cells expressing GFP-H2A or GFP-H2A.Z were precipitated and the levels of H3 and H3K4me2 were detected by ELISA (Absorbance at 450 nm). Shown are the H3K4me2 levels normalized to H3 and means ± SD from two independent experiments.
doi:10.1371/journal.pone.0036967.g005

are used for different applications. Here, we present a new versatile, high-throughput method to determine *in vitro* binding specificities and to detect endogenous interacting factors of GFP-fusion proteins. We use 96-well micro plates with immobilized GFP-Trap (GFP-multiTrap) for fast and efficient purification of GFP-fusion proteins. We demonstrate the efficiency and purity of the GFP immunoprecipitation (Figure 1), a prerequisite to obtain reliable biochemical data on e.g. binding specificities. Moreover, we measured histone-tail binding, DNA and protein-protein binding ratios underlying the versatility of our approach (Figure 2 and 3 and Table 2). The suitability of the demonstrated assays for high-throughput biochemical and functional studies was assessed by calculating the Z-factors (Table 2). Therefore, our assay is suitable to examine an initial high-throughput screening for potential binding partners. Moreover, the assay can be used for compound screening. Additionally, our method allows for detection of endogenous interaction factors based on an ELISA assay (Figure 4 and 5).

In contrast to other high-throughput techniques like conventional microarrays, it does not require time-consuming recombinant protein expression and purification but allows for the direct biochemical analyses of GFP-fusion proteins expressed in mammalian cells. The versatile GFP-multiTrap combined with the widespread use of fluorescent fusion proteins now enables a fast and direct quantitative correlation of microscopic data concerning the subcellular localization and mobility of fluorescent fusion proteins with their enzymatic activity, interacting factors, and DNA binding properties combining cell biology and biochemistry with mutual benefits.

Materials and Methods

Expression Constructs, Cell Culture and Transfection

Mammalian expression constructs encoding GFP-Dnmt1, GFP-Dnmt1ΔPBD, GFP-PBD, GFP-PCNA, RFP-PCNA, GFP-Ligase III, mRFP, GFP, MBD-YFP, GFP-Fen1 and RFP-Xrcc1 were described previously [7,20,29–37]. Note that all constructs encode fusion proteins of GFP, RFP or yellow fluorescent protein (YFP). The Cbx1 expression construct was derived by PCR from mouse cDNA, cloned into pEGFP-C1 (Clontech, USA) and verified by DNA sequencing. Throughout this study enhanced GFP (eGFP) constructs were used and for simplicity referred to as GFP-fusions. HEK293T cells [30] and HeLa Kyoto [29] were cultured in DMEM supplemented with either 50 μg/ml gentamicin (HEK293T) or 1% penicillin/streptomycin (HeLa Kyoto) and 10% fetal calf serum. For expression of GFP/RFP/YFP fusion proteins, HEK293T cells were transfected with the corresponding expression constructs using polyethylenimine (Sigma, USA). 2. HeLa Kyoto cells were transfected using FuGene HD (Roche, Germany) according to the manufacturer's instructions. The plasmid coding for GFP-H2A (H2A type 1, NP_003501.1) was kindly provided by Emily Bernstein (Mount Sinai Hospital) and the plasmid coding for GFP-Z-1 was a gift from Sachihiro Matsunaga (University of Tokyo). Stable cell lines were selected with 600 μg/ml G418 (PAA, Austria) and individual cell clones sorted by using a FACSAria machine (Becton Dickinson, Germany).

Histone-tail Peptides and DNA Substrate Preparation

Fluorescently labeled DNA substrates were prepared by mixing two HPLC-purified DNA oligonucleotides (IBA GmbH, Germany Table 1) in equimolar amounts, denaturation for 30 sec at 92°C and slow cool-down to 25°C allowing hybridization. Histone-tail peptides were purchased as TAMRA conjugates and/or biotinylated (PSL, Germany) and are listed in Table 1.

Preparation of Protein Extracts

HEK293T cells were cultured and transfected as described [38]. For extract preparation 1 mg/ml DNaseI, 1 mM PMSF and Protease Inhibitor cocktail (Roche, Germany) were included in the lysis buffer (20 mM Tris-HCl pH 7.5, 150 mM NaCl, 2 mM $MgCl_2$, 0.5% NP40) or nuclear extract buffer (10 mM HEPES pH 7.9, 10 mM KCl, 1.5 mM $MgCl_2$, 0.34 M Sucrose, 10%Glycerol, 1 mM β-mercapto-ethanol). Cells were lysed for 30 minutes on ice followed by a centrifugation step (15/12000 rpm/4°C). Extracts from transfected 10 cm plates were diluted to 500 μL with immunoprecipitation buffer (IP buffer; 20 mM Tris-HCl pH 7.5, 150 mM NaCl, 0.5 mM EDTA) or dilution buffer (20 mM HEPES pH 7.9, 150 mM KCl). An aliquot of 10 μL (2%) were added to SDS-containing sample buffer (referred to as Input (I)).

Purification and Elution of GFP/YFP/RFP- Fusions

For purification, 100 μL or 50 μL precleared cellular lysate for full-area plates or half-area plates, respectively, was added per well and incubated for 2 hours at 4°C on a GFP-multiTrap plate by continuous shaking. After removing the supernatant, wells were washed twice with 100 μL of washing buffer (WB; 20 mM Tris-HCl pH 7.5, 100–300 mM NaCl, 0.5 mM EDTA) and 100 μL of IP or dilution buffer was added for measurement. The amounts of bound protein were determined by fluorescence intensity measurements with a Tecan Infinite M1000 plate reader (Tecan, Austria). Wavelengths for excitation and emission of GFP are 490±10 nm and 511±10 nm, for RFP are 586±5 nm and 608±10 nm and for YFP 525±5 nm and 538±5 nm, respectively. The concentration of proteins was calculated using calibration curves that were determined by measuring the fluorescence signal of known concentrations of purified GFP, RFP and YFP. Notably, factors interfering with

fluorescence intensity measurements such as absorption of excitation light by cell lysates, auto fluorescence of the samples and/or scattering of the excitation/emission light by cell debris are negligible (Figure S1). Bound proteins were eluted with 300 mM Glycin pH 2.5 and subsequently buffered with 1 M Tris pH 7.5. Elution fractions were added to SDS-containing sample buffer (referred to as Bound (B)). Bound proteins were visualized by immunoblotting using the anti-GFP mouse monoclonal antibody (Roche, Germany).

In vitro Histone-tail Peptide Binding Assay

The *in vitro* histone-tail binding assay was performed as described previously [10]. After one-step purification of GFP fusion proteins the wells were blocked with 100 µL 3% milk solved in TBS-T (0.075% Tween) for 30 minutes at 4°C on a plate vortex, shaking gently. After blocking, the wells were equilibrated in 50 µL IP buffer supplemented with 0.05% Tween. TAMRA-labeled histone-tail peptides were added either to a final concentration of 0.15 µM or of the indicated concentrations and the binding reaction was performed at RT for 20 min on a plate vortex, shaking gently. After removal of unbound substrate the amounts of protein and histone-tail peptide were determined by fluorescence intensity measurements. The concentrations of bound TAMRA-labeled histone-tail peptides were calculated using calibration curves that were determined by measuring a serial dilution of TAMRA-labeled peptides with known concentrations.

Binding ratios were calculated dividing the concentration of bound histone-tail peptide by the concentration of GFP fusion. Wavelengths for excitation and emission of TAMRA were 560±5 nm and 586±5 nm, respectively.

In vitro DNA Binding Assay

In vitro DNA binding assay was performed as described previously [9,10] with the following modifications. GFP/YFP fusions were purified from HEK293T extracts using the 96-well GFP-binder plates and incubated with two differentially labeled DNA substrates at a final concentration of either 100 nM or of the indicated concentration for 60 min at RT in IP buffer supplemented with 2 mM DTT and 100 ng/µL BSA. After removal of unbound substrate the amounts of protein and DNA were determined by fluorescence intensity measurements. The concentration of bound ATTO-labeled DNA substrates was calculated using calibration curves that were determined by measuring a serial dilution of DNA-coupled fluorophores with known concentrations. Binding ratios were calculated dividing the concentration of bound DNA substrate by the concentration of GFP/YFP fusion, corrected by values from a control experiment using DNA substrates of the same sequence but with different fluorescent label, and normalized by the total amount of bound DNA. Wavelengths for excitation and emission of ATTO550 were 545±5 nm and 575±5 nm and for ATTO700 700±10 nm and 720±10, respectively.

Protein-Protein Interaction

GFP fusions were purified from HEK293T extracts using the 96-well GFP multiTrap plates, blocked with 3% milk and incubated with cellular extracts comprising the RFP fusions with the indicated concentrations for 30 min at RT. After removal of unbound RFP fusion (washing buffer) the amounts of proteins were determined by fluorescence intensity measurements. Binding ratios were calculated dividing the concentration of bound RFP fusion by the concentration of GFP fusion. Wavelengths for excitation and emission of RFP were 586±5 nm and 608±10 nm, respectively. Bound proteins were eluted and separated by SDS-PAGE and visualized by immunoblotting using the anti-GFP rat monoclonal antibody; 3H9, and the anti-red rat monoclonal antibody, 5F8 (both ChromoTek, Germany).

Enzyme-linked Immunosorbent Assay (ELISA)

GFP fusions were purified (from HEK293T extracts) using the 96-well GFP-multiTrap plates and were washed twice with dilution buffer (for nucleosome experiments salt concentration was adjusted to 300 mM). After washing bound fractions were either cross-linked with 2% formaldehyde and/or additionally permeabilized with 100% MeOH. After blocking with 3% milk solved in TBS-T (0.075% Tween) the wells were incubated with primary antibody (monoclonal rat anti-H3-HRP (Abcam, UK), polyclonal rabbit anti-H3K4me2 (Abcam, UK) or monoclonal rat anti-PCNA, 16D10 (ChromoTek, Germany) overnight at 4°C on a plate vortex, shaking gently. The wells were washed three times with 200 µL TBS-T and horseradish peroxidase-conjugated secondary antibody (Sigma, USA) was incubated for 1 h at RT for the detection of PCNA or H3K4me2. The wells were washed again as described above. For PCNA experiments detection was carried out by incubating each well with 100 µL TMB (3,3′,5,5′-tetramethylbenzidine) for 10 minutes at RT. The reactions were stopped with the addition of 100 µL 1 M H_2SO_4. For nucleosome experiments, detection was carried out using OPD (Sigma, USA) according to the manufacturers instructions. Bound histone H3, PCNA or H3K4me2 levels were quantified by determination of the absorbance at 450 nm using a Tecan Infinite M1000 plate reader (Tecan, Austria).

Preparation of Mononucleosomes

$2\times10^7-10\times10^7$ HeLa cells, expressing either GFP-H2A or GFP-H2A.Z, were incubated in PBS, 0.3% Triton X-100 and Protease Inhibitor Cocktail (Roche, Germany) for 10 min at 4°C. Nuclei were pelleted and supernatant (SN) transferred and retained. The pellet was washed once in PBS, resuspended in EX100 buffer (10 mM Hepes pH 7.6, 100 mM NaCl, 1.5 mM $MgCl_2$, 0.5 mM EGTA, 10% (v/v) glycerol, 10 mM β-glycerol phosphate 1 mM DTT, Protease Inhibitor Cocktail (Roche, Germany)) and $CaCl_2$ concentration adjusted to 2 mM. Resuspended nuclei were digested with 1.5 U MNase (Sigma, USA) for 20 min at 26°C. The reaction was stopped by addition of EGTA to a final concentration of 10 mM followed by centrifugation for 10 min at 1000 rcf, 4°C. Mononucleosome containing supernatant (MN) was retained.

Calculation of the Z-factors

To assess the suitability of the assay for high-throughput biochemical and functional studies, the Z-factor was calculated using the equation $Z=1-\frac{3\times(\sigma_p+\sigma_n)}{|\mu_p-\mu_n|}$ [39]. In this equation, σ is the standard deviation of the positive (p) and the negative (n) control; µ is the mean value for the molar binding ratio (for positive (μ_p) and negative (μ_n) controls). The values of three independent experiments were used to calculate the Z-factor and all values are listed in Table 2.

Supporting Information

Figure S1 Factors interfering the measured fluorescence intensities. (**A**) The concentrations of GFP and RFP expressed in HEK293T cells were measured in serial dilutions of crude cell extracts. Shown are means ± SD from two independent experiments. Fluorescence intensities were measured via a plate reader and the GFP and RFP concentrations were determined as described in the Material and Methods part. (**B**) Background GFP

and RFP signals in cell lysates of untransfected HEK293T cells. The fluorescence intensities (FI) were measured via a plate reader and the concentrations were determined as described in the Material and Methods part.
(DOC)

Acknowledgments

We thank Heinrich Leonhardt and Ulrich Rothbauer for comments on the manuscripts and discussion. We also thank ChromoTek for the supply of GFP-multiTrap.

Author Contributions

Conceived and designed the experiments: GP SBH. Performed the experiments: GP AJ PW. Analyzed the data: GP AJ PW. Contributed reagents/materials/analysis tools: SBH. Wrote the paper: GP SBH.

References

1. Walther TC, Mann M (2010) Mass spectrometry-based proteomics in cell biology. J Cell Biol 190: 491–500. doi:10.1083/jcb.201004052.
2. Chalfie M, Tu Y, Euskirchen G, Ward WW, Prasher DC (1994) Green fluorescent protein as a marker for gene expression. Science 263: 802–805.
3. Cristea IM, Williams R, Chait BT, Rout MP (2005) Fluorescent proteins as proteomic probes. Mol Cell Proteomics 4: 1933–1941. doi:10.1074/mcp.M500227-MCP200.
4. Rottach A, Kremmer E, Nowak D, Leonhardt H, Cardoso MC (2008) Generation and characterization of a rat monoclonal antibody specific for multiple red fluorescent proteins. Hybridoma 27: 337–343. doi:10.1089/hyb.2008.0031.
5. Aslan K, Lakowicz JR, Geddes CD (2005) Plasmon light scattering in biology and medicine: new sensing approaches, visions and perspectives. Curr Opin Chem Biol 9: 538–544. doi:10.1016/j.cbpa.2005.08.021.
6. Kaushansky A, Allen JE, Gordus A, Stiffler MA, Karp ES, et al. (2010) Quantifying protein-protein interactions in high throughput using protein domain microarrays. Nat Protoc 5: 773–790. doi:10.1038/nprot.2010.36.
7. Rothbauer U, Zolghadr K, Muyldermans S, Schepers A, Cardoso MC, et al. (2008) A versatile nanotrap for biochemical and functional studies with fluorescent fusion proteins. Mol Cell Proteomics 7: 282–289. doi:10.1074/mcp.M700342-MCP200.
8. Trinkle-Mulcahy L, Boulon S, Lam YW, Urcia R, Boisvert FM, et al. (2008) Identifying specific protein interaction partners using quantitative mass spectrometry and bead proteomes. J Cell Biol 183: 223–239. doi:10.1083/jcb.200805092.
9. Frauer C, Leonhardt H (2009) A versatile non-radioactive assay for DNA methyltransferase activity and DNA binding. Nucleic Acids Research 37: e22–e22. doi:10.1093/nar/gkn1029.
10. Pichler G, Wolf P, Schmidt CS, Meilinger D, Schneider K, et al. (2011) Cooperative DNA and histone binding by Uhrf2 links the two major repressive epigenetic pathways. J Cell Biochem doi:10.1002/jcb.23185.
11. Kaustov L, Quyang H, Amaya M, Lemak A, Nady N, et al. (2010) Recognition and specificity determinants of the human Cbx chromodomains. J Biol Chem doi:10.1074/jbc.M110.191411.
12. Jacobs SA, Taverna SD, Zhang Y, Briggs SD, Li J, et al. (2001) Specificity of the HP1 chromo domain for the methylated N-terminus of histone H3. EMBO J 20: 5232–5241. doi:10.1093/emboj/20.18.5232.
13. Fischle W, Tseng BS, Dormann HL, Ueberheide BM, Garcia BA, et al. (2005) Regulation of HP1-chromatin binding by histone H3 methylation and phosphorylation. Nature 438: 1116–1122. doi:10.1038/nature04219.
14. Valinluck V, Tsai H-H, Rogstad DK, Burdzy A, Bird A, et al. (2004) Oxidative damage to methyl-CpG sequences inhibits the binding of the methyl-CpG binding domain (MBD) of methyl-CpG binding protein 2 (MeCP2). Nucleic Acids Research 32: 4100–4108. doi:10.1093/nar/gkh739.
15. Nan X, Meehan RR, Bird A (1993) Dissection of the methyl-CpG binding domain from the chromosomal protein MeCP2. Nucleic Acids Research 21: 4886–4892.
16. Free A, Wakefield RI, Smith BO, Dryden DT, Barlow PN, et al. (2001) DNA recognition by the methyl-CpG binding domain of MeCP2. J Biol Chem 276: 3353–3360. doi:10.1074/jbc.M007224200.
17. Leonhardt H, Page AW, Weier HU, Bestor TH (1992) A targeting sequence directs DNA methyltransferase to sites of DNA replication in mammalian nuclei. Cell 71: 865–873.
18. Chuang LS, Ian HI, Koh TW, Ng HH, Xu G, et al. (1997) Human DNA-(cytosine-5) methyltransferase-PCNA complex as a target for p21WAF1. Science 277: 1996–2000.
19. Mortusewicz O, Leonhardt H (2007) XRCC1 and PCNA are loading platforms with distinct kinetic properties and different capacities to respond to multiple DNA lesions. BMC Mol Biol 8: 81. doi:10.1186/1471-2199-8-81.
20. Mortusewicz O, Rothbauer U, Cardoso MC, Leonhardt H (2006) Differential recruitment of DNA Ligase I and III to DNA repair sites. Nucleic Acids Research 34: 3523–3532. doi:10.1093/nar/gkl492.
21. Hiragami-Hamada K, Shinmyozu K, Hamada D, Tatsu Y, Uegaki K, et al. (2011) N-terminal phosphorylation of HP1{alpha} promotes its chromatin binding. Mol Cell Biol 31: 1186–1200. doi:10.1128/MCB.01012–10.
22. Bestor TH (2000) The DNA methyltransferases of mammals. Human Molecular Genetics 9: 2395–2402. doi:10.1093/hmg/9.16.2395.
23. Caldecott KW (2003) XRCC1 and DNA strand break repair. DNA repair 2: 955–969.
24. Tom S, Henricksen LA, Bambara RA (2000) Mechanism whereby proliferating cell nuclear antigen stimulates flap endonuclease 1. J Biol Chem 275: 10498–10505.
25. Chen U, Chen S, Saha P, Dutta A (1996) p21Cip1/Waf1 disrupts the recruitment of human Fen1 by proliferating-cell nuclear antigen into the DNA replication complex. Proc Natl Acad Sci USA 93: 11597–11602.
26. Jónsson ZO, Hindges R, Hübscher U (1998) Regulation of DNA replication and repair proteins through interaction with the front side of proliferating cell nuclear antigen. EMBO J 17: 2412–2425. doi:10.1093/emboj/17.8.2412.
27. Jacobs SA, Khorasanizadeh S (2002) Structure of HP1 chromodomain bound to a lysine 9-methylated histone H3 tail. Science 295: 2080–2083. doi:10.1126/science.1069473.
28. Viens A, Mechold U, Brouillard F, Gilbert C, Leclerc P, et al. (2006) Analysis of human histone H2AZ deposition in vivo argues against its direct role in epigenetic templating mechanisms. Molecular and Cellular Biology 26: 5325–5335. doi:10.1128/MCB.00584–06.
29. Neumann B, Held M, Liebel U, Erfle H, Rogers P, et al. (2006) High-throughput RNAi screening by time-lapse imaging of live human cells. Nat Methods 3: 385–390. doi:10.1038/nmeth876.
30. DuBridge RB, Tang P, Hsia HC, Leong PM, Miller JH, et al. (1987) Analysis of mutation in human cells by using an Epstein-Barr virus shuttle system. Molecular and Cellular Biology 7: 379–387.
31. Brero A (2005) Methyl CpG-binding proteins induce large-scale chromatin reorganization during terminal differentiation. J Cell Biol 169: 733–743. doi:10.1083/jcb.200502062.
32. Sporbert A, Domaing P, Leonhardt H, Cardoso MC (2005) PCNA acts as a stationary loading platform for transiently interacting Okazaki fragment maturation proteins. Nucleic Acids Research 33: 3521–3528. doi:10.1093/nar/gki665.
33. Leonhardt H, Rahn HP, Weinzierl P, Sporbert A, Cremer T, et al. (2000) Dynamics of DNA replication factories in living cells. J Cell Biol 149: 271–280.
34. Schermelleh L, Spada F, Easwaran HP, Zolghadr K, Margot JB, et al. (2005) Trapped in action: direct visualization of DNA methyltransferase activity in living cells. Nat Methods 2: 751–756. doi:10.1038/nmeth794.
35. Easwaran HP, Schermelleh L, Leonhardt H, Cardoso MC (2004) Replication-independent chromatin loading of Dnmt1 during G2 and M phases. EMBO Rep 5: 1181–1186. doi:10.1038/sj.embor.7400295.
36. Mortusewicz O, Schermelleh L, Walter J, Cardoso MC, Leonhardt H (2005) Recruitment of DNA methyltransferase I to DNA repair sites. Proc Natl Acad Sci USA 102: 8905–8909. doi:10.1073/pnas.0501034102.
37. Campbell RE, Tour O, Palmer AE, Steinbach PA, Baird GS, et al. (2002) A monomeric red fluorescent protein. Proc Natl Acad Sci USA 99: 7877–7882. doi:10.1073/pnas.082243699.
38. Schermelleh L, Haemmer A, Spada F, Rosing N, Meilinger D, et al. (2007) Dynamics of Dnmt1 interaction with the replication machinery and its role in postreplicative maintenance of DNA methylation. Nucleic Acids Research 35: 4301–4312. doi:10.1093/nar/gkm432.
39. Zhang J, Chung T, Oldenburg K (1999) A Simple Statistical Parameter for Use in Evaluation and Validation of High Throughput Screening Assays. J Biomol Screen 4: 67–73.

Supporting material

A

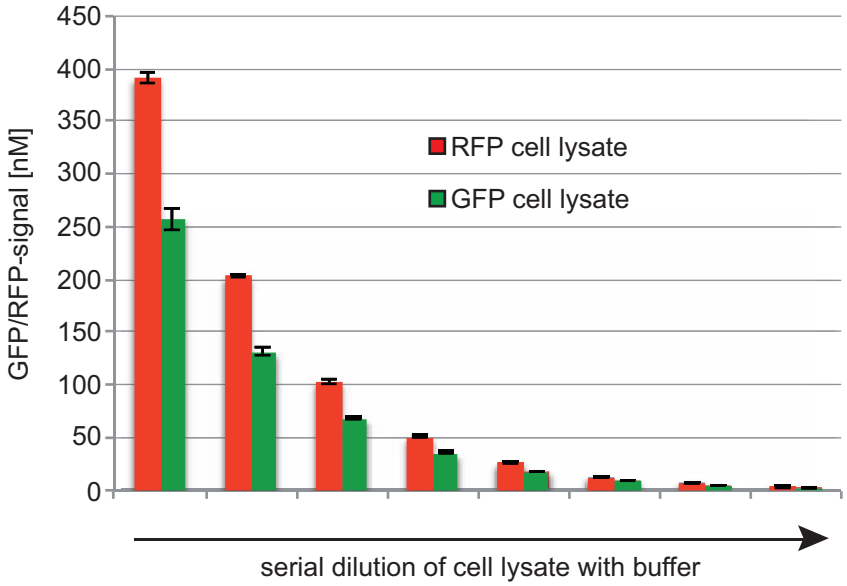

B

	GFP channel		RFP channel	
	cell lysate untransfected	blank	cell lysate untransfected	blank
FI	**33**	**14.5**	**206**	**228**
FI - blank	**18.5**	**0**	**0**	**0**
[nM]	**0.78**	**0**	**0**	**0**

Figure S1: Factors interfering the measured fluorescence intensities. (**A**) The concentrations of GFP and RFP expressed in HEK293T cells were measured in serial dilutions of crude cell extracts. Shown are means ± SD from two independent experiments. Fluorescence intensities were measured via a plate reader and the GFP and RFP concentrations were determined as described in the Material and Methods part. (**B**) Background GFP and RFP signals in cell lysates of untransfected HEK293T cells. The fluorescence intensities (FI) were measured via a plate reader and the concentrations were determined as described in the Material and Methods part.

3.3 The multi-domain protein Np95 connects DNA methylation and histone modification

1796–1804 *Nucleic Acids Research, 2010, Vol. 38, No. 6* *Published online 21 December 2009*
doi:10.1093/nar/gkp1152

The multi-domain protein Np95 connects DNA methylation and histone modification

Andrea Rottach[1], Carina Frauer[1], Garwin Pichler[1], Ian Marc Bonapace[2], Fabio Spada[1] and Heinrich Leonhardt[1,*]

[1]Ludwig Maximilians University Munich, Department of Biology II and Center for Integrated Protein Science Munich (CIPS[M]), Großhaderner Str. 2, 82152 Planegg-Martinsried, Germany and [2]University of Insubria, Department of Structural and Functional Biology, Via da Giussano 12, 21052 Busto Arsizio (VA), Italy

Received April 24, 2009; Revised November 17, 2009; Accepted November 23, 2009

ABSTRACT

DNA methylation and histone modifications play a central role in the epigenetic regulation of gene expression and cell differentiation. Recently, Np95 (also known as UHRF1 or ICBP90) has been found to interact with Dnmt1 and to bind hemimethylated DNA, indicating together with genetic studies a central role in the maintenance of DNA methylation. Using *in vitro* binding assays we observed a weak preference of Np95 and its SRA (SET- and Ring-associated) domain for hemimethylated CpG sites. However, the binding kinetics of Np95 in living cells was not affected by the complete loss of genomic methylation. Investigating further links with heterochromatin, we could show that Np95 preferentially binds histone H3 N-terminal tails with trimethylated (H3K9me3) but not acetylated lysine 9 via a tandem Tudor domain. This domain contains three highly conserved aromatic amino acids that form an aromatic cage similar to the one binding H3K9me3 in the chromodomain of HP1ß. Mutations targeting the aromatic cage of the Np95 tandem Tudor domain (Y188A and Y191A) abolished specific H3 histone tail binding. These multiple interactions of the multi-domain protein Np95 with hemimethylated DNA and repressive histone marks as well as with DNA and histone methyltransferases integrate the two major epigenetic silencing pathways.

INTRODUCTION

DNA methylation and histone modifications are crucially involved in the regulation of gene expression, inheritance of chromatin states, genome stability and differentiation (1–3). Although the biochemical networks controlling these epigenetic marks have been the subject of intensive investigation, their interconnection is still not well resolved in mammals. DNA methylation patterns are established by *de novo* DNA methyltransferases Dnmt3a and 3b, while Dnmt1 is largely responsible for maintaining genomic methylation after DNA replication (4,5). Dnmt1 possesses an intrinsic preference for hemimethylated DNA substrates (6,7) and associates with proliferating cell nuclear antigen (PCNA) at replication sites *in vivo* (8–10). The transient interaction of Dnmt1 with PCNA enhances methylation efficiency but is not strictly required to maintain genomic methylation in human and mouse cells (11,12).

Recently, Np95 has emerged as a central regulatory factor for DNA methylation and interacts with all three Dnmts (13). Np95 localizes at replication foci and its genetic ablation leads to genomic hypomethylation and developmental arrest (14–19). Np95 and its SET- and Ring- associated (SRA) domain were shown to bind hemimethylated DNA with higher affinity than corresponding symmetrically methylated or unmethylated sequences both *in vitro* and *in vivo* (17,18,20–22). In addition, crystal structures of the SRA domain complexed with hemimethylated oligonucleotides revealed flipping of the 5-methylcytosine out of the DNA double helix, a configuration that would stabilize the SRA–DNA interaction (20–22). Thus, recruitment of Dnmt1 to hemimethylated CpG sites by Np95 has been proposed as mechanism for the maintenance of genomic methylation.

In addition to its role in controlling DNA methylation, Np95 has been shown to take part in several other chromatin transactions. Np95 or its human homolog ICBP90/UHRF1 were reported to interact with the histone deacetylase HDAC1 and the histone methyltransferase G9a and to mediate silencing of a viral promoter, suggesting a role of Np95 in gene silencing through histone modification (13,23,24). Np95 binds histone H3 and displays a Ring domain-mediated E3 ubiquitin ligase activity for core histones *in vitro* and possibly histone H3 *in vivo* (25,26). The plant

*To whom correspondence should be addressed. Tel: +49 89 218074232; Fax: +49 89 218074236; Email: h.leonhardt@lmu.de

homeodomain (PHD) of Np95 has been linked to decondensation of replicating pericentric heterochromatin (PH), but it is still unclear which domains recognize specific histone modifications (16,26,27).

In this study we systematically analyzed the binding properties of Np95 and its individual domains to DNA and histone tails *in vitro* and their binding kinetics in living cells. Our data reveal a multi-functional modular structure of Np95 interconnecting DNA methylation and histone modification pathways.

MATERIALS AND METHODS

Expression constructs

Expression construct for GFP–Dnmt1 and RFP–PCNA were described previously (10,28,29). All Np95 constructs were derived by PCR from corresponding myc- and His_6-tagged Np95 constructs (25). To obtain GFP– and Cherry-fusion constructs the Dnmt1 cDNA in the pCAG–GFP–Dnmt1-IRESblast construct (11) or the pCAG–Cherry–Dnmt1–IRESblast was replaced by Np95 encoding PCR fragments. The GFP–Np95ΔTudor expression construct was derived from the GFP–Np95 construct by overlap extension PCR (30). The GFP–Tudor mutant (Y188A, Y191A) was derived from the GFP–Np95 construct by PCR-based mutagenesis (31). All constructs were verified by DNA sequencing. Throughout this study enhanced GFP (eGFP) or monomeric Cherry (mCherry) constructs were used and for simplicity referred to as GFP– or Cherry-fusions.

Cell culture, transfection and immunofluorescence staining

HEK293T cells and embryonic stem cells (ESCs) were cultured and transfected as described (11), with the exception that FuGENE HD (Roche) was used for transfection of ESCs. The *dnmt1*$^{-/-}$ J1 ESCs used in this study are homozygous for the c allele (4). For immunofluorescence staining, TKO ESCs were grown on cover slips, fixed with 3.7% formaldehyde in PBS for 10 min and permeabilized with 0.5% Triton X-100 for 5 min. After blocking with 3% BSA in PBS for 1 h endogenous Np95 was detected with a polyclonal rabbit anti-Np95 serum (32). The secondary antibody was conjugated to Alexa Fluor 568 (Molecular Probes). Nuclear counterstaining was performed with DAPI and cells were mounted in Vectashield (Vector Laboratories). Images were obtained using a TCS SP5 AOBS confocal laser scanning microscope (Leica) using a 63x/1.4 NA Plan-Apochromat oil immersion objective. Fluorophores were excited with 405 and 561 nm lasers.

In vitro DNA binding assay

The *in vitro* DNA binding assay was performed as described previously (33) with the following modifications. Two different double-stranded DNA probes were labeled with distinct fluorophores and used in direct competition (see Supplementary Figures S3 and S6 for details). DNA oligos were controlled for CG methylation state by digestion with either a CG methylation-sensitive (HpaII) or -insensitive (MspI) enzyme (Supplementary Figure S4). For extract preparation 2 mM $MgCl_2$ and 1 mg/ml DNaseI were included in the lysis buffer. Extracts from 1-3 transfected 10 cm plates were diluted to 500-1000 µl with immunoprecipitation (IP) buffer and 1 µg of GFP–Trap (34) (ChromoTek, Germany) per final assay condition was added. After washing and equilibration beads were resuspended in 500 µl of binding buffer (20 mM Tris-HCl pH 7.5, 150 mM NaCl, 0.5 mM EDTA, 1 mM DTT, 100 ng/µl BSA). Two oligonucleotide substrates were added to a final concentration of 50 nM each and incubated at room temperature (RT) for 60 min with constant mixing. Fluorescence intensity measurements were performed with a Tecan Infinite M1000 plate reader using the following excitation/emission wavelengths: 490 ± 10 nm/511 ± 10 nm for GFP, 550 ± 15 nm/580 ± 15 nm for ATTO550 and 650 ± 10 nm/670 ± 10 nm for ATTO647N. Values were adjusted using standard curves obtained with ATTO-dye coupled oligonucleotide primers and purified GFP. Binding activity was expressed as the ratio between the fluorescent signals of bound DNA probe and GFP fusion protein bound to the beads, so that the signals from bound probes are normalized to the amount of GFP fusion. Furthermore, values were normalized using a control set of DNA probes having identical sequences but distinct fluorescent labels (see Supplementary Figures S3 and S6 for details).

Peptide pull-down assay

Peptides were purchased as TAMRA conjugates (PSL, Germany) and are listed in Supplementary Figure S7. The peptide pull-down assay was performed analogously to the DNA binding assay described above. After one-step purification of GFP fusion proteins with the GFP–Trap (ChromoTek, Germany), the beads were equilibrated in 1 ml IP buffer and resuspended in 500 µl binding buffer supplemented with 100 ng/µl of BSA. Peptides were added to a final concentration of 0.74 µM and the binding reaction was performed at RT for 15 min to 60 min with constant mixing. The beads were washed twice with 1 ml of IP buffer and resuspended in 100 µl of the same. Wavelengths for excitation and measurement of TAMRA were 490 ± 5 nm and 511 ± 5 nm, respectively. Fluorescence intensity measurements were adjusted using standard curves from TAMRA coupled peptide and purified GFP.

Live cell microscopy and fluorescence recovery after photobleaching analysis

Live cell imaging and fluorescence recovery after photobleaching (FRAP) analysis were performed as described previously (11). For presentation, we used linear contrast enhancement on entire images.

Statistical analysis

Results were expressed as mean ± SEM. The difference between two mean values was analyzed by Student's *t*-test and was considered to be statistically significant in case of $P < 0.05$ and highly significant with $P < 0.001$.

Electrophoretic mobility shift and supershift assays

Un- and hemimethylated DNA substrates (1 pmol UMB550 and HMB647N, respectively) were incubated with 0.6 pmol purified GFP–Np95 and 0.4 pmol GFP–antibody (mouse monoclonal antibody, Roche). Samples were subjected to a 3.5% non-denaturing PAGE and analyzed with a fluorescence scanner (Typhoon Trio scanner; GE Healthcare) to detect ATTO550 (unmethylated substrate), ATTO647N (hemimethylated substrate) and green fluorescence (GFP–Np95).

RESULTS AND DISCUSSION

Np95 binding kinetics is largely independent of DNA methylation levels *in vivo*

Recent studies showed Np95 bound to hemimethylated DNA, suggesting that the essential function of Np95 in the maintenance of DNA methylation consists of substrate recognition and recruitment of Dnmt1. To investigate the dynamics of these interactions *in vivo* we transiently transfected wild-type (wt) J1 ESCs with expression constructs for Cherry-Np95 and GFP–Dnmt1 and monitored their subcellular distribution using live-cell microscopy (Figure 1A and B). Np95 showed a nuclear distribution with a cell cycle-dependent enrichment at replicating PH, similar to Dnmt1. Consistent with earlier observations (8,12,14–16) we detected co-localization of Np95 and Dnmt1 at sites of DNA replication. We investigated the dynamics of Np95 binding by quantitative fluorescence recovery after photobleaching (FRAP) analysis (Figure 1B). As chromocenters (aggregates of PH) are not homogeneously distributed in the nucleus, we chose to bleach half nuclei to ensure that the bleached region contains a representative number of potential binding sites. We observed a relatively fast and full recovery of relative GFP–Dnmt1 fluorescence intensity (Figure 1B), reflecting a transient and dynamic interaction as described before (11). In contrast, Cherry-Np95 showed a considerably slower and only partial (~80%) recovery within the same observation period. These results indicated a relatively stable binding of Np95 to chromatin and revealed an immobile protein fraction of about 20%. These *in vivo* binding properties would be consistent with tight binding of Np95 to hemimethylated CpG sites and flipping of the methylated cytosines out of the DNA double helix as shown in recent co-crystal structures of the SRA domain of Np95 (20–22).

To directly test the contribution of DNA methylation and the interaction with Dnmt1 to protein mobility, we compared the binding kinetics of GFP–Np95 in wt ESCs and ESCs lacking either Dnmt1 or all three major DNA methyltransferases Dnmt1, 3a and 3b (triple knockout, TKO). Surprisingly, Np95 binding to chromatin was not affected by either drastic reduction (*dnmt1*$^{-/-}$) or even complete loss (TKO) of genomic methylation and showed in both cases remarkably similar FRAP kinetics compared to wt J1 ESCs (Figure 1C). Similar results were obtained with a C-terminal GFP fusion (Np95-GFP; Supplementary Figure S1), arguing against conformational or sterical impairments of the N-terminal fusion protein that could affect the binding kinetics. Also, both, the levels of endogenous Np95 and its degree of accumulation at chromocenters were highly variable in TKO cells, with chromocenter accumulation clearly visible in some cells (Supplementary Figure S2). These results show that DNA methylation and the three DNA methyltransferases do not have a major effect on the overall binding kinetics of Np95 in living cells.

The SRA domain of Np95 is necessary and sufficient for DNA binding *in vitro*

Next, we investigated the DNA binding activity of Np95 and the contribution of distinct Np95 domains by generating a systematic set of individual domains and deletion constructs fused to GFP (Figure 2A). To directly compare the *in vitro* binding affinity of Np95 regarding different methylation states, we synthesized double-stranded DNA-binding substrates with either one or three un- or hemimethylated CpG sites and labeled them with two distinct fluorophores (Supplementary Figure S3). DNA probes were controlled for CG methylation state by digestion with either a CG methylation-sensitive (HpaII) or -insensitive (MspI) enzyme (Supplementary Figure S4). Performing conventional electrophoretic mobility shift and supershift assays we confirmed the DNA binding activity of Np95 and detected a preference for hemimethylated DNA substrates (Figure 2B and Supplementary Figure S5).

As a second line of evidence and to quantify binding preferences, we applied our recently developed non-radioactive DNA binding assay (33) and tested GFP–fused wt Np95 as well as a systematic set of individual domains and deletion constructs for their DNA-binding properties *in vitro* (Figure 2C and Supplementary Figure S6). This assay allows fast comparison of different potential binding substrates in direct competition as well as the simultaneous quantification of GFP–labeled protein to calculate relative binding activity. The different GFP–Np95 fusion constructs were expressed in HEK293T cells, purified with the GFP–Trap (34) and incubated with the fluorescently labeled DNA substrates. GFP–fusion protein and bound DNA substrates were quantified with a fluorescence plate reader (Figure 2C and Supplementary Figure S6). Furthermore, results were corrected for any bias due to incorporation of different fluorescent labels (Supplementary Figures. S3 and S6). Under these assay conditions we observed an up to 2-fold preference (factor 1.6–1.9) of Np95 for DNA substrates containing one or three hemimethylated CpG sites (Supplementary Figure S6). Deletion of the SRA domain completely abolished the DNA-binding activity of Np95, whereas deletion of either the PHD or the Tudor domain had no effect (Figure 2C). Consistently, the isolated PHD and Tudor domains did not bind to DNA, while the SRA domain alone showed similar binding strength and sequence preference as full-length Np95. Together, these results clearly demonstrate that the SRA domain of Np95 preferentially binds to hemimethylated CpG sites, although this

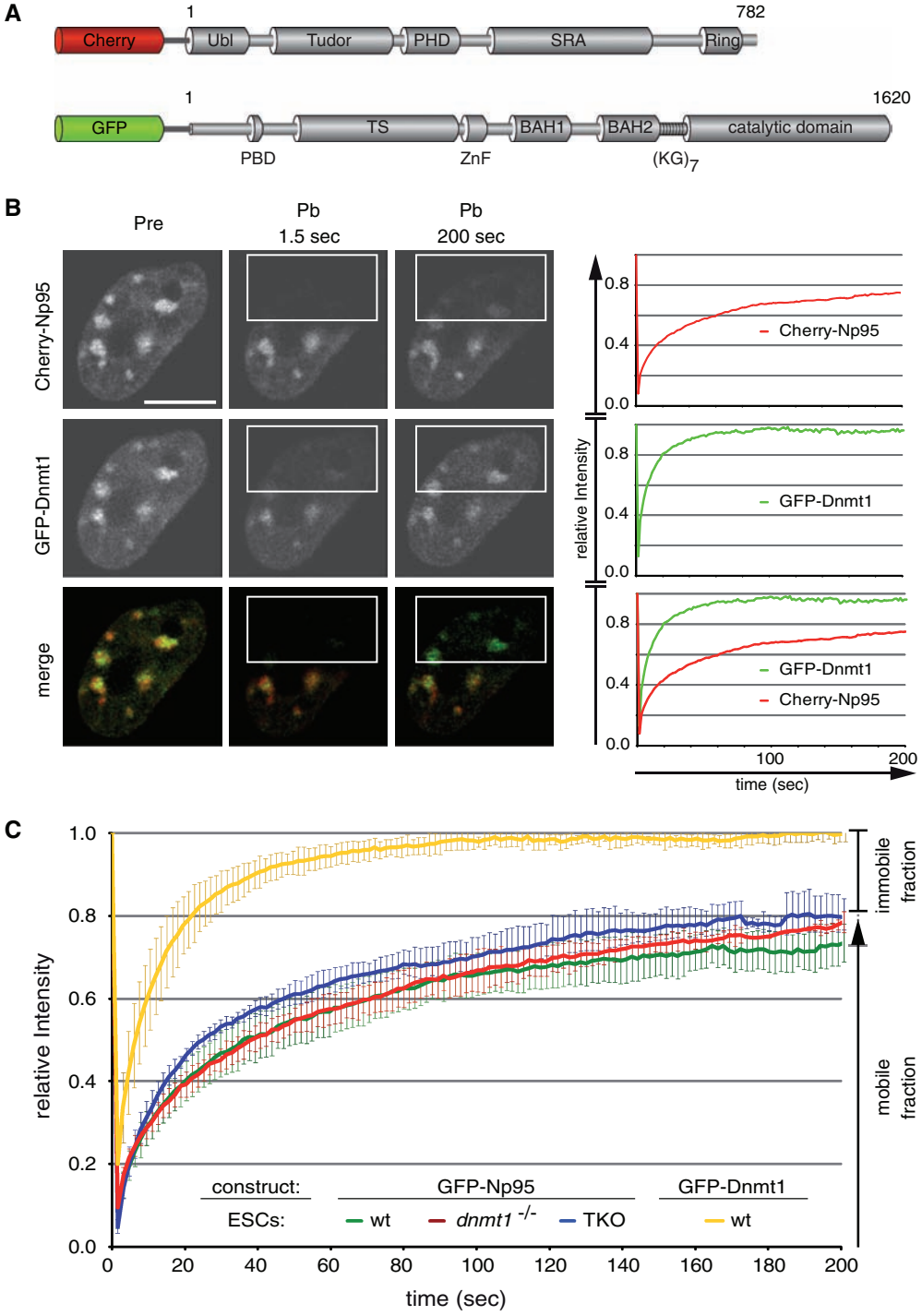

Figure 1. Binding kinetics of Dnmt1 and Np95 in living cells. (**A**) Schematic representation of Np95 and Dnmt1 fluorescent fusions. Ubl, ubiquitin-like domain; Tudor, tandem Tudor domain; PHD, plant homeodomain; SRA, SET- and Ring-associated domain; Ring domain; PBD, PCNA-binding domain; TS, targeting sequence; ZnF, zinc-finger; BAH, bromo adjacent homology domain; $(KG)_7$, lysine-glycine repeat. (**B**) Dnmt1 and Np95 display different kinetics. Representative images from FRAP experiments on wt J1 ESCs transiently co-transfected with Cherry-Np95 and GFP–Dnmt1 constructs. Images show co-localization at chromocenters before (Pre) and at the indicated time points after (Pb) bleaching half of the nucleus. Bleached areas are outlined. Corresponding FRAP curves are shown on the right. Bars, 5 µm. (**C**) FRAP kinetics of GFP–Np95 in J1 ESCs with different genetic backgrounds [wt, *dnmt1*$^{-/-}$ and *dnmt1*$^{-/-}$, 3a$^{-/-}$, 3b$^{-/-}$ (TKO)]. Kinetics of GFP–Dnmt1 is shown for comparison. Mobile and immobile fractions are indicated on the right. Values represent mean ± SEM.

preference is only about 2-fold with purified proteins and substrates *in vitro*.

The SRA domain dominates binding kinetics but not localization of Np95

Next, we investigated the role of distinct Np95 domains in nuclear interactions *in vivo*. To this aim, we expressed the same GFP–Np95 constructs in *np95*$^{-/-}$ ESCs and tested their binding kinetics with FRAP experiments (Figure 2D). Importantly, GFP–Np95 showed similar FRAP kinetics in Np95 deficient, wt or Dnmt-deficient ESCs (Figures 1C and 2D). Among all domains tested, only the SRA domain showed similar kinetics as full-length Np95, including the relatively slow recovery and an immobile fraction of about 20%, while the Tudor and PHD domain displayed the same high mobility as GFP. Also, FRAP curves of the corresponding deletion constructs indicated that the Tudor and the PHD domains have only a minor contribution to *in vivo* binding kinetics, while deletion of the SRA domain drastically increased the mobility of Np95. These data indicate that the SRA domain dominates the binding kinetics of Np95 *in vivo*. Curiously, the addition of the PHD to the SRA domain (GFP–PHD-SRA) resulted in intermediate kinetics and loss of the immobile fraction. This effect was, however, not observed in the context of the full-length protein, suggesting that nuclear interactions of Np95 are controlled by a complex interplay among its domains. To directly study the role of the SRA domain in controlling the subcellular localization of Np95 we co-transfected *np95*$^{-/-}$ ESCs with expression constructs for Cherry-Np95 and either GFP–SRA or GFP–Np95ΔSRA (Figure 2E). This direct comparison showed that the isolated SRA domain does not co-localize with full-length Np95 at PH. Together, these results indicate that the SRA domain of Np95 is necessary and sufficient for DNA binding *in vitro* and also dominates the binding kinetics *in vivo*, but is *per se* not sufficient for proper subnuclear localization. The fact that the Np95ΔSRA construct co-localized with Np95 suggests that other domains than the SRA control the subcellular targeting of Np95.

Np95 binds to histone H3 via a tandem Tudor domain

Database searches showed that the sequence between the Ubl and PHD domains of Np95 is highly conserved in vertebrates and displays structural similarity to the family of Tudor domains [(35); PDB 3db4; Figure 3A and B]. The crystal structure revealed that the Tudor domain is composed of two subdomains (tandem Tudor) forming a hydrophobic pocket that accommodates a histone H3 N-terminal tail trimethylated at K9 (H3K9me3) (PDB 3db3; Figure 3C). This hydrophobic-binding pocket is created by three highly conserved amino acids (Phe152, Tyr188, Tyr191) forming an aromatic cage (Figure 3A and C). Interestingly, a very similar hydrophobic cage structure has been described for the chromodomain of the heterochromatin protein 1ß (HP1ß) (Supplementary Figure S7) that is known to bind trimethylated lysine 9 of histone H3 and associates with PH (36).

To further investigate the histone tail-binding properties of Np95, we mutated two amino acids of the aromatic cage (Y188A, Y191A) and tested the isolated tandem Tudor domain and corresponding mutant in comparison with Np95 using a peptide binding assay. GFP–Np95, GFP–Tudor and GFP–Tudor (Y188A, Y191A) were expressed in HEK293T cells, purified with the GFP–Trap and incubated with TAMRA-labeled histone tail peptides. The fluorescence intensity of GFP fusion proteins and bound peptides was quantified and the relative binding activity calculated (Figure 3D and Supplementary Figure S7). The tandem Tudor domain showed a highly significant preference for the trimethylated (H3K9me3) peptide, while this effect was less pronounced in the full-length Np95. Interestingly, acetylation of K9 (H3K9ac), a modification largely underrepresented in silent chromatin, prevented binding of the tandem Tudor domain. Remarkably, point mutations targeting aromatic cage residues within the tandem Tudor domain completely abolished specific binding to N-terminal histone H3 peptides.

Consistent with these binding data the tandem Tudor domain also showed a weak enrichment at PH, while the PHD domain, previously proposed as potential histone H3-binding motif (26), did neither bind to H3K9 peptides *in vitro* nor to PH *in vivo* (Supplementary Figure S8). These results indicate that the tandem Tudor domain of Np95 features a peptide binding pocket with structural and functional striking similarity to HP1ß and confers selective binding to histone modification states associated with silent chromatin.

These multiple interactions of Np95 with heterochromatin components correlate well with functional data. The depletion of Np95 in mouse cells resulted in increased transcription of major satellite repeats (16). Also, an interaction of Np95 with G9a was described and both were found to be essential for transcriptional regulation (24) and epigenetic silencing of transgenes (13).

In summary, we showed that the SRA domain is necessary and sufficient for DNA binding of Np95 *in vitro*. Photobleaching experiments further indicated that the SRA domain also dominates the binding kinetics of Np95 in living cells which was however largely independent of the DNA methylation level. These results suggest that the SRA domain may also bind to unmethylated DNA or undergo additional, still unidentified interactions *in vivo*. While the essential role of Np95 in the maintenance of DNA methylation is well established, it is still unclear how a relatively weak preference for hemimethylated DNA can be sufficient to maintain DNA methylation patterns over many cell division cycles for an entire life time. We suggest that the multiple interactions of the multi-domain protein Np95 with hemimethylated DNA and H3K9 methylated histone tails as well as with histone (G9a) and DNA (Dnmt1, 3a and 3b) methyltransferases may add up to the necessary specificity *in vivo*. Clearly, these multiple interactions place Np95 at the center of various epigenetic silencing mechanisms and likely mediate epigenetic crosstalk.

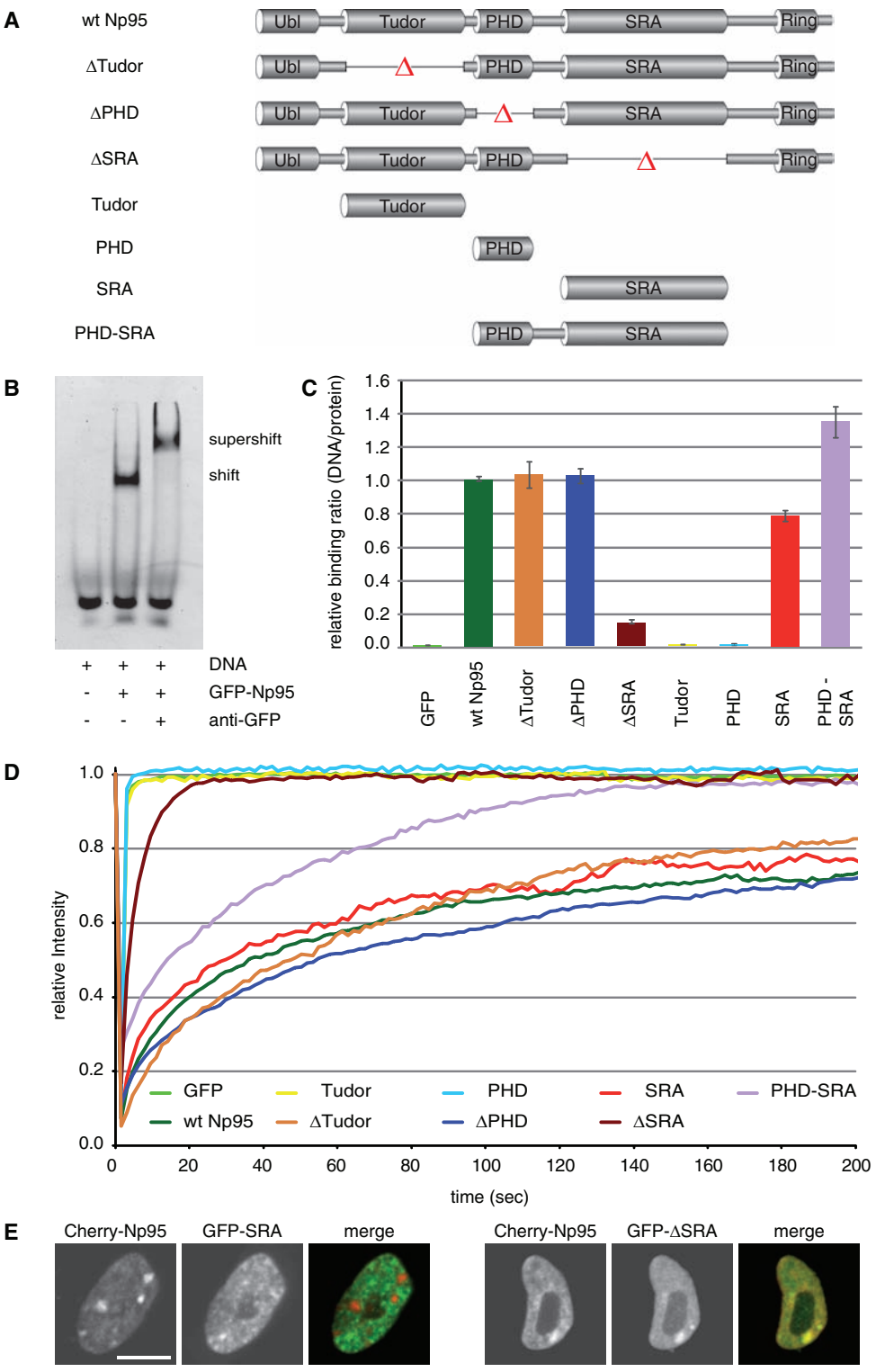

Figure 2. *In vitro* DNA binding and *in vivo* mobility of Np95 domains. (**A**) Schematic representation of the analyzed GFP–Np95 fusion constructs. (**B**) Electrophoretic mobility shift and supershift assay. GFP–Np95 binding to hemimethylated DNA substrates is shown by the shifted GFP–Np95:DNA complex. The addition of a GFP–antibody supershifted the GFP–Np95:DNA complex (supershift assay with unmethylated DNA substrates in direct competition with hemimethylated DNA substrates is shown in Supplementary Figure S6). (**C**) *In vitro* DNA-binding properties of Np95 constructs. Binding assays were performed using fluorescently labeled double stranded oligonucleotide probes containing one central hemimethylated CpG site. Shown are fluorescence intensity ratios of bound probe/bound GFP fusion. Values represent means and SD of three to six independent experiments. GFP was used as control. Further control experiments with either one or three central CpG sites and alternating fluorescent labels are shown in Supplementary Figure S3. (**D**) Kinetics of Np95 constructs in living *np95*$^{-/-}$ ESCs determined by half nucleus FRAP analysis. GFP is shown as reference. Curves represent mean values from 6 to 15 nuclei. SEM (0.001–0.005) is not shown for clarity of illustration. (**E**) Confocal mid-sections of living *np95*$^{-/-}$ ESCs transiently expressing the indicated Np95 fusion constructs (left and mid-panels). Merged images are displayed on the right. Bar, 5 μm.

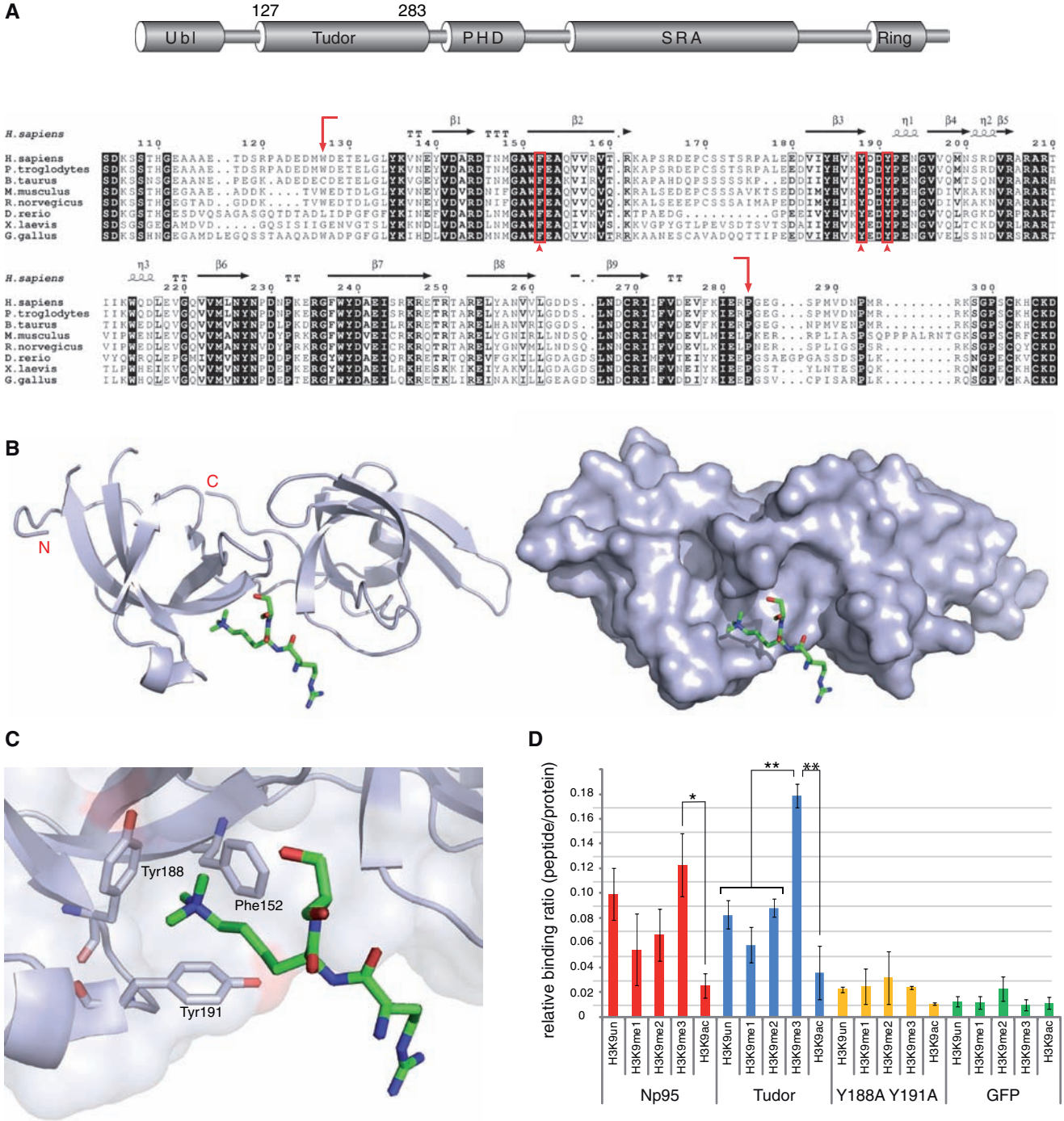

Figure 3. Structure and H3 N-terminal tail binding of the tandem Tudor domain. (**A**) Schematic drawing of the multi-domain architecture of Np95 (top) and alignment of tandem Tudor domains from vertebrate Np95 homologs (bottom). Arrows show the end and start positions of the crystallized tandem Tudor domain shown in (**B**). Residues forming the aromatic cage shown in (**C**) are indicated by arrowheads. Absolutely conserved residues of the tandem Tudor domain are black shaded, while positions showing conservative substitutions are boxed with residues in bold face. Secondary-structure elements were generated with EsPript (37) using the crystal structure of human UHRF1 (PDB 3db3 and 3db4) and are shown above the amino acid sequence: α-helices (η), β-strands, strict alpha turns (TT) and strict beta turns (TTT). Accession numbers: *Homo sapiens* Q96T88.1; *Pan troglodytes* XP_001139916.1; *Bos Taurus* AAI51672.1; *Mus musculus* Q8VDF2.2; *Rattus norvergicus* Q7TPK1.2; *Dario rerio* NP_998242.1; *Xenopus laevis* ABY28114.1, *Gallus gallus* XP_418269.2. (B) Side view of the tandem Tudor domain as a cartoon model (left) and as surface representation (right) in complex with a histone H3 N-terminal tail peptide trimethylated at lysine 9 (green stick model; only Arg8-Lys9-Ser10 of the H3 peptide are resolved). The image was generated with PyMOL (38). (C) An aromatic cage is formed by Phe152, Tyr188 and Tyr191 and accommodates the trimethylated lysine 9 of H3 (H3K9me3). (**D**) Histone H3 N-terminal tail binding specificity of GFP–Np95, GFP–Tudor and GFP–Tudor (Y188A Y191A) *in vitro*. Shown are fluorescence intensity ratios of bound probe/bound GFP fusion. GFP was used as negative control. Shown are means ± SEM from four to ten independent experiments and two-sample t-tests were performed that do or do not assume equal variances, respectively. Statistical significance compared to the binding ratio of H3K9me3 is indicated: $*P < 0.05$, $**P < 0.001$.

SUPPLEMENTARY DATA

Supplementary Data are available at NAR Online.

ACKNOWLEDGMENTS

The authors are grateful to Masahiro Muto and Haruhiko Koseki (RIKEN Research Center for Allergy and Immunology, Yokohama, Japan) for providing wild-type and *np95*$^{-/-}$ E14 ESCs, to En Li (Novartis Institutes for Biomedical Research, Boston, MA) for *dnmt1*$^{-/-}$ and J1 ESCs and to Masaki Okano (RIKEN Center for Developmental Biology, Kobe, Japan) for the TKO ESCs.

FUNDING

This work was supported by the Nanosystems Initiative Munich (NIM), the BioImaging Network Munich (BIN) and by grants from the Deutsche Forschungsgemeinschaft (DFG) to H.L. IMB was supported by the Italian Association for Cancer Research (AIRC), the Fondazione CARIPLO Progetto NOBEL. C.F. and G.P. were supported by the International Doctorate Program NanoBioTechnology (IDK-NBT) and the International Max Planck Research School for Molecular and Cellular Life Sciences (IMPRS-LS). Funding for open access charges: DFG.

Conflict of interest statement. None declared.

REFERENCES

1. Bird,A. (2002) DNA methylation patterns and epigenetic memory. *Genes Dev.*, **16**, 6–21.
2. Kouzarides,T. (2007) Chromatin modifications and their function. *Cell*, **128**, 693–705.
3. Reik,W. (2007) Stability and flexibility of epigenetic gene regulation in mammalian development. *Nature*, **447**, 425–432.
4. Lei,H., Oh,S., Okano,M., Juttermann,R., Goss,K., Jaenisch,R. and Li,E. (1996) De novo DNA cytosine methyltransferase activities in mouse embryonic stem cells. *Development*, **122**, 3195–3205.
5. Okano,M., Bell,D.W., Haber,D.A. and Li,E. (1999) DNA methyltransferases Dnmt3a and Dnmt3b are essential for de novo methylation and mammalian development. *Cell*, **99**, 247–257.
6. Bestor,T.H. and Ingram,V.M. (1983) Two DNA methyltransferases from murine erythroleukemia cells: purification, sequence specificity, and mode of interaction with DNA. *Proc. Natl Acad. Sci. USA*, **80**, 5559–5563.
7. Pradhan,S., Talbot,D., Sha,M., Benner,J., Hornstra,L., Li,E., Jaenisch,R. and Roberts,R. (1997) Baculovirus-mediated expression and characterization of the full-length murine DNA methyltransferase. *Nucleic Acids Res.*, **25**, 4666–4673.
8. Leonhardt,H., Page,A.W., Weier,H.U. and Bestor,T.H. (1992) A targeting sequence directs DNA methyltransferase to sites of DNA replication in mammalian nuclei. *Cell*, **71**, 865–873.
9. Chuang,L.S.-H., Ian,H.-I., Koh,T.-W., Ng,H.-H., Xu,G. and Li,B.F.L. (1997) Human DNA-(cytosine-5) methyltransferase-PCNA complex as a target for p21WAF1. *Science*, **277**, 1996–2000.
10. Easwaran,H.P., Schermelleh,L., Leonhardt,H. and Cardoso,M.C. (2004) Replication-independent chromatin loading of Dnmt1 during G2 and M phases. *EMBO Rep.*, **5**, 1181–1186.
11. Schermelleh,L., Haemmer,A., Spada,F., Rosing,N., Meilinger,D., Rothbauer,U., Cristina Cardoso,M. and Leonhardt,H. (2007) Dynamics of Dnmt1 interaction with the replication machinery and its role in postreplicative maintenance of DNA methylation. *Nucleic Acids Res.*, **35**, 4301–43012.
12. Spada,F., Haemmer,A., Kuch,D., Rothbauer,U., Schermelleh,L., Kremmer,E., Carell,T., Langst,G. and Leonhardt,H. (2007) DNMT1 but not its interaction with the replication machinery is required for maintenance of DNA methylation in human cells. *J. Cell Biol.*, **176**, 565–571.
13. Meilinger,D., Fellinger,K., Bultmann,S., Rothbauer,U., Bonapace,I.M., Klinkert,W.E., Spada,F. and Leonhardt,H. (2009) *EMBO Rep*, **10**, 1259–1264.
14. Uemura,T., Kubo,E., Kanari,Y., Ikemura,T., Tatsumi,K. and Muto,M. (2000) Temporal and spatial localization of novel nuclear protein NP95 in mitotic and meiotic cells. *Cell Struct. Funct.*, **25**, 149–159.
15. Miura,M., Watanabe,H., Sasaki,T., Tatsumi,K. and Muto,M. (2001) Dynamic changes in subnuclear NP95 location during the cell cycle and its spatial relationship with DNA replication foci. *Exp. Cell Res.*, **263**, 202–208.
16. Papait,R., Pistore,C., Negri,D., Pecoraro,D., Cantarini,L. and Bonapace,I.M. (2007) Np95 is implicated in pericentromeric heterochromatin replication and in major satellite silencing. *Mol. Biol. Cell*, **18**, 1098–1106.
17. Bostick,M., Kim,J.K., Esteve,P.-O., Clark,A., Pradhan,S. and Jacobsen,S.E. (2007) UHRF1 plays a role in maintaining dna methylation in mammalian cells. *Science*, **317**, 1760–1764.
18. Sharif,J., Muto,M., Takebayashi,S., Suetake,I., Iwamatsu,A., Endo,T.A., Shinga,J., Mizutani-Koseki,Y., Toyoda,T., Okamura,K. *et al.* (2007) The SRA protein Np95 mediates epigenetic inheritance by recruiting Dnmt1 to methylated DNA. *Nature*, **450**, 908–912.
19. Achour,M., Jacq,X., Ronde,P., Alhosin,M., Charlot,C., Chataigneau,T., Jeanblanc,M., Macaluso,M., Giordano,A., Hughes,A.D. *et al.* (2008) The interaction of the SRA domain of ICBP90 with a novel domain of DNMT1 is involved in the regulation of VEGF gene expression. *Oncogene*, **27**, 2187–2197.
20. Arita,K., Ariyoshi,M., Tochio,H., Nakamura,Y. and Shirakawa,M. (2008) Recognition of hemi-methylated DNA by the SRA protein UHRF1 by a base-flipping mechanism. *Nature*, **455**, 818–821.
21. Avvakumov,G.V., Walker,J.R., Xue,S., Li,Y., Duan,S., Bronner,C., Arrowsmith,C.H. and Dhe-Paganon,S. (2008) Structural basis for recognition of hemi-methylated DNA by the SRA domain of human UHRF1. *Nature*, **455**, 822–825.
22. Qian,C., Li,S., Jakoncic,J., Zeng,L., Walsh,M.J. and Zhou,M.M. (2008) Structure and hemimethylated CpG binding of the SRA domain from human UHRF1. *J. Biol. Chem.*, **283**, 34490–34494.
23. Unoki,M., Nishidate,T. and Nakamura,Y. (2004) ICBP90, an E2F-1 target, recruits HDAC1 and binds to methyl-CpG through its SRA domain. *Oncogene*, **23**, 7601–7610.
24. Kim,J.K., Esteve,P.O., Jacobsen,S.E. and Pradhan,S. (2009) UHRF1 binds G9a and participates in p21 transcriptional regulation in mammalian cells. *Nucleic Acids Res.*, **37**, 493–505.
25. Citterio,E., Papait,R., Nicassio,F., Vecchi,M., Gomiero,P., Mantovani,R., Di Fiore,P.P. and Bonapace,I.M. (2004) Np95 is a histone-binding protein endowed with ubiquitin ligase activity. *Mol. Cell Biol.*, **24**, 2526–2535.
26. Karagianni,P., Amazit,L., Qin,J. and Wong,J. (2008) ICBP90, a novel methyl K9 H3 binding protein linking protein ubiquitination with heterochromatin formation. *Mol. Cell Biol.*, **28**, 705–717.
27. Papait,R., Pistore,C., Grazini,U., Babbio,F., Cogliati,S., Pecoraro,D., Brino,L., Morand,A.L., Dechampesme,A.M., Spada,F. *et al.* (2008) The PHD domain of Np95 (mUHRF1) is involved in large-scale reorganization of pericentromeric heterochromatin. *Mol. Biol. Cell*, **19**, 3554–3563.
28. Schermelleh,L., Spada,F., Easwaran,H.P., Zolghadr,K., Margot,J.B., Cardoso,M.C. and Leonhardt,H. (2005) Trapped in action: direct visualization of DNA methyltransferase activity in living cells. *Nat. Methods*, **2**, 751–756.
29. Sporbert,A., Domaing,P., Leonhardt,H. and Cardoso,M.C. (2005) PCNA acts as a stationary loading platform for transiently interacting Okazaki fragment maturation proteins. *Nucleic Acids Res.*, **33**, 3521–3528.

30. Ho,S.N., Hunt,H.D., Horton,R.M., Pullen,J.K. and Pease,L.R. (1989) Site-directed mutagenesis by overlap extension using the polymerase chain reaction. *Gene*, **77**, 51–59.
31. Ko,J.K. and Ma,J. (2005) A rapid and efficient PCR-based mutagenesis method applicable to cell physiology study. *Am. J. Physiol. Cell Physiol.*, **288**, C1273–1278.
32. Bonapace,I.M., Latella,L., Papait,R., Nicassio,F., Sacco,A., Muto,M., Crescenzi,M. and Di Fiore,P.P. (2002) Np95 is regulated by E1A during mitotic reactivation of terminally differentiated cells and is essential for S phase entry. *J. Cell Biol.*, **157**, 909–914.
33. Frauer,C. and Leonhardt,H. (2009) A versatile non-radioactive assay for DNA methyltransferase activity and DNA binding. *Nucleic Acids Res.*, **37**, e22.
34. Rothbauer,U., Zolghadr,K., Muyldermans,S., Schepers,A., Cardoso,M.C. and Leonhardt,H. (2008) A versatile nanotrap for biochemical and functional studies with fluorescent fusion proteins. *Mol. Cell Proteomics*, **7**, 282–289.
35. Adams-Cioaba,M.A. and Min,J. (2009) Structure and function of histone methylation binding proteins. *Biochem. Cell Biol.*, **87**, 93–105.
36. Jacobs,S.A. and Khorasanizadeh,S. (2002) Structure of HP1 chromodomain bound to a lysine 9-methylated histone H3 tail. *Science*, **295**, 2080–2083.
37. Gouet,P., Courcelle,E., Stuart,D.I. and Metoz,F. (1999) ESPript: analysis of multiple sequence alignments in PostScript. *Bioinformatics*, **15**, 305–308.
38. DeLano,W.L. (2008) The PyMOL Molecular Graphics System. *DeLano Scientific LLC*. Palo Alto, CA, USA.

SUPPLEMENTARY INFORMATION

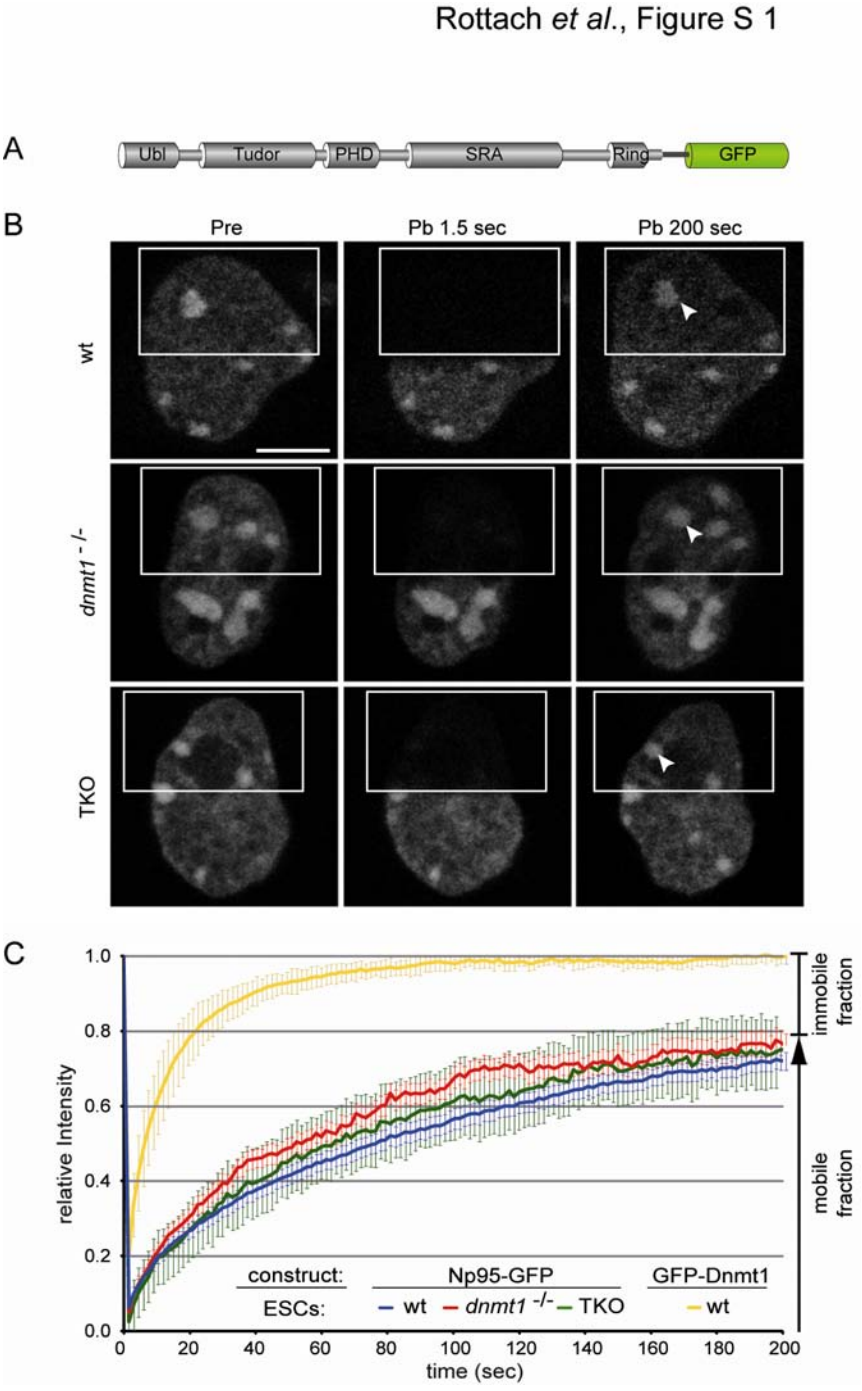

Supplementary Figure 1. Nuclear localization, FRAP kinetics and DNA binding specificity for an Np95 construct C-terminally fused to GFP (Np95-GFP, respectively). (**A**) Schematic drawing of Np95-GFP. Abbreviations are as in Fig. 1. (**B**) Representative images from FRAP experiments for Np95-GFP transiently expressed in wt, *dnmt1*$^{-/-}$ and TKO J1 ESCs as indicated on the left. Images show confocal mid-sections of nuclei before (Pre) and at the indicated time points after bleaching (Pb) half of the nucleus. Bleached areas are outlined. Arrowheads mark pericentric heterochromatin. Bars, 5 µm. **(C**) FRAP kinetics of Np95-GFP in J1 ESCs with different genetic backgrounds as shown in B and Fig. 1C. Kinetics of GFP-Dnmt1 is shown for comparison. Mobile and immobile fractions are indicated on the right. Values represent mean ± SEM. Note that the kinetics are similar to those shown for GFP-Np95 in Fig. 1C and that there is no significant difference in cells with different genetic backgrounds.

Rottach *et al.*, Figure S 2

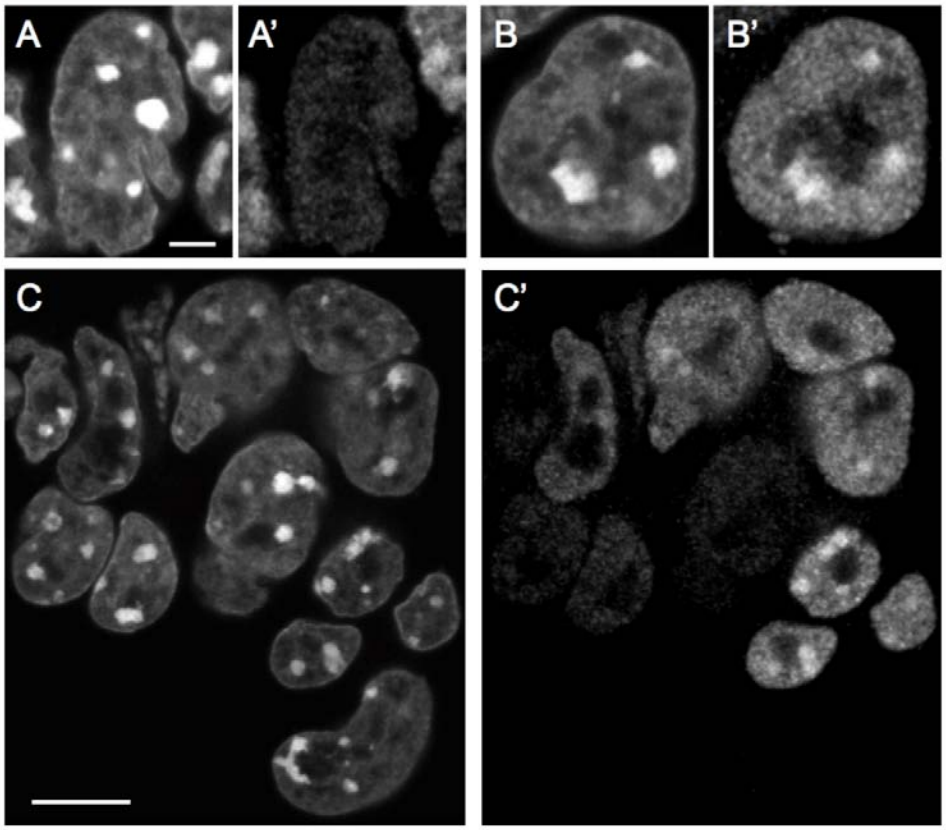

Supplementary Figure 2. Variable expression levels and localization of Np95 in TKO cells. TKO cells were stained with DAPI (A, B and C) and an anti-Np95 antibody (A', B' and C'). A-A' and B-B' show examples of cells with very low and high Np95 levels, respectively. In B' accumulation of endogenous Np95 at chromocenters is evident. C and C' show a field containing cells with very different Np95 levels and degrees of Np95 accumulation at chromocenters. Scale bars are 3 μm (A-B') and 10 μm (C and C').

Rottach *et al.*, Figure S 3

A

Oligo name	DNA sequence
CG-up	5'- CTCAACAACTAACTACCATCCGGACCAGAAGAGTCATCATGG -3'
MG-up	5'- CTCAACAACTAACTACCATCMGGACCAGAAGAGTCATCATGG -3'
3CG-up	5'-CTCAACAACTAACTACCATCCGGACCTCATCCGGACCTCATCCGGACCAGAAGAGTCATCATGG -3'
Fill-In-550	5'- ATTO550-CCATGATGACTCTTCTGGTC -3'
Fill-In-647N	5'- ATTO647N-CCATGATGACTCTTCTGGTC -3'

B

Substrate	CpG site	Label	Oligo I	Oligo II	dCTP reaction
UMB-550	unmethylated	550	CG-up	Fill-In-550	dCTP
UMB-647N		647N		Fill-In-647N	
HMB-550	hemimethylated	550	MG-up	Fill-In-550	dCTP
HMB-647N		647N		Fill-In-647N	
UMB-3CG-550	unmethylated	550	3CG-up	Fill-In-550	dCTP
UMB-3CG-647N		647N		Fill-In-647N	
HMB-3CG-550	hemimethylated	550	3CG-up	Fill-In-550	5methyl dCTP
HMB-3CG-647N		647N		Fill-In-647N	

Supplementary Figure 3. Oligo design for the *in vitro* DNA binding assay (**A**) DNA oligonucleotides used for the preparation of double stranded probes for *in vitro* DNA binding assays. M: 5-methyl-cytosine. (**B**) Description of double stranded probes used for *in vitro* DNA binding assays. Name, status of the central CpG site, fluorescent label, as well as DNA oligonucleotides and nature of the dCTP used in the primer extension reaction are specified. By using a control set of two probes with identical sequence but different fluorescent labels we observed effects due to probe preparation and/or unspecific binding of ATTO dyes (data not shown). The values obtained from the control set were used to normalize every probe / protein pair.

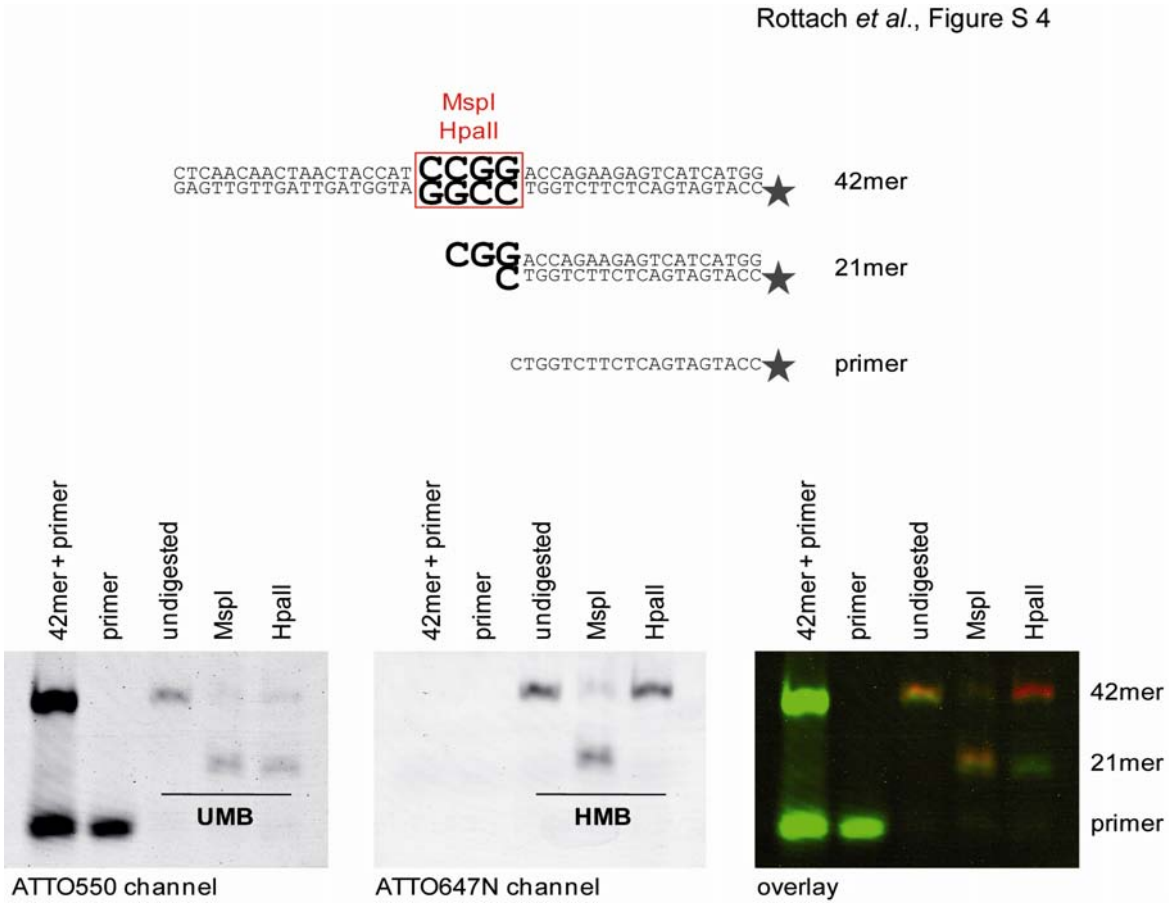

Supplementary Figure 4. Quality control of un- and hemi-methylated DNA substrates

Unmethylated and hemimethylated DNA substrates (UMB550 and HMB647N, respectively) were digested with MspI or HpaII and analyzed by 15 % non-denaturing PAGE for CG methylation. DNA substrates were detected via their fluorescent ATTO label using the Typhoon Trio scanner. Note that the unmethylated DNA substrate is digested by both MspI and HpaII, whereas the hemimethylated substrate is cut by MspI, but not by the methylation sensitive HpaII. Sequences of the double stranded probes before (42mer) and after cut (21mer) as well as the unextended primer are displayed above. Enzyme recognition motifs are boxed and asterisks represent fluorescent ATTO label.

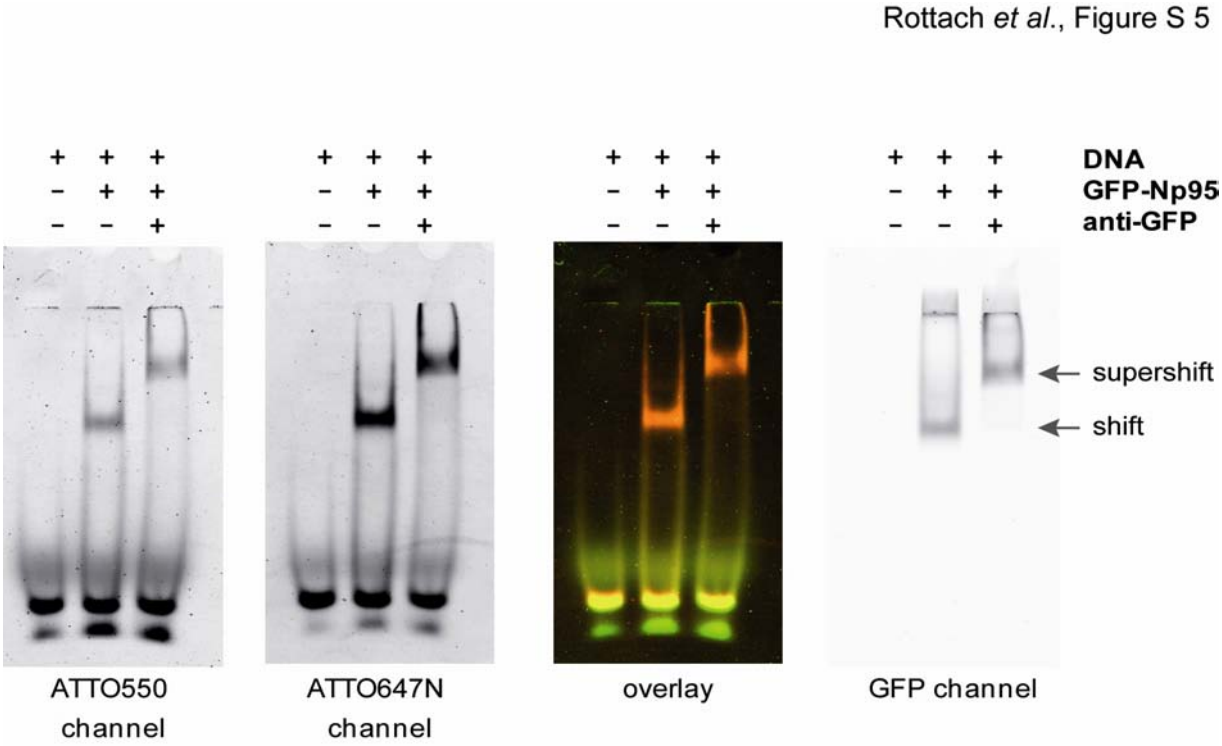

Supplementary Figure 5. Electrophoretic mobility shift and supershift assays with GFP-Np95. Un- and hemimethylated DNA substrates (1 pmol UMB550 and HMB647N, respectively) were incubated with 0.6 pmol purified GFP-Np95 and 0.4 pmol GFP-antibody. Samples were subjected to a 3.5 % non-denaturing PAGE and analyzed by the Typhoon Trio scanner to detect ATTO550 (unmethylated substrate), ATTO647N (hemimethylated substrate) and green fluorescence (GFP). Note that the DNA:GFP-Np95:GFP-antibody complex is shifting higher than the DNA:GFP-Np95 complex (arrows).

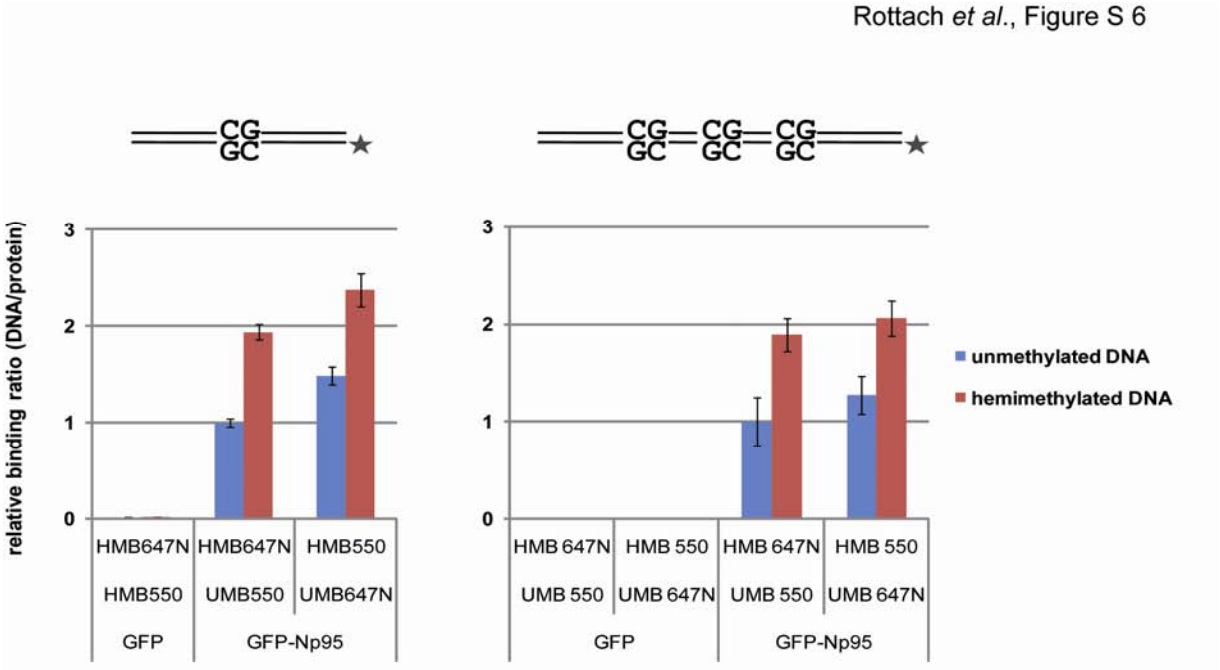

Supplementary Figure 6. DNA binding specificity of GFP-Np95

The sequence specific DNA binding activity of Np95 was tested with an *in vitro* binding assays using GFP-Np95 with un- and hemimethylated substrates in direct competition. The DNA substrates included either one (left) or three (right) CG sites. Note that regardless of the attached fluorescent label (indicated by asterisks) and number of CG sites the hemimethylated DNA substrates are preferentially bound (1.6- to 1.9-fold). Shown are the means ± SEM from two (left) or four (right) independent experiments.

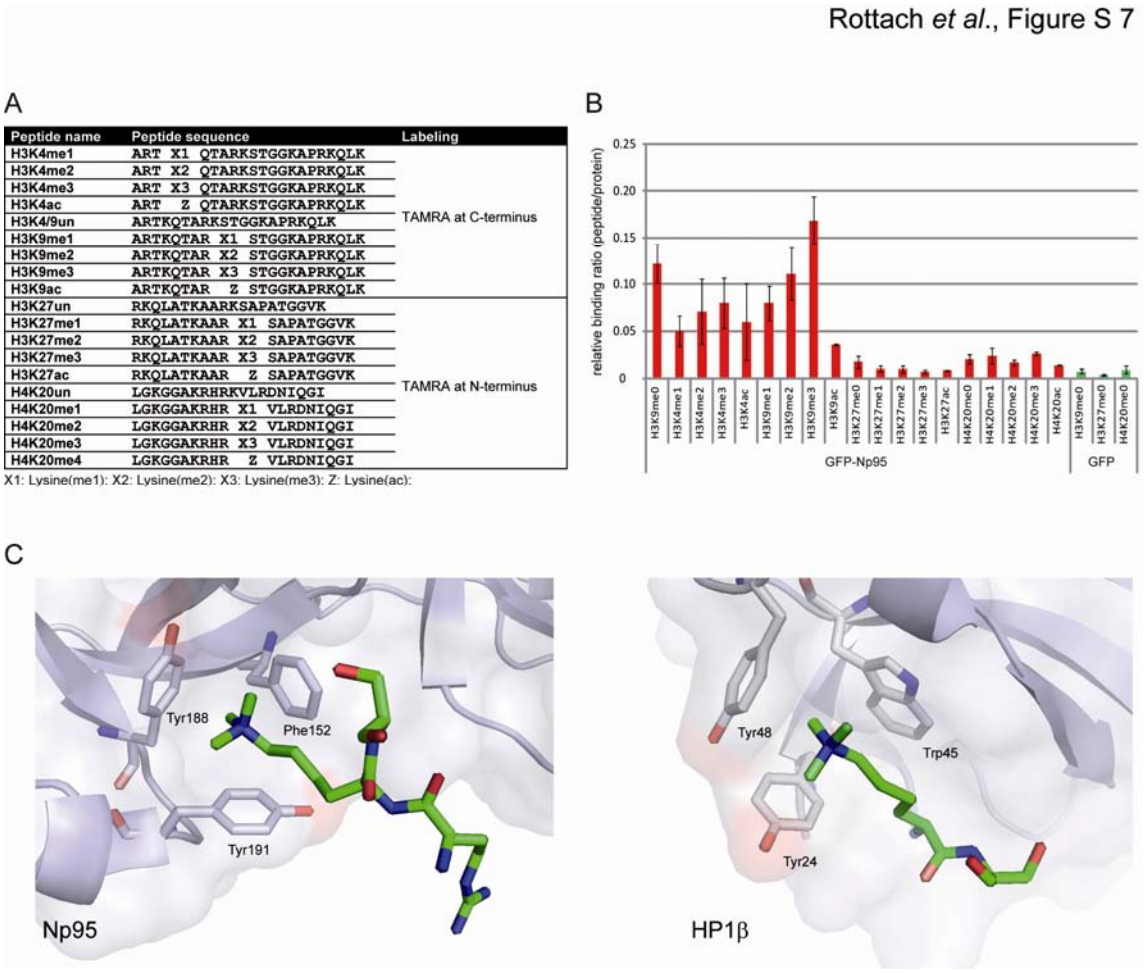

Peptide name	Peptide sequence	Labeling
H3K4me1	ART X1 QTARKSTGGKAPRKQLK	TAMRA at C-terminus
H3K4me2	ART X2 QTARKSTGGKAPRKQLK	
H3K4me3	ART X3 QTARKSTGGKAPRKQLK	
H3K4ac	ART Z QTARKSTGGKAPRKQLK	
H3K4/9un	ARTKQTARKSTGGKAPRKQLK	
H3K9me1	ARTKQTAR X1 STGGKAPRKQLK	
H3K9me2	ARTKQTAR X2 STGGKAPRKQLK	
H3K9me3	ARTKQTAR X3 STGGKAPRKQLK	
H3K9ac	ARTKQTAR Z STGGKAPRKQLK	
H3K27un	RKQLATKAARKSAPATGGVK	TAMRA at N-terminus
H3K27me1	RKQLATKAAR X1 SAPATGGVK	
H3K27me2	RKQLATKAAR X2 SAPATGGVK	
H3K27me3	RKQLATKAAR X3 SAPATGGVK	
H3K27ac	RKQLATKAAR Z SAPATGGVK	
H4K20un	LGKGGAKRHRKVLRDNIQGI	
H4K20me1	LGKGGAKRHR X1 VLRDNIQGI	
H4K20me2	LGKGGAKRHR X2 VLRDNIQGI	
H4K20me3	LGKGGAKRHR X3 VLRDNIQGI	
H4K20me4	LGKGGAKRHR Z VLRDNIQGI	

X1: Lysine(me1): X2: Lysine(me2): X3: Lysine(me3): Z: Lysine(ac):

Supplementary Figure 7. Histone tail binding of Np95 and HP1ß (**A**) Amino acid sequences of TAMRA-labeled histone tail peptides used for the peptide binding assay. (**B**) Histone H3 and H4-tail binding specificity of GFP-Np95 *in vitro*. Ratios of bound TAMRA-labeled peptide over bound GFP fusion were determined and normalized to the ratio of H3K4/9un peptide over GFP-Np95. GFP was used as negative control. Shown are means ± SEM from six independent experiments. (**C**) Structural comparison of the H3K9me3-binding aromatic cages formed by the tandem Tudor domain of Np95 (left) and the chromodomain of HP1ß (right, PDB 1kne). In these structures, only Arg8-Lys9-Ser10 and Lys9-Ser10 from histone H3 are resolved peptides, respectively (green stick models). The image was generated with PyMOL (1).

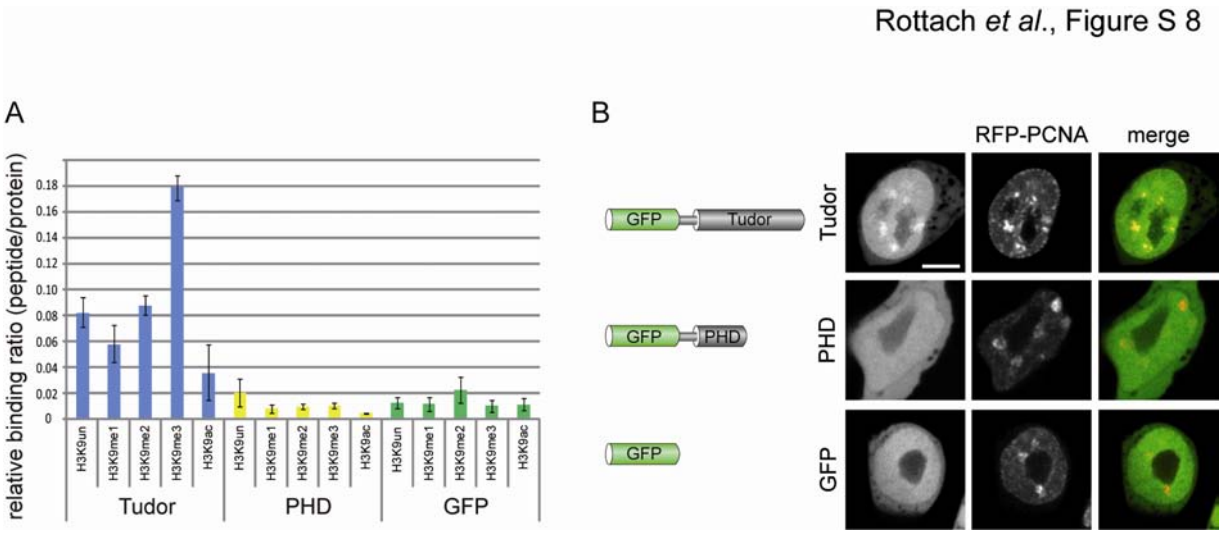

Supplementary Figure 8. Histone tail binding and subcellular distribution of PHD and Tudor domain of Np95 (**A**) Histone H3 N-terminal tail binding specificity of GFP-Tudor, GFP-PHD and GFP *in vitro*. Shown are fluorescence intensity ratios of bound probe / bound GFP fusion. GFP was used as negative control. Shown are means ± SEM from four to six independent experiments. Only the tandem Tudor domain shows preferential binding of H3K9 trimethylated histone tails. (**B**) Schematic representation of the analyzed Np95 constructs. All constructs were N-terminal GFP fusions (left panel). Confocal mid sections of living *np95*$^{-/-}$ ESCs transiently expressing the indicated Np95 fusion constructs and RFP-PCNA as S phase marker (left and mid panels). Merged images are displayed on the right. Bars, 5 µm. Only the GFP-Tudor fusion protein showed slight enrichment at pericentric heterochromatin.

References:

1. DeLano, W.L. (2002) *The PyMOL User's Manual*.

3.4 Cooperative DNA and histone binding by Uhrf2 links the two major repressive epigenetic pathways

ARTICLE
Journal of Cellular Biochemistry 112:2585–2593 (2011)

Journal of Cellular Biochemistry

Cooperative DNA and Histone Binding by Uhrf2 Links the Two Major Repressive Epigenetic Pathways

Garwin Pichler, Patricia Wolf, Christine S. Schmidt, Daniela Meilinger, Katrin Schneider, Carina Frauer, Karin Fellinger, Andrea Rottach, and Heinrich Leonhardt*

Ludwig Maximilians University Munich, Department of Biology II and Center for Integrated Protein Science Munich (CIPS^{M}), Großhaderner Str. 2, 82152 Planegg-Martinsried, Germany

ABSTRACT

Gene expression is regulated by DNA as well as histone modifications but the crosstalk and mechanistic link between these epigenetic signals are still poorly understood. Here we investigate the multi-domain protein Uhrf2 that is similar to Uhrf1, an essential cofactor of maintenance DNA methylation. Binding assays demonstrate a cooperative interplay of Uhrf2 domains that induces preference for hemimethylated DNA, the substrate of maintenance methylation, and enhances binding to H3K9me3 heterochromatin marks. FRAP analyses revealed that localization and binding dynamics of Uhrf2 in vivo require an intact tandem Tudor domain and depend on H3K9 trimethylation but not on DNA methylation. Besides the cooperative DNA and histone binding that is characteristic for Uhrf2, we also found an opposite expression pattern of *uhrf1* and *uhrf2* during differentiation. While *uhrf1* is mainly expressed in pluripotent stem cells, *uhrf2* is upregulated during differentiation and highly expressed in differentiated mouse tissues. Ectopic expression of Uhrf2 in *uhrf1*$^{-/-}$ embryonic stem cells did not restore DNA methylation at major satellites indicating functional differences. We propose that the cooperative interplay of Uhrf2 domains may contribute to a tighter epigenetic control of gene expression in differentiated cells. J. Cell. Biochem. 112: 2585–2593, 2011.

KEY WORDS: UHRF1; UHRF2; DNA METHYLATION; HISTONE MODIFICATIONS; EPIGENETICS

DNA methylation and histone modifications are major epigenetic marks involved in the regulation of gene expression, inheritance of chromatin states, genome stability, and cellular differentiation [Bird, 2002; Kouzarides, 2007; Reik, 2007]. Misregulation of epigenetic pathways, like erroneous DNA methylation, may lead to cancer and other diseases [Jones and Baylin, 2007]. Open questions concern the crosstalk and mechanistic link between different epigenetic signals.

Genome-scale DNA methylation studies revealed a connection between DNA methylation and histone modifications. Specifically, DNA methylation correlates with the absence of H3K4 methylation and presence of H3K9 methylation [Meissner et al., 2008]. This correlation may in part be caused by DNA methyltransferases specifically recognizing histone modifications. For instance, the de novo DNA methyltransferase Dnmt3a and its cofactor Dnmt3L specifically recognize unmethylated H3K4 mediated by the ATRX-Dnmt3-Dnmt3L (ADD) domain [Ooi et al., 2007; Otani et al., 2009]. Dnmt1, which is involved in maintenance methylation during DNA replication and DNA repair [Leonhardt et al., 1992; Mortusewicz et al., 2005], specifically methylates hemimethylated DNA [Bestor and Ingram, 1983; Pradhan et al., 1997] and associates with constitutive heterochromatin via its targeting sequence (TS) domain [Easwaran et al., 2004].

Recently, Uhrf1 (also known as Np95 or ICBP90) has been shown to link DNA and histone modifications and has emerged as an essential cofactor for the maintenance of genomic DNA methylation. Genetic ablation of *uhrf1* leads to remarkable genomic hypomethylation, a phenotype similar to *dnmt1*$^{-/-}$ embryonic stem cells (ESCs) [Bostick et al., 2007; Sharif et al., 2007]. Uhrf1 binds hemimethylated DNA via a SET and RING associated domain (SRA) domain and targets Dnmt1 to its substrate of maintenance DNA methylation [Bostick et al., 2007; Sharif et al., 2007; Arita et al., 2008; Avvakumov et al., 2008; Hashimoto et al., 2008; Qian et al., 2008; Rottach et al., 2010]. This targeting activity of Uhrf1 is based on specific binding to the heterochromatin mark H3K9me3 via a tandem Tudor domain (TTD) [Karagianni et al., 2008; Rottach et al.,

Additional supporting information may be found in the online version of this article.

Grant sponsor: Deutsche Forschungsgemeinschaft (DFG).

Karin Fellinger's present address is Intervet International GmbH, Unterschleissheim, Germany.

*Correspondence to: Dr. Heinrich Leonhardt, Department of Biology II, Ludwig Maximilians University Munich, 82152 Planegg-Martinsried, Germany. E-mail: h.leonhardt@lmu.de

Received 1 April 2011; Accepted 11 May 2011 • DOI 10.1002/jcb.23185 • © 2011 Wiley-Liss, Inc.
Published online 19 May 2011 in Wiley Online Library (wileyonlinelibrary.com).

2010]. In addition, Uhrf1 interacts with Dnmt3a and Dnmt3b and with histone modifying enzymes like HDAC1, G9a, and Tip60 [Unoki et al., 2004; Achour et al., 2009; Kim et al., 2009; Meilinger et al., 2009]. Finally, Uhrf1 displays E3 ubiquitin ligase activity for histone H3 [Citterio et al., 2004] and is involved in large scale reorganization of chromocenters [Papait et al., 2008].

Interestingly, a second member of the Uhrf family, Uhrf2, harbors similar domains [Bronner et al., 2007]. Until now, the only known function of Uhrf2 is a role in intranuclear degradation of polyglutamine aggregates [Iwata et al., 2009]. In this study, we systematically investigated the function and interplay of distinct Uhrf2 domains in DNA and histone tail substrate recognition and report first hints on cell-type specific functions of Uhrf1 and Uhrf2.

MATERIALS AND METHODS

EXPRESSION CONSTRUCTS

Expression constructs for GFP, RFP-PCNA, Uhrf1-GFP, and GFP constructs of Dnmt1 were described previously [Sporbert et al., 2005; Fellinger et al., 2009; Meilinger et al., 2009]. All Uhrf2 expression constructs were derived by PCR from mouse *uhrf2*-myc cDNA (MR210744, ORIGENE). To obtain GFP fusion constructs, the *uhrf1* cDNA [Rottach et al., 2010] was replaced by *uhrf2* encoding PCR fragments in the pCAG-*uhrf1*-GFP vector. The deletion and point mutant expression constructs were derived from the corresponding wild-type constructs by overlap extension PCR [Ho et al., 1989] and PCR-based mutagenesis. The following start and end amino acids were chosen: Uhrf2 tandem Tudor domain, amino acids 118–312; Uhrf2 PHD domain, amino acids 325–395; Uhrf2 tandem Tudor–PHD domain, amino acids 118–395; Uhrf1 tandem Tudor–PHD domain, amino acids 121–370. The linker exchange constructs were derived by PCR using overlapping primers that contained the partial linker sequence. Amino acid sequences of the linkers: Uhrf1: KERRPLIASPSQPPA; Uhrf2: GAHPISFADGKF. All constructs were verified by DNA sequencing. Throughout this study enhanced GFP constructs were used and for simplicity referred to as GFP fusions.

CELL CULTURE, TRANSFECTION, CELL SORTING, AND DIFFERENTIATION

HEK293T cells, MEFs, and ESCs were cultured and transfected as described [Schermelleh et al., 2007; Rottach et al., 2010] with the exception that Lipofectamin (Invitrogen) was used for transfection of MEFs. E14 *uhrf1*$^{-/-}$ ESCs were transfected with Uhrf1-GFP and Uhrf2-GFP expression constructs using FuGENE HD (Roche) according to the manufacturer's instructions. ESCs were sorted for GFP positive cells 48 h after transfection with a FACS Aria II instrument (Becton Dikinson). ESC strains wt E14, wt J1, and E14 *uhrf1*$^{-/-}$ were cultured and differentiated to embryoid bodies as described [Szwagierczak et al., 2010]. The ESC strain wt JM8A3.N1 (EUCOMM, Germany) was cultured in Knockout D-MEM (Gibco-BRL, Grand-Island, NY) medium containing 10% fetal bovine serum (PAA Laboratories GmbH, Austria), 0.1 mM β-mercaptoethanol (Gibco-BRL), 2 mM L-glutamine, 100 U/ml penicillin, 100 μg/ml streptomycin (PAA Laboratories GmbH). The medium was supplemented with 1,000 U/ml recombinant mouse LIF (Millipore, Temecula, CA).

RNA ISOLATION, CDNA SYNTHESIS, AND QUANTITATIVE REAL-TIME PCR

RNA isolation and cDNA synthesis were performed as described [Szwagierczak et al., 2010]. Equal amounts of cDNA were used for Real-time PCR with TaqMan Gene Expression Master Mix (Applied Biosystems) on the 7500 Fast Real-time PCR System (Applied Biosystems) according to the manufacturer's instructions. The following TaqMan Gene expression assays were used: Gapdh (Assay ID: Mm99999915_g1), uhrf1 (Assay ID: Mm00477865_m1) and uhrf2 (Assay ID: Mm00520043_m1). Gene expression levels were normalized to Gapdh and calculated using the comparative C_T Method ($\Delta\Delta C_T$ Method).

IN VITRO DNA BINDING AND HISTONE-TAIL PEPTIDE BINDING ASSAY

The in vitro binding assays were performed as described previously [Frauer and Leonhardt, 2009; Rottach et al., 2010]. NoCpG DNA substrates were produced in a primer extension reaction [Frauer and Leonhardt, 2009] others by hybridization of two DNA oligos (Supplementary Fig. S7B–D). Histone-tail peptides were purchased as TAMRA conjugates (PSL, Germany; Supplementary Fig. S7A). Peptides were added in a molar ratio 1.5:1 (peptide/GFP fusion) and the binding reaction was performed at RT for 15 min with constant mixing. For combined assays, samples were additionally incubated with either H3K9me3 or H3K9ac histone-tail peptides in a molar ratio 1.5:1 (peptide/GFP fusion) or increasing amount of DNA substrate as indicated. The binding reaction was performed at RT for 60 min with constant mixing.

IMMUNOFLOURESCENCE STAINING AND ANTIBODIES

For immunostaining, MEF cells and ESCs were grown on cover slips and transiently transfected with Uhrf2-GFP (MEF cells), or co-transfected with Uhrf2-GFP and RFP-PCNA (ESCs). Cells were fixed with 2.0% or 3.7% formaldehyde in PBS and permeabilized in PBS containing 0.2% Triton X-100. The post-translational histone modification H3K9me3 was detected via a rabbit primary antibody (Active Motif) and a secondary anti-rabbit antibody conjugated to Alexa Fluor 594 (Molecular Probes, Eugene, OR). The antibodies were diluted 1:1,000 or 1:500, respectively, in PBS containing 0.02% Tween-20 and 2% BSA. GFP-Binder (ChromoTek, Germany) was used to boost GFP signals and was labeled with Alexa Fluor 488. Cells were counterstained with DAPI and mounted in Vectashield (Vector Laboratories, Burlingame, CA). Images of the cells were obtained using a TCS SP5 AOBS confocal laser scanning microscope (Leica, Wetzlar, Germany) with a 63x/1.4 NA Plan-Apochromat oil immersion objective. GFP, Alexa Fluor 488, RFP, and Alexa Fluor 594 were excited with a 488-nm argon laser and a 561-nm diode laser, respectively. Image series were recorded with a frame size of 512 × 512 pixels, a pixel size of 100 nm and with a detection pinhole size of 1 Airy Unit.

LIVE CELL MICROSCOPY AND FLUORESCENCE RECOVERY AFTER PHOTOBLEACHING (FRAP) ANALYSIS

Live cell imaging and FRAP analyses were performed as described [Schermelleh et al., 2007] with the exception that imported images were intensity normalized, converted to 8-bit and Gauss-filtered (2 pixel radius). Data sets showing lateral movement were corrected by image registration using the StackReg plug-in of ImageJ [Abramoff et al., 2004] starting with a frame when approximately half recovery was reached. Within the first 30 s after bleaching, images were taken every 150 ms and then in intervals of 1 s.

DNA METHYLATION ANALYSIS

Genomic DNA was isolated with the QIAmp DNA Mini Kit (Qiagen) and 1.5 μg were bisulfite converted using the EZ DNA Methylation-Gold Kit (Zymo research) according to the manufacturer's instructions. Primer sequences for major satellites were AAAAT-GAGAAACATCCACTTG (forward primer) and CCATGATTTT-CAGTTTTCTT (reverse primer). For amplification we used Qiagen Hot Start Polymerase in 1× Qiagen Hot Start Polymerase buffer supplemented with 0.2 mM dNTPs, 0.2 μM forward primer, 0.2 μM reverse primer, 1.3 mM betaine (Sigma) and 60 mM tetramethylammonium-chloride (TMAC, Sigma). Major satellites were amplified in a single amplification and pyrosequencing reactions were carried out by Varionostic GmbH (Ulm, Germany).

STATISTICAL ANALYSIS

Results were expressed as means ± SD or means ± SEM. The difference between two mean values was analyzed by Student's *t*-test and was considered as statistically significant in case of $P < 0.05$ (*) and highly significant for $P < 0.001$ (**).

RESULTS

OPPOSITE EXPRESSION PATTERN OF *UHRF1* AND *UHRF2* DURING DIFFERENTIATION

Recently, Uhrf1 has emerged as an essential factor for the maintenance of DNA methylation. Sequence analyses revealed that Uhrf2 harbors five recognizable domains similar to Uhrf1 (Fig. 1A), but its role in the regulation of DNA methylation is still unclear. We compared the expression pattern of *uhrf1* and *uhrf2* in ESCs and somatic cells, during differentiation and in differentiated mouse tissues (Fig. 1B–D and Supplementary Fig. S1). Interestingly, both genes show opposite expression patterns; while *uhrf1* is expressed in ESCs and down regulated during differentiation, which is consistent with previous reports [Muto et al., 1995; Fujimori et al., 1998; Hopfner et al., 2000], *uhrf2* is upregulated and highly expressed in differentiated mouse tissues. The switch in the expression pattern argues against a functional redundancy of both genes and is consistent with the drastic loss of DNA methylation in *uhrf1*$^{-/-}$ ESCs despite the presence of intact *uhrf2* alleles. Therefore, the opposite expression pattern of both genes suggests different functional roles of *uhrf1* and *uhrf2* in development.

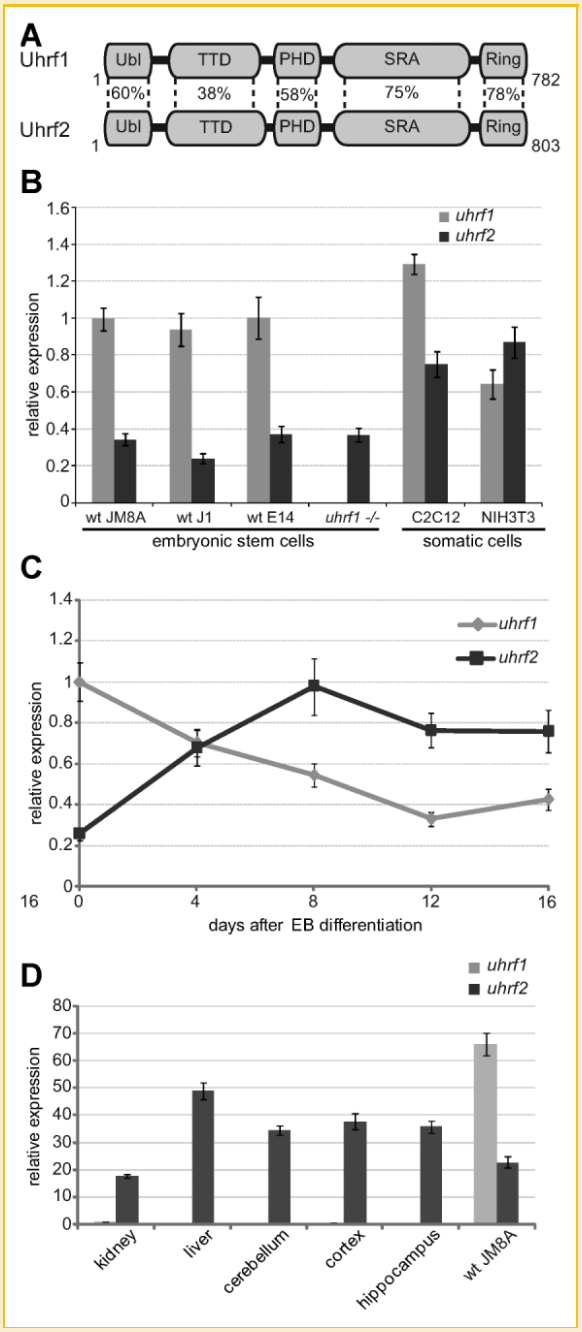

Fig. 1. Opposite expression pattern of *uhrf1* and *uhrf2* during differentiation. A: Schematic outline of the multi-domain architecture of Uhrf1 in comparison to Uhrf2. An N-terminal ubiquitin-like domain (Ubl) is followed by a tandem Tudor domain (TTD), a plant homeodomain (PHD), a SET and RING associated (SRA) domain and a C-terminal really interesting new gene (RING) domain. Numbers indicate primary sequence similarities of single domains determined by BlastP search [Altschul, 1991]. Expression analysis of *uhrf1* and *uhrf2* by Real-time PCR in ESCs and somatic cells (B), during differentiation of wt J1 ESCs (C) and in various adult mouse tissues in comparison to the expression data in ESCs (D). Expression levels are relative to *uhrf1* in wtJM8A (B), day 0 of differentiation (C) and to kidney (D) (*uhrf1* set to 1). Shown are means ± SD of at least two independent experiments.

COOPERATIVE BINDING OF REPRESSIVE EPIGENETIC MARKS BY UHRF2

To investigate DNA and histone-tail binding preferences of Uhrf2 in vitro, we used a versatile binding assay developed for GFP fusion proteins [Rothbauer et al., 2008; Frauer and Leonhardt, 2009; Rottach et al., 2010]. Similar to Uhrf1, histone-tail peptide binding assays revealed that Uhrf2 preferentially binds to H3(1–20) and H3K9me3 peptides (Fig. 2A). This binding activity of Uhrf2 is mediated by the TTD but not the PHD domain (Fig. 2B). Consistently, acetylation of H3K9, underrepresented in heterochromatin,

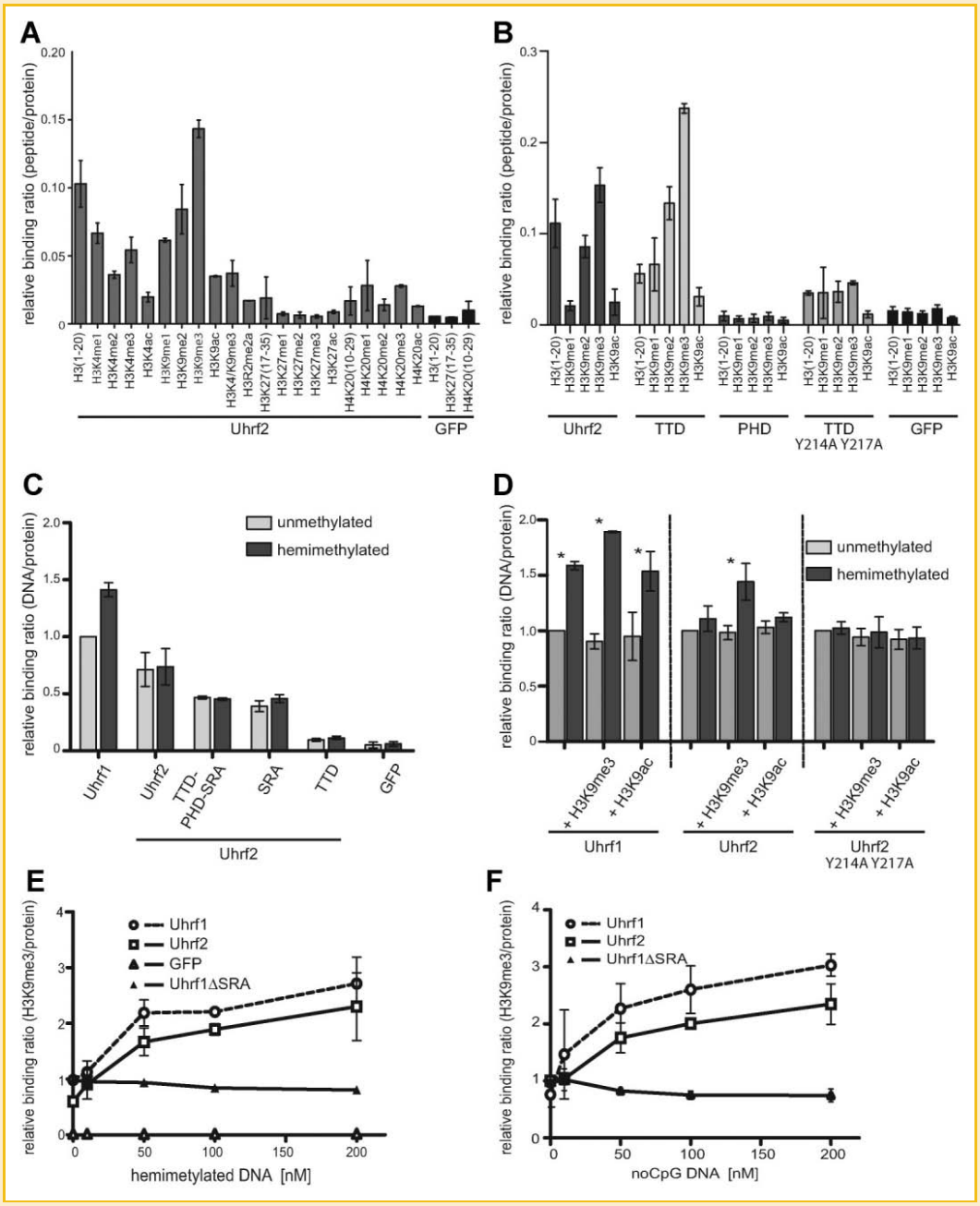

Fig. 2. Cooperative binding of repressive epigenetic marks by Uhrf2. In vitro binding ratios of fluorescently labeled substrate over bound GFP fusion proteins were determined. A: Histone H3- and H4-tail binding specificities of Uhrf2. Shown are means ± SD of biological duplicates. B: Histone H3 tail binding specificity of Uhrf2, its tandem Tudor domain (TTD), its PHD domain and its TTD mutant (Y214A Y217A). Shown are means ± SEM of at least three independent experiments. C: DNA binding properties of Uhrf1, Uhrf2 and of single (SRA, TTD) and combined Uhrf2 domains (TTD–PHD–SRA). Shown are means ± SEM of three independent experiments. D: DNA binding properties of Uhrf1, Uhrf2 and Uhrf2 Y214A Y217A in combination with histone-tail peptide binding. Shown are means ± SD of three independent experiments (Uhrf1, Uhrf2) and of two independent experiments (Uhrf2 Y214A Y217A). Values were normalized to the binding ratio of each GFP fusion for unmethylated DNA without histone-tail peptide. Statistical significance of differences between the binding ratios with un- and hemimethylated DNA is indicated; $^{*}P < 0.05$. E + F: H3K9me3 peptide binding by Uhrf1, Uhrf2, and Uhrf1ΔSRA with increasing concentrations of DNA substrate containing either one central hemimethylated (E) or noCpG site (F). Shown are means ± SD of biological duplicates. Values were normalized to the binding ratio of Uhrf1ΔSRA without DNA.

prevented the binding of Uhrf2 and its TTD. The binding of Uhrf1 to H3K9me3 is mediated by an aromatic cage in the TTD [Rottach et al., 2010]. Site-directed mutagenesis of Uhrf2 changing the two conserved tyrosine residues to alanine (Y214A Y217A) (Supplementary Fig. S2) abolished specific peptide binding (Fig. 2B) and supports a function of the aromatic cage in H3K9me3 recognition.

Whereas Uhrf1 preferentially binds to hemimethylated DNA, Uhrf2 failed to show a preference for hemi-over unmethylated DNA (Fig. 2C). These differences in DNA binding preferences between Uhrf1 and Uhrf2 were confirmed by electrophoretic mobility shifts (Supplementary Fig. S3). To further investigate the functional interplay between DNA and histone binding we performed combined binding assays (Fig. 2D). Interestingly, binding to heterochromatin-specific H3K9me3 peptides induced a significant preference of Uhrf2 for hemi-over unmethylated DNA. Uhrf1 already on its own showed preference for hemimethylated DNA that was further enhanced by binding to H3K9me3 peptides. To test the specificity of this cooperativity we mutated the aromatic cage in Uhrf2 that is necessary for H3K9me3 histone-tail peptide binding. The mutated Uhrf2 (Y214A Y217A) showed comparable DNA binding activity as the wild-type Uhrf2 but addition of heterochromatin-specific H3K9me3 peptides did not induce preference for hemi-over unmethylated DNA (Fig. 2D).

In the reverse experiment, addition of DNA enhanced binding of Uhrf1 and Uhrf2 to the H3K9me3 peptide (Fig. 2E,F). This was not observed for the DNA binding mutant of Uhrf1 (Uhrf1ΔSRA) which showed constant peptide binding with increasing DNA concentrations. These findings suggest that single binding events of distinct Uhrf2 domains lead to multivalent engagement of different repressive epigenetic marks. In fact, multivalent engagement of DNA and histone tail peptides via the SRA domain and the TTD, respectively, results in affinity enhancement and additional specificity for hemimethylated DNA, the substrate of maintenance methylation.

CELLULAR LOCALIZATION AND DYNAMICS OF UHRF2 DEPEND ON HISTONE H3K9 METHYLATION

To monitor the subcellular localization of Uhrf2, we expressed Uhrf2-GFP constructs in cells with different genetic backgrounds. In wild type (wt) ESCs, Uhrf2 is localized in the nucleus and is enriched at pericentric heterochromatin (PH) (Fig. 3A,B and Supplementary Fig. S4A–C). To investigate which epigenetic marks at PH are recognized by Uhrf2 we determined the localization of Uhrf2 in genetically modified ESCs either lacking all three major DNA methyltransferases Dnmt1, Dnmt3a, and Dnmt3b (TKO) [Tsumura et al., 2006] or ESCs lacking the two major H3K9 methyltransferases Suv39H1/H2 (*Suv39h dn*) [Lehnertz et al., 2003]. TKO cells are practically devoid of genomic DNA methylation and *Suv39h dn* ESCs show substantially reduced H3K9me3 levels. We found Uhrf2 localized at PH in TKO but not in *Suv39h dn* ESCs, indicating that localization of Uhrf2 is dependent on H3K9 but not on DNA methylation (Fig. 3A). Consistently, immunostaining of wt mouse embryonic fibroblasts (MEFs) showed co-localization of Uhrf2 and H3K9me3 marks at PH, which was not observed in *Suv39h dn* MEFs [Peters et al., 2001] (Fig. 3B). Also, mutations in the TTD (Uhrf2 Y214A Y217A) that abolished binding to H3K9me3 peptides in vitro

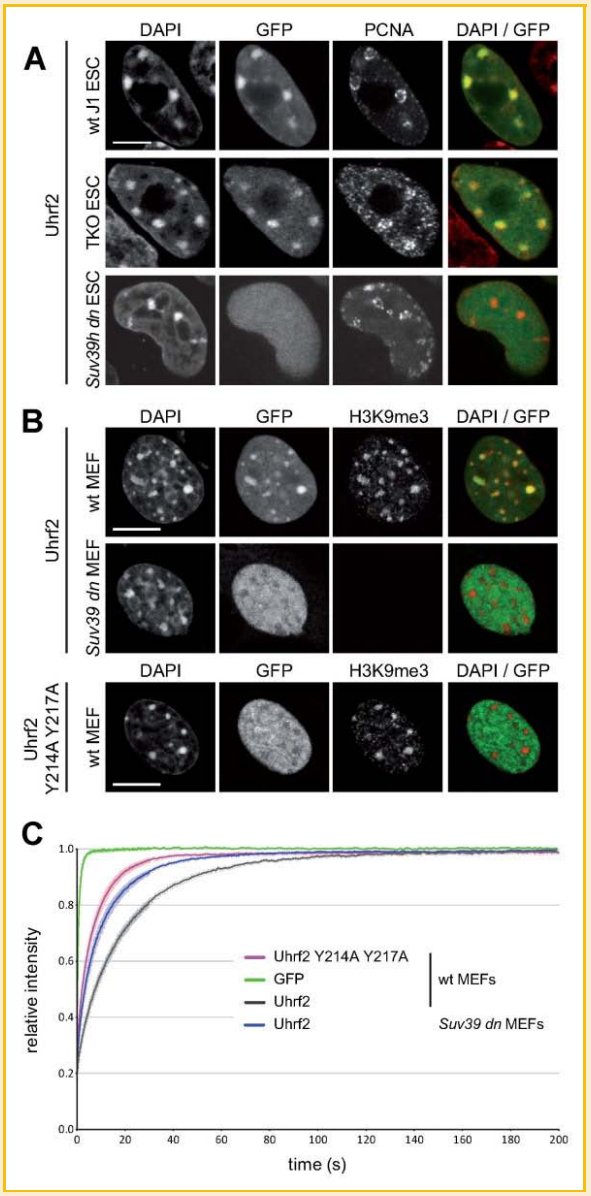

Fig. 3. Cellular localization and dynamics of Uhrf2 depend on histone H3K9 methylation. A: Confocal mid sections of fixed wt J1, TKO and *Suv39h dn* ESCs transiently expressing Uhrf2-GFP and RFP-PCNA and counterstained with DAPI, which preferentially highlights PH. Merged images are displayed on the right side (GFP: green; DAPI: red). Scale bar 5 μm. B: Confocal mid sections of fixed wt MEFs and *Suv39h dn* MEFs transiently expressing Uhrf2-GFP or Uhrf2 Y214A Y217A-GFP were immunostained for H3K9me3 and counterstained with DAPI. Merged images are displayed on the right side (GFP: green; DAPI: red). Scale bar 5 μm. C: Dynamics of Uhrf2-GFP and Uhrf2 Y214A Y217A-GFP in living MEFs determined by half nucleus FRAP analysis. GFP is shown as reference. Curves represent means ± SEM from at least 8 nuclei.

disrupted enrichment at PH in wt MEFs (Fig. 3B). The dependence of Uhrf2 localization on H3K9me3 was also confirmed by quantitative correlation analysis (Supplementary Fig. S4D,E).

To investigate the effect of H3K9me3 on the dynamics of Uhrf2 in living cells we performed quantitative fluorescence recovery after photobleaching (FRAP) analyses in wt and *Suv39h dn* MEFs. We chose to bleach half nuclei to include a representative number of

interactions from different nuclear domains and structures in the bleached area [Rottach et al., 2010]. Recovery of Uhrf2-GFP fluorescence in *Suv39h dn* MEFs (half-time $t_{1/2} = 5.9 \pm 0.6$ s) and of the TTD mutant in wt MEFs ($t_{1/2} = 3.2 \pm 0.4$ s) was considerably faster than the recovery of Uhrf2-GFP in wt MEFs ($t_{1/2} = 11.8 \pm 0.6$ s) pointing to a crucial role of H3K9me3 in Uhrf2 dynamics in living cells (Fig. 3C). Taken together, these results clearly demonstrate that the interaction of Uhrf2 with the heterochromatin mark H3K9me3 is required for the localization at PH and affects binding dynamics in living cells.

COOPERATIVE BINDING OF THE COMBINED UHRF2 TTD–PHD DOMAIN

Recently, several studies showed multivalent binding to histone-tail peptides [Ruthenburg et al., 2007]. In case of Uhrf1 and Uhrf2, the TTD is followed by a second histone-tail binding domain, a PHD domain (Fig. 1A). As the isolated PHD domains of Uhrf1 and Uhrf2 did not show binding to H3 histone-tail peptides (Fig. 2B) [Rottach et al., 2010], we tested whether the combination of the PHD and the TTD results in cooperative histone-tail binding. Surprisingly, the combined TTD–PHD domain of Uhrf2 displayed a fourfold increased binding to H3K9me2/me3 in comparison to the single TTD, which was not observed for the corresponding construct of Uhrf1 (Figs. 2B and 4A).

Sequence alignments of the combined domains revealed two striking differences between Uhrf1 and Uhrf2. Firstly, Uhrf2 harbors an additional stretch of 33 highly conserved amino acids present in the TTD (Supplementary Fig. S5A). Secondly, the linker region between the TTD and PHD domain of Uhrf2 is highly conserved, whereas this region is highly diverse in Uhrf1 (Supplementary Fig. S5A). To test which sequence is responsible for the observed cooperative interplay between PHD and TTD, we generated and tested different hybrid and deletion constructs (Supplementary Fig. S5B). Notably, replacement of the native linker in the Uhrf2 TTD–PHD construct by the Uhrf1 linker caused decreased relative binding ratios to H3K9me2/3 comparable to the single Uhrf2 TTD (Fig. 4B). Transferring the Uhrf2 linker to the Uhrf1 TTD–PHD construct as well as deletion of the Uhrf2 stretch region did not affect the binding to H3K9me3 peptides (Fig. 4B).

These results suggest that the cooperative interplay of different Uhrf2 domains, which is responsible for the increased binding to heterochromatin marks, is dependent on the highly conserved linker region connecting the TTD and PHD domains. A similar functional importance of linker sequences has been described for BPTF and histone lysine demethylases [Li et al., 2006; Horton et al., 2010].

UHRF1 AND UHRF2 ARE NOT FUNCTIONALLY REDUNDANT IN ESCS

To investigate whether Uhrf1 and Uhrf2 are functionally redundant we performed interaction and rescue assays. Like Uhrf1, also Uhrf2 interacts with Dnmts (Supplementary Fig. S6) suggesting a similar function in DNA methylation. To test for such a functional role, we ectopically expressed Uhrf2-GFP or Uhrf1-GFP in *uhrf1*$^{-/-}$ ESCs and determined DNA methylation levels at major satellites by pyrosequencing. While ectopic expression of Uhrf1-GFP led to significant increase of DNA methylation levels at CpG sites of major satellite DNA in *uhrf1*$^{-/-}$ ESCs, Uhrf2-GFP did not restore DNA methylation at these sites (Fig. 5). These results point to functional differences between Uhrf1 and Uhrf2 in vivo.

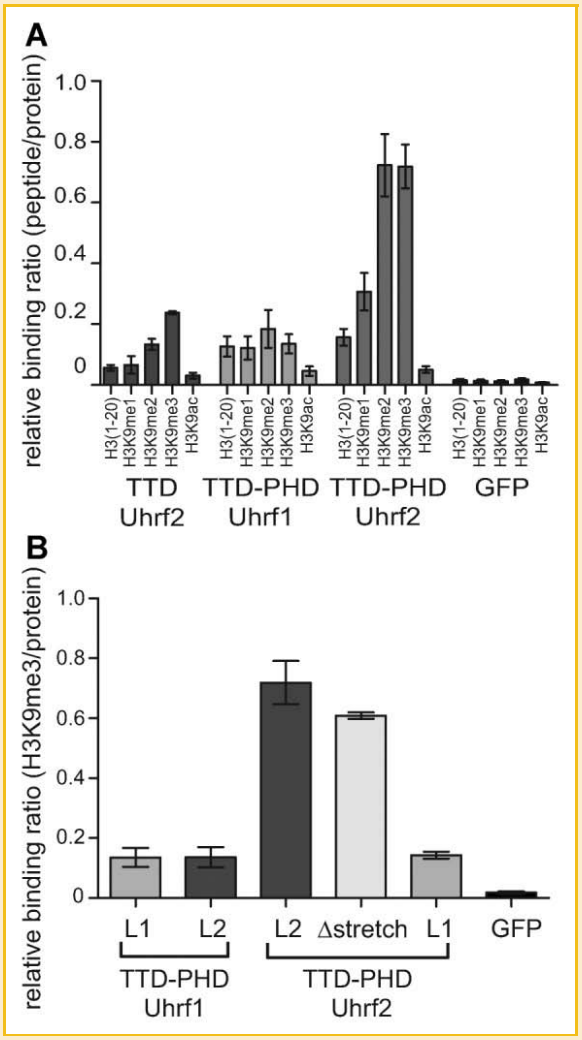

Fig. 4. Cooperative binding of the combined tandem Tudor–PHD domain of Uhrf2. A: Histone H3 N-terminal tail binding specificity of the TTD of Uhrf2 and of the combined TTD and PHD domain (TTD–PHD) of Uhrf1 and Uhrf2. Shown are means ± SEM from at least six independent experiments. B: Histone H3K9me3 binding of the combined TTD–PHD domains of Uhrf1 and Uhrf2, hybrid proteins (L1 and L2 specify inserted linker sequences derived from Uhrf1 and Uhrf2, respectively) and a stretch deletion Uhrf2 construct. Shown are means ± SEM from at least three independent experiments.

DISCUSSION

Over the past decades many different histone modifications were discovered that are involved in epigenetic gene regulation. A key question is how these histone marks are linked to DNA methylation pattern and how this complex epigenetic information is integrated and translated into defined chromatin structures and gene expression levels. Epigenetic regulators that bind DNA and histone marks are ideally suited to link these pathways and intramolecular interactions between different binding domains may contribute to

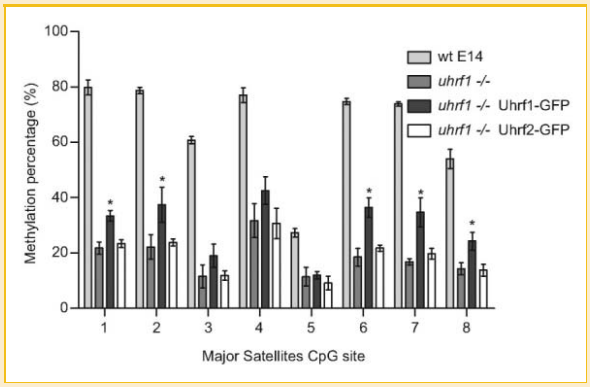

Fig. 5. Uhrf1 and Uhrf2 are not functionally redundant in ESCs. DNA methylation analysis of wt E14 ESCs, *uhrf1*$^{-/-}$ ESCs and of *uhrf1*$^{-/-}$ ESCs ectopically expressing Uhrf1-GFP or Uhrf2-GFP. ESCs transiently expressing Uhrf1-GFP and Uhrf2-GFP were isolated by FACS sorting 48 h after transfection and CpG methylation levels of major satellites repeats were analysed by bisulfite treatment, PCR amplification and direct pyrosequencing. Statistical significance of differences in DNA methylation levels between *uhrf1*$^{-/-}$ ESCs and *uhrf1*$^{-/-}$ ESCs with ectopically expressed Uhrf1-GFP or Uhrf2-GFP are indicated; $^{*}P < 0.05$. Shown are means ± SD from three independent experiments.

substrate specificity and epigenetic regulation [Hashimoto et al., 2009].

Recently, Uhrf1, an essential factor for the maintenance of DNA methylation, has been shown to bind to repressive DNA and histone modifications via an SRA and a tandem Tudor domain, respectively. Here we provide the first systematic characterization of the second member of the Uhrf family, Uhrf2, and demonstrate that Uhrf2 binds to the H3K9me3 heterochromatin mark via an aromatic cage of a tandem Tudor domain (TTD). Mutations in the aromatic cage abolished binding to H3K9me3 histone-tail peptides in vitro and prevented enrichment of Uhrf2 at pericentric heterochromatin in vivo. Interestingly, similar mutations in the aromatic cage of Uhrf1 prevented repression of $p16^{INK4A}$ [Nady et al., 2011] suggesting a link between H3K9me3 binding and a function of Uhrf proteins in gene repression.

Our results point to a complex regulation of substrate recognition by Uhrf2 involving cooperative binding domains and critical linker sequences. In contrast to Uhrf1, preferential binding of Uhrf2 to hemimethylated DNA, the substrate of DNA maintenance methylation, was only induced upon simultaneous binding to H3K9me3 histone-tail peptides. Binding of Uhrf1 and Uhrf2 to DNA in turn enhanced binding to H3K9me3 histone-tail peptides. Consistently, SILAC-based proteomic analysis identified enrichment of UHRF1 at nucleosomes containing repressive DNA and H3K9 methylation marks [Bartke et al., 2010]. Together, these data demonstrate a cooperative interplay between DNA and histone tail binding domains of Uhrf1 and Uhrf2. A similar effect was reported for MSL3 that specifically binds to H4K20me1 via a chromodomain only in the presence of DNA [Kim et al., 2010].

An additional level of complexity was added by recent studies showing multivalent binding of histone-tail peptides by mixed two-effector modules [Ruthenburg et al., 2007]. Notably, the combined TTD–PHD domain of Uhrf2, but not of Uhrf1, showed enhanced binding to H3K9me3 histone-tail peptides. This cooperativity was dependent on the highly conserved linker region connecting the TTD and PHD domains. Similarly, an important role was attributed to the linker sequence between the histone binding domain (PHD) and the histone modifying domain of jumanji histone lysine demethylases [Horton et al., 2010].

The dramatic loss of DNA methylation in *uhrf1*$^{-/-}$ ESCs [Bostick et al., 2007; Sharif et al., 2007] is remarkable, especially considering the presence of the *uhrf2* gene, which encodes a highly similar protein as demonstrated in this study. As one possible explanation for this lack of functional redundancy we found, in contrast to *uhrf1*, relatively low *uhrf2* mRNA levels in ESCs, which were not affected by genetic *uhrf1* ablation. Moreover, both genes also show opposite expression patterns during differentiation. The failure of ectopically expressed Uhrf2 to restore DNA methylation in *uhrf1* deficient cells clearly points to functional differences between both proteins in vivo. However, more definitive insights into the specific function(s) of Uhrf2 will require targeted mutations and subsequent analyses of pluripotent as well as differentiated cells. Based on the cooperative binding of Uhrf2 domains to repressive DNA and histone marks we propose that Uhrf2 might contribute to a tighter control of gene repression in differentiated cells as compared to a less stringent control by Uhrf1 in pluripotent ESCs.

ACKNOWLEDGMENTS

The authors are grateful to En Li (Novartis Institutes for Biomedical Research, Boston, MA) for J1 ESCs, to Masaki Okano (RIKEN Center for Developmental Biology, Kobe, Japan) for TKO ESCs, to Thomas Jenuwein (Max-Planck Institute of Immunobiology and Epigenetics, Freiburg, Germany) for the *Suv39h dn* MEFs and to Gunnar Schotta (Adolf-Butenandt-Institute, Faculty of Medicine, Ludwig Maximilians University Munich, Germany) for the *Suv39h dn* ESCs. This work was supported by the Nanosystems Initiative Munich (NIM) and by grants from the Deutsche Forschungsgemeinschaft (DFG) SFB646 and SFB684 to H.L. G.P., C.S.S., K.S., and C.F. were supported by the International Doctorate Program NanoBioTechnology (IDK-NBT) and the International Max Planck Research School for Molecular and Cellular Life Sciences (IMPRS-LS). PW is a fellow of the Graduate School Life Science Munich (LSM).

REFERENCES

Abramoff MD, Magelhaes PJ, Ram SJ. 2004. Image processing with ImageJ. Biophotonics Int 11:36–42.

Achour M, Fuhrmann G, Alhosin M, Ronde P, Chataigneau T, Mousli M, Schini-Kerth VB, Bronner C. 2009. UHRF1 recruits the histone acetyltransferase Tip60 and controls its expression and activity. Biochem Biophys Res Commun 390:523–528.

Altschul SF. 1991. Amino acid substitution matrices from an information theoretic perspective. J Mol Biol 219:555–565.

Arita K, Ariyoshi M, Tochio H, Nakamura Y, Shirakawa M. 2008. Recognition of hemi-methylated DNA by the SRA protein UHRF1 by a base-flipping mechanism. Nature 455:818–821.

Avvakumov GV, Walker JR, Xue S, Li Y, Duan S, Bronner C, Arrowsmith CH, Dhe-Paganon S. 2008. Structural basis for recognition of hemi-methylated DNA by the SRA domain of human UHRF1. Nature 455:822–825.

Bartke T, Vermeulen M, Xhemalce B, Robson SC, Mann M, Kouzarides T. 2010. Nucleosome-interacting proteins regulated by DNA and histone methylation. Cell 143:470–484.

Bestor TH, Ingram VM. 1983. Two DNA methyltransferases from murine erythroleukemia cells: Purification, sequence specificity, and mode of interaction with DNA. Proc Natl Acad Sci USA 80:5559–5563.

Bird A. 2002. DNA methylation patterns and epigenetic memory. Genes Dev 16:6–21.

Bostick M, Kim JK, Esteve PO, Clark A, Pradhan S, Jacobsen SE. 2007. UHRF1 plays a role in maintaining DNA methylation in mammalian cells. Science 317:1760–1764.

Bronner C, Achour M, Arima Y, Chataigneau T, Saya H, Schini-Kerth VB. 2007. The UHRF family: Oncogenes that are drugable targets for cancer therapy in the near future? Pharmacol Ther 115:419–434.

Citterio E, Papait R, Nicassio F, Vecchi M, Gomiero P, Mantovani R, Di Fiore PP, Bonapace IM. 2004. Np95 is a histone-binding protein endowed with ubiquitin ligase activity. Mol Cell Biol 24:2526–2535.

Easwaran HP, Schermelleh L, Leonhardt H, Cardoso MC. 2004. Replication-independent chromatin loading of Dnmt1 during G2 and M phases. EMBO Rep 5:1181–1186.

Fellinger K, Rothbauer U, Felle M, Langst G, Leonhardt H. 2009. Dimerization of DNA methyltransferase 1 is mediated by its regulatory domain. J Cell Biochem 106:521–528.

Frauer C, Leonhardt H. 2009. A versatile non-radioactive assay for DNA methyltransferase activity and DNA binding. Nucleic Acids Res 37:e22.

Fujimori A, Matsuda Y, Takemoto Y, Hashimoto Y, Kubo E, Araki R, Fukumura R, Mita K, Tatsumi K, Muto M. 1998. Cloning and mapping of Np95 gene which encodes a novel nuclear protein associated with cell proliferation. Mamm Genome 9:1032–1035.

Hashimoto H, Horton JR, Zhang X, Bostick M, Jacobsen SE, Cheng X. 2008. The SRA domain of UHRF1 flips 5-methylcytosine out of the DNA helix. Nature 455:826–829.

Hashimoto H, Horton JR, Zhang X, Cheng X. 2009. UHRF1, a modular multi-domain protein, regulates replication-coupled crosstalk between DNA methylation and histone modifications. Epigenetics 4:8–14.

Ho SN, Hunt HD, Horton RM, Pullen JK, Pease LR. 1989. Site-directed mutagenesis by overlap extension using the polymerase chain reaction. Gene 77:51–59.

Hopfner R, Mousli M, Jeltsch JM, Voulgaris A, Lutz Y, Marin C, Bellocq JP, Oudet P, Bronner C. 2000. ICBP90, a novel human CCAAT binding protein, involved in the regulation of topoisomerase IIalpha expression. Cancer Res 60:121–128.

Horton JR, Upadhyay AK, Qi HH, Zhang X, Shi Y, Cheng X. 2010. Enzymatic and structural insights for substrate specificity of a family of jumonji histone lysine demethylases. Nat Struct Mol Biol 17:38–43.

Iwata A, Nagashima Y, Matsumoto L, Suzuki T, Yamanaka T, Date H, Deoka K, Nukina N, Tsuji S. 2009. Intranuclear degradation of polyglutamine aggregates by the ubiquitin-proteasome system. J Biol Chem 284:9796–9803.

Jones PA, Baylin SB. 2007. The epigenomics of cancer. Cell 128:683–692.

Karagianni P, Amazit L, Qin J, Wong J. 2008. ICBP90, a novel methyl K9 H3 binding protein linking protein ubiquitination with heterochromatin formation. Mol Cell Biol 28:705–717.

Kim JK, Esteve PO, Jacobsen SE, Pradhan S. 2009. UHRF1 binds G9a and participates in p21 transcriptional regulation in mammalian cells. Nucleic Acids Res 37:493–505.

Kim D, Blus BJ, Chandra V, Huang P, Rastinejad F, Khorasanizadeh S. 2010. Corecognition of DNA and a methylated histone tail by the MSL3 chromodomain. Nat Struct Mol Biol 17:1027–1029.

Kouzarides T. 2007. Chromatin modifications and their function. Cell 128:693–705.

Lehnertz B, Ueda Y, Derijck AA, Braunschweig U, Perez-Burgos L, Kubicek S, Chen T, Li E, Jenuwein T, Peters AH. 2003. Suv39h-mediated histone H3 lysine 9 methylation directs DNA methylation to major satellite repeats at pericentric heterochromatin. Curr Biol 13:1192–1200.

Leonhardt H, Page AW, Weier HU, Bestor TH. 1992. A targeting sequence directs DNA methyltransferase to sites of DNA replication in mammalian nuclei. Cell 71:865–873.

Li H, Ilin S, Wang W, Duncan EM, Wysocka J, Allis CD, Patel DJ. 2006. Molecular basis for site-specific read-out of histone H3K4me3 by the BPTF PHD finger of NURF. Nature 442:91–95.

Meilinger D, Fellinger K, Bultmann S, Rothbauer U, Bonapace IM, Klinkert WE, Spada F, Leonhardt H. 2009. Np95 interacts with de novo DNA methyltransferases, Dnmt3a and Dnmt3b, and mediates epigenetic silencing of the viral CMV promoter in embryonic stem cells. EMBO Rep 10:1259–1264.

Meissner A, Mikkelsen TS, Gu H, Wernig M, Hanna J, Sivachenko A, Zhang X, Bernstein BE, Nusbaum C, Jaffe DB, Gnirke A, Jaenisch R, Lander ES. 2008. Genome-scale DNA methylation maps of pluripotent and differentiated cells. Nature 454:766–770.

Mortusewicz O, Schermelleh L, Walter J, Cardoso MC, Leonhardt H. 2005. Recruitment of DNA methyltransferase I to DNA repair sites. Proc Natl Acad Sci USA 102:8905–8909.

Muto M, Utsuyama M, Horiguchi T, Kubo E, Sado T, Hirokawa K. 1995. The characterization of the monoclonal antibody Th-10a, specific for a nuclear protein appearing in the S phase of the cell cycle in normal thymocytes and its unregulated expression in lymphoma cell lines. Cell Prolif 28:645–657.

Nady N, Lemak A, Walker JR, Avvakumov GV, Kareta MS, Achour M, Xue S, Duan S, Allali-Hassani A, Zuo X, Wang YX, Bronner C, Chedin F, Arrowsmith CH, Dhe-Paganon S. 2011. Recognition of multivalent histone states associated with heterochromatin by UHRF1. J Biol Chem. [Epub ahead of print].

Ooi SK, Qiu C, Bernstein E, Li K, Jia D, Yang Z, Erdjument-Bromage H, Tempst P, Lin SP, Allis CD, Cheng X, Bestor TH. 2007. DNMT3L connects unmethylated lysine 4 of histone H3 to de novo methylation of DNA. Nature 448:714–717.

Otani J, Nankumo T, Arita K, Inamoto S, Ariyoshi M, Shirakawa M. 2009. Structural basis for recognition of H3K4 methylation status by the DNA methyltransferase 3A ATRX-DNMT3-DNMT3L domain. EMBO Rep 10:1235–1241.

Papait R, Pistore C, Grazini U, Babbio F, Cogliati S, Pecoraro D, Brino L, Morand AL, Dechampesme AM, Spada F, Leonhardt H, McBlane F, Oudet P, Bonapace IM. 2008. The PHD domain of Np95 (mUHRF1) is involved in large-scale reorganization of pericentromeric heterochromatin. Mol Biol Cell 19: 3554–3563.

Peters AH, O'Carroll D, Scherthan H, Mechtler K, Sauer S, Schofer C, Weipoltshammer K, Pagani M, Lachner M, Kohlmaier A, Opravil S, Doyle M, Sibilia M, Jenuwein T. 2001. Loss of the Suv39h histone methyltransferases impairs mammalian heterochromatin and genome stability. Cell 107:323–337.

Pradhan S, Talbot D, Sha M, Benner J, Hornstra L, Li E, Jaenisch R, Roberts RJ. 1997. Baculovirus-mediated expression and characterization of the full-length murine DNA methyltransferase. Nucleic Acids Res 25:4666–4673.

Qian C, Li S, Jakoncic J, Zeng L, Walsh MJ, Zhou MM. 2008. Structure and hemimethylated CpG binding of the SRA domain from human UHRF1. J Biol Chem 283(50):34490–34494.

Reik W. 2007. Stability and flexibility of epigenetic gene regulation in mammalian development. Nature 447:425–432.

Rothbauer U, Zolghadr K, Muyldermans S, Schepers A, Cardoso MC, Leonhardt H. 2008. A versatile nanotrap for biochemical and functional studies with fluorescent fusion proteins. Mol Cell Proteomics 7:282–289.

Rottach A, Frauer C, Pichler G, Bonapace IM, Spada F, Leonhardt H. 2010. The multi-domain protein Np95 connects DNA methylation and histone modification. Nucleic Acids Res 38:1796–1804.

Ruthenburg AJ, Li H, Patel DJ, Allis CD. 2007. Multivalent engagement of chromatin modifications by linked binding modules. Nat Rev Mol Cell Biol 8:983–994.

Schermelleh L, Haemmer A, Spada F, Rosing N, Meilinger D, Rothbauer U, Cardoso MC, Leonhardt H. 2007. Dynamics of Dnmt1 interaction with the replication machinery and its role in postreplicative maintenance of DNA methylation. Nucleic Acids Res 35:4301–4312.

Sharif J, Muto M, Takebayashi S, Suetake I, Iwamatsu A, Endo TA, Shinga J, Mizutani-Koseki Y, Toyoda T, Okamura K, Tajima S, Mitsuya K, Okano M, Koseki H. 2007. The SRA protein Np95 mediates epigenetic inheritance by recruiting Dnmt1 to methylated DNA. Nature 450:908–912.

Sporbert A, Domaing P, Leonhardt H, Cardoso MC. 2005. PCNA acts as a stationary loading platform for transiently interacting Okazaki fragment maturation proteins. Nucleic Acids Res 33:3521–3528.

Szwagierczak A, Bultmann S, Schmidt CS, Spada F, Leonhardt H. 2010. Sensitive enzymatic quantification of 5-hydroxymethylcytosine in genomic DNA. Nucleic Acids Res 38:e181.

Tsumura A, Hayakawa T, Kumaki Y, Takebayashi S, Sakaue M, Matsuoka C, Shimotohno K, Ishikawa F, Li E, Ueda HR, Nakayama J, Okano M. 2006. Maintenance of self-renewal ability of mouse embryonic stem cells in the absence of DNA methyltransferases Dnmt1, Dnmt3a and Dnmt3b. Genes Cells 11:805–814.

Unoki M, Nishidate T, Nakamura Y. 2004. ICBP90, an E2F-1 target, recruits HDAC1 and binds to methyl-CpG through its SRA domain. Oncogene 23: 7601–7610.

Supplementary Information

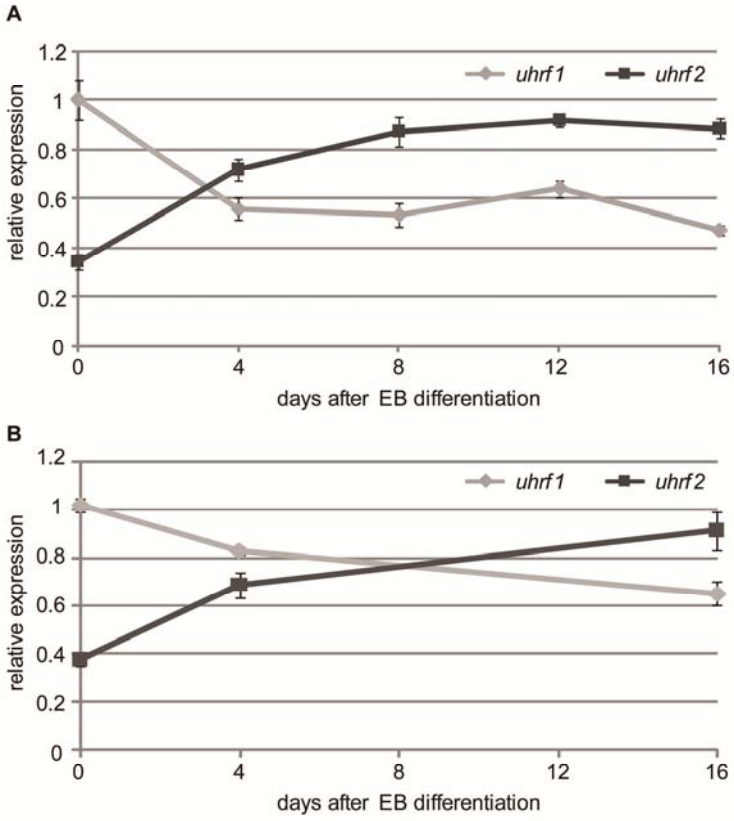

Supplementary Figure S1. Opposite expression pattern of *uhrf1* and *uhrf2*. Expression analyses of *uhrf1* and *uhrf2* by Real-time PCR during differentiation of ESCs with two different genetic backgrounds (wt E14 (**A**) and wt JM8A (**B**)). Transcript levels of *uhrf1* at day 0 of EB formation are used as reference point (set to 1). Shown are means ± SD from three technical replicates of one biological experiment.

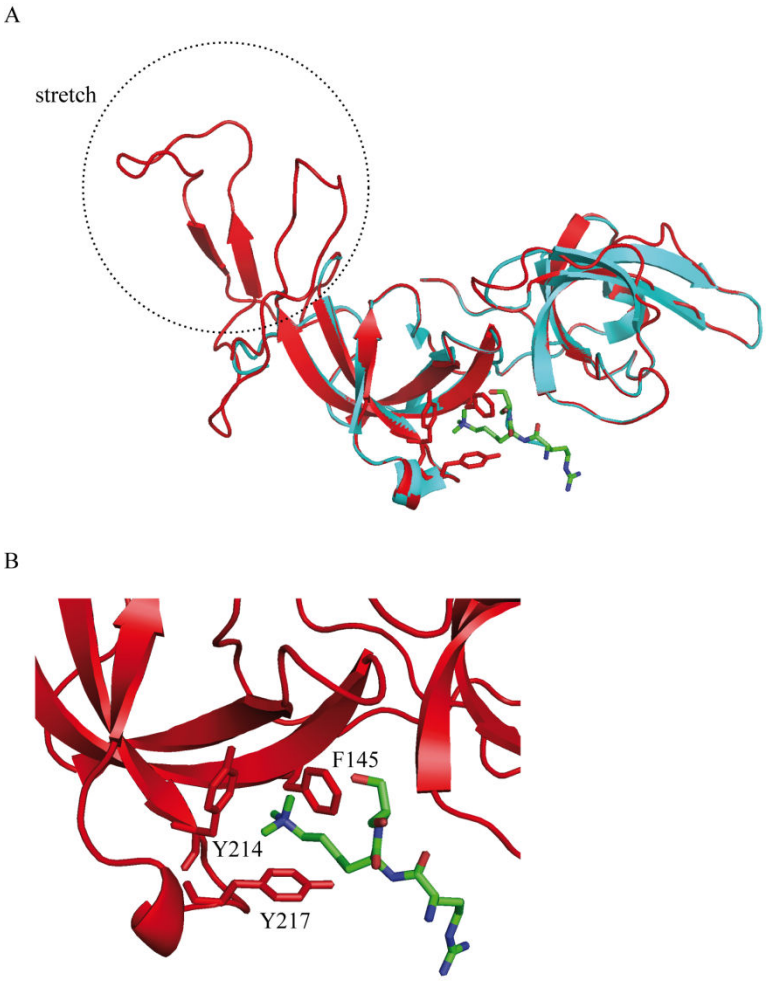

Supplementary Figure S2. Model of the tandem Tudor domain (TTD) of Uhrf2. (**A**) A model of the TTD of Uhrf2 was generated using SWISS Model [Arnold et al., 2006; Guex and Peitsch, 1997] with the solved structure of the TTD of Uhrf1 (PDB: 3DB3) as template. Both structures, the Uhrf2 model in red and the Uhrf1 template in cyan, are superimposed in PyMOL [Schrodinger, 2010]. (**B**) H3K9me3 is embedded in an aromatic cage formed by three aromatic residues of Uhrf2.

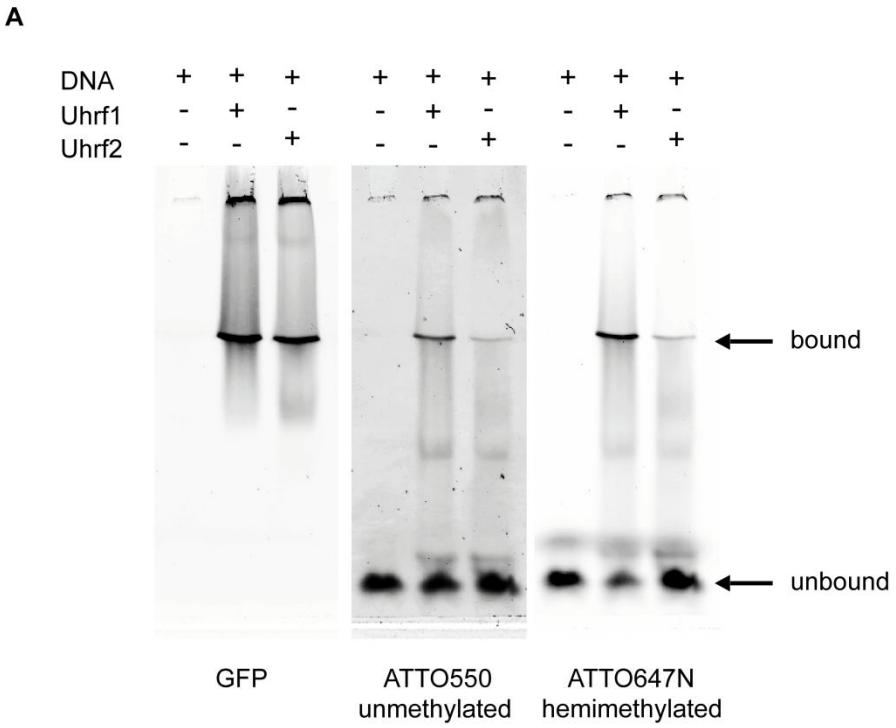

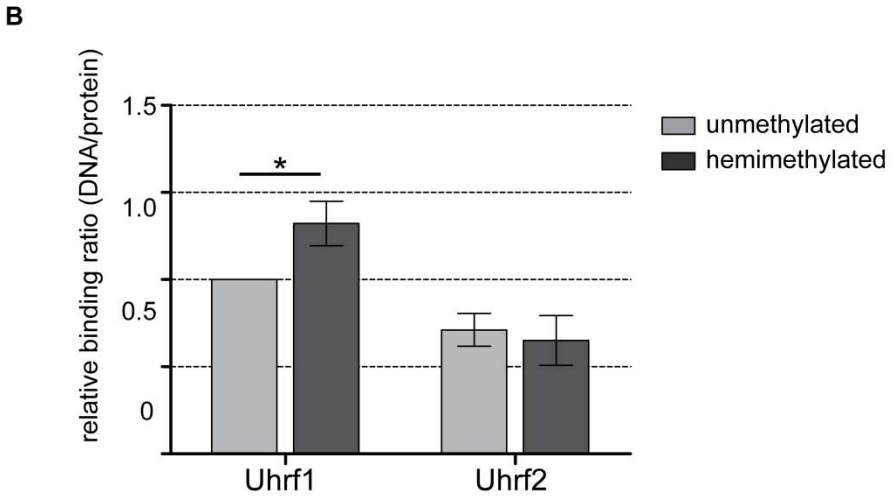

Supplementary Figure S3. Electrophoretic mobility shift of Uhrf1 and Uhrf2. (**A**) Un- and hemimethylated DNA substrates (1 pmol each in direct competition) were incubated with 0.63 pmol purified Uhrf1-GFP or Uhrf2-GFP. Samples were subjected to 3.5% non-denaturing PAGE and analyzed with a fluorescence scanner (Typhoon TRIO scanner, GE Healthcare) to detect ATTO550 (unmethylated substrate), ATTO647N (hemimethylated substrate) and GFP. (**B**) Band intensities were quantified with ImageJ [Abramoff, 2004]. To quantify bound DNA/protein ratios, grey values of unbound DNA bands were subtracted from the corresponding DNA input bands and subsequently normalized by the grey values of the GFP bands. All values were normalized to the relative binding ratio of Uhrf1 to unmethylated substrate. Shown are means ± SD from three independent experiments. Statistical significance between the binding ratios of un- and hemimethylated DNA is indicated; *$P < 0.05$.

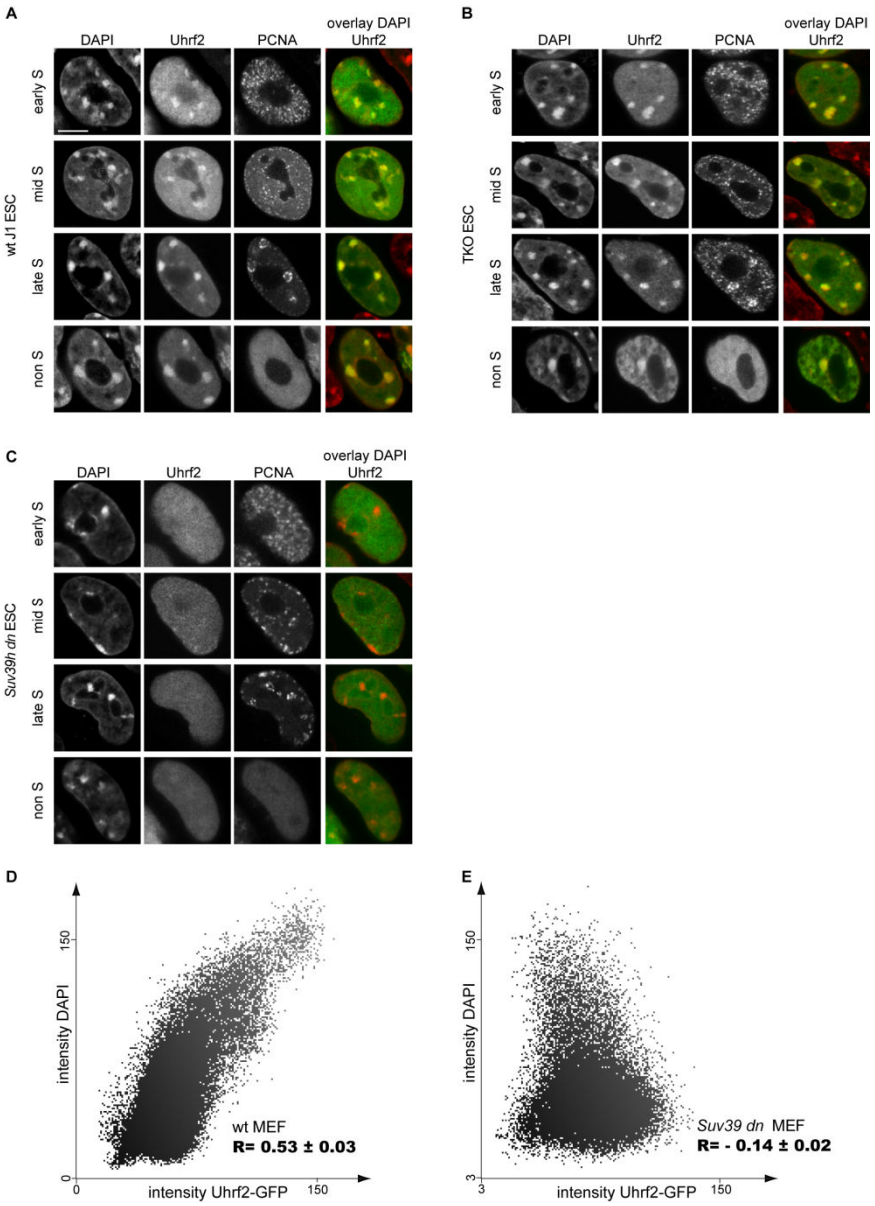

Supplementary Figure S4. Cell-cycle dependent localization of Uhrf2 in cells with different genetic backgrounds. Confocal mid sections of fixed wt J1 (**A**), TKO (**B**) and *Suv39h dn* ESCs (**C**), transiently expressing Uhrf2-GFP. Cells were co-transfected with a RFP-PCNA expression vector to distinguish S phase stages [Sporbert et al., 2005] and counterstained with DAPI. Merged images are displayed on the right. Scale bar 5 µm. In wt J1 and TKO ESCs the Uhrf2 fusion protein accumulates at pericentric heterochromatin independent of the cell-cycle stage and methylation levels (**A**) (**B**). In contrast, Uhrf2-GFP shows a fully dispersed nuclear distribution in *Suv39h dn* cells indicating the dependency on H3K9me3 methylation for localization at PH *in vivo* (**C**). (**D**) and (**E**) Scatter blot of GFP-Uhrf2 and DAPI signals in wt MEFs and *Suv39h dn* MEFs. The corresponding Pearson correlation coefficients R ± SEM are calculated from ten analysed cells. The software Volocity (Perkin Elmer) was used for analysis, selecting the cell nucleus as region of interest. Note that Pearson correlation coefficients range from +1 to -1 for perfect to no co-localization.

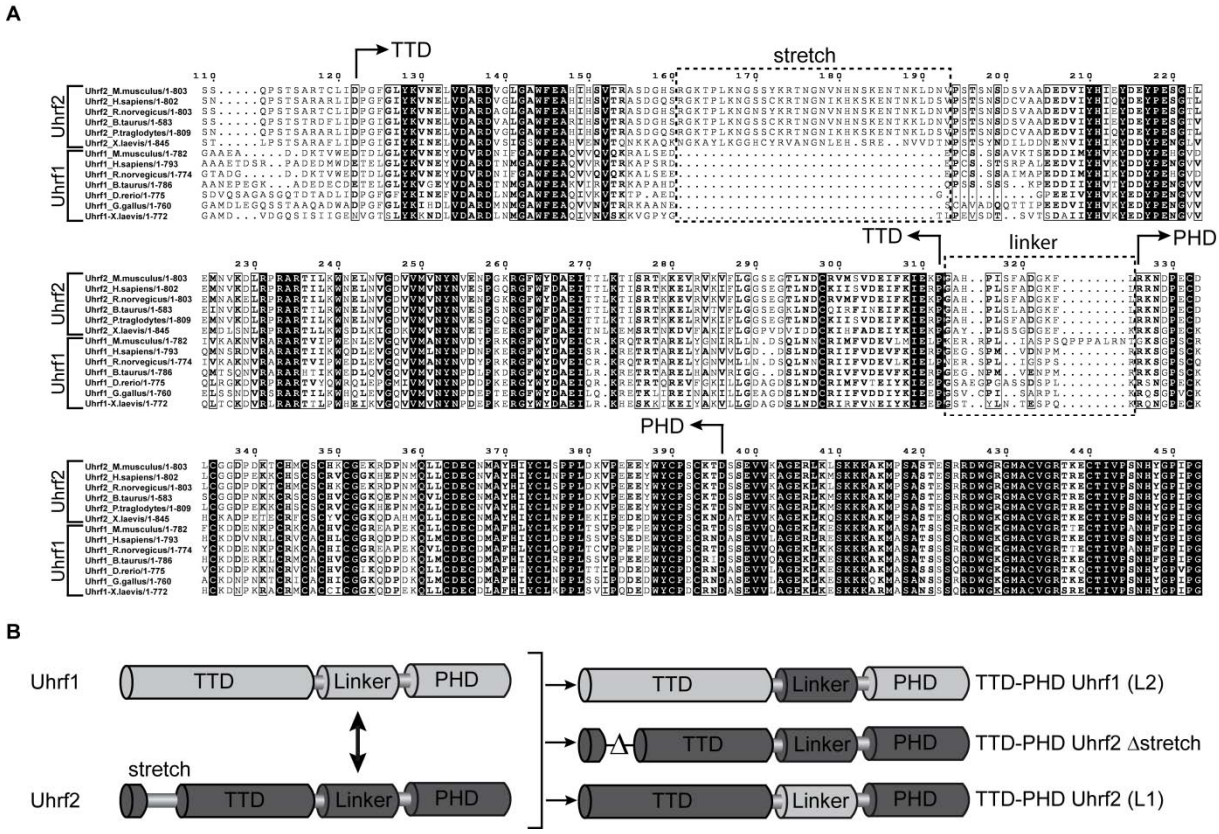

Supplementary Figure S5. Alignment and recombination of Uhrf1 and Uhrf2 domains. (**A**) Alignment of the tandem Tudor domain (TTD) and PHD domains from vertebrate Uhrf2 and Uhrf1 orthologs. Accession numbers for Uhrf2: *Homo sapiens* CAH74119.1; *Bos taurus* AAI48950.1; *Mus musculus* Q7TMI3; *Rattus norvegicus* NP_001101055.1; *Pan troglodytes* XP_528534.2; *Xenopus laevis* AAI28674.1. Accession numbers for Uhrf1: *Homo sapiens* Q96T88.1; *Bos taurus* AAI51672.1; *Mus musculus* Q8VDF2.2; *Rattus norvegicus* Q7TPK1.2; *Dario rerio* NP_998242.1; *Xenopus laevis* AAI28674.1, *Gallus gallus* XP_418269.2. Arrows show the start and end positions of the TTD and PHD domains. Absolutely conserved residues are black shaded, while positions showing conservative substitutions are boxed with residues in bold face. The additional stretch region found in the TTD of Uhrf2 and the linker region between TTD and PHD finger are boxed with dotted black lines. (**B**) Schematic outline of engineered constructs including the deletion of the stretch region and the swapping of linker sequences.

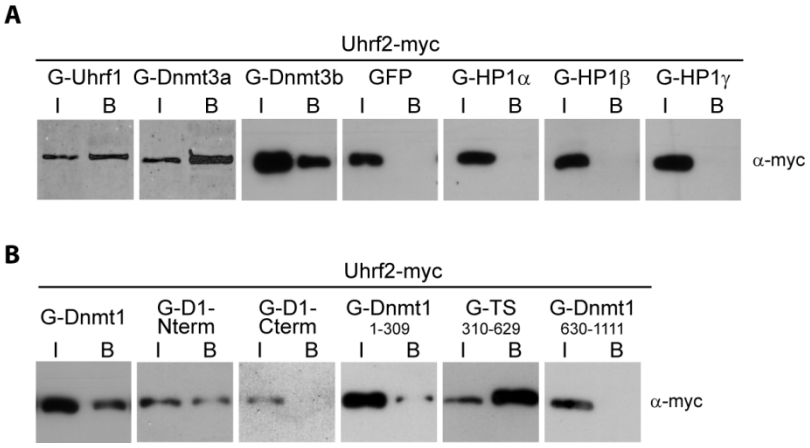

Supplementary Figure S6. Uhrf2 interacts with Uhrf1, Dnmt1 and Dnmt3a/b. (**A**) Co-immunoprecipation of Uhrf2-myc and GFP-Uhrf1, GFP-Dnmt3a, GFP-Dnmt3b, GFP-HP1α, GFP-HP1β, GFP-HP1γ or GFP transiently co-expressed in HEK293T cells. Note that Uhrf2 interacts with Uhrf1, Dnmt3a and Dnmt3b. (**B**) Co-immunoprecipation of Uhrf2-myc and GFP-Dnmt1 constructs transiently co-expressed in HEK293T cells: GFP-Dnmt1 (G-Dnmt1), GFP-fusions of the N-terminal and C-terminal part of Dnmt1 (G-D1-Nterm, G-D1-Cterm) and truncated Dnmt1 constructs (G-Dnmt1 1-309, G-TS 310-629, G-Dnmt1 630-1111). Note that Uhrf2 interacts with full-length Dnmt1, the N-terminal part and the targeting sequence (G-TS 310-629). One percent of input (I) relative to bound fractions (B) was loaded. Co-immunoprecipitation was performed using the GFP trap [Rothbauer et al., 2008]. Co-precipitated myc-tagged proteins were detected using a mouse monoclonal primary anti-myc antibody (Invitrogen, Germany) and an HRP- or Cy5-conjugated secondary anti-mouse antibody (Sigma, Germany, or Jackson ImmunoResearch Laboratories, USA, respectively).

A

Peptide name	Peptide sequence	Peptide labelling
H3K4me1	ART X1 QTARKSTGGKAPRKQLK	TAMRA at C-terminus
H3K4me2	ART X2 QTARKSTGGKAPRKQLK	
H3K4me3	ART X3 QTARKSTGGKAPRKQLK	
H3K4ac	ART Z QTARKSTGGKAPRKQLK	
H3K4/9un	ARTKQTARKSTGGKAPRKQLK	
H3K9me1	ARTKQTAR X1 STGGKAPRKQLK	
H3K9me2	ARTKQTAR X2 STGGKAPRKQLK	
H3K9me3	ARTKQTAR X3 STGGKAPRKQLK	
H3K9ac	ARTKQTAR Z STGGKAPRKQLK	
H3R2me2a	A X4 TKQTARSTGGKAPRKQLK	
H3K4me3K9me3	ART X3 QTAR X3 STGGKAPRKQLK	
H3K27un	RKQLATKAARKSAPATGGVK	TAMRA at N-terminus
H3K27me1	RKQLATKAAR X1 SAPATGGVK	
H3K27me2	RKQLATKAAR X2 SAPATGGVK	
H3K27me3	RKQLATKAAR X3 SAPATGGVK	
H3K27ac	RKQLATKAAR Z SAPATGGVK	
H4K20un	LGKGGAKRHRKVLRDNIQGI	
H4K20me1	LGKGGAKRHR X1 VLRDNIQGI	
H4K20me2	LGKGGAKRHR X2 VLRDNIQGI	
H4K20me3	LGKGGAKRHR X3 VLRDNIQGI	
H4K20ac	LGKGGAKRHR Z VLRDNIQGI	

X1: Lysine(me1); X2: Lysine(me2); X3: Lysine(me3); X4: Arginine(me2 asymmetric) Z: Lysine(ac)

B

DNA substrate	DNA sequence	DNA labelling
CGup	CTCAACAACTAACTACCATCCGGACCAGAAGAGTCATCATGG	no
MGup	CTCAACAACTAACTACCATCMGGACCAGAAGAGTCATCATGG	no
noCpG	CTCAACAACTAACTACCATCCTGACCAGAAGAGTCATCATGG	no
um647N	CCATGATGACTCTTCTGGTCCGGATGGTAGTTAGTTGTTGAG	ATTO647N at 5´end
um700	CCATGATGACTCTTCTGGTCCGGATGGTAGTTAGTTGTTGAG	ATTO700 at 5´end
Fill-In-550	CCATGATGACTCTTCTGGTC	ATTO550 at 5´end
Fill-In-590	CCATGATGACTCTTCTGGTC	ATTO590 at 5´end
Fill-In-647N	CCATGATGACTCTTCTGGTC	ATTO647N at 5´end
Fill-In-700	CCATGATGACTCTTCTGGTC	ATTO700 at 5´end

C

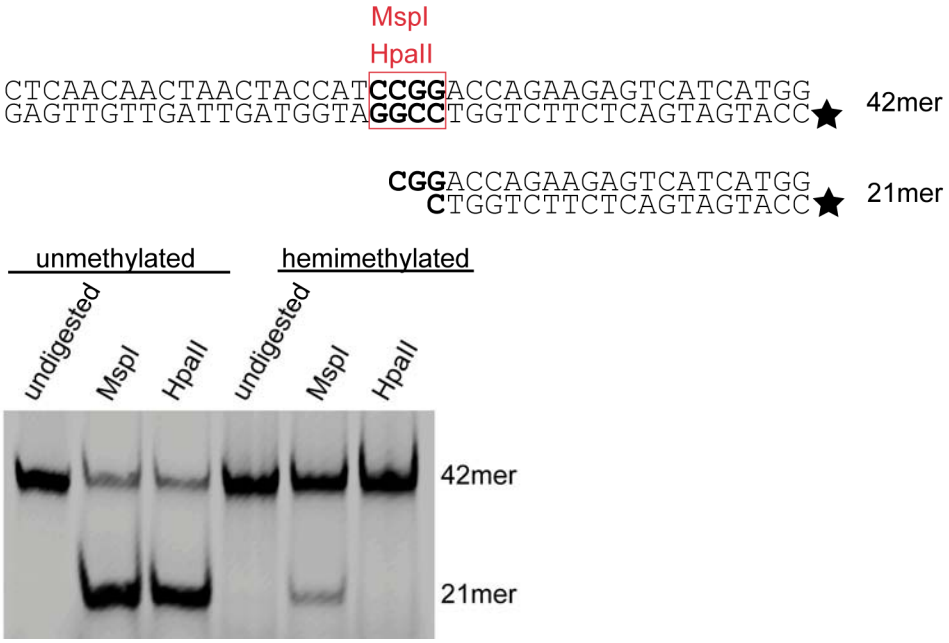

Supplementary Figure S7. Histone-tail peptide and DNA sequences and quality control of DNA substrates. (**A**) Amino acid sequence of TAMRA-labelled peptides for *in vitro* histone-tail peptide binding assays. Histone-tail peptides were purchased as TAMRA conjugates (PSL, Germany). (**B**) DNA oligos used for preparation of double-stranded probes for *in vitro*

DNA binding assays. M: 5-methyl-cytosine. For hybridization, DNA oligos were mixed in equimolar amounts, heated to 92°C and cooled down to room temperature. DNA substrates for Figure 2F were completed in a primer extension reaction. By using a control set of DNA probes with identical sequence but different fluorescent labels we observed effects due to probe preparation and/or unspecific binding of ATTO dyes (data not shown). The values obtained from the control set were used to normalize every probe/protein pair. (**C**) Quality control of DNA substrates. Un- and hemimethylated DNA substrates (2 pmol; Atto647N labelled) were digested with 1 unit MspI or HpaII and analyzed by 15% non-denaturing PAGE for CpG methylation. Note that unmethylated DNA substrate is digested by both enzymes, whereas hemimethylated substrate is only cut by MspI. Enzyme recognition motifs are boxed and asterisks represent ATTO labels.

Supplementary References

Abramoff MD, Magelhaes, P.J., Ram, S.J. 2004. Image Processing with ImageJ. Biophotonics International 11:36-42.

Arnold K, Bordoli L, Kopp J, Schwede T. 2006. The SWISS-MODEL workspace: a web-based environment for protein structure homology modelling. Bioinformatics 22:195-201.

Guex N, Peitsch MC. 1997. SWISS-MODEL and the Swiss-PdbViewer: an environment for comparative protein modeling. Electrophoresis 18:2714-23.

Rothbauer U, Zolghadr K, Muyldermans S, Schepers A, Cardoso MC, Leonhardt H. 2008. A versatile nanotrap for biochemical and functional studies with fluorescent fusion proteins. Mol Cell Proteomics 7:282-9.

Schrodinger, LLC. 2010. The PyMOL Molecular Graphics System, Version 1.3editor^editors.

Sporbert A, Domaing P, Leonhardt H, Cardoso MC. 2005. PCNA acts as a stationary loading platform for transiently interacting Okazaki fragment maturation proteins. Nucleic Acids Res 33:3521-8.

3.5 DNMT1 regulation by interactions and modifications

Nucleus 2:5, 392-402; September/October 2011; © 2011 Landes Bioscience

Regulation of DNA methyltransferase 1 by interactions and modifications

Weihua Qin, Heinrich Leonhardt* and Garwin Pichler

Center for Integrated Protein Science; Department of Biology II; Ludwig Maximilians University; Munich, Germany

Key words: DNMT1, Dnmts, DNA methylation, epigenetics, DNA methyltransferases, post-translational modifications, protein interactions

DNA methylation plays a central role in the epigenetic regulation of gene expression during development and disease. Remarkably, the complex and changing patterns of genomic DNA methylation are established and maintained by only three DNA methyltransferases. Here we focus on DNMT1, the major and ubiquitously expressed DNA methyltransferase in vertebrates, to outline possible regulatory mechanisms. A list of all protein interactions and post-translational modifications reported for DNMT1 clearly shows that DNMT1, and by extension also DNA methylation in general, are functionally linked with several other epigenetic pathways and cellular processes. General themes of these interactions and modifications include the activation, stabilization and recruitment of DNMT1 at specific sites and heterochromatin regions. For a comprehensive understanding of the regulation of DNA methylation it is now necessary to systematically quantify the interactions and modifications of DNMT1, to elucidate their function at the molecular level and to integrate these data at the cellular level.

Introduction

Multicellular organisms contain a variety of highly specialized cells that despite their morphological and functional differences possess the same genetic information. During development, different sets of genes are activated and repressed to generate the cell type-specific functionality. It has become increasingly clear that cell type-specific gene expression patterns are established and maintained by a complex interplay of transcriptions factors and epigenetic regulators. In particular, DNA and histone modifications control the composition, structure and dynamics of chromatin and thereby regulate gene expression.[1-3]

DNA methylation was the first epigenetic modification to be identified and has been intensively studied for half a century. DNA methylation is the post-replicative addition of methyl groups to the C5 position of cytosines catalyzed by a family of DNA methyltransferases (Dnmts). All C5 Dnmts share the same conserved motifs involved in the complex molecular mechanism of methyl group transfer best studied in the prokaryotic Dnmt M.HhaI (**Fig. 1A**).[6] This mechanism involves Dnmt binding to the DNA, flipping the target cytosine out of the DNA double helix, covalent bond formation between a conserved cysteine nucleophile and the cytosine C6, transfer of a methyl group from S-adenosyl-l-methionine to the activated cytosine C5 and Dnmt release by β-elimination.[6,7]

In vertebrates, there are five known members of the Dnmt family that differ in structure and function and apart from DNMT2, all Dnmts comprise an N-terminal regulatory domain in addition to the C-terminal catalytic domain (**Fig. 1A**). The Dnmt3 subfamily, comprising DNMT3a and DNMT3b, shows activity toward unmethylated DNA and establishes de novo DNA methylation patterns during gametogenesis and embryogenesis.[8-10] The cofactor DNMT3L[11] specifically recognizes unmethylated histone H3K4 [12] and stimulates the activity of DNMT3a and DNMT3b,[13] but by itself lacks enzymatic activity.[14] Established DNA methylation patterns are maintained during DNA replication and DNA repair by the ubiquitously expressed DNMT1,[15,16] which displays a strong preference for hemimethylated CpG sites, the substrate of maintenance DNA methylation.[17] The fifth member of the Dnmt family, DNMT2, shows very weak activity toward DNA and was instead shown to methylate cytoplasmic $tRNA^{Asp}$.[18,19]

Despite their common catalytic mechanism, all three active eukaryotic Dnmts have distinct and non-redundant functions which are likely mediated by their diverse regulatory domains (**Fig. 1A**). In contrast to prokaryotic Dnmts, the tissue-specific de novo Dnmts, DNMT3a and DNMT3b, are only active on a subset of target CpG sites,[20] reflecting a selective control imposed by the N-terminal regulatory domain. The ubiquitously expressed DNMT1 preferentially methylates hemimethylated CpG sites and thereby maintains DNA methylation patterns after DNA replication and DNA repair.[15-17] Remarkably, the catalytic domain of DNMT1—although possessing all conserved motifs—is not catalytically active by itself and requires allosteric activation by the N-terminal regulatory domain.[21-23] In this review we will focus on a detailed description of DNMT1 regulation to illustrate the extremely complex and interconnected regulation of DNA methylation.

Structure and Function of DNMT1

Bioinformatic analysis suggested that mammalian DNMT1 evolved by fusion of at least three ancestral genes.[22] The

*Correspondence to: Heinrich Leonhardt; Email: h.leonhardt@lmu.de
Submitted: 07/01/11; Revised: 08/27/11; Accepted: 08/31/11
http://dx.doi.org/10.4161/nucl.2.5.17928

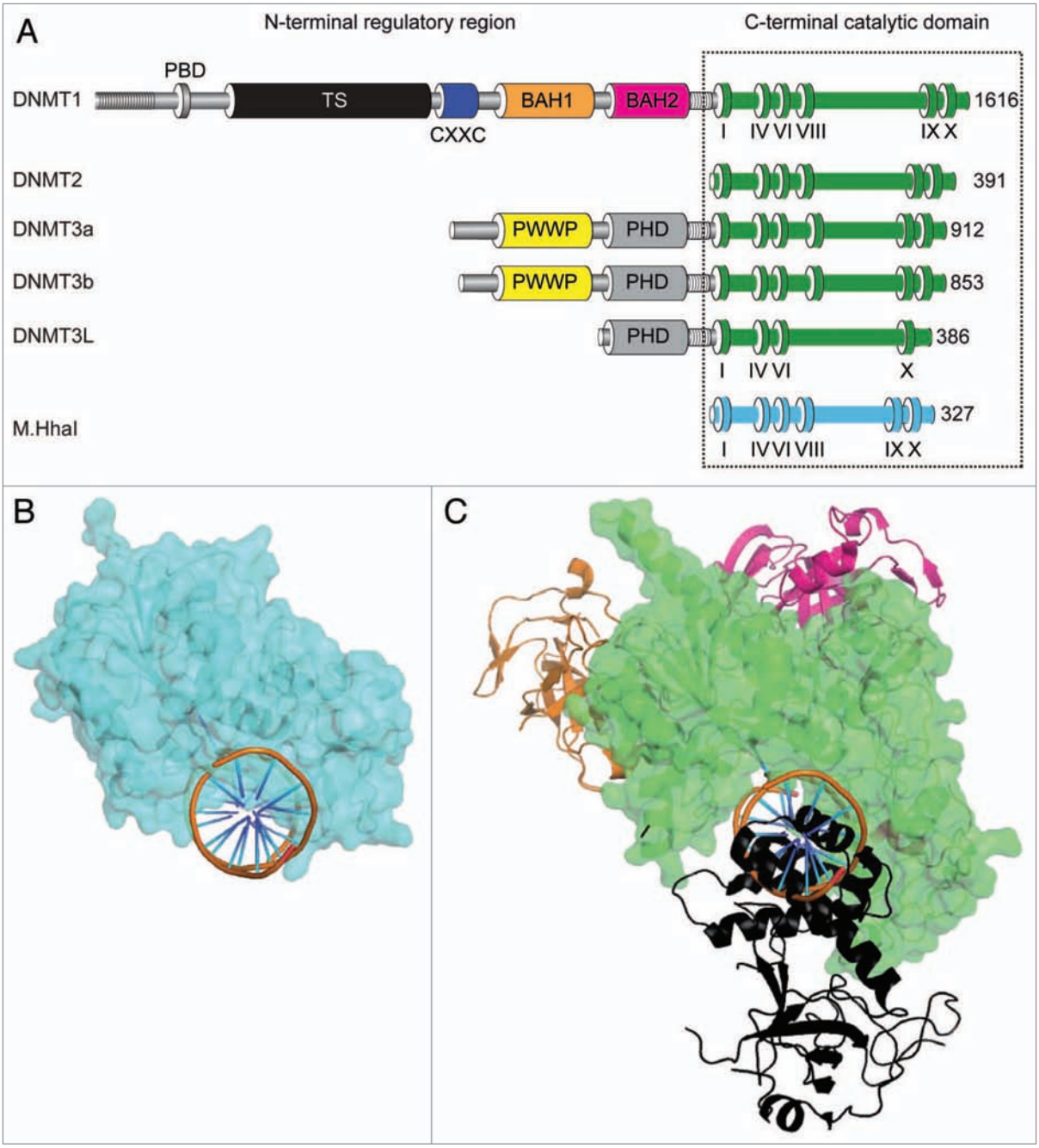

Figure 1. Structural insights into the DNA methyltransferase 1 (DNMT1). (A) Schematic outline of the domain architecture of mammalian Dnmts in comparison to the prokaryotic Dnmt, M.HhaI. All Dnmts harbor highly conserved motifs (I-X) in the C-terminal catalytic domain. In addition, DNMT1 harbors a proliferating cell nuclear antigen (PCNA) binding domain (PBD) followed by the targeting sequence (TS domain), a zinc finger domain (CXXC), two bromo-adjacent homology domains (BAH1/2). DNMT3a and DNMT3b comprise a PWWP domain and a PHD domain that is also found in DNMT3L. (B) Crystal structure of the prokaryotic cytosine-(C5) methyltransferases M.HhaI in complex with hemimethylated DNA (PDB ID code 5mht).[4] (C) Crystal structure of the large fragment (291–1,620) of mouse DNMT1 (PDB ID code 3AV4) [5] in superimposition with the prokaryotic structure (B) showing the expected steric clash between the TS domain and DNA binding in the catalytic pocket. The single domains are color-coded as in (A).

N-terminal domain of DNMT1 harbors a proliferating cell nuclear antigen (PCNA) binding domain (PBD), a targeting sequence (TS domain), a zinc finger domain (CXXC) and two bromo-adjacent homology domains (BAH1/2) and is connected to the C-terminal catalytic domain by seven lysyl-glycyl dipeptide repeats.[24,25] The PBD domain has been shown to mediate the interaction with PCNA leading to the association of DNMT1 with the replication machinery.[15,26,27] The TS domain mediates association with heterochromatin and may lead to dimerization of DNMT1.[15,27,28] The CXXC domain of DNMT1 binds to

unmethylated DNA but its deletion does not alter the activity and specificity of DNMT1.[29] Interestingly, the isolated C-terminal catalytic domain of DNMT1, although harboring all conserved Dnmt motifs, requires an additional, large part of the N-terminal domain for enzymatic activity.[21-23] Fusion of this N-terminal region of DNMT1 to the prokaryotic Dnmt, M.HhaI, induced a preference for hemimethylated DNA.[30] Cleavage between the regulatory and the catalytic domain stimulated the initial velocity of methylation of unmethylated DNA without substantial change in the rate of methylation of hemimethylated DNA.[31] These findings illustrate the role of the N-terminal domain in the selective activation of the catalytic domain to ensure faithful maintenance of DNA methylation patterns.

First insights into the molecular mechanism of DNMT1 regulation were provided by two recently published crystal structures comprising either a large fragment of mouse DNMT1 (aa 291–1,620) (PDB ID code 3AV4) or a shorter fragment (aa 650–1,602) in complex with unmethylated DNA (PDB ID code 3PT6).[5,32] Notably, the overall structure of the eukaryotic catalytic domain is highly similar to the prokaryotic M.HhaI (PDB ID code 5mht) (**Fig. 1B and C**).[4] In addition, both structures showed an interaction of the N-terminal regulatory domain with the C-terminal catalytic domain,[5,32] which is consistent with prior genetic and biochemical studies.[21,33] Remarkably, the TS domain was found deeply inserted into the catalytic pocket and would in this conformation prevent DNMT1 binding to hemimethylated DNA, the substrate for maintenance DNA methylation.[5] These structural insights indicate that DNMT1 most likely undergoes several conformational changes during the methylation reaction. Activation of DNMT1 requires displacement of the TS domain from the DNA binding pocket to allow substrate binding. Indeed, deletion of the TS domain lowered the activation energy[4] and addition of purified TS domains inhibited DNMT1 methylation activity in vitro,[34] clearly pointing to an auto-inhibitory function of the TS domain. These findings suggest that interacting proteins may modulate the interactions of the N-terminal domain with the catalytic domain and thereby regulate the activity of DNMT1 in vivo.

Regulation of DNMT1 Activity by Interacting Factors

Previously, it was proposed that nuclear processes like the replication of genetic and epigenetic information are regulated and coordinated by targeting participating proteins to functional subnuclear structures.[35-37] Over the last two decades, a large variety of proteins were reported to interact with DNMT1, ranging from DNA methyltransferases, DNA binding proteins, chromatin modifiers and chromatin binding proteins to tumor suppressors, cell cycle regulators and transcriptional regulators (**Fig. 2 and Table 1**).

The discrepancy between the high processivity of DNA replication (~0.035 sec per nucleotide) [42] and the low turnover rates (70–450 sec per methyl group) of recombinant DNMT1 [43] in vitro suggests that additional mechanisms increase the activity of DNMT1 in vivo. Indeed, DNMT1 associates with the replication machinery[15] by directly binding to PCNA, a homotrimeric ring which serves as a common loading platform for replication factors.[26,44-46] Binding of DNMT1 to PCNA enhances the methylation activity about 2-fold, but is not strictly required for maintaining DNA methylation in vivo.[47,48] Thus, the transient association between DNMT1 and PCNA alone cannot bridge the gap between the slow in vitro kinetics of DNMT1 and the fast progression of the replication fork in vivo.

Although DNMT1 can bind hemimethlytated CpG sites by itself, it also interacts with methyl-CpG binding proteins like MeCP2,[49] MBD2/3 [50] and the UHRF family.[25,51] MeCP2 binds DNA, induces chromatin compaction[52,53] and interacts with DNMT1 via its transcription repressor domain (TRD).[49] MeCP2 and MBD2, which specifically recognize fully methylated CpG sites,[54] and MBD3 also form complexes with histone deactelyases HDAC1 and HDAC2 which in turn interact with DNMT1.[49,55-58] This set of interactions can explain the correlation between DNA hypermethylation and histone hypoacetylation at transcriptional inactive regions,[59] suggesting a role in transcriptional repression.[60] This complex may also comprise the DNMT1 association protein (DMAP1) [58,61] and the transcriptional co-regulator Daxx[62] mediating repression in an HDAC-independent manner.[58,61] In addition, the interaction with methyl-CpG binding proteins and HDACs may enrich DNMT1 in highly methylated heterochromatic regions to increase local methylation efficiency and/or enhance heterochromatin formation at these highly methylated regions.

Recently, UHRF1 has emerged as an essential co-factor for maintenance DNA methylation. The genetic ablation of *uhrf1* in embryonic stem cells (ESCs) leads to genomic hypomethylation similar to *dnmt1*$^{-/-}$ ESCs.[63,64] UHRF1 co-localizes and interacts with DNMT1 throughout S-phase and preferentially binds to hemimethylated DNA via a SET and Ring associated (SRA) domain and to the H3K9me3 heterochromatin mark via a tandem Tudor domain.[65-69] The crystal structure of the SRA domain in complex with hemimethylated DNA revealed that the 5-methylcytosine is flipped out of the DNA double helix, a configuration that would stabilize the UHRF1-DNA interaction.[65-69] These results suggest that DNMT1 does not directly bind its substrate, the hemimethylated DNA, but is rather recruited by UHRF1. Recently, the second member of the UHRF family, UHRF2, was also shown to interact with DNMT1 and repressive epigenetic marks.[70] The slight differences in the structure and function of UHRF1 and UHRF2 and their opposite expression patterns suggest non-redundant functions during development.[70] In addition, UHRF1 and UHRF2, as well as DNMT1, bind to the de novo Dnmts DNMT3a and DNMT3b.[70-75] These results demonstrate a complex interplay between methyl-CpG binding proteins and Dnmts in establishing genomic DNA methylation patterns.

Besides the interaction with methyl-CpG binding proteins, DNMT1 also associates with a number of proteins involved in the establishment and maintenance of heterochromatin structure. DNMT1 interacts with the major eukaryotic histone methyltransferases Suv39H1 [76] and EHMT2 [77-80] (also known as G9a), which are essential for H3K9 methylation.[73,81] Genetic ablation of *ehmt2* [81,82] and *suv39 h*[73] in mouse ESCs leads to DNA hypomethylation at specific loci in genomic DNA and altered

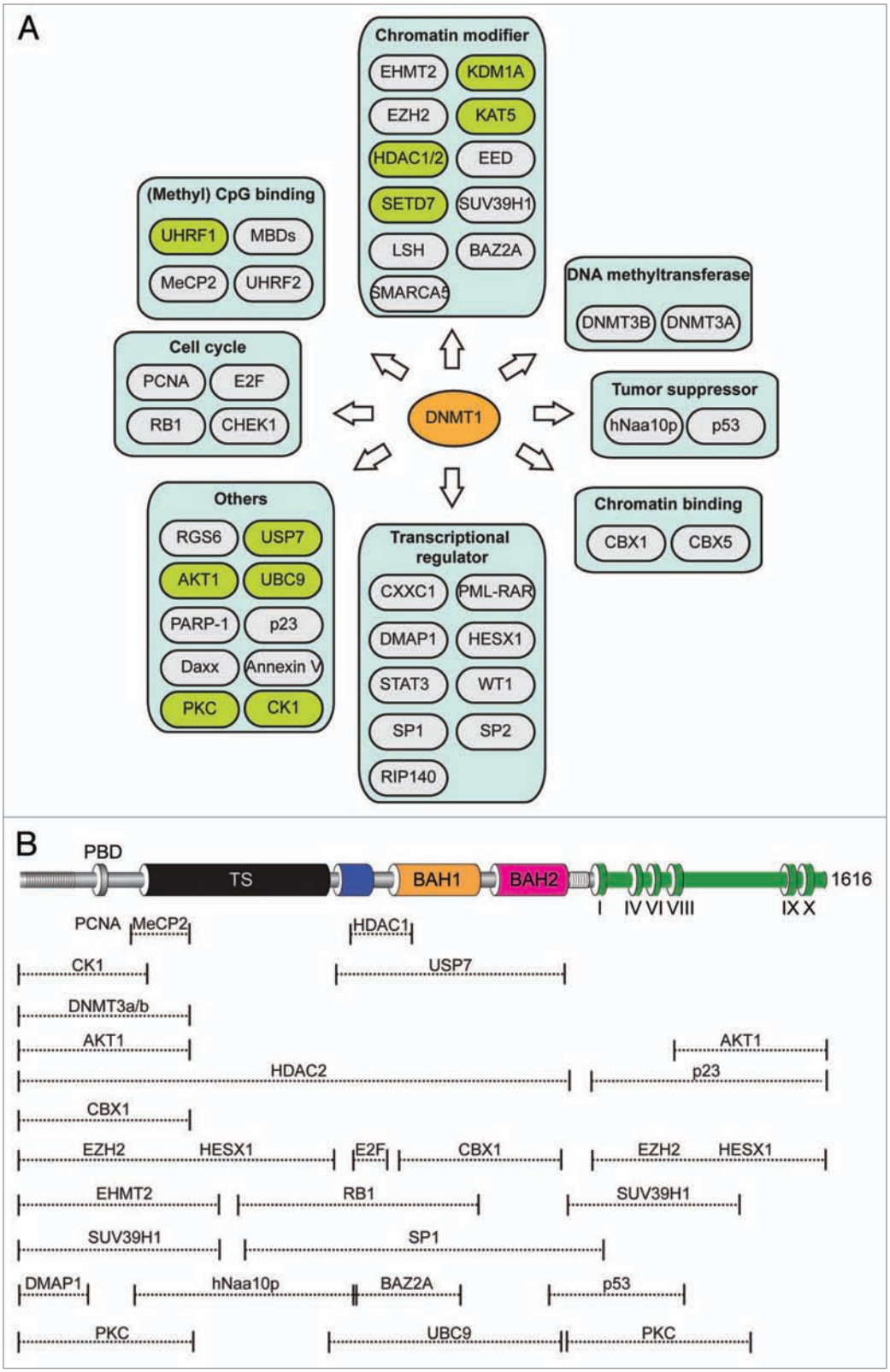

Figure 2. Overview of DNMT1 interacting proteins. (A) Interacting proteins range from DNA methyltransferases, DNA binding proteins, chromatin modifiers and chromatin binding proteins to tumor suppressors, cell cycle regulators and transcriptional regulators. Proteins involved in the post-translational modification of DNMT1 are highlighted in green. (B) Mapped interaction domains are indicated.

Table 1. Overview of DNMT1 interacting proteins

Interacting Protein	Function	Method	Organism	References
		Trancriptional regulator		
DMAP1	Involved in transcription repression and activation Component of the NuA4 histone acetyltransferase (HAT) complex	Yeast 2-hybrid (Y2H) Affinity Capture-western (AC/WB) Reconstituted Complex	*H. sapiens*	Rountree, et al. 2000
PML-RAR	Transcriptional regulator of retinoic acid (RA) target genes; induces gene hypermethylation and silencing by recruiting Dnmt1	AC/WB	*H. sapiens*	Di Croce, et al. 2002
HESX1	Required for the normal development of the forebrain, eyes and other anterior structures; Possible transcriptional repressor	Y2H AC/WB	*H. sapiens*	Sajedi, et al. 2008
CXXC1 (CFP1)	Transcriptional activator that exhibits a unique DNA binding specificity for [AC] CpG[AC] unmethylated CpG motifs	AC/WB	*H. sapiens*	Butler, et al. 2008
SP1	Transcription factor	AC/WB	*H. sapiens*	Esteve, et al. 2007
SP3	Transcription factor	AC/WB	*H. sapiens*	Esteve, et al. 2007
STAT3	Transcription factor that binds to the interleukin-6 (IL-6)-responsive elements	AC/WB Co-localization	*H. sapiens*	Zhang, et al. 2005
WT1	Transcription factor that plays an important role in cellular development and cell survival	AC/WB	*H. sapiens*	Xu, et al. 2011
RIP140	Modulates transcriptional activation and repression	AC/WB	*H. sapiens*	Kiskinis, et al. 2007
		Chromatin modifier		
HDAC1/2	Deacetylation of lysine residues on the N-terminal part of the core histones (H2A, H2B, H3 and H4)	AC/WB Co-fractionation Reconstituted Complex Y2H	*H. sapiens* *M. musculus*	Fuks, et al. 2000; Rountree, et al. 2000; Achour, et al. 2008; Kimura, et al. 2003; Robertson, et al. 2000; Myant, et al. 2008;
KDM1A (AOF2; LSD1)	Histone demethylation of H3K4me and H3K9me; Demethylation of DNMT1	AC/WB	*M. musculus*	Wang, et al. 2008
SUV39H1	Histone methyltransferase that specifically trimethylates H3K9	AC/WB	*H. sapiens*	Fuks, et al. 2003; Estève, et al. 2006
EHMT2 (G9a)	Histone methyltransferase that specifically mono- and dimethylates H3K9	AC/WB	*H. sapiens*	Estève, et al. 2006; Kim, et al. 2009; Tachibana, et al 2002; Peters, et al. 2003
EZH2	Polycomb group (PcG) protein. Catalytic subunit of the PRC2/EED-EZH2 complex	AC/WB Reconstituted complex	*H. sapiens*	Vire, et al. 2006; Xu, et al; 2011
EED	Polycomb group (PcG) protein. Component of the PRC2/EED-EZH2 complex	AC/WB Co-localization	*H. sapiens*	Vire, et al. 2006
SETD7	Histone methyltransferase that specifically monomethylates H3K9	AC/WB Biochemical Activity	*H. sapiens*	Esteve, et al. 2009
KAT5 (TIP60)	Catalytic subunit of the NuA4 histone acetyltransferase complex	AC/WB	*H. sapiens*	Du, et al. 2010
LSH	Chromatin remodeling	AC/WB	*H. sapiens*	Myant and Stancheva, 2008
SMARCA5 (SNF2H)	Helicase that possesses intrinsic ATP-dependent nucleosome-remodeling activity	AC/WB	*H. sapiens*	Robertson, et al. 2004

The function of proteins is according to the UniProt database[38,39] and the applied method is according to the BioGRID[40] database apart from the fluorescent two-hybrid (F2H) assay.[41] All protein names are according to the human nomenclature unless noted otherwise. Proteins involved in the post-translational modification of DNMT1 are highlighted in green.

Table 1. Overview of DNMT1 interacting proteins

BAZ2A (TIP5)	Essential component of the NoRC (nucleolar remodeling complex) complex	Reconstituted Complex	*H. sapiens*	Zhou, et al. 2005
(Methyl) CpG binding proteins				
MeCP2	Methylated CpG binding protein	AC/WB Reconstituted complex	*R. norvegicus*	Kimura and Shiota, 2003
MBD2/MBD3	Methylated CpG binding protein	AC/WB	*H. sapiens*	Tatematsu, et al. 2000
UHRF1	Hemimethylated CpG binding protein; essential for maintenance DNA methylation	Y2H AC/WB Reconstituted complex Co-localization	*H. sapiens* *M. musculus*	Bostick, et al. 2007 ; Sharif, et al. 2007; Arita, et al. 2008 ; Awakumov, et al. 2008; Qian, et al. 2008; Achour, et al. 2008; Meilinger, et al. 2009
UHRF2	E3 ubiquitin-protein ligase which mediates ubiquitination and subsequent proteasomal degradation of PCNP; Hemimethylated CpG binding protein	AC/WB	*M. musculus*	Pichler, et al. 2011
Tumor suppressor				
p53	Tumor suppressor in many tumor types	AC/WB	*H. sapiens*	Esteve, et al. 2005
hNaa10p	Tumor suppressor Stimulate Dnmt1 activity	AC/WB	*H. sapiens*	Lee, et al. 2010
DNA methyltransferase				
DNMT3a	Required for genome wide de novo methylation and is essential for the establishment of DNA methylation patterns during development	AC/WB Reconstituted Complex	*H. sapiens* *M. musculus*	Fatemi, et al. 2002; Kim, et al. 2002
DNMT3b	Required for genome wide de novo methylation and is essential for the establishment of DNA methylation patterns during development	AC/WB Reconstituted Complex	*H. sapiens*	Rhee, et al. 2002; Kim, et al. 2002; Lehnertz, et al. 2003; Geiman 2004
Chromatin binding protein				
HP1β	Recognizes and binds methylated H3K9	Reconstituted Complex	*H. sapiens*	Fuks, et al. 2003
CBX5	Recognizes and binds methylated H3K9	AC/WB	*H. sapiens*	Lehnertz, et al. 2003
Cell cycle regulator				
PCNA	Targeting Dnmt1 to replication foci	AC/WB Reconstituted Complex Co-localization	*H.sapiens*	Leonhardt, et al. 1992; Chuang, et al. 1997; Rountree, et al. 2000
RB1	Cell cycle regulator	AC/WB Reconstituted Complex Co-fractionation	*H. sapiens*	Robertson, et al. 2000; Pradhan, et al. 2002
E2F1	Transcription factor Play a role in controlling cell cycle entry	Co-fractionation	*H. sapiens*	Robertson, et al. 2000
CHEK1 (CHK1)	checkpoint mediated cell cycle arrest in response to DNA damage or the presence of unreplicated DNA	AC/WB	*H. sapiens*	Palii, et al. 2008
Others				
RGS6	Regulator of G-protein signaling	Reconstituted Complex	*H. sapiens*	Liu, et al. 2004
USP7	Hydrolase that deubiquitinates target proteins	AC/Mass Spectrometry AC/WB F2H	*H. sapiens* *M. musculus*	Sowa, et al. 2009; Qin, et al. 2010; Du, et al. 2010

The function of proteins is according to the UniProt database[38,39] and the applied method is according to the BioGRID[40] database apart from the fluorescent two-hybrid (F2H) assay.[41] All protein names are according to the human nomenclature unless noted otherwise. Proteins involved in the post-translational modification of DNMT1 are highlighted in green.

Table 1. Overview of DNMT1 interacting proteins

UBC9	E2 ubiquitin-conjugating enzyme	AC/WB	*H. sapiens*	Lee, et al. 2009
AKT1	RAC-alpha serine/threonine-protein kinase	AC/WB Co-localization	*H. sapiens*	Esteve, et al. 2011
PARP-1	Poly [ADP-ribose] polymerase 1	AC/WB Reconstituted Complex	*H. sapiens*	Reale, et al. 2005; Zampieri, et al. 2009
p23	Molecular chaperone	AC/WB	*H. sapiens*	Zhang and Verdine 1996
Daxx	Adapter protein in a MDM2-DAXX-USP7 complex	AC/WB Co-localization	*H. sapiens*	Muromoto, et al. 2004
Annexin V	Anticoagulant protein	AC/WB	*R. norvegicus*	Ohsawa, et al. 1996
PKCs	Protein kinase C	AC/WB Co-localization	*H. sapiens*	Lavoie, et al. 2011
CK1 δ/ε	Casein kinase 1δ/ε	AC/WB	*M. musculus*	Sugiyama, et al. 2010

The function of proteins is according to the UniProt database[38,39] and the applied method is according to the BioGRID[40] database apart from the fluorescent two-hybrid (F2H) assay.[41] All protein names are according to the human nomenclature unless noted otherwise. Proteins involved in the post-translational modification of DNMT1 are highlighted in green.

DNA methylation of pericentric satellite repeats, respectively. Interestingly, also the H3K9me3 binding heterochromatin protein HP1β was shown to interact with DNMT1,[76] but localization of DNMT1 at late replicating chromocenters seemed to be independent of SUV39H1/2 and HP1β.[27] In addition, DNMT1 interacts with Polycomb group (PcG) proteins EZH2 [83,84] and EED,[83] which are subunits of the PRC2/EED-EZH2 complex that methylates H3K27. EZH2 was shown to recruit DNMT1 to target genes and thereby mediate promoter methylation.[83] A recent study showed that DNMT1 inhibition decreased the expression levels of PcG proteins and induced cellular senescence, providing a possible link between DNA methylation, maintenance of stem cell self-renewal and multipotency.[85]

In addition to the histone modifying enzymes, also chromatin remodeling ATPases like LSH are required for maintaining DNA methylation in mammals. LSH is related to the SNF2 family of chromatin-remodeling ATPases and forms a complex with DNMT1, DNMT3b and HDACs, suggesting a role in transcriptional repression.[86,87] Similarly, BAZ2A (also known as TIP5), the large subunit of the nucleolar remodeling complex (NoRC), forms a complex with DNMT1, DNMT3s, HDACs and hSNF2H, mediating recruitment to rDNA.[88] One component of this complex, the chromatin remodeler hSNF2H, increases the binding affinity of DNMT1 to mononucleosomes.[89] The interaction with these chromatin remodeling factors may help DNMT1 to access substrate sites in heterochromatic regions.

Besides indirect connections to transcriptional regulation, also direct interactions of DNMT1 with transcription regulators and factors have been described. CXXC1 (CFP1), a component of the SetD1A/B methyltransferase complex, binds to DNMT1, and *Cxxc1*-deficient ESCs display reduced levels of global DNA methylation.[90] Moreover, DNMT1 was shown to interact with the transcription factors SP1,[91] SP3 [91] and STAT3.[92] A STAT3-DNMT1-HDAC1 complex binds to the promoter of *shp1,* encoding a negative regulator of cell signaling, inducing cell transformation.[92] Also RIP140, a co-repressor for nuclear receptors, interacts with DNMT1 and DNMT3s in gene repression.[93]

Additional DNMT1 interactions have been reported with various tumor suppressor genes including WT1,[84] Rb,[57,94] p53[95] and hNaa10p.[96] The Wilms tumor suppressor protein (WT1) recruits DNMT1 to the *Pax2* promoter resulting in DNA hypermethylation.[84] The retinoblastoma (Rb) tumor supressor gene product associates with DNMT1 and the transcription factor, E2F1, resulting in transcriptional repression of E2F1-responsive promoters.[57] The interaction with p53 stimulates DNMT1 activity leading to hypermethylation.[95] In addition, studies showed that either deletion of *p53* in the HCT116 human colon carcinoma cell line or knockdown of p53 in human B-lymphoblast TK6 cells results in an increased level of DNMT1.[97,98] Interestingly, clinical data from lung cancer patients indicated that p53 mutations were associated with overexpression of DNMT1, providing a mechanistic link between the p53-DNMT1 interaction and cancerogenesis.[99] Finally, the tumor suppressor, hNaa10p, recruits DNMT1 to promoters of tumor suppressor genes and increases the DNA binding affinity of DNMT1.[96] Besides a role in normal gene regulation, connections with deregulated gene expression in cancer were also reported. The leukemia-promoting PML-RAR fusion recruits DNMT1 to target promoters, inducing gene hypermethylation, an early step of carcinogenesis.[100]

For the sake of completeness, the following DNMT1 interacting proteins should be mentioned even though the function of these interactions is still unclear. The first described interacting partners of DNMT1 were Annexin V[101] and the molecular chaperone p23.[102] The functional importance of DNMT1 interactions with RGS6, a protein that negatively regulates the heterotrimeric G protein signaling,[103] with PARP-1 [104,105] and with HESX1 [106] also remain elusive. The diversity of proteins reported to interact with DNMT1 provides a first insight into the complexity of the epigenetic network and illustrates the central role of DNMT1 in these regulatory pathways.

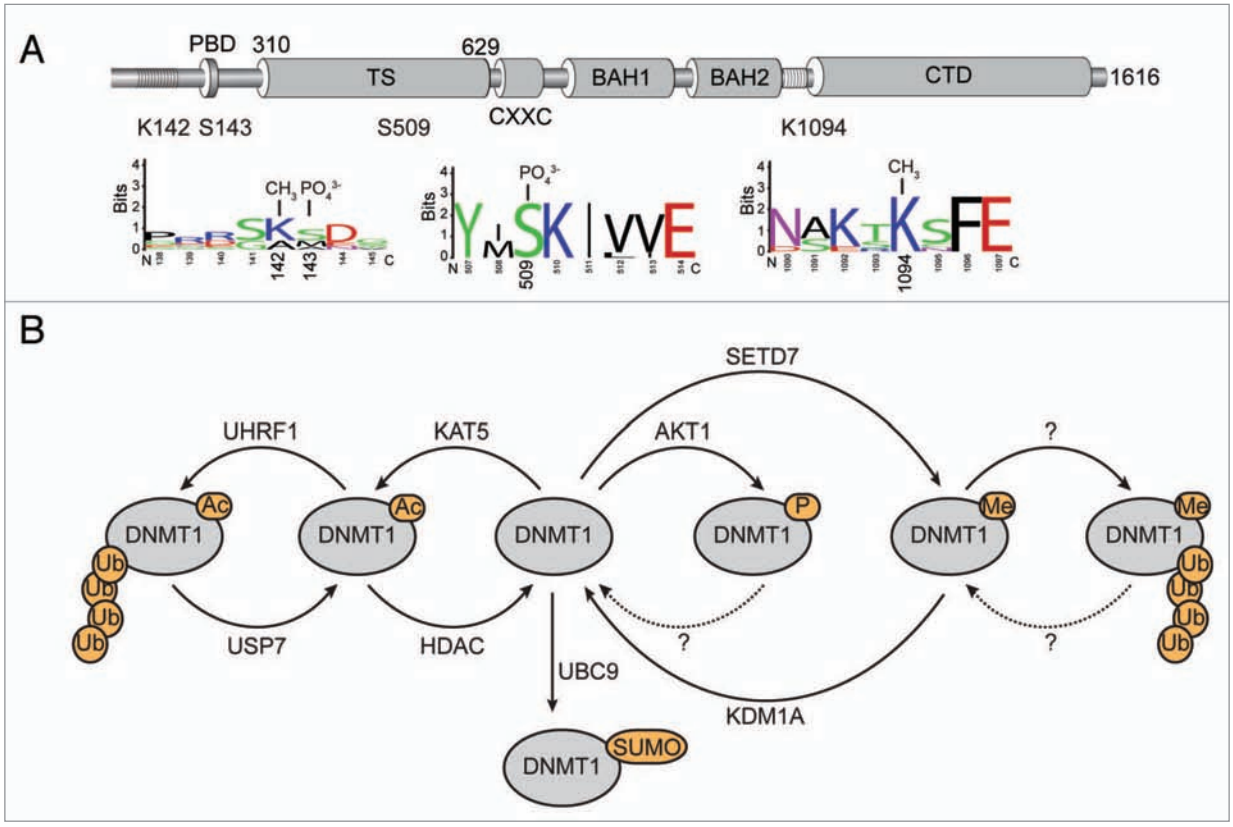

Figure 3. Regulation of DNMT1 by post-translational modifications. (A) Schematic outline of the domain architecture of DNMT1. The lysine residues K142 and K1094 are methylated and the serine residues S143 and S509 phosphorylated. In addition, the murine Dnmt1 is phosphorylated at S146. The conservation of known modified sites are shown in sequence logos by WebLogo.[107] The input to WebLogo was a ClustalW[108] alignment of DNMT1 from different species (*Homo sapiens* P26358.2; *Bos Taurus* DAA27999.1; *Mus musculus* P13864.5; *Rattus norvegicus* Q9Z330.2; *Gallus gallus* Q92072.1; *Paracentrotus lividus* Q27746.1 and *Danio rerio* AAI63894.1). (B) Crosstalk between DNMT1 and interacting proteins leading to post-translational modifications of DNMT1. The following abbreviations are used: Ac = Acetylation; Ub = Ubiquitination; SUMO = Sumoylation; p = Phosphorylation; Me = Methylation. The dotted line indicates a hypothetical dephosphorylation.

Regulation of DNMT1 Activity by Modifications

While most of the interacting factors regulate DNMT1 activity by recruitment to specific DNA sequences and target genes, some of them have been described to modulate DNMT1 activity by post-translational modifications (**Fig. 3**). Recent publications have described several different post-translational modifications that influence the stability, abundance and activity of DNMT1.

DNMT1 was shown to undergo cell cycle-dependent changes in acetylation and ubiquitination.[109-111] On the one hand, DNMT1 is acetylated by KAT5 and subsequently ubiquitinated by the E3 ubiquitin ligase, UHRF1, marking DNMT1 for proteolytic degradation. The abundance of DNMT1 increases in early S phase and starts to decrease during late S or G_2 phase, a pattern which inversely correlates with the abundance of KAT5, suggesting that KAT5-mediated DNMT1 acetylation triggers DNMT1 degradation.[110] On the other hand, DNMT1 is deubiquitinated by USP7 (also known as Herpes virus-associated ubiquitin-specific protease HAUSP) and deacetylated by HDAC1, protecting DNMT1 from proteolytic degradation.[110,111] The interaction between DNMT1 and USP7 is disrupted during mid-late S phase, showing that a physical interaction is required for the stabilization of DNMT1. Furthermore, the interaction of UHRF1 and DNMT1 increases during late S phase leading to destabilization of DNMT1.[110]

In fact, the first post-translational modification to be described was the phosphorylation of Dnmt1 at Ser515 (DNMT1 Ser509)[112] (**Fig. 3A**), which was suggested to modulate the interaction between the regulatory and catalytic domain.[113] In addition, Dnmt1 is phosphorylated at Ser146 (in mice only) by the casein kinase 1δ/ε, decreasing the DNA binding affinity,[114] and at sites in the regulatory domain, which have yet to be mapped, by members of the PKC family.[115] Notably, it has been reported that the phosphorylation of DNMT1 disrupts the DNMT1/PCNA/UHRF1 interaction, promoting global DNA hypomethylation in human gliomas.[116] Phosphorylation of Ser143 by AKT1 during early and mid-S phase has been described to stabilize DNMT1.[117] S143 phosphorylation in turn blocks methylation of the adjacent Lys142 by SETD7, which marks DNMT1 for proteolytic degradation during late S phase and G_2.[117,118]

Besides Lys142, SET7/9 can also methylate the Lys1096 residue of Dnmt1 (Lys1094 of DNMT1), which destabilizes the enzyme. The corresponding demethylation by KDM1A (also

known as lysine-specific demethylase LSD1 and AOF2) in turn increases the stability of Dnmt1.[119] Consistently, the genetic ablation of *kdm1a* in ESCs led to a progressive loss of DNA methylation[119] and caused cellular differentiation.[120] Finally, DNMT1 is also sumoylated by the ubiquitin-conjugating enzyme, UBC9, leading to the increased catalytic activity of DNMT1 on genomic DNA in vitro.[121] In summary, post-translational modifications influence the abundance and activity of DNMT1, and may thus play a role during normal development and disease.

Perspective

The ever-increasing list of interacting factors and post-translational modifications reported for Dnmt1 impressively illustrates the complexity of the regulation of DNA methylation in vivo. Many of these interactions and modifications were identified in different cells and species, using varied and mostly qualitative methods. It is now essential to systematically and quantitatively analyze the different combinations in which they occur, in which cell types they take place, during which phase of the cell cycle, at which stage of cellular differentiation, and finally which fractions of the cellular DNMT1 protein pool are involved. Clearly, the availability of first structural data of DNMT1 helps to elucidate the function of these interactions and modifications in the regulation of DNMT1 at the molecular level.[5,32,122] The biggest challenge however will be the integration of all these data to comprehend DNMT1 regulation in the context of living cells, taking into account the complexity and dynamics of its natural substrate, the chromatin, as well as the competition or cooperation with countless other cellular proteins and processes.

Acknowledgments

We thank Carina Frauer and Simon Vyse for comments on the manuscript and discussions. Projects in HL's lab are supported by grants from the Deutsche Forschungsgemeinschaft (DFG SFB646, SFB684 and TR5). G.P. is supported by the International Doctorate Program NanoBioTechnology (IDK-NBT) and the International Max Planck Research School for Molecular and Cellular Life Science (IMPRS-LS). W.Q. is supported by the China Scholarship Council (CSC).

References

1. Bird A. DNA methylation patterns and epigenetic memory. Genes Dev 2002; 16:6-21; PMID:11782440; DOI:10.1101/gad.947102.
2. Kouzarides T. Chromatin modifications and their function. Cell 2007; 128:693-705; PMID:17320507; DOI:10.1016/j.cell.2007.02.005.
3. Reik W. Stability and flexibility of epigenetic gene regulation in mammalian development. Nature 2007; 447:425-32; PMID:17522676; DOI:10.1038/nature05918.
4. O'Gara M, Roberts RJ, Cheng X. A structural basis for the preferential binding of hemimethylated DNA by HhaI DNA methyltransferase. J Mol Biol 1996; 263:597-606; PMID:8918941; DOI:10.1006/jmbi.1996.0601.
5. Takeshita K, Suetake I, Yamashita E, Suga M, Narita H, Nakagawa A, et al. Structural insight into maintenance methylation by mouse DNA methyltransferase 1 (Dnmt1). Proc Natl Acad Sci USA 2011; 108:9055-9; PMID:21518897; DOI:10.1073/pnas.1019629108.
6. Klimasauskas S, Kumar S, Roberts RJ, Cheng X. HhaI methyltransferase flips its target base out of the DNA helix. Cell 1994; 76:357-69; PMID:8293469; DOI:10.1016/0092-8674(94)90342-5.
7. Cheng X, Blumenthal RM. Mammalian DNA methyltransferases: a structural perspective. Structure 2008; 16:341-50; PMID:18334209; DOI:10.1016/j.str.2008.01.004.
8. Kaneda M, Okano M, Hata K, Sado T, Tsujimoto N, Li E, et al. Essential role for de novo DNA methyltransferase Dnmt3a in paternal and maternal imprinting. Nature 2004; 429:900-3; PMID:15215868; DOI:10.1038/nature02633.
9. Okano M, Bell DW, Haber DA, Li E. DNA methyltransferases Dnmt3a and Dnmt3b are essential for de novo methylation and mammalian development. Cell 1999; 99:247-57; PMID:10555141; DOI:10.1016/S0092-8674(00)81656-6.
10. Okano M, Xie S, Li E. Cloning and characterization of a family of novel mammalian DNA (cytosine-5) methyltransferases. Nat Genet 1998; 19:219-20; PMID:9662389; DOI:10.1038/890.
11. Aapola U, Kawasaki K, Scott HS, Ollila J, Vihinen M, Heino M, et al. Isolation and initial characterization of a novel zinc finger gene, DNMT3L, on 21q22.3, related to the cytosine-5-methyltransferase 3 gene family. Genomics 2000; 65:293-8; PMID:10857753; DOI:10.1006/geno.2000.6168.
12. Ooi SK, Qiu C, Bernstein E, Li K, Jia D, Yang Z, et al. DNMT3L connects unmethylated lysine 4 of histone H3 to de novo methylation of DNA. Nature 2007; 448:714-7; PMID:17687327; DOI:10.1038/nature05987.
13. Suetake I, Shinozaki F, Miyagawa J, Takeshima H, Tajima S. DNMT3L stimulates the DNA methylation activity of Dnmt3a and Dnmt3b through a direct interaction. J Biol Chem 2004; 279:27816-23; PMID:15105426; DOI:10.1074/jbc.M400181200.
14. Hata K, Okano M, Lei H, Li E. Dnmt3L cooperates with the Dnmt3 family of de novo DNA methyltransferases to establish maternal imprints in mice. Development 2002; 129:1983-93; PMIDHYPERLINK "http://www.ncbi.nlm.nih.gov/entrez/query.fcgi?cmd=Retrieve&db=PubMed&list_uids=11934864&dopt=Abstract":11934864.
15. Leonhardt H, Page AW, Weier HU, Bestor TH. A targeting sequence directs DNA methyltransferase to sites of DNA replication in mammalian nuclei. Cell 1992; 71:865-73; PMID:1423634; DOI:10.1016/0092-8674(92)90561-P.
16. Mortusewicz O, Schermelleh L, Walter J, Cardoso MC, Leonhardt H. Recruitment of DNA methyltransferase I to DNA repair sites. Proc Natl Acad Sci USA 2005; 102:8905-9; PMID:15956212; DOI:10.1073/pnas.0501034102.
17. Bestor TH, Ingram VM. Two DNA methyltransferases from murine erythroleukemia cells: purification, sequence specificity, and mode of interaction with DNA. Proc Natl Acad Sci USA 1983; 80:5559-63; PMID:6577443; DOI:10.1073/pnas.80.18.5559.
18. Goll MG, Kirpekar F, Maggert KA, Yoder JA, Hsieh CL, Zhang X, et al. Methylation of tRNAAsp by the DNA methyltransferase homolog Dnmt2. Science 2006; 311:395-8; PMID:16424344; DOI:10.1126/science.1120976.
19. Hermann A, Gowher H, Jeltsch A. Biochemistry and biology of mammalian DNA methyltransferases. Cell Mol Life Sci 2004; 61:2571-87; PMID:15526163; DOI:10.1007/s00018-004-4201-1.
20. Hsieh CL. In vivo activity of murine de novo methyltransferases, Dnmt3a and Dnmt3b. Mol Cell Biol 1999; 19:8211-8; PMID:10567546.
21. Fatemi M, Hermann A, Pradhan S, Jeltsch A. The activity of the murine DNA methyltransferase Dnmt1 is controlled by interaction of the catalytic domain with the N-terminal part of the enzyme leading to an allosteric activation of the enzyme after binding to methylated DNA. J Mol Biol 2001; 309:1189-99; PMID:11399088; DOI:10.1006/jmbi.2001.4709.
22. Margot JB, Aguirre-Arteta AM, Di Giacco BV, Pradhan S, Roberts RJ, Cardoso MC, et al. Structure and function of the mouse DNA methyltransferase gene: Dnmt1 shows a tripartite structure. J Mol Biol 2000; 297:293-300; PMID:10715201; DOI:10.1006/jmbi.2000.3588.
23. Zimmermann C, Guhl E, Graessmann A. Mouse DNA methyltransferase (MTase) deletion mutants that retain the catalytic domain display neither de novo nor maintenance methylation activity in vivo. Biol Chem 1997; 378:393-405; PMID:9191026; DOI:10.1515/bchm.1997.378.5.393.
24. Goll MG, Bestor TH. Eukaryotic cytosine methyltransferases. Annu Rev Biochem 2005; 74:481-514; PMID:15952895; DOI:10.1146/annurev.biochem.74.010904.153721.
25. Rottach A, Leonhardt H, Spada F. DNA methylation-mediated epigenetic control. J Cell Biochem 2009; 108:43-51; PMID:19565567; DOI:10.1002/jcb.22253.
26. Chuang LS, Ian HI, Koh TW, Ng HH, Xu G, Li BF. Human DNA-(cytosine-5) methyltransferase-PCNA complex as a target for $p21^{WAF1}$. Science 1997; 277:1996-2000; PMID:9302295; DOI:10.1126/science.277.5334.1996.
27. Easwaran HP, Schermelleh L, Leonhardt H, Cardoso MC. Replication-independent chromatin loading of Dnmt1 during G_2 and M phases. EMBO Rep 2004; 5:1181-6; PMID:15550930; DOI:10.1038/sj.embor.7400295.
28. Fellinger K, Rothbauer U, Felle M, Langst G, Leonhardt H. Dimerization of DNA methyltransferase 1 is mediated by its regulatory domain. J Cell Biochem 2009; 106:521-8; PMID:19173286; DOI:10.1002/jcb.22071.
29. Frauer C, Rottach A, Meilinger D, Bultmann S, Fellinger K, Hasenoder S, et al. Different binding properties and function of CXXC zinc finger domains in Dnmt1 and Tet1. PLoS ONE 2011; 6:16627; PMID:21311766; DOI:10.1371/journal.pone.0016627.

30. Pradhan S, Roberts RJ. Hybrid mouse-prokaryotic DNA (cytosine-5) methyltransferases retain the specificity of the parental C-terminal domain. EMBO J 2000; 19:2103-14; PMID:10790376; DOI:10.1093/emboj/19.9.2103.
31. Bestor TH. Activation of mammalian DNA methyltransferase by cleavage of a Zn binding regulatory domain. EMBO J 1992; 11:2611-7; PMID:1628623.
32. Song J, Rechkoblit O, Bestor TH, Patel DJ. Structure of DNMT1-DNA complex reveals a role for autoinhibition in maintenance DNA methylation. Science 2011; 331:1036-40; PMID:21163962; DOI:10.1126/science.1195380.
33. Margot JB, Ehrenhofer-Murray AE, Leonhardt H. Interactions within the mammalian DNA methyltransferase family. BMC Mol Biol 2003; 4:7; PMID:12777184; DOI:10.1186/1471-2199-4-7.
34. Syeda F, Fagan RL, Wean M, Avvakumov GV, Walker JR, Xue S, et al. The RFTS domain is a DNA-competitive inhibitor of Dnmt1. J Biol Chem 2011.
35. Cardoso MC, Leonhardt H. Protein targeting to subnuclear higher order structures: a new level of regulation and coordination of nuclear processes. J Cell Biochem 1998; 70:222-30; PMID:9671228; DOI:10.1002/(SICI)1097-4644(19980801)70:2222::AID-JCB83.0.CO;2-Q.
36. Leonhardt H, Cardoso MC. Targeting and association of proteins with functional domains in the nucleus: the insoluble solution. Int Rev Cytol 1995; 162:303-35; PMID:8557490.
37. Leonhardt H, Rahn HP, Cardoso MC. Functional links between nuclear structure, gene expression, DNA replication and methylation. Crit Rev Eukaryot Gene Expr 1999; 9:345-51; PMID:10651251.
38. UniProt C. Ongoing and future developments at the Universal Protein Resource. Nucleic Acids Res 2011; 39:214-9; PMID:21051339; DOI:10.1093/nar/gkq1020.
39. Jain E, Bairoch A, Duvaud S, Phan I, Redaschi N, Suzek BE, et al. Infrastructure for the life sciences: design and implementation of the UniProt website. BMC Bioinformatics 2009; 10:136; PMID:19426475; DOI:10.1186/1471-2105-10-136.
40. Stark C, Breitkreutz BJ, Chatr-Aryamontri A, Boucher L, Oughtred R, Livstone MS, et al. The BioGRID Interaction Database: 2011 update. Nucleic Acids Res 2011; 39:698-704; PMID:21071413; DOI:10.1093/nar/gkq1116.
41. Zolghadr K, Mortusewicz O, Rothbauer U, Kleinhans R, Goehler H, Wanker EE, et al. A fluorescent two-hybrid assay for direct visualization of protein interactions in living cells. Mol Cell Proteomics 2008; 7:2279-87; PMID:18622019; DOI:10.1074/mcp.M700548-MCP200.
42. Jackson DA, Pombo A. Replicon clusters are stable units of chromosome structure: evidence that nuclear organization contributes to the efficient activation and propagation of S phase in human cells. J Cell Biol 1998; 140:1285-95; PMID:9508763; DOI:10.1083/jcb.140.6.1285.
43. Pradhan S, Bacolla A, Wells RD, Roberts RJ. Recombinant human DNA (cytosine-5) methyltransferase. I. Expression, purification and comparison of de novo and maintenance methylation. J Biol Chem 1999; 274:33002-10; PMID:10551868; DOI:10.1074/jbc.274.46.33002.
44. Bravo R, Frank R, Blundell PA, Macdonald-Bravo H. Cyclin/PCNA is the auxiliary protein of DNA polymerase-delta. Nature 1987; 326:515-7; PMID:2882423; DOI:10.1038/326515a0.
45. Kelman Z, O'Donnell M. Structural and functional similarities of prokaryotic and eukaryotic DNA polymerase sliding clamps. Nucleic Acids Res 1995; 23:3613-20; PMID:7478986; DOI:10.1093/nar/23.18.3613.
46. Wyman C, Botchan M. DNA replication. A familiar ring to DNA polymerase processivity. Curr Biol 1995; 5:334-7; PMID:7627541; DOI:10.1016/S0960-9822(95)00065-0.
47. Schermelleh L, Haemmer A, Spada F, Rosing N, Meilinger D, Rothbauer U, et al. Dynamics of Dnmt1 interaction with the replication machinery and its role in postreplicative maintenance of DNA methylation. Nucleic Acids Res 2007; 35:4301-12; PMID:17576694; DOI:10.1093/nar/gkm432.
48. Spada F, Haemmer A, Kuch D, Rothbauer U, Schermelleh L, Kremmer E, et al. DNMT1 but not its interaction with the replication machinery is required for maintenance of DNA methylation in human cells. J Cell Biol 2007; 176:565-71; PMID:17312023; DOI:10.1083/jcb.200610062.
49. Kimura H, Shiota K. Methyl-CpG-binding protein, MeCP2, is a target molecule for maintenance DNA methyltransferase, Dnmt1. J Biol Chem 2003; 278:4806-12; PMID:12473678; DOI:10.1074/jbc.M209923200.
50. Tatematsu KI, Yamazaki T, Ishikawa F. MBD2-MBD3 complex binds to hemi-methylated DNA and forms a complex containing DNMT1 at the replication foci in late S phase. Genes Cells 2000; 5:677-88; PMID:10947852; DOI:10.1046/j.1365-2443.2000.00359.x.
51. Bronner C, Achour M, Arima Y, Chataigneau T, Saya H, Schini-Kerth VB. The UHRF family: oncogenes that are drugable targets for cancer therapy in the near future? Pharmacol Ther 2007; 115:419-34; PMID:17658611; DOI:10.1016/j.pharmthera.2007.06.003.
52. Brero A, Easwaran HP, Nowak D, Grunewald I, Cremer T, Leonhardt H, et al. Methyl CpG-binding proteins induce large-scale chromatin reorganization during terminal differentiation. J Cell Biol 2005; 169:733-43; PMID:15939760; DOI:10.1083/jcb.200502062.
53. Georgel PT, Horowitz-Scherer RA, Adkins N, Woodcock CL, Wade PA, Hansen JC. Chromatin compaction by human MeCP2. Assembly of novel secondary chromatin structures in the absence of DNA methylation. J Biol Chem 2003; 278:32181-8; PMID:12788925; DOI:10.1074/jbc.M305308200.
54. Hendrich B, Tweedie S. The methyl-CpG binding domain and the evolving role of DNA methylation in animals. Trends Genet 2003; 19:269-77; PMID:12711219; DOI:10.1016/S0168-9525(03)00080-5.
55. Achour M, Jacq X, Ronde P, Alhosin M, Charlot C, Chataigneau T, et al. The interaction of the SRA domain of ICBP90 with a novel domain of DNMT1 is involved in the regulation of VEGF gene expression. Oncogene 2008; 27:2187-97; PMID:17934516; DOI:10.1038/sj.onc.1210855.
56. Fuks F, Burgers WA, Brehm A, Hughes-Davies L, Kouzarides T. DNA methyltransferase Dnmt1 associates with histone deacetylase activity. Nat Genet 2000; 24:88-91; PMID:10615135; DOI:10.1038/71750.
57. Robertson KD, Ait-Si-Ali S, Yokochi T, Wade PA, Jones PL, Wolffe AP. DNMT1 forms a complex with Rb, E2F1 and HDAC1 and represses transcription from E2F-responsive promoters. Nat Genet 2000; 25:338-42; PMID:10888886; DOI:10.1038/77124.
58. Rountree MR, Bachman KE, Baylin SB. DNMT1 binds HDAC2 and a new co-repressor, DMAP1, to form a complex at replication foci. Nat Genet 2000; 25:269-77; PMID:10888872; DOI:10.1038/77023.
59. Eden S, Hashimshony T, Keshet I, Cedar H, Thorne AW. DNA methylation models histone acetylation. Nature 1998; 394:842; PMID:9732866; DOI:10.1038/29680.
60. Wade PA. Methyl CpG-binding proteins and transcriptional repression. Bioessays 2001; 23:1131-7; PMID:11746232; DOI:10.1002/bies.10008.
61. Mohan KN, Ding F, Chaillet JR. Distinct roles of DMAP1 in mouse development. Mol Cell Biol 2011; 31:1861-9; PMID:21383065; DOI:10.1128/MCB.01390-10.
62. Muromoto R, Sugiyama K, Takachi A, Imoto S, Sato N, Yamamoto T, et al. Physical and functional interactions between Daxx and DNA methyltransferase 1-associated protein, DMAP1. J Immunol 2004; 172:2985-93; PMID:14978102.
63. Bostick M, Kim JK, Esteve PO, Clark A, Pradhan S, Jacobsen SE. UHRF1 plays a role in maintaining DNA methylation in mammalian cells. Science 2007; 317:1760-4; PMID:17673620; DOI:10.1126/science.1147939.
64. Sharif J, Muto M, Takebayashi S, Suetake I, Iwamatsu A, Endo TA, et al. The SRA protein Np95 mediates epigenetic inheritance by recruiting Dnmt1 to methylated DNA. Nature 2007; 450:908-12; PMID:17994007; DOI:10.1038/nature06397.
65. Arita K, Ariyoshi M, Tochio H, Nakamura Y, Shirakawa M. Recognition of hemi-methylated DNA by the SRA protein UHRF1 by a base-flipping mechanism. Nature 2008; 455:818-21; PMID:18772891; DOI:10.1038/nature07249.
66. Avvakumov GV, Walker JR, Xue S, Li Y, Duan S, Bronner C, et al. Structural basis for recognition of hemi-methylated DNA by the SRA domain of human UHRF1. Nature 2008; 455:822-5; PMID:18772889; DOI:10.1038/nature07273.
67. Hashimoto H, Horton JR, Zhang X, Bostick M, Jacobsen SE, Cheng X. The SRA domain of UHRF1 flips 5-methylcytosine out of the DNA helix. Nature 2008; 455:826-9; PMID:18772888; DOI:10.1038/nature07280.
68. Qian C, Li S, Jakoncic J, Zeng L, Walsh MJ, Zhou MM. Structure and hemimethylated CpG binding of the SRA domain from human UHRF1. J Biol Chem 2008; 283:34490-4; PMID:18945682; DOI:10.1074/jbc.C800169200.
69. Rottach A, Frauer C, Pichler G, Bonapace IM, Spada F, Leonhardt H. The multi-domain protein Np95 connects DNA methylation and histone modification. Nucleic Acids Res 2010; 38:1796-804; PMID:20026581; DOI:10.1093/nar/gkp1152.
70. Pichler G, Wolf P, Schmidt CS, Meilinger D, Schneider K, Frauer C, et al. Cooperative DNA and histone binding by Uhrf2 links the two major repressive epigenetic pathways. J Cell Biochem 2011.
71. Fatemi M, Hermann A, Gowher H, Jeltsch A. Dnmt3a and Dnmt1 functionally cooperate during de novo methylation of DNA. Eur J Biochem 2002; 269:4981-4; PMID:12383256; DOI:10.1046/j.1432-1033.2002.03198.x.
72. Kim GD, Ni J, Kelesoglu N, Roberts RJ, Pradhan S. Co-operation and communication between the human maintenance and de novo DNA (cytosine-5) methyltransferases. EMBO J 2002; 21:4183-95; PMID:12145218; DOI:10.1093/emboj/cdf401.
73. Lehnertz B, Ueda Y, Derijck AA, Braunschweig U, Perez-Burgos L, Kubicek S, et al. Suv39 h-mediated histone H3 lysine 9 methylation directs DNA methylation to major satellite repeats at pericentric heterochromatin. Curr Biol 2003; 13:1192-200; PMID:12867029; DOI:10.1016/S0960-9822(03)00432-9.
74. Meilinger D, Fellinger K, Bultmann S, Rothbauer U, Bonapace IM, Klinkert WE, et al. Np95 interacts with de novo DNA methyltransferases, Dnmt3a and Dnmt3b, and mediates epigenetic silencing of the viral CMV promoter in embryonic stem cells. EMBO Rep 2009; 10:1259-64; PMID:19798101; DOI:10.1038/embor.2009.201.
75. Rhee I, Bachman KE, Park BH, Jair KW, Yen RW, Schuebel KE, et al. DNMT1 and DNMT3b cooperate to silence genes in human cancer cells. Nature 2002; 416:552-6; PMID:11932749; DOI:10.1038/416552a.
76. Fuks F, Hurd PJ, Deplus R, Kouzarides T. The DNA methyltransferases associate with HP1 and the SUV39H1 histone methyltransferase. Nucleic Acids Res 2003; 31:2305-12; PMID:12711675; DOI:10.1093/nar/gkg332.

77. Estève PO, Chin HG, Smallwood A, Feehery GR, Gangisetty O, Karpf AR, et al. Direct interaction between DNMT1 and G9a coordinates DNA and histone methylation during replication. Genes Dev 2006; 20:3089-103; PMID:17085482; DOI:10.1101/gad.1463706.
78. Kim JK, Esteve PO, Jacobsen SE, Pradhan S. UHRF1 binds G9a and participates in p21 transcriptional regulation in mammalian cells. Nucleic Acids Res 2008; 37:493-505; PMID:19056828; DOI:10.1093/nar/gkn961.
79. Peters AH, Kubicek S, Mechtler K, O'Sullivan RJ, Derijck AA, Perez-Burgos L, et al. Partitioning and plasticity of repressive histone methylation states in mammalian chromatin. Mol Cell 2003; 12:1577-89; PMID:14690609; DOI:10.1016/S1097-2765(03)00477-5.
80. Tachibana M, Sugimoto K, Nozaki M, Ueda J, Ohta T, Ohki M, et al. G9a histone methyltransferase plays a dominant role in euchromatic histone H3 lysine 9 methylation and is essential for early embryogenesis. Genes Dev 2002; 16:1779-91; PMID:12130538; DOI:10.1101/gad.989402.
81. Dong KB, Maksakova IA, Mohn F, Leung D, Appanah R, Lee S, et al. DNA methylation in ES cells requires the lysine methyltransferase G9a but not its catalytic activity. EMBO J 2008; 27:2691-701; PMID:18818693; DOI:10.1038/emboj.2008.193.
82. Ikegami K, Iwatani M, Suzuki M, Tachibana M, Shinkai Y, Tanaka S, et al. Genome-wide and locus-specific DNA hypomethylation in G9a deficient mouse embryonic stem cells. Genes Cells 2007; 12:1-11; PMID:17212651; DOI:10.1111/j.1365-2443.2006.01029.x.
83. Viré E, Brenner C, Deplus R, Blanchon L, Fraga M, Didelot C, et al. The Polycomb group protein EZH2 directly controls DNA methylation. Nature 2006; 439:871-4; PMID:16357870; DOI:10.1038/nature04431.
84. Xu B, Zeng DQ, Wu Y, Zheng R, Gu L, Lin X, et al. Tumor suppressor menin represses paired box gene 2 expression via Wilms tumor suppressor protein-polycomb group complex. J Biol Chem 2011; 286:13937-44; PMID:21378168; DOI:10.1074/jbc.M110.197830.
85. So AY, Jung JW, Lee S, Kim HS, Kang KS. DNA methyltransferase controls stem cell aging by regulating BMI1 and EZH2 through microRNAs. PLoS ONE 2011; 6:19503; PMID:21572997; DOI:10.1371/journal.pone.0019503.
86. Jeddeloh JA, Stokes TL, Richards EJ. Maintenance of genomic methylation requires a SWI2/SNF2-like protein. Nat Genet 1999; 22:94-7; PMID:10319870; DOI:10.1038/8803.
87. Myant K, Stancheva I. LSH cooperates with DNA methyltransferases to repress transcription. Mol Cell Biol 2008; 28:215-26; PMID:17967891; DOI:10.1128/MCB.01073-07.
88. Zhou Y, Grummt I. The PHD finger/bromodomain of NoRC interacts with acetylated histone H4K16 and is sufficient for rDNA silencing. Curr Biol 2005; 15:1434-8; PMID:16085498; DOI:10.1016/j.cub.2005.06.057.
89. Robertson AK, Geiman TM, Sankpal UT, Hager GL, Robertson KD. Effects of chromatin structure on the enzymatic and DNA binding functions of DNA methyltransferases DNMT1 and Dnmt3a in vitro. Biochem Biophys Res Commun 2004; 322:110-8; PMID:15313181; DOI:10.1016/j.bbrc.2004.07.083.
90. Butler JS, Lee JH, Skalnik DG. CFP1 interacts with DNMT1 independently of association with the Setd1 Histone H3K4 methyltransferase complexes. DNA Cell Biol 2008; 27:533-43; PMID:18680430; DOI:10.1089/dna.2007.0714.
91. Estève PO, Chin HG, Pradhan S. Molecular mechanisms of transactivation and doxorubicin-mediated repression of survivin gene in cancer cells. J Biol Chem 2006; 282:2615-25; PMID:17124180; DOI:10.1074/jbc.M606203200.
92. Zhang Q, Wang HY, Marzec M, Raghunath PN, Nagasawa T, Wasik MA. STAT3- and DNA methyltransferase 1-mediated epigenetic silencing of SHP-1 tyrosine phosphatase tumor suppressor gene in malignant T lymphocytes. Proc Natl Acad Sci USA 2005; 102:6948-53; PMID:15870198; DOI:10.1073/pnas.0501959102.
93. Kiskinis E, Hallberg M, Christian M, Olofsson M, Dilworth SM, White R, et al. RIP140 directs histone and DNA methylation to silence Ucp1 expression in white adipocytes. EMBO J 2007; 26:4831-40; PMID:17972916; DOI:10.1038/sj.emboj.7601908.
94. Pradhan S, Kim GD. The retinoblastoma gene product interacts with maintenance human DNA (cytosine-5) methyltransferase and modulates its activity. EMBO J 2002; 21:779-88; PMID:11847125; DOI:10.1093/emboj/21.4.779.
95. Estève PO, Chin HG, Pradhan S. Human maintenance DNA (cytosine-5)-methyltransferase and p53 modulate expression of p53-repressed promoters. Proc Natl Acad Sci USA 2005; 102:1000-5; PMID:15657147; DOI:10.1073/pnas.0407729102.
96. Lee CF, Ou DS, Lee SB, Chang LH, Lin RK, Li YS, et al. hNaa10p contributes to tumorigenesis by facilitating DNMT1-mediated tumor suppressor gene silencing. J Clin Invest 2010; 120:2920-30; PMID:20592467; DOI:10.1172/JCI42275.
97. Guo Z, Tsai MH, Shiao YH, Chen LH, Wei ML, Lv X, et al. DNA (cytosine-5)-methyltransferase 1 as a mediator of mutant p53-determined p16(ink4A) downregulation. J Biomed Sci 2008; 15:163-8; PMID:18038118; DOI:10.1007/s11373-007-9222-y.
98. Peterson EJ, Bogler O, Taylor SM. p53-mediated repression of DNA methyltransferase 1 expression by specific DNA binding. Cancer Res 2003; 63:6579-82; PMID:14583449.
99. Lin RK, Wu CY, Chang JW, Juan LJ, Hsu HS, Chen CY, et al. Dysregulation of p53/Sp1 control leads to DNA methyltransferase-1 overexpression in lung cancer. Cancer Res 2010; 70:5807-17; PMID:20570896; DOI:10.1158/0008-5472.CAN-09-4161.
100. Di Croce L, Raker VA, Corsaro M, Fazi F, Fanelli M, Faretta M, et al. Methyltransferase recruitment and DNA hypermethylation of target promoters by an oncogenic transcription factor. Science 2002; 295:1079-82; PMID:11834837; DOI:10.1126/science.1065173.
101. Ohsawa K, Imai Y, Ito D, Kohsaka S. Molecular cloning and characterization of annexin V-binding proteins with highly hydrophilic peptide structure. J Neurochem 1996; 67:89-97; PMID:8667030; DOI:10.1046/j.1471-4159.1996.67010089.x.
102. Zhang X, Verdine GL. Mammalian DNA cytosine-5 methyltransferase interacts with p23 protein. FEBS Lett 1996; 392:179-83; PMID:8772199; DOI:10.1016/0014-5793(96)00810-1.
103. Liu Z, Fisher RA. RGS6 interacts with DMAP1 and DNMT1 and inhibits DMAP1 transcriptional repressor activity. J Biol Chem 2004; 279:14120-8; PMID:14734556; DOI:10.1074/jbc.M309547200.
104. Reale A, Matteis GD, Galleazzi G, Zampieri M, Caiafa P. Modulation of DNMT1 activity by ADP-ribose polymers. Oncogene 2005; 24:13-9; PMID:15637587; DOI:10.1038/sj.onc.1208005.
105. Zampieri M, Passananti C, Calabrese R, Perilli M, Corbi N, De Cave F, et al. Parp1 localizes within the Dnmt1 promoter and protects its unmethylated state by its enzymatic activity. PLoS ONE 2009; 4:4717; PMID:19262751; DOI:10.1371/journal.pone.0004717.
106. Sajedi E, Gaston-Massuet C, Andoniadou CL, Signore M, Hurd PJ, Dattani M, Martinez-Barbera JP. DNMT1 interacts with the developmental transcriptional repressor HESX1. Biochim Biophys Acta 2008; 1783:131-43.
107. Crooks GE, Hon G, Chandonia JM, Brenner SE. WebLogo: a sequence logo generator. Genome Res 2004; 14:1188-90; PMID:15173120; DOI:10.1101/gr.849004.
108. Thompson JD, Higgins DG, Gibson TJ. CLUSTAL W: improving the sensitivity of progressive multiple sequence alignment through sequence weighting, position-specific gap penalties and weight matrix choice. Nucleic Acids Res 1994; 22:4673-80; PMID:7984417; DOI:10.1093/nar/22.22.4673.
109. Bronner C. Control of DNMT1 abundance in epigenetic inheritance by acetylation, ubiquitylation and the histone code. Sci Signal 2011; 4:3; PMID:21266713; DOI:10.1126/scisignal.2001764.
110. Du Z, Song J, Wang Y, Zhao Y, Guda K, Yang S, et al. DNMT1 stability is regulated by proteins coordinating deubiquitination and acetylation-driven ubiquitination. Sci Signal 2010; 3:80; PMID:21045206; DOI:10.1126/scisignal.2001462.
111. Qin W, Leonhardt H, Spada F. Usp7 and Uhrf1 control ubiquitination and stability of the maintenance DNA methyltransferase Dnmt1. J Cell Biochem 2011; 112:439-44; PMID:21268065; DOI:10.1002/jcb.22998.
112. Glickman JF, Pavlovich JG, Reich NO. Peptide mapping of the murine DNA methyltransferase reveals a major phosphorylation site and the start of translation. J Biol Chem 1997; 272:17851-7; PMID:9211941; DOI:10.1074/jbc.272.28.17851.
113. Goyal R, Rathert P, Laser H, Gowher H, Jeltsch A. Phosphorylation of serine-515 activates the Mammalian maintenance methyltransferase Dnmt1. Epigenetics 2007; 2:155-60; PMID:17965600; DOI:10.4161/epi.2.3.4768.
114. Sugiyama Y, Hatano N, Sueyoshi N, Suetake I, Tajima S, Kinoshita E, et al. The DNA-binding activity of mouse DNA methyltransferase 1 is regulated by phosphorylation with casein kinase 1delta/epsilon. Biochem J 2010; 427:489-97; PMID:20192920; DOI:10.1042/BJ20091856.
115. Lavoie G, Esteve PO, Bibens-Laulan N, Predhan S, St-Pierre Y. PKC isoforms interact with and phosphorylate DNMT1. BMC Biol 2011; 9:31; PMID:21619587; DOI:10.1186/1741-7007-9-31.
116. Hervouet E, Lalier L, Debien E, Cheray M, Geairon A, Rogniaux H, et al. Disruption of Dnmt1/PCNA/UHRF1 interactions promotes tumorigenesis from human and mice glial cells. PLoS ONE 2010; 5:11333; PMID:20613874; DOI:10.1371/journal.pone.0011333.
117. Esteve PO, Chang Y, Samaranayake M, Upadhyay AK, Horton JR, Feehery GR, et al. A methylation and phosphorylation switch between an adjacent lysine and serine determines human DNMT1 stability. Nat Struct Mol Biol 2011.
118. Estève PO, Chin HG, Benner J, Feehery GR, Samaranayake M, Horwitz GA, et al. Regulation of DNMT1 stability through SET7-mediated lysine methylation in mammalian cells. Proc Natl Acad Sci USA 2009; 106:5076-81; PMID:19282482; DOI:10.1073/pnas.0810362106.
119. Wang J, Hevi S, Kurash JK, Lei H, Gay F, Bajko J, et al. The lysine demethylase LSD1 (KDM1) is required for maintenance of global DNA methylation. Nat Genet 2009; 41:125-9; PMID:19098913; DOI:10.1038/ng.268.
120. Adamo A, Sese B, Boue S, Castano J, Paramonov I, Barrero MJ, et al. LSD1 regulates the balance between self-renewal and differentiation in human embryonic stem cells. Nat Cell Biol 2011; 13:652-9; PMID:21602794; DOI:10.1038/ncb2246.
121. Lee B, Muller MT. SUMOylation enhances DNA methyltransferase 1 activity. Biochem J 2009; 421:449-61; PMID:19450230; DOI:10.1042/BJ20090142.
122. Frauer C, Leonhardt H. Twists and turns of DNA methylation. Proc Natl Acad Sci USA 2011; 108:8919-20; PMID:21593412; DOI:10.1073/pnas.1105804108.

3.6 Cell Cycle-dependent Interactions of Dnmt1

Cell Cycle-dependent Interactions of Dnmt1

Introduction and Aims

DNA methylation plays a central role in the epigenetic regulation of gene expression during development. Remarkably, the complex and changing patterns of genomic DNA methylation are established and maintained by only three DNA methyltransferases. In mammalian cells, Dnmt1 copies the DNA methylation pattern from parental to daughter strand during DNA replication, thereby maintaining an important epigenetic mark. Crucial for this process is not only the intrinsic preference of Dnmt1 for hemimethylated DNA, the substrate of maintenance DNA methylation, but also the interaction of Dnmt with a variety of different cellular structures and cofactors at different cell cycle and developmental stages. Although, many interacting proteins have been identified in the last two decades, the exact and dynamic regulation of Dnmt1 is still poorly understood. Recent studies showed that interacting proteins could have different impact on Dnmt1 depending on the cell cycle phase the interaction occurs. One striking example for cell cycle-dependent regulation is the interaction of Dnmt1 with Uhrf1. On one hand, Uhrf1 is an essential co-factor for maintenance DNA methylation and its genetic ablation in ESCs leads to remarkable genomic hypomethylation, a phenotype similar to *dnmt1*$^{-/-}$ ESCs (Bostick et al., 2007; Sharif et al., 2007). Uhrf1 co-localizes and interacts with Dnmt1 throughout S-phase, preferentially binds to hemimethylated DNA via a SET and Ring associated (SRA) domain and to the H3K9me3 heterochromatin mark via a tandem Tudor domain, suggesting a role in recruiting Dnmt1 to replication foci. On the other hand, Dnmt1 is ubiquitinated by Uhrf1 triggered by Kat5-mediated acetylation of Dnmt1 (Qin et al., 2011a; Du et al., 2010). Interestingly, the abundance of Dnmt1 increases in early S phase and starts to decrease during late S and/or G_2 phase, a pattern which inversely correlates with the abundance of Kat5, suggesting that Kat5-mediated Dnmt1 acetylation triggers Dnmt1 degradation. These data suggest, that Uhrf1 plays a dual role dependent on the cell cycle phase. Uhrf1 either "activates" Dnmt1 by recruiting it to hemimethylated CpG sites or "inactivates" Dnmt1 by triggering its proteosomal degradation by ubiquitination. The ever-increasing list of interacting factors and post-translational modifications reported for Dnmt1 impressively illustrates the complexity of the regulation of DNA methylation *in vivo*. For a comprehensive understanding of the regulation of DNA methylation it is now necessary to systematically quantify the interactions and modifications of Dnmt1, to elucidate their function at the molecular level and to integrate these data at the cellular level. It is now essential to analyze the different combinations in which Dnmt1 interactions occur, in which cell types they take place, during which phase of the cell cycle, at which stage of cellular differentiation, and finally which

fractions of the cellular Dnmt1 protein pool are involved. In this study, we use a combination of stable isotope labelling with amino acids in cell culture(SILAC) and mass spectrometry to quantify cell cycle-specific interactions of Dnmt1.

Work ow for quantitative analysis of Dnmt1 interactions

For a comprehensive understanding how Dnmt1 and DNA methylation is regulated over the cell cycle it is crucial to quantify and analyze cell cycle-dependent interactions of Dnmt1. Here, we use a combination of SILAC-based quantitative proteomics (Ong et al., 2002) with immunoprecipitation of endogenous Dnmt1 from HeLa (derived from cervical cancer cells taken from Henrietta Lacks) cells, synchronized at different phases of the cell cycle. A standard workflow for SILAC-based analysis of protein interaction partners in pull-down experiments is summarized in (Figure 10).
In brief, HeLa cells are grown in either "light" media (containing ^{12}C and ^{14}N lysine and arginine) or "heavy" media (containing ^{13}C and ^{15}N substituted lysine and arginine). Cells grown in "light" or "heavy" media represent the non-labelled samples or the SILAC standard, respectively. After culturing the cells for 12 days, which is sufficient for complete labelling of the proteins, the cells are synchronized in G_1 by adding 0.8 mM mimosine to the media. It has been demonstrated, that the rare non- protein amino acid mimosine induces a cell cycle arrest of human somatic cells in late G_1 phase, before establishment of active DNA replication forks (Krude, 1999). After 24 h mimosine treatment, the HeLa cells are released from G_1 and harvested immediately (G_1 phase) or after 5 h (early S phase) and 10 h (late S phase). In this approach, SILAC is only used to produce heavy labelled reference proteins or proteomes. these are added to the proteomes under investigation after cell lysis and before protein digestion. The actual experiment is therefore completely decoupled from the labeling procedure (Geiger et al., 2011). In addition, the effective experimental variability, that inevitably occurs when the samples are processed independently, reduces (Trinkle-Mulcahy et al., 2008). The cells were lysed, protein concentrations were measured and equivalent amounts of cell lysates were mixed. After a pre-clearing step, using not-functionalized beads, endogenous Dnmt1 is immunoprecipitated using a Dnmt1 binding protein coupled to agarose beads (DBP) provided by ChromoTek (Germany). The specific DBP was engineered based on a 13-kDa Dnmt1 binding fragment derived from a llama single chain antibody (Rothbauer et al., 2008). After washing four times with 150 mM NaCl, the bound proteins were eluted by on-beads trypsination and analysed by high sensitivity mass spectrometry in the Core Facility of the Max-Planck-Institute of Biochemistry.

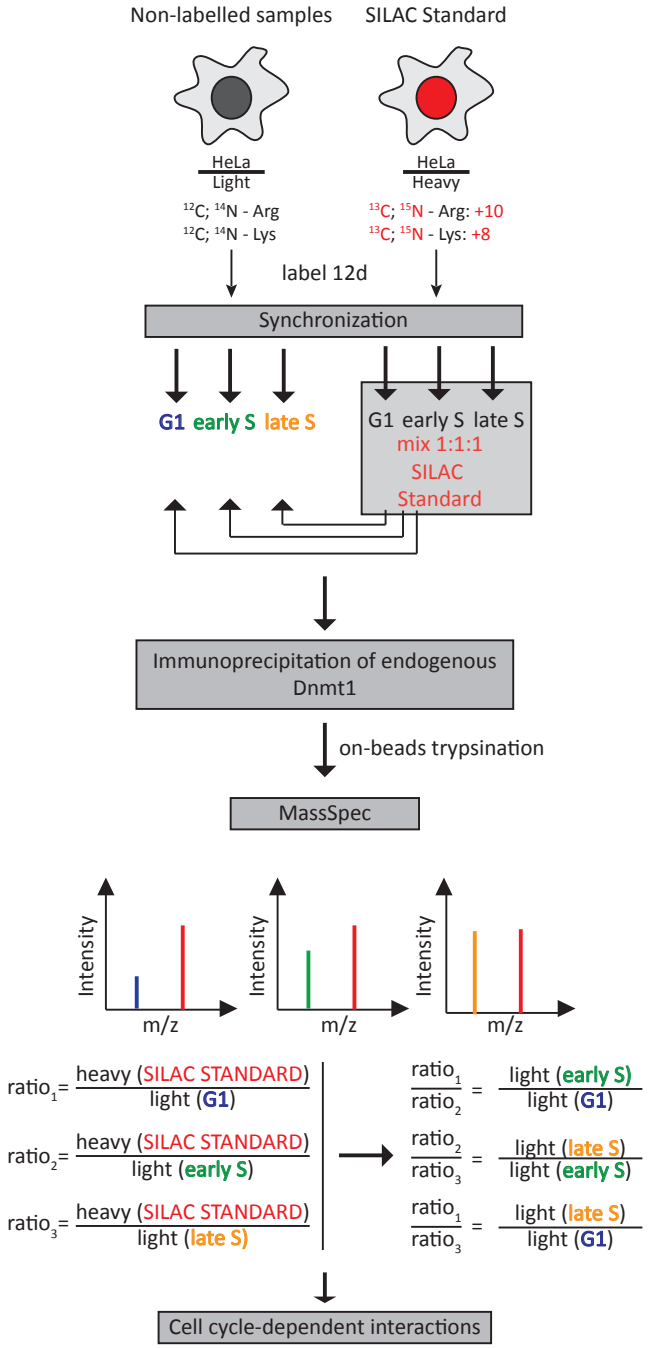

Figure 10: Work ow of SILAC-based quantification of cell cycle-dependent interactions of Dnmt1

Firstly, HeLa cells are cultured for 12 days in SILAC media containing either "light" or "heavy" lysines and arginines. Secondly, the HeLa cells are synchronized for 24 h with 0.8 mM mimosine, released and harvested either in G_1, early S or late S of the cell cycle. HeLa cells labelled with "heavy" media and sychronized in the corresponding cell cycle phases are mixed 1:1:1 and represent the SILAC standard. Thirdly, the SILAC standard is mixed 1:1 with non-labelled HeLa cells synchronized either in G_1, early S or late S of the cell cycle. Endogenous Dnmt1 is immunoprecipitated with a specific Dnmt1 Binder coupled to agarose-beads and the interactions are quantitatively determined by mass-spectrometry.

Immunoprecipitation of endogenous Dnmt1 from crude cell extracts

As a first test, we determined the efficiency of the specific DBP to immunoprecipitate endogenous Dnmt1. Initially, we tested 5 different DBP provided by ChromoTek (Germany). These specific binding proteins are based on approximately 13-kDa Dnmt1 binding fragment derived from a llama single chain antibody. Previous studies demonstrated, that specific binders such as the GFP-Trap (ChromoTek, Germany), a GFP-binding protein coupled to agarose beads, has several decisive advantages over conventional antibodies (Rothbauer et al., 2006; 2008). Firstly, typical high affinities of single chain antibodies allow short (30-60 min) incubations to isolate endogenous proteins and even transiently bound factors from different cellular compartments. Secondly, its small size of about 13 kDa minimizes unspecific binding and entirely avoids contamination by heavy and light chains of conventional antibodies (50 and 25 kDa) that normally interfere with subsequent analyses. Initially, we tested the influence of the DBP on the catalytic activity of Dnmt1. We expressed GFP-Dnmt1 in human embryonic kidney (HEK293T) cells and one-step purified GFP-Dnmt1 via the GFP-Trap (ChromoTek, Germany) as described before (Frauer and Leonhardt, 2009). Briefly, cells were lysed, incubated with the GFP-Trap (ChromoTek, Germany) and washed. Next, we incubated the purified GFP-Dnmt1 with DNA trapping substrate containing the mechanism-based inhibitor 5-aza-cytosine at a central hemi- (hemi) or unmethylated (un) CpG site with different fluorescent labels (Frauer and Leonhardt, 2009). The immobilized GFP-Dnmt1 was incubated with trapping substrate, alone or in the presence of a 10-fold molar excess of purified DBPs, and the catalytic activity of Dnmt1 was calculated. Those initial measurements did not reveal any inhibiting or activating effects of the DBP on the catalytic activity of Dnmt1 (Figure 11A).

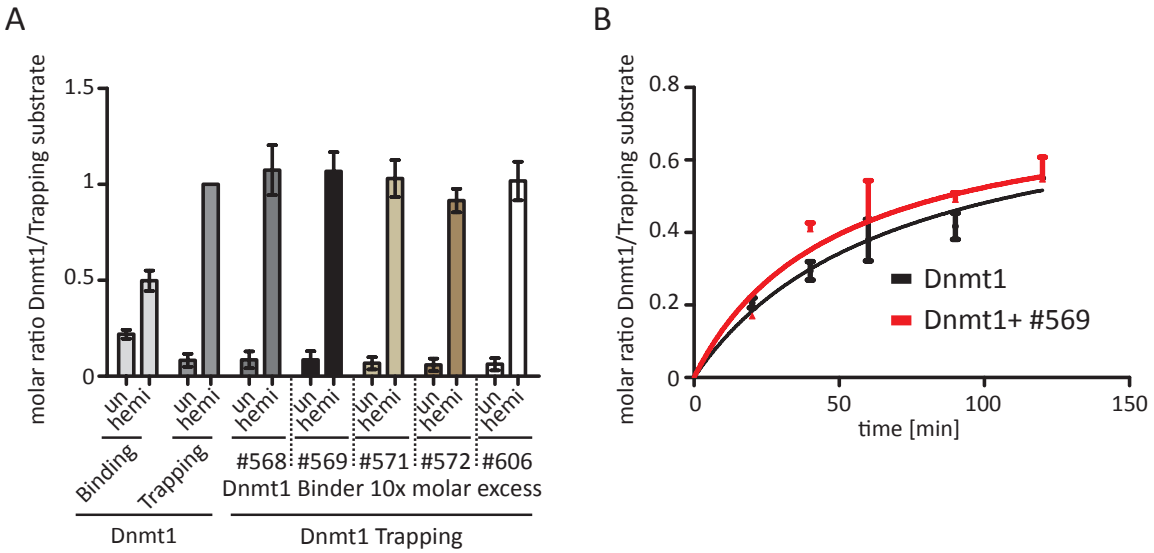

Figure 11: Initial testing of different Dnmt1 binder

A) The catalytic activity of Dnmt1 on hemi- and unmethylated DNA was measured in direct competition in the presence of a 10-fold molar excess of different Dnmt1 binder. The DNA binding and trapping activity of Dnmt1 alone was measured as positive control. Shown are means ± SEM of at least three independent experiments (except for Dnmt1 trapping). **B)** The catalytic activity was measured at different time points for Dnmt1 with a 10-fold molar excess of Dnmt1 binder #569. Shown are means ± SEM of two independent experiments.

Next, we examined the influence of the DBP #569 on the enzyme kinetics of Dnmt1. We performed the described trapping assay and measured the catalytic activity of Dnmt1 at different time points. Samples containing a 10-fold molar excess of DBP #569 did not show an altered enzymatic kinetic in comparison to the positive control (Figure 11B). In addition, we tested the ability of the DBP to precipitate its antigen from crude cell extracts and measured the catalytic activity of immunoprecipitated Dnmt1 (Figure 12). First, the DBP #569 was added to protein extracts of HEK293T cells expressing GFP-Dnmt1. Precipitated proteins were separated by SDS-PAGE and visualized by Coomassie Blue or immunoblot analysis (Figure 12A). After precipitation with the DBP the major protein band corresponded to GFP-Dnmt1. Next, we immunoprecipitated endogenous Dnmt1 from HeLa cells or Dnmt1 from mouse embryonic fibroblast (MEF) cells and determined the catalytic activity towards hemimethylated CpG sites with the trapping assay (Figure 12B). We could detect catalytic activity in samples from HeLa and MEF cells incubated with DBP coupled to agarose beads but not in samples obtained with not-functionalized beads (Figure 12B).

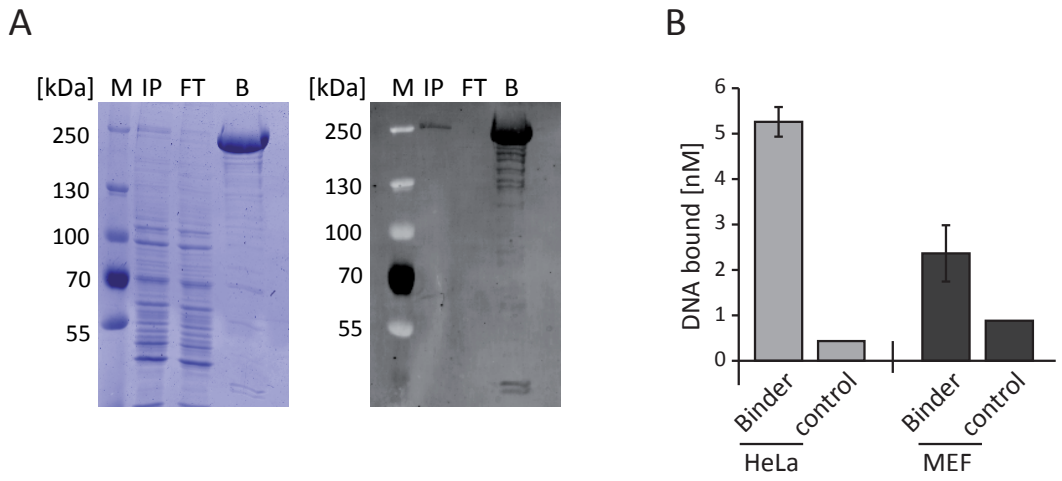

Figure 12: Immunoprecipitation of Dnmt1 with the Dnmt1 binder

A) Immunoprecipitation of GFP-Dnmt1 transiently expressed in HEK293T cells with DBP #569. Aliquots of input (IP) flow trough (FT) and bound fraction were separated by SDS-PAGE and visualized either by Coomassie staining (left) or by immunoblot analysis using a GFP-antibody (right). **B)** Endogenous Dnmt1 from HeLa or MEF cells was purified with the Dnmt1 binder. Purified Dnmt1 was incubated with hemimethylated trapping substrate and the catalytic activity was measured after 90 minutes. Not-functionalized beads were used as negative control. Shown are means $\pm$ SD of two independent experiments.

In summary, the DBP allows a fast and efficient (one-step) isolation of endogenous, active Dnmt1 for biochemical analyses including DNA methyltransferase activity

Cell cycle synchronization of HeLa cells with mimosine

In this study, we wanted to quantify the interactions of Dnmt1 over the cell cycle. As described above, interacting proteins can have different impacts on the activity of Dnmt1 at different cell cycle stages. Here, we used mimosine to synchronize the HeLa cells in G_1. Mimosine, a plant-derived amino acid whose cellular target is still unclear, blocks cells either in late G_1 phase (Lalande, 1990) or at the G_1/S boundary (Mosca et al., 1992). Also, it has been shown, that mimosine can induce a cell cycle arrest before establishment of active DNA replication forks (Krude, 1999). Mimosine is an effective inhibitor of S-phase entry in mammalian fibroblastic cell lines and human leukemic cell lines, and it inhibits DNA replication in Xenopus extracts (Gilbert et al., 1995). Mimosine is a stable inhibitor of cell cycle progression and is a relatively non-toxic compared with other chemical inhibitors, such as aphidicolin. To synchronize the cells, we cultured them in media containing 0.8 mM mimosine for 24 h. After washing with PBS, the cells were released and harvested at different time points (Figure 13). We stained the DNA with propidium iodide and analysed the DNA content by flow cytometry.

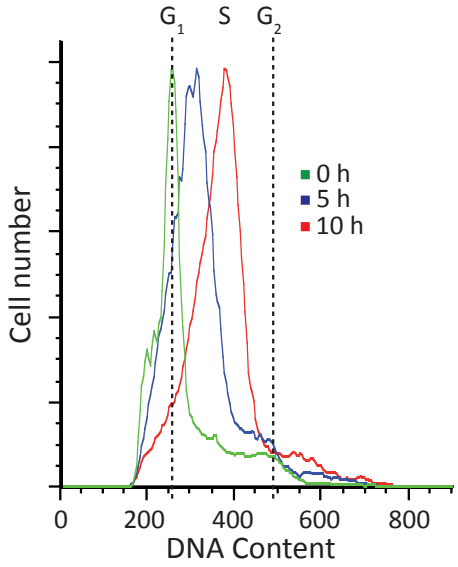

Figure 13: Cell cycle synchronization of HeLa cells using mimosine

HeLa cells were synchronized with 0.8 mM mimosine for 24 h, released and harvested after the indicated time intervals (green: 0 h; blue: 5 h; red: 10 h). The cells were stained with propidium iodide (PI) and analysed by flow cytometry.

The cells were efficiently synchronized in late G_1 after 24 h incubation with mimosine (Figure 13, green). After release in "light" media, we obtained a homogenous cell fraction in early S ((Figure 13, blue) or mid-late S (Figure 13, red) after 5 h or 10 h, respectively.

Identification of Dnmt1 interactions using the Dnmt1 binder

Then, we were interested whether we could detect known interaction partners of endogenous Dnmt1 immunoprecipitated from HeLa or HEK293T cells using the DBP #569 coupled to beads. We, immunoprecipitated endogenous Dnmt1, washed the beads four times with 150 mM NaCl and all proteins bound to the beads were digested with trypsin. All mass spectrometry analyses were performed by the Core Facility of the Max-Planck-Institute of Biochemistry.

Protein	Description	Uniprot Accession	Cell Type	Unique Peptides HEK293T/HeLa
Transcription and Development Regulation				
PSIP1	Transcriptional co-activator involved in neuroepithelial stem cell differentiation and neurogenesis	O75475	Both	6/4
KAP1	Mediates gene silencing	Q13263	HEK293T	5/0
TRIM25	Ubiquitin E3 ligase	Q14258	HeLa	0/2
FXR1	RNA-binding protein required for embryonic and postnatal development of muscle tissue.	P51114	Both	3/2
Histones				
Histone H1.3	Linker Histone	P16402	Both	8/3
Histone H2B type	Core Component of nucleosome	Q16778	Both	5/2
Histone H4	Core Component of nucleosome	P62805	Both	8/6
Chromatin-associated				
HDAC6	Histone deacetylase	Q6NT75	Both	7/14
HDAC10	Histone deacetylase	Q969S8	HeLa	0/3
HDAC2	Histone deacetylase	Q92769	Both	2/0
SMARCA5	Helicase that possesses intrinsic ATP-dependent nucleosome-remodelling activity	O60264	HEK293T	5/0
CHD4	Component of the histone deacetylase NuRD complex.	Q14839	HEK293T	2/0
CBX1	Recognizes and binds methylated H3K9	Q6IBN6	HEK293T	2/0
DNA damage				
XRCC5	Single stranded DNA-dependent ATP-dependent helicase.	P13010	Both	3/4
XRCC6	Single stranded DNA-dependent ATP-dependent helicase.	P12956	Both	7/7
DDB1	Required for DNA repair.	Q16531	Both	2/2
PARP1	Poly [ADP-ribose] polymerase 1	P09874	HEK293T	18/0
ZC3HAV1L	Phosphorylated upon DNA damage.	Q96H79	Both	2/2
DNA methylation				
DNMT1	Maintenance DNA methylation	P26358	Both	3/3
Cell cycle regulator				
PCNA	Targeting DNMT1 to replication foci	P12004	Both	13/7
Others				
PRMT1	Protein arginine methyltransferase	Q99873	Both	4/3
USP7	Hydrolase that deubiquitinates target proteins	A6NMY8	Both	2/6
SET	Multitasking protein, involved in transcription, nucleosome assembly and histone binding	Q01105	Both	2/4
Annexin	Calcium-regulated membrane-binding protein	P07355	HeLa	0/4

Table 1: Interaction partners of Dnmt1

Endogenous Dnmt1 was purified from HeLa or HEK293T cells using the Dnmt1 Binder and interaction partners were determined by mass spectrometry

We summarized the interaction partner of Dnmt1 in Table 1. Notably, we found proteins that are known to interact with Dnmt1 such as HDAC2 (Rountree et al., 2000; Robertson et al., 2000), Smarca5 (Robertson et al., 2004), Cbx1 (Fuks et al., 2003), Parp1 (Reale et al., 2005; Zampieri et al., 2009), Usp7 (Du et al., 2010; Qin et al., 2011a), Annexin (Ohsawa et al., 1996) and Kap1 (Quenneville et al., 2011), demonstrating the reliability of our approach. Besides known interactions, we could identify proteins involved in DNA damage repair such as Xrcc5, Xrcc6 and Ddb1 (Table 1). It has been shown, that Dnmt1 and PCNA accumulate at DNA damage sites, whereas recruit-

ment of Dnmt3a or b was not observed (Mortusewicz et al., 2005), indicating a direct role of Dnmt1 in the restoration of epigenetic information. In addition, Dnmt1 interacts with Mbd4, a mismatch-specific DNA N-glycosylase, further supporting a role of Dnmt1 in DNA damage repair (Ruzov et al., 2009). Also, Dnmt1 interacts with different chromatin-associated proteins like HDAC6 and HDAC10, which are both class IIb histone deacetylases. Notably, only the interactions with HDAC1 and 2 have been described so far (Robertson et al., 2000; Rountree et al., 2000). In summary, we could detect known interactions and could discover several new interactions, demonstrating the reliability and usefulness of our approach.

SILAC-based quantification of cell cycle-dependent interactions

The samples were prepared as described in Figure 10 and the mass spectrometry data was analysed by MaxQuant (Cox and Mann, 2008). A false discovery rate (FDR) of 0.01 for proteins and peptides and a minimum peptide length of 6 amino acids were required. MS/MS spectra were searched by Andromeda against the IPI human database (version 3.68) combined with 262 common contaminants and concatenated with the reversed versions of all sequences. For the Andromeda search trypsin allowing for cleavage N-terminal to Arginine and Lysine was chosen as enzyme specificity. MaxQuant was used for scoring of the peptides for identification. It also determined the SILAC state of peptides by the mass differences between SILAC peptide pairs and this information was used to perform searches with fixed Arg10 and Lys8 modifications as appropriate. Maximally two missed cleavages and three labelled amino acids were allowed. Initial mass deviation of precursor ion was up to 7 ppm, mass deviation for fragment ions was 0.5 units on the m/z scale. Protein identification required two peptides one of which had to be unique to the protein group. Data analysis plots were performed in the MaxQuant environment (Perseus). We created a heat map of the SILAC pull-down ratios and performed a one-way hierarchical clustering.

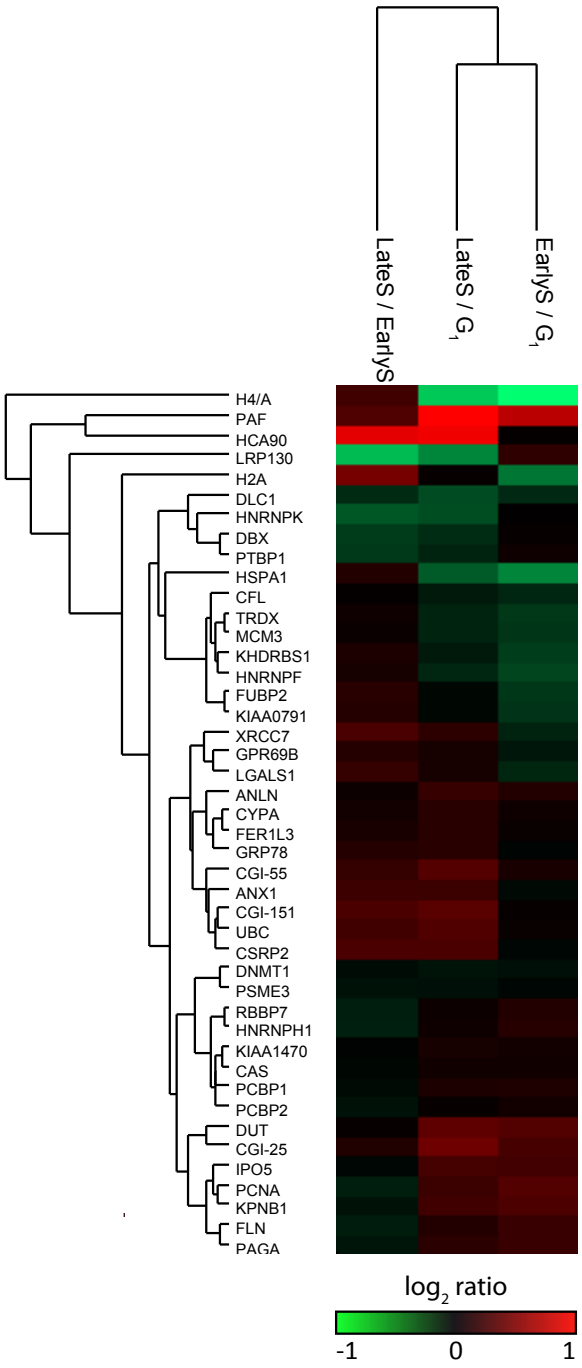

Figure 14: Dynamic Dnmt1 interactome visualized by a heat map and one-way hierarchical clustering
The columns represent ratios of either late S to early S, late S to G_1 or early S to G_1. Green values represents a negative ratio, red values represent a positive ratio. Shown are the median of three independent experiments. Only nuclear proteins with at least two SILAC ratio in each group are plotted. All ratio intensities are shown in $\log_2$ scale.

We found 44 nuclear proteins and our Dnmt1 interactome includes well-know binders

such as PCNA and different histone proteins.

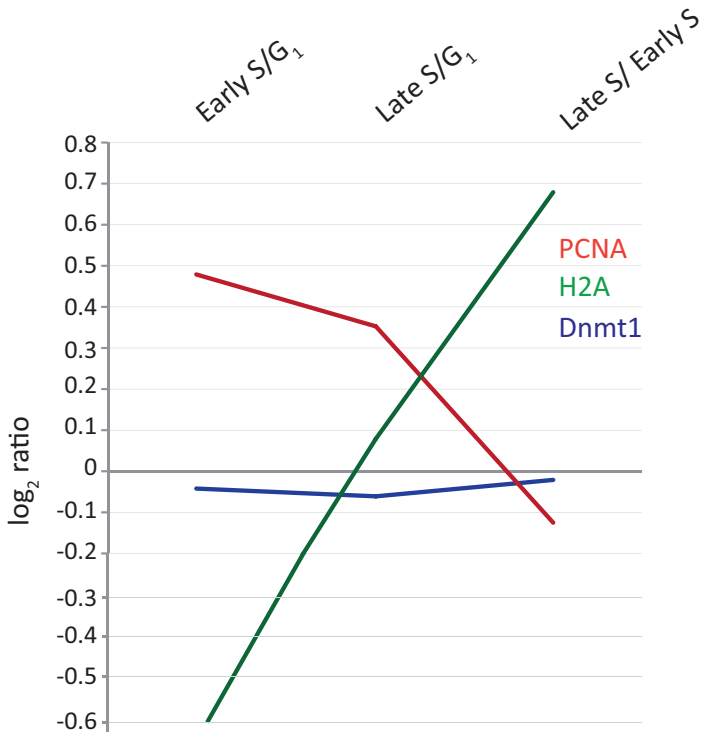

Figure 15: SILAC ratios for Dnmt1, PCNA and H2A

SILAC ratios taken from (Figure 14) between different cell cycle phases of Dnmt1, PCNAand Histone H2A.

Notably, the SILAC ratio of Dnmt1 is constant, demonstrating a non-varying Dnmt1 protein concentration over the cell cycle (Figure 15). Interestingly, PCNA interacts predominantly during early S phase with Dnmt1 while several histones interact with Dnmt1 in late S (Figure 15). Consistently, it is known that Dnmt1 interacts with PCNA in early to mid S phase (Schermelleh et al., 2007) and with histones at late replicating chromocenters in late S phase (Easwaran et al., 2004), demonstrating changing interactions of Dnmt1 during S phase of the cell cycle. In summary, we have described a streamlined interaction screen, which accurately discover and characterize dynamic interactions of endogenous Dnmt1 in the same experiment.

4 Discussion

Epigenetic modifications such as DNA methylation, histone modifications and nucleosome positioning play a role in the regulation of gene expression. However, the crosstalk and mechanistic links between these epigenetic signals are still poorly understood.

Over the past decade, a large variety of different interacting factors and post-translational modifications were reported for the eukaryotic DNA methyltransferase, Dnmt1, illustrating the complexity of DNA methylation *in vivo*. In this PhD thesis, I investigated the role of Dnmt1 interacting factors such as Uhrf1 and Uhrf2 and examined their role in connecting different epigenetic pathways. To gain further insights into the function of these proteins, I established a high-throughput histone-tail peptide, DNA and protein-protein binding assay. Applying this method, I provided further insights into the crosstalk of DNA methylation and histone modifications. I could show that Uhrf1 and Uhrf2 specifically bind to the predominant heterochromatin mark H3K9me3, mediated by highly conserved aromatic amino acids forming an aromatic cage structure. Moreover, binding assays demonstrated a cooperative interplay of Uhrf2 domains that induces preference for hemimethylated DNA, the substrate of maintenance methylation, and enhances binding to H3K9me3 heterochromatin marks. Furthermore, I established and applied protocols to quantify and discover interactions of Dnmt1 over the cell cycle.

4.1 Versatile Toolbox for High-Throughput Biochemical and Functional Studies with Fluorescent Proteins

In the past, a variety of different *in vivo* and *in vitro* assays have been developed to determine protein binding specificities and affinities to different substrates like DNA, histones and proteins. These include the yeast two-hybrid assay (Fields and Song, 1989; Chien et al., 1991), the protein complementation assay (Johnsson and Varshavsky, 1994), peptide phage display (Smith, 1985), microarrays, isothermal titration calorimetry (ITC) (Ababou and Ladbury, 2007), surface plasmon resonance (SPR) (Aslan et al., 2005) and conventional pull-down experiments with mass spectrometry (Gavin et al., 2002; Ho et al., 2002) or immunoblot analyses. All these techniques are powerful tools to quantify and identify binding events but have certain disadvantages. On the one hand, techniques like ITC and SPR need large amounts of proteins. To gain large amounts, those proteins have to be expressed and purified from bacterial systems (e.g. *E.coli*) or lower eukaryotes such as yeast (e.g. *S. cerevisiae*). Thus, the recombinant proteins might lack essential post-translational modifications or are not folded properly

which could lead to different binding properties and inaccurate results. The expression of proteins in higher eukaryotes like insects ensures post-translational modifications but is very time-consuming and expensive. In addition SPR and ITC measurements one can only determine the binding affinity to one substrate, which does not reflect the *in vivo* situation where most proteins have the choice between many different binding substrates inparallel. On the other hand, conventional methods like pull-downs require proteins fused to a small epitope tag such as FLAG or c-Myc. In contrast, *in vivo* data are acquired using fluorosescent tags like GFP and RFP. The integration of these *in vitro* data with *in vivo* data obtained with fluorescently labelled proteins has in part been impeded by the simple fact that different protein tags are used for different applications. In Chapter 3.1, we provide protocols for two specific GFP- and RFP- binding proteins based on antibody fragments derived from llama single chain antibodies. The binding proteins can be produced in bacteria and coupled to monovalent matrixes generating so-called Nanotraps. We provide protocols for precipitation of fluorescent fusion proteins from crude cell extracts to identify and map protein-protein interactions as well as specific histone-tail peptide binding in an easy and reliable manner. Furthermore, we expanded the presented assays to 96-well micro plates to generate a versatile toolbox for high throughput biochemical and functional studies with fluorescent fusion proteins (Chapter 3.2 and Figure 16).

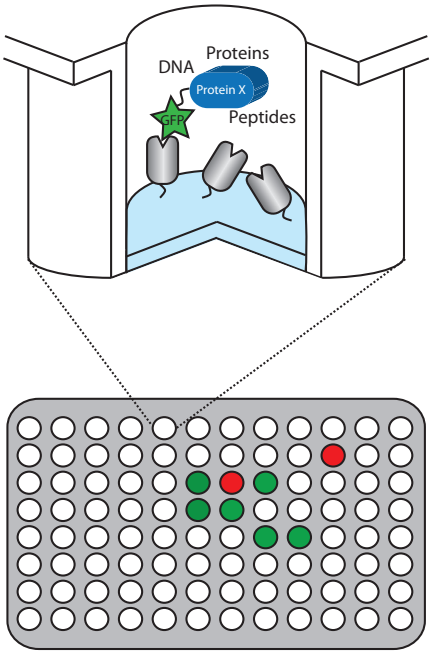

Figure 16: Schematic drawing of the GFP-multiTrap

A specific GFP-binding protein is immobilized in the wells. Purified GFP-fusions can be tested for histone-tail peptide, DNA and protein binding.

Using a new system based on 96-well micro plates comprising an immobilized GFP-binding protein (GFP-Trap, GFP-multiTrap), we performed fast and efficient one-step purification of different GFP- and YFP-fusion proteins from crude cell lysate. After immobilization we determined highly reproducible binding ratios of the cellular expressed GFP-fusion proteins to histone-tail peptides, DNA or RFP-fusion proteins. Briefly, after expression of GFP-fusion proteins, we generated crude cell extracts by cell lysis and centrifugation and transferred the soluble supernatant to single wells of the GFP-multiTrap. After binding, the single wells were subjected to several washing steps and incubated with fluorescently labelled substrates such as histone-tail peptides and DNA substrates or with RFP-fusion proteins (Figure 16). After removal of unbound substrate, the absolute amounts and molar ratios of GFP-fusion proteins and bound substrates were determined by fluorescence measurements. As proof of principle, we tested histone-tail peptide binding specificities of Cbx1, the DNA binding specificities of the MBD domain of MeCP2 and the protein-protein interactions of different epigenetic regulators. We found that Cbx1 preferentially binds to di- and trimethylated H3K9 histone-tail peptides and this specific binding is abolished by phosphorylation of the adjacent serine. Notably, previous studies (Jacobs et al., 2001) measured binding affinities of 7 and 2.5 µM for H3K9me2 and H3K9me3 for the HP1 chromo domain, the Drosophila homolog of mammalian Cbx1. These measurements indicated a clear preference for trimethylated H3K9. However, we could not detect a preference for H3K9me3. One explanation could be the use of different expression systems. While the binding ratios for the HP1 chromo domain were determined using bacterial expressed protein we used a fluorescent fusion protein derived from mammalian cells. In this context a recent study revealed that recombinant HP1 prepared from mammalian cultured cells exhibited a stronger binding affinity for K9-methylated histone H3 (H3K9me) in comparison to protein produced in *E.coli* due to multiple post-translational phosphorylation at N-terminal serine residues (Hiragami-Hamada et al., 2011). This demonstrates the impact of post-translational modifications on biochemical properties of specific proteins and emphasizes the advantage of using GFP-fusion proteins expressed in mammalian systems. Furthermore, we could measure a preference of the isolated MBD domain of MeCP2 for symmetrically methylated over unmethylated DNA, consistent to previous studies (Nan et al., 1993; Free et al., 2001) using conventional electrophoretic mobility shift assays (EMSA). In addition to the detection of substrate specificity, the analysis of the interaction with other cellular components and factors is essential to understand the function of proteins. The use of fluorescently labelled fusion proteins to study protein-protein interactions *in vitro*, provides a new and simple method since binding events can be detected by measuring the fluorescence, avoiding laborious and inaccurate protein detection using conventional immunoblotting systems. Using our new assay, we determined quantitative binding ratios between nuclear located

proteins involved in DNA replication, DNA methylation as well as in DNA repair. In particular, we could show that the PBD domain of Dnmt1 binds to PCNA and that deletion of this domain abolishes binding of full-length Dnmt1 to PCNA. In parallel, we used an ELISA-based assay to detect endogenous interaction factors bound to immunoprecipitated GFP-fusion proteins. Notably, using this appraoch, we found endogenous PCNA bound to Dnmt1, Fen1 and PCNA itself but not binding to Dnmt1 lacking the PBD domain. Also, we could detect endogenous Histone H3 bound on Cbx1. Remarkably, we quantified the level of H3 and H3K4me2 at nucleosomes comprising different histone variants. In particular, we found higher levels of H3K4me2 at nucleosomes comprising H2A.Z in comparison to H2A.
In summary, we established a new versatile medium/high-throughput approach to analyse binding specificities of fluorescently labelled fusion proteins and to detect endogenous interacting factors in a fast and reliable manner.

4.2 Uhrf proteins connect different pathways

4.2.1 Uhrf1 coordinates repressive epigenetic pathways

As described in Chapter 1.2.2, Dnmt1 interacts with a large variety of different proteins including chromatin binding and modifying proteins. It is known, that DNA and H3K9 methylation correlate and form a complex regulatory network contributing to gene repression (Cedar and Bergman, 2009; Esteve et al., 2006). These two repressive epigenetic modifications seem to mutually influence each other *in vivo*. On the one hand, the knockdown of the DNA methyltransferase Dnmt1 results in decreased levels in H3K9 di-and trimethylation (Espada et al., 2004; Ikegami et al., 2007; Dong et al., 2008). On the other hand, the knockdown of the histone methyltransferase Suv39H1/H2 or G9a, that are both known to interact with Dnmt1, leads to decreased DNA methylation in mammals (Lehnertz et al., 2003; Tachibana et al., 2002). However, how histone marks are linked to DNA methylation pattern and how this complex epigenetic information is integrated and translated into defined chromatin structures and gene expression levels still remains elusive. In this context, multi-domain proteins that bind DNA and histone marks are ideally suited to link epigenetic pathways and intra-molecular interactions between different binding domains may contribute to substrate specificity and epigenetic regulation (Hashimoto et al., 2009).
The multi-domain protein Uhrf1 has recently emerged as key factor to connect two repressive epigenetic pathways by binding to hemimethylated DNA and to histones (Citterio et al., 2004; Avvakumov et al., 2008; Arita et al., 2008). Moreover, Uhrf1 interacts with both DNA and H3K9 methyltransferases including Dnmt1 and G9a (Kim et al.,

2009; Meilinger et al., 2009; Unoki et al., 2004; Achour et al., 2009) and genetic ablation in ESCs leads to genome- wide hypomethylation, a phenotype similar to *dnmt1*$^{-/-}$ ESCs (Bostick et al., 2007; Sharif et al., 2007). Based on these data, Uhrf1 was suggested to recruit Dnmt1 to hemimethylated CpG sites at replication forks. The SRA domain of Uhrf1 is sufficient to recognize hemimethylated DNA but it was still unclear which domain or combination of domains is binding to histones and which specific histone modifications are recognized. Using *in vitro* DNA and histone-tail peptide binding assays in combination with *in vivo* fluorescence recovery after photobleaching (FRAP) studies in ESCs, we characterized the various interactions mediated by Uhrf1 and the single Uhrf1 domains (Chapter 3.3). We found that Uhrf1 binds to hemi- over unmethylated DNA substrates with only an about two-fold preference. Consistently, we found that complete loss of genomic DNA methylation does not affect binding kinetics of Uhrf1 *in vivo*. Moreover, the isolated SRA domain is sufficient for DNA binding of Uhrf1 *in vitro*. However, the subcellular localization of the isolated SRA domain is different in comparison to the full-length Uhrf1, pointing to an additional role of other domains in the proper subcellular localization. Using our*in vitro* histone-tail peptide-binding assay, we could demonstrate that Uhrf1 preferentially binds to the predominant heterochromatin mark H3K9me3. Interestingly, the specific recognition is mediated by three highly conserved aromatic amino acids in the tandem Tudor domain forming an aromatic cage structure. Together, our data support the hypothesis that Uhrf1 possess a multi-functional modular structure connecting DNA methylation and histone modification pathways.

4.2.2 Uhrf2 coordinates repressive epigenetic pathways

Interestingly, a second member of the Uhrf family, Uhrf2, harbours similar domains (Bronner et al., 2007). Until now, Uhrf2 has been described to play a role in intranuclear degradation of polyglutamine aggregates (Iwata et al., 2009) and cell cycle control (Mori et al., 2002; Li et al., 2004; Mori et al., 2011). However, a potential function of Uhrf2 in maintenance DNA methylation has not been reported. We systematically investigated the function and interplay of distinct Uhrf2 domains in DNA and histone tail substrate recognition and reported first data on cell-type specific functions of Uhrf1 and Uhrf2 (Chapter 3.4). Firstly, we compared the expression pattern of *uhrf1* and *uhrf2* in ESCs and somatic cells, during differentiation and in differentiated mouse tissues and found opposite expression patterns; while *uhrf1* is expressed in ESCs and down regulated during differentiation, which is consistent with previous reports (Fujimori et al., 1998; Hopfner et al., 2000), *uhrf2* is up regulated and highly expressed in differentiated mouse tissues. Using our *in vitro* binding assays, we investigated the DNA and histone-tail peptide binding preferences of Uhrf2. Similar to Uhrf1, Uhrf2 preferentially

binds to unmodified histone H3 and H3K9me3 mediated by an aromatic cage in the tandem Tudor domain. Consistently, acetylation of H3K9, underrepresented in heterochromatin, prevented the binding of Uhrf2. Notably, in contrast to recent publications, we could not detect any histone binding for the isolated PHD domains of Uhrf1 and Uhrf2 *in vitro*. It was shown, that the PHD domain, which is located adjacent to the tandem Tudor domain, binds to histone H3 unmodified arginine 2 (H3R2) (Rajakumara et al., 2011; Xie et al., 2011; Wang et al., 2011; Hu et al., 2011). The binding of the PHD domain to H3 is abolished by methylation of H3R2 but not by H3K4 and H3K9 methylation. ChIP studies demonstrated that Uhrf1's ability to repress its direct target gene expression is dependent on PHD binding to unmodified H3R2, thereby demonstrating the functional importance of this recognition event and supporting the potential for crosstalk between histone arginine methylation and Uhrf1 function (Rajakumara et al., 2011). In general, arginine methylation is catalysed by the PRMT family of proteins and physiological roles for protein arginine methylation have been established in several biological processes like signal transduction, mRNA splicing, transcriptional control, DNA repair and protein translocation (Bedford and Clarke, 2009). However, little is known about how histone arginine residues are recognized and to what extent protein arginine methylation and demethylation occurs. Interestingly, we could demonstrate that the combination of the PHD and the tandem Tudor domain of Uhrf2 displayed an increased binding to H3K9me2/me3 in comparison to the single TTD, which was not observed for the corresponding construct of Uhrf1. The increased binding depends on the highly conserved linker region between the tandem Tudor and PHD domain of Uhrf2, suggesting a cooperative interplay of different Uhrf2 domains. A similar functional importance of linker sequences has been described for BPTF and histone lysine demethylases (Li et al., 2006; Horton et al., 2010). In case of BPTF, the largest subunit of the ATP-dependent chromatin-remodelling complex, NURF, a PHD and a bromo domain are connected via a -helical linker (Li et al., 2006). Both investigated histone demethylases harbour a PHD that binds H3K4me3 and a jumonji domain that demethylates either H3K9me2 or H3K27me2 and the substrate specificity is controlled by the linker connecting both functional domains (Horton et al., 2010). These data demonstrate an additional level of complexity involving multivalent binding of histone-tail peptides by mixed two- effector modules (Ruthenburg et al., 2007).

In contrast to Uhrf1, Uhrf2 did not show a DNA binding preference for hemimethylated DNA. However, binding to heterochromatin-specific H3K9me3 peptides induced a significant preference of Uhrf2 for hemi- over unmethylated DNA. Vice versa, binding to DNA enhanced binding of Uhrf1 and Uhrf2 to the H3K9me3 peptide. Consistently, SILAC-based proteomic analysis identified enrichment of Uhrf1 at nucleosomes containing repressive DNA and H3K9 methylation marks (Bartke et al., 2010). A similar effect was reported for MSL3 that specifically binds to H4K20me1 via a chromodomain

only in the presence of DNA (Kim et al., 2010).
Similar to Uhrf1, the subcellular localization and binding dynamics of Uhrf2 *in vivo* are dependent on histone H3K9 methylation but not on DNA methylation. Consistently, mutant Uhrf1 protein deficient for H3K4me0/K9me3 binding fails to reduce the expression of a target gene, p16INK4A, when overexpressed (Nady et al., 2011). Remarkably, transient expression of Uhrf2 in *uhrf1*$^{-/-}$ ESCs did not restore the DNA methylation pattern at major satellites, pointing to functional differences between Uhrf1 and Uhrf2 *in vivo*. Notably, a recent publication reveals that Uhrf fails to recruit Dnmt1 to replication foci during S phase of the cell cycle, demonstrating that the cell cycle-dependent interaction between Uhrf1 and Dnmt1 is a key regulatory mechanism for DNA methylation (Zhang et al., 2011). Also, the opposite expression pattern argues against a functional redundancy of both genes and explain the drastic loss of DNA methylation in *uhrf1*$^{-/-}$ ESCs despite the presence of intact *uhrf2* alleles.

4.2.3 Diverse function of Uhrf proteins

As illustrated in Figure 9, Uhrf proteins harbour several distinct functional domains, suggesting diverse functional roles in different cellular pathways. It was suggested, that Uhrf1 binds to hemimethylated DNA, flips the base out of the DNA helix and recruits Dnmt1 to its substrate. However, conventional *in vitro* DNA methyltransferase activity assays argue against that simple model. Dnmt1 is active on hemimethylated naked DNA and less active on DNA wrapped around mononucleosomes (Figure 17). Remarkably, the addition of Uhrf1 abolished the catalytic activity of Dnmt1, suggesting a tight binding of Uhrf1 to hemimethylated DNA that occludes the DNA from Dnmt1. These data indicate that the base flipping mediated by Uhrf1 does not facilitate the DNA methylation reaction by Dnmt1. Likely, Uhrf1 recruit other proteins to ensure maintenance DNA methylation by Dnmt1.

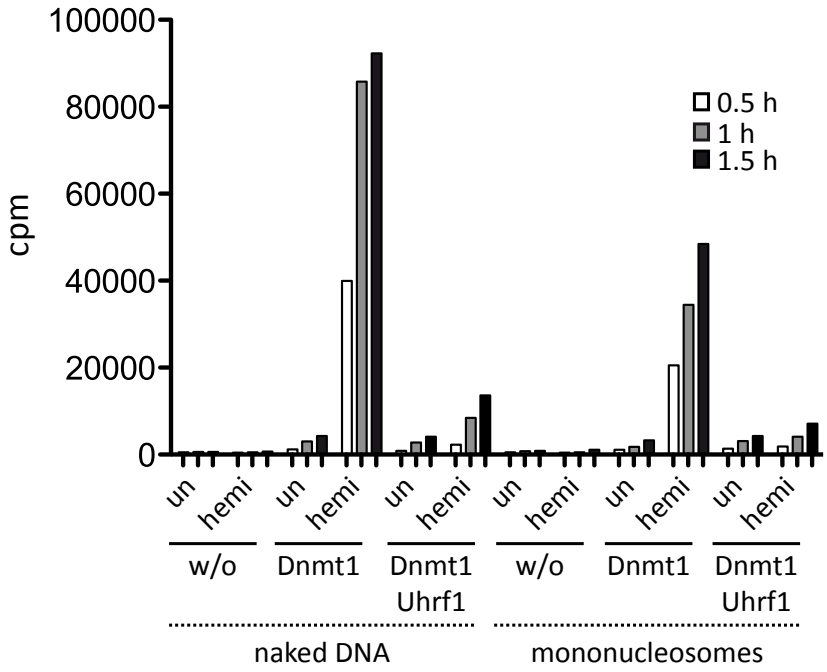

Figure 17: Radioactive *in vitro* DNA methyltransferase assay

Dnmt1 and Uhrf1 were expressed recombinantly in insect cells. Un- or hemimethylated DNA substrates, either naked or wrapped around mononucleosomes, were incubated with Dnmt1 alone or with Dnmt1 and Uhrf1 in molar ratio of 1:2. All reactions were performed in the presence of S-Adenosyl-L-Methionine (SAM (^{3}H)) at 37°. Reactions were stopped after 0.5, 1 or 1.5 h, precipitated in TCA and counts per minute (cpm) were measured. Carina Frauer purified Dnmt1 from insect cells and Henrike Klinker (Becker lab) prepared the mononucleosomes.

Indeed, interactomics of both Uhrf proteins discovered a broad range of proteins with different functions (Table 2) that are involved in many different pathways (Table 3).

Protein	Description	Uniprot Accesion	Bait	Unique Peptides Uhrf1/Uhrf2
Transcription Regulation				
DMAP1	Involved in transcription repression and activation	Q9NPF5	Uhrf2	0/3
PRDM10	May be involved in transcriptional regulation	Q17R90	Uhrf2	0/2
ZNF618	May be involved in transcriptional regulation.	Q5T7W0	Uhrf2	0/2
PSIP1	Transcriptional co-activator	O75475	Both	6/8
ADNP	Potential transcription factor.	Q9H2P0	Uhrf2	0/9
MTA2	May be involved in the regulation of gene expression as repressor and activator	O94776	Uhrf1	2/0
Cell Cycle Regulation				
ANP32A	Implicated in a number of cellular processes,	P39687	Both	2/6
ANP32B	Implicated in a number of cellular processes,	P39687	Both	2/6
Histones				
Histone H4	Core Component of nucleosome	P62805	Both	11/13
HIST2H2BE	Core Component of nucleosome	Q16778	Uhrf2	0/5
HIST1H2BN	Core Component of nucleosome	Q99877	Uhrf1	3/0
H2A.Z	Histone variant	P0C0S5	Uhrf1	4/4
macro-H2A.2	Histone variant	Q9P0M6	Uhrf2	0/8
Chromatin-associated				
SMARCA5	Helicase that possesses intrinsic ATP-dependent nucleosome-remodelling activity	O60264	Both	16/17
RSF1	Required for assembly of regular nucleosome arrays by the RSF chromatin-remodelling complex.	Q96T23	Both	9/4
BAZ1A	Component of the ACF complex	Q9NRL2	Both	5/5
BAZ1B	Atypical tyrosine-protein kinase	Q9UIG0	Uhrf1	2/0
HDAC1	Histone deacetylase	Q13547	Uhrf1	2/3
RNF2	E3 ubiquitin-protein ligase	Q99496	Uhrf2	0/4
CBX8	Component of a Polycomb group (PcG)	Q9HC52	Uhrf2	0/4
CBX3	Recognizes and binds methylated H3K9	Q13185	Both	2/3
RCC1	Binds both to the nucleosomes and double-stranded DNA.	Q16269	Uhrf1	7/0
PBRM1	Involved in transcriptional activation and repression of select genes by chromatin remodelling	Q86U86	Uhrf1	3/0
CHD4	Component of the histone deacetylase NuRD complex	Q14839	Uhrf2	0/10
DNA binding				
UHRF2	E3 ubiquitin-protein ligase	Q96PU4	Uhrf2	0/24
UHRF1	Hemimethylated CpG binding protein	A8K024	Both	10/4
DNMT1	Maintenance DNA methylation	P26358	Uhrf1	2/0
DNA damage				
PARP1	Poly [ADP-ribose] polymerase 1	P09874	Both	39/47
PARP2	Involved in the base excision repair (BER) pathway	Q9UGN5	Uhrf1	6/0
XRCC1	Corrects defective DNA strand-break repair and sister chromatid exchange	P18887	Uhrf1	3/0
XRCC5	Single stranded DNA-dependent ATP-dependent helicase.	P13010	Uhrf1	6/0
XRCC6	Single stranded DNA-dependent ATP-dependent helicase.	P12956	Uhrf1	4/0
MSH6	Component of the post-replicative DNA mismatch repair system	P52701	Uhrf1	9/0
DDB1	Required for DNA repair.	Q16531	Both	4/17
RFC5	Elongation of primed DNA templates by DNA polymerase delta	P40937	Uhrf1	2/0
MPG	Hydrolysis of the deoxyribose N-glycosidic bond for base excision	P29372	Uhrf2	0/2
Ligase III	Corrects defective DNA strand-break repair and sister chromatid exchange	P49916	Uhrf1	2/0
RAD23B	Multiubiquitin chain receptor involved in modulation of proteosomal degradation.	P54727	Uhrf2	0/2
Others				
USP7	Hydrolase that deubiquitinates target proteins	A6NMY8	Both	30/28
SET	Multitasking protein, involved	Q01105	Uhrf2	0/11

Table 2: Interaction partners of Uhrf1-GFP and Uhrf2-GFP

GFP-fusions were expressed in HEK293T cells and purified via GFP-Trap. Interaction partner were determined by mass spectrometry.

As mentioned, Uhrf1 and Uhrf2 have been shown to interact with DNA methyltransferases (Dnmt1, Dnmt3a and b) and histone methyltransferases (G9a), demonstrating their role in connecting different epigenetic pathways. Uhrf1 forms a repressive complex with G9a/GLP in euchromatic regions to regulate transcription of p21 and $p16^{INK4A}$ (Nady et al., 2011; Kim et al., 2009) and Suv39H1/H2-mediated H3K9 methylation has been demonstrated to be essential for proper localization of Uhrf proteins (Pichler et al., 2011; Karagianni et al., 2008). Notably, the major H3K9 methyltransferases Suv39H1,

G9a, GLP and SetDB1 have recently been demonstrated to coexist in a multimeric complex, and these enzymes cooperate to mediate H3K9 methylation in both eu- and heterochromatin (Fritsch et al., 2010).

Uhrf1			Uhrf2		
KEGG pathways	**Count**	**Percentage**	**KEGG pathways**	**Count**	**Percentage**
Spliceosome	5	7.69	Spliceosome	24	17.27
SLE	4	6.15	SLE	7	5.04
Base excision repair	4	6.15	RNA transport	7	5.04
Nucleotide excision repair	3	4.62	Ribosome	7	5.04
NHEJ	3	4.62	mRNA surveillance	4	2.88
Mismatch repair	3	4.62	Ribosome biogenesis	3	2.16
Wnt signaling pathway	2	3.08	Cancer pathway	3	2.16
Ub-mediated proteolysis	2	3.08	Nucleotide excision repair	3	2.16
RNA transport	2	3.08	Base excision repair	3	2.16
Ribosome biogenesis	2	3.08	Wnt signaling pathway	2	1.44
Ribosome	2	3.08	Ub-mediated proteolysis	2	1.44
DNA replication	2	3.08	Protein processing	2	1.44
			Mismatch repair	2	1.44
			Colorectal cancer	2	1.44
			Cell cycle	2	1.44

Table 3: Uhrf proteins associate with a broad range of proteins

The immunoprecipitated proteins were grouped and counted according to the KEGG pathways. Rows indicate the KEGG pathway and how many proteins in relation to the total number of immunoprecipitated proteins are annotated in this particular pathway. Following abbreviations were used: SLE: Systemic lupus erythematosus; NHEJ: Non-homologous end joining; Ub: Ubiquitin. Notably, histone proteins are involved in the SLE KEGG pathway.

Both, Uhrf1 and Uhrf2 bind to methylated H3K9, generated by H3K9 methyltransferases through the tandem Tudor domain and PHD finger module, which may recruit H3K9 methyltransferases to methylate the adjacent H3K9 of neighbouring nucleosomes. That may help to establish and maintain H3K9me3 states on both heterochromatic and certain silenced euchromatic regions (Barski et al., 2007; Bilodeau et al., 2009). Therefore, it is highly possible that the propagation of DNA methylation and H3K9me3 mutually reinforce each other to ensure the stability of heterochromatic states through Uhrf1- and Uhrf2- associated repressive complex (Hashimoto et al., 2009; Xie et al., 2011). In addition, our interactomics data identified Cbx3 binding to both Uhrf proteins (Table 2). Cbx3 binds to trimethylated H3K9 (Kaustov et al., 2010) and may help to maintain heterochromatin similar to HP1 (Maison and Almouzni, 2004). Notably, we could also detect proteins involved in ATP-dependent chromatin remodelling such as Smarca5, Baz1a and Baz1b (Table 2). These interaction data suggest that Uhrf proteins bind to histones and DNA and recruit chromatin remodeller that may "open" the chromatin to facilitate the maintenance of DNA methylation. Interestingly, Dnmt1 also interacts with

Smarca5 that increases the binding affinity of Dnmt1 to mononucleosomes that may help Dnmt1 to access substrate sites in heterochromatic regions. (Robertson et al., 2004). Indeed, Smarca5, also known as Snf5h, is the catalytic subunit of ACF complex that regulates spacing of nucleosomes using ATP to generate evenly spaced nucleosomes along the chromatin. It was shown that Snf2h becomes specifically enriched in replicating pericentric heterochromatin and *in vivo* depletion of Snf2h slows the progression of DNA replication, demonstrating a role in enabling DNA replication through highly condensed regions of chromatin (Collins et al., 2002).
In addition, Uhrf proteins harbour a Ring domain, which possesses ubiquitin E3 ligase activity and might function in modulating chromatin structure through its ubiquitin activity. *In vitro*, H2A, H2B and H3 were identified as substrates of Uhrf1 with similar efficiency (Citterio et al., 2004) and we could detect several core histones interacting with both Uhrf proteins (Table 2). Compared to acetylation, methylation, and phosphorylation, very little is known about the function of histone ubiquitylation. Recently, the histone H3 and H4 ubiquitin ligase complex, CUL4-DDB-ROC1, has been characterized. Biochemical studies indicate that CUL4-DDB-ROC1-mediated histone ubiquitylation weakens the interaction between histones and DNA and facilitates the recruitment of repair proteins to damaged DNA (Wang et al., 2006). Also, we could show (Qin et al.; unpublished data,), that ubiquitination activity of Uhrf1 was required for maintenance of DNA methylation by Dnmt1. These data suggest, that besides the role of Uhrf proteins in propagating histone methylation they control the overall structure of nucleosomes by ubiquitination.
In addition, Uhrf1 and Uhrf2 associate with the deubiquitinase Usp7, which also bind to Dnmt1, suggesting a dynamic complex including Dnmt1, Uhrf1 and Usp7 in mammalian cells (Qin et al., 2011a). Notably, genetic ablation of *usp7* in human tumor cell lines did not affect global DNA methylation but led to a 65 % decreased DNA methylation level at the imprinted gene H19 (Du et al., 2010). Consistently, Usp7 and Uhrf1 were reported to modulate Dnmt1 stability by ubiquitination and deubiquitination (Qin et al., 2011a; Du et al., 2010), and in addition Usp7 stimulates both the maintenance and de novo methylation activity of Dnmt1 *in vitro* (Felle et al., 2011).
As mentioned, ubiquitination of H3 and H4 participates in the cellular response to DNA damage (Wang et al., 2006) and Uhrf proteins were suggested to ubiquitinate histones. Consistently, the loss of Uhrf1 increases the sensitivity of cells to DNA damage (Tien et al., 2011). It was shown, that Uhrf1-depleted cells exhibit increased sensitivity to -irradiation and that these cells show impaired cell cycle arrest and an impaired accumulation of histone H2A.X phosphorylation (H2A.X) in response to -irradiation (Mistry et al., 2010). Notably, several proteins involved in DNA damage repair such as Parp1/2, Xrcc1 and 6 and Ddb1 interact with both Uhrf proteins.
Taken together, Uhrf proteins may function in the propagation of repressive chromatin

states, gene expression/repression, protein and histone ubiquitination, cell cycle regulation and DNA damage response (Figure 18).

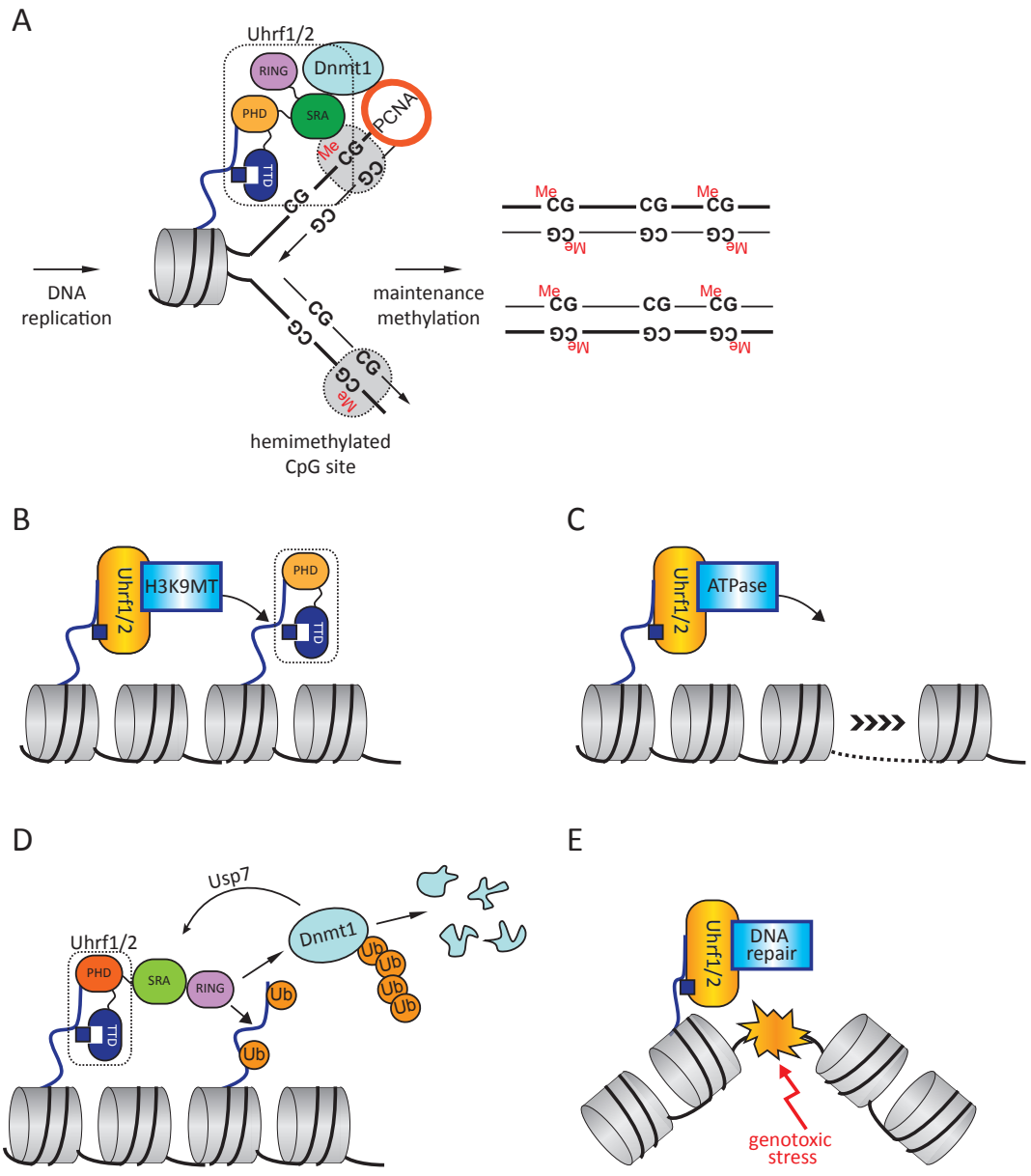

Figure 18: Diverse functions of Uhrf proteins

A) Uhrf proteins bind to repressive epigenetic modifications and Uhrf1 recruits Dnmt1 to replication foci. **B)** Uhrf proteins bind to H3K9me3 and recruit H3K9 methyltransferases (H3K9MT), propagating heterochromatic regions. **C)** Uhrf proteins bind to ATP-dependent chromatin remodeller. D) Uhrf proteins harbour an E3 ubiquitin ligase, RING, domain, that ubiquitinates proteins like Dnmt1 and histones. **E)** Uhrf proteins play a role in DNA damage repair and interact with proteins involved in DNA repair.

4.3 Dynamic interactions of Dnmt1

Over the past decade, a large variety of different interacting factors and post-translational modifications were reported for the eukaryotic DNA methyltransferase Dnmt1. The ever-increasing list impressively illustrates the complexity of Dnmt1 regulation. Furthermore, some of these interactions are highly dynamic over the cell cycle, illustrating an additional level of regulation. One example of cell cycle-dependent regulation is described in Chapter 1.2.3. During early S to mid S phase, Dnmt1 interacts with PCNA and is localized at replication foci. In addition, Dnmt1 is stabilized by Akt1-mediated phosphorylation (Esteve et al., 2011) to guarantee a necessary level of active Dnmt1. Whereas in late S phase, Dnmt1 is localized at late replication chromocenters and Uhrf1-dependent ubiquitination destabilizes Dnmt1 (Easwaran et al., 2004; Du et al., 2010). These examples illustrate the interplay of specific interactions recruiting Dnmt1 to specific foci and/or mediating post-translational modifications.
However, many of the known interactions and modifications were identified in different cells and species regardless of the cell cycle phase using varied and mostly qualitative methods. To gain further insights into the complexity of Dnmt1 regulation, it is essential to systematically and quantitatively analyse the different interactions dependent on the cell cycle phase.
We used a quantitative SILAC-based mass spectrometry approach to discover and characterize dynamic interactions of endogenous Dnmt1 in the same experiment. Consistent to *in vivo* data, we could show that Dnmt1 interacts with PCNA predominantly in early S phase and binds to core histones during late S phase of the cell cycle. However, we could not quantify the interactions such as with the chromatin remodeller Smarca5 or with transcriptional regulator such as Kap1. we initially found with convential mass spectrometry (Table 1). Further experiments with other synchronization techniques like Thymidin treatment and using different SILAC standards such as HEK293T cells and/or only unsynchcronized cells may be necessary to detect and quantifiy additional interactions.
The biggest challenge however will be the integration of all these data to comprehend Dnmt1 regulation in the context of living cells, taking into account the complexity and dynamics of its natural substrate, the chromatin, as well as the competition or cooperation with countless other cellular proteins and processes We are convinced that the combination of future quantitative interaction and *in vivo* studies will provide valuable insights into the epigenetic regulation of gene expression

5 Annex

5.1 References

Aapola, U., K. Shibuya, H.S. Scott, J. Ollila, M. Vihinen, M. Heino, A. Shintani, K. Kawasaki, S. Minoshima, K. Krohn, S.E. Antonarakis, N. Shimizu, J. Kudoh, and P. Peterson. 2000. Isolation and Initial Characterization of a Novel Zinc Finger Gene, DNMT3L, on 21q22.3, Related to the Cytosine-5- Methyltransferase 3 Gene Family. Genomics. 65:293-298.

Ababou, A., and J.E. Ladbury. 2007. Survey of the year 2005: literature on applications of isothermal titration calorimetry. J. Mol. Recognit. 20:4-14.

Abbady, A.-Q., C. Bronner, M.-A. Trotzier, R. Hopfner, K. Bathami, C.D. Muller, M. Jeanblanc, and M. Mousli. 2003. ICBP90 expression is downregulated in apoptosis-induced Jurkat cells. Ann. N. Y. Acad. Sci. 1010:300-303.

Abbott, D.W., V.S. Ivanova, X. Wang, W.M. Bonner, and J. Ausio. 2001. Characterization of the stability and folding of H2A.Z chromatin particles: implications for transcriptional activation. J. Biol. Chem. 276:41945-41949.

Achour, M., G. Fuhrmann, M. Alhosin, P. Ronde, T. Chataigneau, M. Mousli, V.B. Schini-Kerth, and C. Bronner. 2009. UHRF1 recruits the histone acetyltransferase Tip60 and controls its expression and activity. Biochem. Biophys. Res. Commun. 390:523-528.

Achour, M., X. Jacq, P. Ronde, M. Alhosin, C. Charlot, T. Chataigneau, M. Jeanblanc, M. Macaluso, A. Giordano, A.D. Hughes, V.B. Schini-Kerth, and C. Bronner. 2007. The interaction of the SRA domain of ICBP90 with a novel domain of DNMT1 is involved in the regulation of VEGF gene expression. Oncogene. 27:2187-2197.

Adamo, A., B. Sesé, S. Boue, J. Castano, I. Paramonov, M.J. Barrero, and J.C.I. Belmonte. 2011. LSD1 regulates the balance between self-renewal and differentiation in human embryonic stem cells. Nature Publishing Group. 13:652-660.

Ahn, S.-H., W.L. Cheung, J.-Y. Hsu, R.L. Diaz, M.M. Smith, and C.D. Allis. 2005. Sterile 20 kinase phosphorylates histone H2B at serine 10 during hydrogen peroxide-induced apoptosis in S. cerevisiae. Cell. 120:25-36.

Antequera, F., and A. Bird. 1993. Number of CpG islands and genes in human and mouse. Proc. Natl. Acad. Sci. U.S.A. 90:11995-11999.

Arima, Y., T. Hirota, C. Bronner, M. Mousli, T. Fujiwara, S.-I. Niwa, H. Ishikawa, and H. Saya. 2004. Down-regulation of nuclear protein ICBP90 by p53/p21Cip1/WAF1-dependent DNA-damage checkpoint signals contributes to cell cycle arrest at G1/S transition.

Genes Cells. 9:131-142.

Arita, K., M. Ariyoshi, H. Tochio, Y. Nakamura, and M. Shirakawa. 2008. Recognition of hemi-methylated DNA by the SRA protein UHRF1 by a base-flipping mechanism. Nature. 455:818-821.

Aslan, K., J.R. Lakowicz, and C.D. Geddes. 2005. Plasmon light scattering in biology and medicine: new sensing approaches, visions and perspectives. Curr Opin Chem Biol. 9:538-544.

Avvakumov, G.V., J.R. Walker, S. Xue, Y. Li, S. Duan, C. Bronner, C.H. Arrowsmith, and S. Dhe-Paganon. 2008. Structural basis for recognition of hemi-methylated DNA by the SRA domain of human UHRF1. Nature. 455:822-825.

Barski, A., S. Cuddapah, K. Cui, T.-Y. Roh, D.E. Schones, Z. Wang, G. Wei, I. Chepelev, and K. Zhao. 2007. High-resolution profiling of histone methylations in the human genome. Cell. 129:823-837.

Bartke, T., M. Vermeulen, B. Xhemalce, S.C. Robson, M. Mann, and T. Kouzarides. 2010. Nucleosome-interacting proteins regulated by DNA and histone methylation. Cell. 143:470-484.

Bedford, M.T., and S.G. Clarke. 2009. Protein Arginine Methylation in Mammals: Who, What, and Why. Molecular Cell. 33:1-13.

Berger, S.L. 2007. The complex language of chromatin regulation during transcription. Nature. 447:407-412.

Bernstein, B.E., A. Meissner, and E.S. Lander. 2007. The mammalian epigenome. Cell. 128:669-681.

Bernstein, B.E., T.S. Mikkelsen, X. Xie, M. Kamal, D.J. Huebert, J. Cuff, B. Fry, A. Meissner, M. Wernig, K. Plath, R. Jaenisch, A. Wagschal, R. Feil, S.L. Schreiber, and E.S. Lander. 2006. A bivalent chromatin structure marks key developmental genes in embryonic stem cells. Cell. 125:315-326.

Bestor, T.H. 1992. Activation of mammalian DNA methyltransferase by cleavage of a Zn binding regulatory domain. EMBO J. 11:2611-2617.

Bestor, T.H., and V.M. Ingram. 1983. Two DNA methyltransferases from murine erythroleukemia cells: purification, sequence specificity, and mode of interaction with DNA. Proc. Natl. Acad. Sci. U.S.A. 80:5559-5563.

Bilodeau, S., M.H. Kagey, G.M. Frampton, P.B. Rahl, and R.A. Young. 2009. SetDB1 con-

tributes to repression of genes encoding developmental regulators and maintenance of ES cell state. Genes & Development. 23:2484-2489.

Bird, A. 2002. DNA methylation patterns and epigenetic memory. Genes & Development. 16:6-21.

Bonapace, I.M. 2002. Np95 is regulated by E1A during mitotic reactivation of terminally differentiated cells and is essential for S phase entry. The Journal of Cell Biology. 157:909-914.

Bostick, M., J.K. Kim, P.O. Estève, A. Clark, S. Pradhan, and S.E. Jacobsen. 2007. UHRF1 Plays a Role in Maintaining DNA Methylation in Mammalian Cells. Science. 317:1760-1764.

Bourc'his, D., G.L. Xu, C.S. Lin, B. Bollman, and T.H. Bestor. 2001. Dnmt3L and the establishment of maternal genomic imprints. Science. 294:2536-2539.

Brero, A. 2005. Methyl CpG-binding proteins induce large-scale chromatin reorganization during terminal differentiation. J. Cell Biol. 169:733-743.

Bronner, C. 2011. Control of DNMT1 Abundance in Epigenetic Inheritance by Acetylation, Ubiquitylation, and the Histone Code. Science Signaling. 4:pe3-pe3.

Bronner, C., G. Fuhrmann, F.L. Chédin, M. Macaluso, and S. Dhe-Paganon. 2010. UHRF1 Links the Histone code and DNA Methylation to ensure Faithful Epigenetic Memory Inheritance. Genet Epigenet. 2009:29-36.

Bronner, C., M. Achour, Y. Arima, T. Chataigneau, H. Saya, and V.B. Schini-Kerth. 2007. The UHRF family: Oncogenes that are drugable targets for cancer therapy in the near future? Pharmacology & Therapeutics. 115:419-434.

Butler, J.S., J.H. Lee, and D.G. Skalnik. 2008. CFP1 interacts with DNMT1 independently of association with the Setd1 Histone H3K4 methyltransferase complexes. DNA Cell Biol. 27:533-543.

Cairns, B.R. 2009. The logic of chromatin architecture and remodelling at promoters. Nature. 461:193-198.

Campos, E.I., and D. Reinberg. 2009. Histones: annotating chromatin. Annu. Rev. Genet. 43:559-599.

Cao, R., L. Wang, H. Wang, L. Xia, H. Erdjument-Bromage, P. Tempst, R.S. Jones, and Y. Zhang. 2002. Role of histone H3 lysine 27 methylation in Polycomb-group silencing. Science. 298:1039-1043.

Cedar, H., and Y. Bergman. 2009. Linking DNA methylation and histone modification: patterns and paradigms. Nat Rev Genet. 10:295-304.

Chan, S.W.-L., I.R. Henderson, and S.E. Jacobsen. 2005. Gardening the genome: DNA methylation in Arabidopsis thaliana. Nat Rev Genet. 6:351-360.

Cheng, X., and R.M. Blumenthal. 2008. Mammalian DNA Methyltransferases: A Structural Perspective. Structure. 16:341-350.

Chien, C.T., P.L. Bartel, R. Sternglanz, and S. Fields. 1991. The two-hybrid system: a method to identify and clone genes for proteins that interact with a protein of interest. Proc. Natl. Acad. Sci. U.S.A. 88:9578-9582.

Chu, J., E.A. Loughlin, N.A. Gaur, S. Senbanerjee, V. Jacob, C. Monson, B. Kent, A. Oranu, Y. Ding, C. Ukomadu, and K.C. Sadler. 2011. UHRF1 phosphorylation by Cyclin A2/CDK2 is required for zebrafish embryogenesis. Mol Biol Cell.

Chuang, L.S., H.I. Ian, T.W. Koh, H.H. Ng, G. Xu, and B.F. Li. 1997. Human DNA-(cytosine-5) methyltransferase-PCNA complex as a target for p21WAF1. Science. 277:1996-2000.

Cimmino, L., O. Abdel-Wahab, R.L. Levine, and I. Aifantis. 2011. TET Family Proteins and Their Role in Stem Cell Differentiation and Transformation. Cell Stem Cell. 9:193-204.

Citterio, E., R. Papait, F. Nicassio, M. Vecchi, P. Gomiero, R. Mantovani, P.P. Di Fiore, and I.M. Bonapace. 2004. Np95 is a histone-binding protein endowed with ubiquitin ligase activity. Mol. Cell. Biol. 24:2526-2535.

Clapier, C.R., and B.R. Cairns. 2009. The biology of chromatin remodeling complexes. Annu. Rev. Biochem. 78:273-304.

Collins, N., R.A. Poot, I. Kukimoto, C. García-Jiménez, G. Dellaire, and P.D. Varga-Weisz. 2002. An ACF1-ISWI chromatin-remodeling complex is required for DNA replication through heterochromatin. Nat Genet. 32:627-632.

Cox, J., and M. Mann. 2008. MaxQuant enables high peptide identification rates, individualized p.p.b.-range mass accuracies and proteome-wide protein quantification. Nat Biotechnol. 26:1367-1372.

Cristea, I.M., R. Williams, B.T. Chait, and M.P. Rout. 2005. Fluorescent proteins as proteomic probes. Mol. Cell Proteomics. 4:1933-1941.

Crnogorac-Jurcevic, T., R. Gangeswaran, V. Bhakta, G. Capurso, S. Lattimore, M. Akada, M. Sunamura, W. Prime, F. Campbell, T.A. Brentnall, E. Costello, J. Neoptolemos, and N.R. Lemoine. 2005. Proteomic analysis of chronic pancreatitis and pancreatic ade-

nocarcinoma. Gastroenterology. 129:1454-1463.

Cuthbert, G.L., S. Daujat, A.W. Snowden, H. Erdjument-Bromage, T. Hagiwara, M. Yamada, R. Schneider, P.D. Gregory, P. Tempst, A.J. Bannister, and T. Kouzarides. 2004. Histone deimination antagonizes arginine methylation. Cell. 118:545-553.

Deaton, A.M., and A. Bird. 2011. CpG islands and the regulation of transcription. Genes & Development. 25:1010-1022.

Dehal, P., Y. Satou, R.K. Campbell, J. Chapman, B. Degnan, A. De Tomaso, B. Davidson, A. Di Gregorio, M. Gelpke, D.M. Goodstein, N. Harafuji, K.E.M. Hastings, I. Ho, K. Hotta, W. Huang, T. Kawashima, P. Lemaire, D. Martinez, I.A. Meinertzhagen, S. Necula, M. Nonaka, N. Putnam, S. Rash, H. Saiga, M. Satake, A. Terry, L. Yamada, H.-G. Wang, S. Awazu, K. Azumi, J. Boore, M. Branno, S. Chin-Bow, R. DeSantis, S. Doyle, P. Francino, D.N. Keys, S. Haga, H. Hayashi, K. Hino, K.S. Imai, K. Inaba, S. Kano, K. Kobayashi, M. Kobayashi, B.-I. Lee, K.W. Makabe, C. Manohar, G. Matassi, M. Medina, Y. Mochizuki, S. Mount, T. Morishita, S. Miura, A. Nakayama, S. Nishizaka, H. Nomoto, F. Ohta, K. Oishi, I. Rigoutsos, M. Sano, A. Sasaki, Y. Sasakura, E. Shoguchi, T. Shin-i, A. Spagnuolo, D. Stainier, M.M. Suzuki, O. Tassy, N. Takatori, M. Tokuoka, K. Yagi, F. Yoshizaki, S. Wada, C. Zhang, P.D. Hyatt, F. Larimer, C. Detter, N. Doggett, T. Glavina, T. Hawkins, P. Richardson, S. Lucas, Y. Kohara, M. Levine, N. Satoh, and D.S. Rokhsar. 2002. The draft genome of Ciona intestinalis: insights into chordate and vertebrate origins. Science. 298:2157-2167.

Delhommeau, F., S. Dupont, V. Della Valle, C. James, S. Trannoy, A. Massé, O. Kosmider, J.-P. Le Couedic, F. Robert, A. Alberdi, Y. Lécluse, I. Plo, F.J. Dreyfus, C. Marzac, N. Casadevall, C. Lacombe, S.P. Romana, P. Dessen, J. Soulier, F. Viguié, M. Fontenay, W. Vainchenker, and O.A. Bernard. 2009. Mutation in TET2 in myeloid cancers. N. Engl. J. Med. 360:2289-2301.

Dhalluin, C., J.E. Carlson, L. Zeng, C. He, A.K. Aggarwal, and M.M. Zhou. 1999. Structure and ligand of a histone acetyltransferase bromodomain. Nature. 399:491-496.

Di Croce, L., V.A. Raker, M. Corsaro, F. Fazi, M. Fanelli, M. Faretta, F. Fuks, F. Lo Coco, T. Kouzarides, C. Nervi, S. Minucci, and P.G. Pelicci. 2002. Methyltransferase recruitment and DNA hypermethylation of target promoters by an oncogenic transcription factor. Science. 295:1079-1082.

Doi, A., I.-H. Park, B. Wen, P. Murakami, M.J. Aryee, R. Irizarry, B. Herb, C. Ladd-Acosta, J. Rho, S. Loewer, J. Miller, T. Schlaeger, G.Q. Daley, and A.P. Feinberg. 2009. Differential methylation of tissue- and cancer-specific CpG island shores distinguishes human induced pluripotent stem cells, embryonic stem cells and fibroblasts. Nat Genet.

41:1350-1353.

Dong, K.B., I.A. Maksakova, F. Mohn, D. Leung, R. Appanah, S. Lee, H.W. Yang, L.L. Lam, D.L. Mager, D. Sch¨ubeler, M. Tachibana, Y. Shinkai, and M.C. Lorincz. 2008. DNA methylation in ES cells requires the lysine methyltransferase G9a but not its catalytic activity. EMBO J. 27:2691-2701.

Du, Z., J. Song, Y. Wang, Y. Zhao, K. Guda, S. Yang, H.Y. Kao, Y. Xu, J. Willis, S.D. Markowitz, D. Sedwick, R.M. Ewing, and Z. Wang. 2010. DNMT1 Stability Is Regulated by Proteins Coordinating Deubiquitination and Acetylation-Driven Ubiquitination. Science Signaling. 3:ra80-ra80.

Duan, Q., H. Chen, M. Costa, and W. Dai. 2008. Phosphorylation of H3S10 blocks the access of H3K9 by specific antibodies and histone methyltransferase. Implication in regulating chromatin dynamics and epigenetic inheritance during mitosis. J. Biol. Chem. 283:33585-33590.

Easwaran, H.P., L. Schermelleh, H. Leonhardt, and M.C. Cardoso. 2004. Replication-independent chromatin loading of Dnmt1 during G2 and M phases. EMBO Rep. 5:1181-1186.

Eden, S., T. Hashimshony, I. Keshet, H. Cedar, and A.W. Thorne. 1998. DNA methylation models histone acetylation. Nature. 394:842.

Espada, J., E. Ballestar, M.F. Fraga, A. Villar-Garea, A. Juarranz, J.C. Stockert, K.D. Robertson, F. Fuks, and M. Esteller. 2004. Human DNA methyltransferase 1 is required for maintenance of the histone H3 modification pattern. J. Biol. Chem. 279:37175-37184.

Esteller, M. 2007. Epigenetic gene silencing in cancer: the DNA hypermethylome. Hum. Mol. Genet. 16 Spec No 1:R50-9.

Esteller, M. 2008. Epigenetics in cancer. N. Engl. J. Med. 358:1148-1159.

Estève, P.O., H.G. Chin, A. Smallwood, G.R. Feehery, O. Gangisetty, A.R. Karpf, M.F. Carey, and S. Pradhan. 2006. Direct interaction between DNMT1 and G9a coordinates DNA and histone methylation during replication. Genes & Development. 20:3089-3103.

Estève, P.O., H.G. Chin, and S. Pradhan. 2005. Human maintenance DNA (cytosine-5)-methyltransferase and p53 modulate expression of p53-repressed promoters. Proc. Natl. Acad. Sci. U.S.A. 102:1000-1005.

Estève, P.O., H.G. Chin, J. Benner, G.R. Feehery, M. Samaranayake, G.A. Horwitz, S.E. Jacobsen, and S. Pradhan. 2009. Regulation of DNMT1 stability through SET7-mediated

lysine methylation in mammalian cells. Proc. Natl. Acad. Sci. U.S.A. 106:5076-5081.

Estève, P.O., Y. Chang, M. Samaranayake, A.K. Upadhyay, J.R. Horton, G.R. Feehery, X. Cheng, and S. Pradhan. 2011. A methylation and phosphorylation switch between an adjacent lysine and serine determines human DNMT1 stability. Nature Publishing Group.

Estève, P.-O., H.G. Chin, and S. Pradhan. 2007. Molecular mechanisms of transactivation and doxorubicin-mediated repression of survivin gene in cancer cells. J. Biol. Chem. 282:2615-2625.

Fan, J.Y., F. Gordon, K. Luger, J.C. Hansen, and D.J. Tremethick. 2002. The essential histone variant H2A.Z regulates the equilibrium between different chromatin conformational states. Nat. Struct. Biol. 9:172-176.

Fatemi, M., A. Hermann, H. Gowher, and A. Jeltsch. 2002. Dnmt3a and Dnmt1 functionally cooperate during de novo methylation of DNA. Eur J Biochem. 269:4981-4984.

Fatemi, M., A. Hermann, S. Pradhan, and A. Jeltsch. 2001. The activity of the murine DNA methyltransferase Dnmt1 is controlled by interaction of the catalytic domain with the N-terminal part of the enzyme leading to an allosteric activation of the enzyme after binding to methylated DNA1. Journal of Molecular Biology. 309:1189-1199.

Faust, C., K.A. Lawson, N.J. Schork, B. Thiel, and T. Magnuson. 1998. The Polycomb-group gene eed is required for normal morphogenetic movements during gastrulation in the mouse embryo. Development. 125:4495-4506.

Felle, M., S. Joppien, A. Németh, S. Diermeier, V. Thalhammer, T. Dobner, E. Kremmer, R. Kappler, and G. L¨angst. 2011. The USP7/Dnmt1 complex stimulates the DNA methylation activity of Dnmt1 and regulates the stability of UHRF1. Nucleic Acids Research. 39:8355-8365.

Fellinger, K., U. Rothbauer, M. Felle, G. Langst, and H. Leonhardt. 2009. Dimerization of DNA methyltransferase 1 is mediated by its regulatory domain. J. Cell. Biochem. 106:521-528.

Feng, S., S.J. Cokus, X. Zhang, P.-Y. Chen, M. Bostick, M.G. Goll, J. Hetzel, J. Jain, S.H. Strauss, M.E. Halpern, C. Ukomadu, K.C. Sadler, S. Pradhan, M. Pellegrini, and S.E. Jacobsen. 2010. Conservation and divergence of methylation patterning in plants and animals. Proceedings of the National Academy of Sciences. 107:8689-8694.

Fields, S., and O. Song. 1989. A novel genetic system to detect protein-protein interactions. Nature. 340:245-246.

Fischle, W., B.S. Tseng, H.L. Dormann, B.M. Ueberheide, B.A. Garcia, J. Shabanowitz, D.F. Hunt, H. Funabiki, and C.D. Allis. 2005. Regulation of HP1-chromatin binding by histone H3 methylation and phosphorylation. Nature. 438:1116-1122.

Francis, N.J., and R.E. Kingston. 2001. Mechanisms of transcriptional memory. Nat. Rev. Mol. Cell Biol. 2:409-421.

Frauer, C., A. Rottach, D. Meilinger, S. Bultmann, K. Fellinger, S. Hasen¨oder, M. Wang, W. Qin, J. S¨oding, F. Spada, and H. Leonhardt. 2011. Different binding properties and function of CXXC zinc finger domains in Dnmt1 and Tet1. PLoS ONE. 6:e16627.

Frauer, C., and H. Leonhardt. 2009. A versatile non-radioactive assay for DNA methyltransferase activity and DNA binding. Nucleic Acids Research. 37:e22-e22.

Free, A., R.I. Wakefield, B.O. Smith, D.T. Dryden, P.N. Barlow, and A.P. Bird. 2001. DNA recognition by the methyl-CpG binding domain of MeCP2. J. Biol. Chem. 276:3353-3360.

Fritsch, L., P. Robin, J.R.R. Mathieu, M. Souidi, H. Hinaux, C. Rougeulle, A. Harel-Bellan, M. Ameyar-Zazoua, and S. Ait-Si-Ali. 2010. A subset of the histone H3 lysine 9 methyltransferases Suv39h1, G9a, GLP, and SETDB1 participate in a multimeric complex. Mol. Cell. 37:46-56.

Fujimori, A., Y. Matsuda, Y. Takemoto, Y. Hashimoto, E. Kubo, R. Araki, R. Fukumura, K. Mita, K. Tatsumi, and M. Muto. 1998. Cloning and mapping of Np95 gene which encodes a novel nuclear protein associated with cell proliferation. Mamm. Genome. 9:1032-1035.

Fuks, F., P.J. Hurd, R. Deplus, and T. Kouzarides. 2003. The DNA methyltransferases associate with HP1 and the SUV39H1 histone methyltransferase. Nucleic Acids Research. 31:2305-2312.

Fuks, F., W.A. Burgers, A. Brehm, L. Hughes-Davies, and T. Kouzarides. 2000. DNA methyltransferase Dnmt1 associates with histone deacetylase activity. Nat Genet. 24:88-91.

Gavin, A.-C., M. Bösche, R. Krause, P. Grandi, M. Marzioch, A. Bauer, J. Schultz, J.M. Rick, A.-M. Michon, C.-M. Cruciat, M. Remor, C. H¨ofert, M. Schelder, M. Brajenovic, H. Ruffner, A. Merino, K. Klein, M. Hudak, D. Dickson, T. Rudi, V. Gnau, A. Bauch, S. Bastuck, B. Huhse, C. Leutwein, M.-A. Heurtier, R.R. Copley, A. Edelmann, E. Querfurth, V. Rybin, G. Drewes, M. Raida, T. Bouwmeester, P. Bork, B. Seraphin, B. Kuster, G. Neubauer, and G. Superti-Furga. 2002. Functional organization of the yeast proteome by systematic analysis of protein complexes. Nature. 415:141-147.

Geiger, T., J. Cox, P. Ostasiewicz, J.R. Wisniewski, and M. Mann. 2010. Super-SILAC mix for quantitative proteomics of human tumor tissue. Nat. Methods. 7:383-385.

Geiger, T., J.R. Wisniewski, J. Cox, S. Zanivan, M. Kruger, Y. Ishihama, and M. Mann. 2011. Use of stable isotope labeling by amino acids in cell culture as a spike-in standard in quantitative proteomics. Nat Protoc. 6:147-157.

Georgel, P.T., R.A. Horowitz-Scherer, N. Adkins, C.L. Woodcock, P.A. Wade, and J.C. Hansen. 2003. Chromatin compaction by human MeCP2. Assembly of novel secondary chromatin structures in the absence of DNA methylation. J. Biol. Chem. 278:32181-32188.

Gilbert, D.M., A. Neilson, H. Miyazawa, M.L. DePamphilis, and W.C. Burhans. 1995. Mimosine arrests DNA synthesis at replication forks by inhibiting deoxyribonucleotide metabolism. J. Biol. Chem. 270:9597-9606.

Glickman, J.F., J.G. Pavlovich, and N.O. Reich. 1997. Peptide mapping of the murine DNA methyltransferase reveals a major phosphorylation site and the start of translation. J. Biol. Chem. 272:17851-17857.

Goll, M.G., and T.H. Bestor. 2005. EUKARYOTIC CYTOSINE METHYLTRANSFERASES. Annu. Rev. Biochem. 74:481-514.

Goll, M.G., F. Kirpekar, K.A. Maggert, J.A. Yoder, C.-L. Hsieh, X. Zhang, K.G. Golic, S.E. Jacobsen, and T.H. Bestor. 2006. Methylation of tRNAAsp by the DNA methyltransferase homolog Dnmt2. Science. 311:395-398.

Goyal, R., P. Rathert, H. Laser, H. Gowher, and A. Jeltsch. 2007. Phosphorylation of serine-515 activates the Mammalian maintenance methyltransferase Dnmt1. Epigenetics. 2:155-160.

Guo, J.U., Y. Su, C. Zhong, G.-L. Ming, and H. Song. 2011. Hydroxylation of 5-methylcytosine by TET1 promotes active DNA demethylation in the adult brain. Cell. 145:423-434.

Hajkova, P., S. Erhardt, N. Lane, T. Haaf, O. El-Maarri, W. Reik, J. Walter, and M.A. Surani. 2002. Epigenetic reprogramming in mouse primordial germ cells. Mech. Dev. 117:15-23.

Hajkova, P., S.J. Jeffries, C. Lee, N. Miller, S.P. Jackson, and M.A. Surani. 2010. Genome-wide reprogramming in the mouse germ line entails the base excision repair pathway. Science. 329:78-82.

Hardeland, U., M. Bentele, J. Jiricny, and P. Sch¨ar. 2003. The versatile thymine DNA-

glycosylase: a comparative characterization of the human, Drosophila and fission yeast orthologs. Nucleic Acids Research. 31:2261-2271.

Hashimoto, H., J.R. Horton, X. Zhang, and X. Cheng. 2009. UHRF1, a modular multi-domain protein, regulates replication-coupled crosstalk between DNA methylation and histone modifications. Epigenetics. 4:8-14.

Hashimoto, H., J.R. Horton, X. Zhang, M. Bostick, S.E. Jacobsen, and X. Cheng. 2008. The SRA domain of UHRF1 flips 5-methylcytosine out of the DNA helix. Nature. 455:826-829.

Hassa, P.O., S.S. Haenni, M. Elser, and M.O. Hottiger. 2006. Nuclear ADP-ribosylation reactions in mammalian cells: where are we today and where are we going? Microbiol. Mol. Biol. Rev. 70:789-829.

Hata, K., M. Okano, H. Lei, and E. Li. 2002. Dnmt3L cooperates with the Dnmt3 family of de novo DNA methyltransferases to establish maternal imprints in mice. Development. 129:1983-1993.

He, Y.F., B.Z. Li, Z. Li, P. Liu, Y. Wang, Q. Tang, J. Ding, Y. Jia, Z. Chen, L. Li, Y. Sun, X. Li, Q. Dai, C.X. Song, K. Zhang, C. He, and G.L. Xu. 2011. Tet-Mediated Formation of 5-Carboxylcytosine and Its Excision by TDG in Mammalian DNA. Science. 333:1303-1307.

Hellman, A., and A. Chess. 2007. Gene body-specific methylation on the active X chromosome. Science. 315:1141-1143.

Hendrich, B., and S. Tweedie. 2003. The methyl-CpG binding domain and the evolving role of DNA methylation in animals. Trends Genet. 19:269-277.

Hermann, A., H. Gowher, and A. Jeltsch. 2004. Biochemistry and biology of mammalian DNA methyltransferases. Cell Mol Life Sci. 61:2571-2587.

Hervouet, E., L. Lalier, E. Debien, M. Cheray, A. Geairon, H. Rogniaux, D. Loussouarn, S.A. Martin, F.M. Vallette, and P.-F. Cartron. 2010. Disruption of Dnmt1/PCNA/UHRF1 Interactions Promotes Tumorigenesis from Human and Mice Glial Cells. PLoS ONE. 5:e11333.

Hiragami-Hamada, K., K. Shinmyozu, D. Hamada, Y. Tatsu, K. Uegaki, S. Fujiwara, and J.-I. Nakayama. 2011. N-terminal phosphorylation of HP1alpha promotes its chromatin binding. Mol. Cell. Biol. 31:1186-1200.

Ho, Y., A. Gruhler, A. Heilbut, G.D. Bader, L. Moore, S.-L. Adams, A. Millar, P. Taylor, K. Bennett, K. Boutilier, L. Yang, C. Wolting, I. Donaldson, S. Schandorff, J. Shewnarane, M. Vo, J. Taggart, M. Goudreault, B. Muskat, C. Alfarano, D. Dewar, Z. Lin, K. Michalickova, A.R.

Willems, H. Sassi, P.A. Nielsen, K.J. Rasmussen, J.R. Andersen, L.E. Johansen, L.H. Hansen, H. Jespersen, A. Podtelejnikov, E. Nielsen, J. Crawford, V. Poulsen, B.D. Sorensen, J. Matthiesen, R.C. Hendrickson, F. Gleeson, T. Pawson, M.F. Moran, D. Durocher, M. Mann, C.W.V. Hogue, D. Figeys, and M. Tyers. 2002. Systematic identification of protein complexes in Saccharomyces cerevisiae by mass spectrometry. Nature. 415:180-183.

Honeybee Genome Sequencing Consortium. 2006. Insights into social insects from the genome of the honeybee Apis mellifera. Nature. 443:931-949.

Hopfner, R., M. Mousli, J.M. Jeltsch, A. Voulgaris, Y. Lutz, C. Marin, J.P. Bellocq, P. Oudet, and C. Bronner. 2000. ICBP90, a novel human CCAAT binding protein, involved in the regulation of topoisomerase IIalpha expression. Cancer Res. 60:121-128.

Hopfner, R., M. Mousli, P. Oudet, and C. Bronner. 2002. Overexpression of ICBP90, a novel CCAAT-binding protein, overcomes cell contact inhibition by forcing topoisomerase II alpha expression. Anticancer Res. 22:3165-3170.

Horton, J.R., A.K. Upadhyay, H.H. Qi, X. Zhang, Y. Shi, and X. Cheng. 2010. Enzymatic and structural insights for substrate specificity of a family of jumonji histone lysine demethylases. Nature Publishing Group. 17:38-43.

Hsieh, C.L. 1999. In vivo activity of murine de novo methyltransferases, Dnmt3a and Dnmt3b. Mol. Cell. Biol. 19:8211-8218.

Hu, L., Z. Li, P. Wang, Y. Lin, and Y. Xu. 2011. Crystal structure of PHD domain of UHRF1 and insights into recognition of unmodified histone H3 arginine residue 2. Cell Res. 21:1374-1378.

Ikegami, K., M. Iwatani, M. Suzuki, M. Tachibana, Y. Shinkai, S. Tanaka, J.M. Greally, S. Yagi, N. Hattori, and K. Shiota. 2007. Genome-wide and locus-specific DNA hypomethylation in G9a deficient mouse embryonic stem cells. Genes Cells. 12:1-11.

Illingworth, R.S., and A.P. Bird. 2009. CpG islands–'a rough guide'. FEBS Lett. 583:1713-1720.

Irizarry, R.A., C. Ladd-Acosta, B. Wen, Z. Wu, C. Montano, P. Onyango, H. Cui, K. Gabo, M. Rongione, M. Webster, H. Ji, J.B. Potash, S. Sabunciyan, and A.P. Feinberg. 2009. The human colon cancer methylome shows similar hypo- and hypermethylation at conserved tissue-specific CpG island shores. Nat Genet. 41:178-186.

Ito, S., A.C. D'Alessio, O.V. Taranova, K. Hong, L.C. Sowers, and Y. Zhang. 2010. Role of Tet proteins in 5mC to 5hmC conversion, ES-cell self-renewal and inner cell mass specification. Nature. 466:1129-1133.

Ito, S., L. Shen, Q. Dai, S.C. Wu, L.B. Collins, J.A. Swenberg, C. He, and Y. Zhang. 2011. Tet proteins can convert 5-methylcytosine to 5-formylcytosine and 5-carboxylcytosine. Science. 333:1300-1303.

Iwata, A., Y. Nagashima, L. Matsumoto, T. Suzuki, T. Yamanaka, H. Date, K. Deoka, N. Nukina, and S. Tsuji. 2009. Intranuclear degradation of polyglutamine aggregates by the ubiquitin-proteasome system. J. Biol. Chem. 284:9796-9803.

Iyer, L.M., M. Tahiliani, A. Rao, and L. Aravind. 2009. Prediction of novel families of enzymes involved in oxidative and other complex modifications of bases in nucleic acids. Cell Cycle. 8:1698-1710. Jackson, D.A., and A. Pombo. 1998. Replicon clusters are stable units of chromosome structure: evidence that nuclear organization contributes to the efficient activation and propagation of S phase in human cells. J. Cell Biol. 140:1285-1295.

Jacobs, S.A., and S. Khorasanizadeh. 2002. Structure of HP1 chromodomain bound to a lysine 9-methylated histone H3 tail. Science. 295:2080-2083.

Jacobs, S.A., S.D. Taverna, Y. Zhang, S.D. Briggs, J. Li, J.C. Eissenberg, C.D. Allis, and S. Khorasanizadeh. 2001. Specificity of the HP1 chromo domain for the methylated N-terminus of histone H3. EMBO J. 20:5232-5241.

Jaenisch, R., and A. Bird. 2003. Epigenetic regulation of gene expression: how the genome integrates intrinsic and environmental signals. Nat Genet. 33 Suppl:245-254.

Jeanblanc, M., M. Mousli, R. Hopfner, K. Bathami, N. Martinet, A.-Q. Abbady, J.-C. Siffert, E. Mathieu, C.D. Muller, and C. Bronner. 2005. The retinoblastoma gene and its product are targeted by ICBP90: a key mechanism in the G1/S transition during the cell cycle. Oncogene. 24:7337-7345.

Jeddeloh, J.A., T.L. Stokes, and E.J. Richards. 1999. Maintenance of genomic methylation requires a SWI2/SNF2-like protein. Nat Genet. 22:94-97.

Jenkins, Y., V. Markovtsov, W. Lang, P. Sharma, D. Pearsall, J. Warner, C. Franci, B. Huang, J. Huang, G.C. Yam, J.P. Vistan, E. Pali, J. Vialard, M. Janicot, J.B. Lorens, D.G. Payan, and Y. Hitoshi. 2005. Critical role of the ubiquitin ligase activity of UHRF1, a nuclear RING finger protein, in tumor cell growth. Mol Biol Cell. 16:5621-5629.

Ji, H., L.I.R. Ehrlich, J. Seita, P. Murakami, A. Doi, P. Lindau, H. Lee, M.J. Aryee, R.A. Irizarry, K. Kim, D.J. Rossi, M.A. Inlay, T. Serwold, H. Karsunky, L. Ho, G.Q. Daley, I.L. Weissman, and A.P. Feinberg. 2010. Comprehensive methylome map of lineage commitment from haematopoietic progenitors. Nature. 467:338-342.

Johnsson, N., and A. Varshavsky. 1994. Split ubiquitin as a sensor of protein interactions in vivo. Proc. Natl. Acad. Sci. U.S.A. 91:10340-10344.

Kacem, S., and R. Feil. 2009. Chromatin mechanisms in genomic imprinting. Mamm. Genome. 20:544-556.

Kaneda, M., M. Okano, K. Hata, T. Sado, N. Tsujimoto, E. Li, and H. Sasaki. 2004. Essential role for de novo DNA methyltransferase Dnmt3a in paternal and maternal imprinting. Nature. 429:900-903.

Karagianni, P., L. Amazit, J. Qin, and J. Wong. 2008. ICBP90, a novel methyl K9 H3 binding protein linking protein ubiquitination with heterochromatin formation. Mol. Cell. Biol. 28:705-717.

Kaustov, L., H. Quyang, M. Amaya, A. Lemak, N. Nady, S. Duan, G. Wasney, Z. Li, M. Vedadi, M. Schapira, J. Min, and C.H. Arrowsmith. 2010. Recognition and specificity determinants of the human Cbx chromodomains. J. Biol. Chem.

Kim, D., B.J. Blus, V. Chandra, P. Huang, F. Rastinejad, and S. Khorasanizadeh. 2010. Corecognition of DNA and a methylated histone tail by the MSL3 chromodomain. Nature Publishing Group. 17:1027-1029. Kim, G.D., J. Ni, N. Kelesoglu, R.J. Roberts, and S. Pradhan. 2002. Co-operation and communication between the human maintenance and de novo DNA (cytosine-5) methyltransferases. EMBO J. 21:4183-4195.

Kim, J.K., P.O. Estève, S.E. Jacobsen, and S. Pradhan. 2009. UHRF1 binds G9a and participates in p21 transcriptional regulation in mammalian cells. Nucleic Acids Research. 37:493-505.

Kimura, H., and K. Shiota. 2003. Methyl-CpG-binding protein, MeCP2, is a target molecule for maintenance DNA methyltransferase, Dnmt1. J. Biol. Chem. 278:4806-4812.

Kinoshita, T., A. Miura, Y. Choi, Y. Kinoshita, X. Cao, S.E. Jacobsen, R.L. Fischer, and T. Kakutani. 2004. One-way control of FWA imprinting in Arabidopsis endosperm by DNA methylation. Science. 303:521-523.

Kiskinis, E., M. Hallberg, M. Christian, M. Olofsson, S.M. Dilworth, R. White, and M.G. Parker. 2007. RIP140 directs histone and DNA methylation to silence Ucp1 expression in white adipocytes. EMBO J. 26:4831-4840.

Klein, C.J., M.-V. Botuyan, Y. Wu, C.J. Ward, G.A. Nicholson, S. Hammans, K. Hojo, H. Yamanishi, A.R. Karpf, D.C. Wallace, M. Simon, C. Lander, L.A. Boardman, J.M. Cunningham, G.E. Smith, W.J. Litchy, B. Boes, E.J. Atkinson, S. Middha, P.J. B Dyck, J.E. Parisi,

G. Mer, D.I. Smith, and P.J. Dyck. 2011. Mutations in DNMT1 cause hereditary sensory neuropathy with dementia and hearing loss. Nat Genet. 43:595-600.

Klimasauskas, S., S. Kumar, R.J. Roberts, and X. Cheng. 1994. HhaI methyltransferase flips its target base out of the DNA helix. Cell. 76:357-369.

Klose, R.J., and A.P. Bird. 2006. Genomic DNA methylation: the mark and its mediators. Trends Biochem. Sci. 31:89-97.

Koh, K.P., A. Yabuuchi, S. Rao, Y. Huang, K. Cunniff, J. Nardone, A. Laiho, M. Tahiliani, C.A. Sommer, G. Mostoslavsky, R. Lahesmaa, S.H. Orkin, S.J. Rodig, G.Q. Daley, and A. Rao. 2011. Tet1 and Tet2 regulate 5-hydroxymethylcytosine production and cell lineage specification in mouse embryonic stem cells. Cell Stem Cell. 8:200-213.

Konstandin, N., S. Bultmann, A. Szwagierczak, A. Dufour, B. Ksienzyk, F. Schneider, T. Herold, M. Mulaw, P.M. Kakadia, S. Schneider, K. Spiekermann, H. Leonhardt, and S.K. Bohlander. 2011. Genomic 5-hydroxymethylcytosine levels correlate with TET2 mutations and a distinct global gene expression pattern in secondary acute myeloid leukemia. Leukemia. 25:1649-1652.

Korber, P., and P.B. Becker. 2010. Nucleosome dynamics and epigenetic stability. Essays in Biochemistry. 48:63-74.

Kouzarides, T. 2007. Chromatin modifications and their function. Cell. 128:693-705.

Kriaucionis, S., and N. Heintz. 2009. The nuclear DNA base 5-hydroxymethylcytosine is present in Purkinje neurons and the brain. Science. 324:929-930.

Krishnamoorthy, T., X. Chen, J. Govin, W.L. Cheung, J. Dorsey, K. Schindler, E. Winter, C.D. Allis, V. Guacci, S. Khochbin, M.T. Fuller, and S.L. Berger. 2006. Phosphorylation of histone H4 Ser1 regulates sporulation in yeast and is conserved in fly and mouse spermatogenesis. Genes & Development. 20:2580-2592.

Krude, T. 1999. Mimosine arrests proliferating human cells before onset of DNA replication in a dose-dependent manner. Exp. Cell Res. 247:148-159.

Kunert, N., J. Marhold, J. Stanke, D. Stach, and F. Lyko. 2003. A Dnmt2-like protein mediates DNA methylation in Drosophila. Development. 130:5083-5090.

Lalande, M. 1990. A reversible arrest point in the late G1 phase of the mammalian cell cycle. Exp. Cell Res. 186:332-339.

Lan, F., R.E. Collins, R. De Cegli, R. Alpatov, J.R. Horton, X. Shi, O. Gozani, X. Cheng, and Y. Shi. 2007. Recognition of unmethylated histone H3 lysine 4 links BHC80 to LSD1-

mediated gene repression. Nature. 448:718-722.

Langemeijer, S.M.C., R.P. Kuiper, M. Berends, R. Knops, M.G. Aslanyan, M. Massop, E. Stevens-Linders, P. van Hoogen, A.G. van Kessel, R.A.P. Raymakers, E.J. Kamping, G.E. Verhoef, E. Verburgh, A. Hagemeijer, P. Vandenberghe, T. de Witte, B.A. van der Reijden, and J.H. Jansen. 2009. Acquired mutations in TET2 are common in myelodysplastic syndromes. Nat Genet. 41:838-842.

Lao, V.V., A. Darwanto, and L.C. Sowers. 2010. Impact of base analogues within a CpG dinucleotide on the binding of DNA by the methyl-binding domain of MeCP2 and methylation by DNMT1. Biochemistry. 49:10228-10236.

Laurent, L., E. Wong, G. Li, T. Huynh, A. Tsirigos, C.T. Ong, H.M. Low, K.W. Kin Sung, I. Rigoutsos, J. Loring, and C.-L. Wei. 2010. Dynamic changes in the human methylome during differentiation. Genome Res. 20:320-331.

Lavoie, G., P.O. Estève, N. Bibens-Laulan, S. Predhan, and Y. St-Pierre. 2011. PKC isoforms interact with and phosphorylate DNMT1. BMC Biol. 9:31.

Lee, B., and M.T. Muller. 2009. SUMOylation enhances DNA methyltransferase 1 activity. Biochem J. 421:449-461.

Lee, C.F., D.S. Ou, S.B. Lee, L.H. Chang, R.K. Lin, Y.S. Li, A.K. Upadhyay, X. Cheng, Y.C. Wang, H.S. Hsu, M. Hsiao, C.W. Wu, and L.J. Juan. 2010. hNaa10p contributes to tumorigenesis by facilitating DNMT1-mediated tumor suppressor gene silencing. J Clin Invest. 120:2920-2930.

Lee, J., K. Inoue, R. Ono, N. Ogonuki, T. Kohda, T. Kaneko-Ishino, A. Ogura, and F. Ishino. 2002. Erasing genomic imprinting memory in mouse clone embryos produced from day 11.5 primordial germ cells. Development. 129:1807-1817.

Lehnertz, B., Y. Ueda, A.A. Derijck, U. Braunschweig, L. Perez-Burgos, S. Kubicek, T. Chen, E. Li, T. Jenuwein, and A.H. Peters. 2003. Suv39h-mediated histone H3 lysine 9 methylation directs DNA methylation to major satellite repeats at pericentric heterochromatin. Curr. Biol. 13:1192-1200.

Lei, H., S.P. Oh, M. Okano, R. Jüttermann, K.A. Goss, R. Jaenisch, and E. Li. 1996. De novo DNA cytosine methyltransferase activities in mouse embryonic stem cells. Development. 122:3195-3205.

Leonhardt, H., A.W. Page, H.U. Weier, and T.H. Bestor. 1992. A targeting sequence directs DNA methyltransferase to sites of DNA replication in mammalian nuclei. Cell. 71:865-873.

Letunic, I., and P. Bork. 2007. Interactive Tree Of Life (iTOL): an online tool for phylogenetic tree display and annotation. Bioinformatics. 23:127-128.

Letunic, I., and P. Bork. 2011. Interactive Tree Of Life v2: online annotation and display of phylogenetic trees made easy. Nucleic Acids Research. 39:W475-8.

Li, B., M. Carey, and J.L. Workman. 2007. The role of chromatin during transcription. Cell. 128:707-719. Li, H., S. Ilin, W. Wang, E.M. Duncan, J. Wysocka, C.D. Allis, and D.J. Patel. 2006. Molecular basis for site-specific read-out of histone H3K4me3 by the BPTF PHD finger of NURF. Nature. 442:91-95.

Li, Y., T. Mori, H. Hata, Y. Homma, and H. Kochi. 2004. NIRF induces G1 arrest and associates with Cdk2. Biochemical and Biophysical Research Communications. 319:464-468.

Lienert, F., C. Wirbelauer, I. Som, A. Dean, F. Mohn, and D. Sch¨ubeler. 2011. Identification of genetic elements that autonomously determine DNA methylation states. Nat Genet. 43:1091-1097.

Lindroth, A.M., X. Cao, J.P. Jackson, D. Zilberman, C.M. McCallum, S. Henikoff, and S.E. Jacobsen. 2001. Requirement of CHROMOMETHYLASE3 for maintenance of CpXpG methylation. Science. 292:2077-2080.

Lister, R., M. Pelizzola, R.H. Dowen, R.D. Hawkins, G. Hon, J. Tonti-Filippini, J.R. Nery, L. Lee, Z. Ye, Q.-M. Ngo, L. Edsall, J. Antosiewicz-Bourget, R. Stewart, V. Ruotti, A.H. Millar, J.A. Thomson, B. Ren, and J.R. Ecker. 2009. Human DNA methylomes at base resolution show widespread epigenomic differences. Nature. 462:315-322.

Luger, K., A.W. Mader, R.K. Richmond, D.F. Sargent, and T.J. Richmond. 1997. Crystal structure of the nucleosome core particle at 2.8 A resolution. Nature. 389:251-260. Luger, K., and J.C. Hansen. 2005. Nucleosome and chromatin fiber dynamics. Curr. Opin. Struct. Biol. 15:188-196.

Lyko, F., B.H. Ramsahoye, and R. Jaenisch. 2000. DNA methylation in Drosophila melanogaster. Nature. 408:538-540.

Macdonald, N., J.P.I. Welburn, M.E.M. Noble, A. Nguyen, M.B. Yaffe, D. Clynes, J.G. Moggs, G. Orphanides, S. Thomson, J.W. Edmunds, A.L. Clayton, J.A. Endicott, and L.C. Mahadevan. 2005. Molecular basis for the recognition of phosphorylated and phosphoacetylated histone h3 by 14-3-3. Molecular Cell. 20:199-211.

Maison, C., and G. Almouzni. 2004. HP1 and the dynamics of heterochromatin maintenance. Nat. Rev. Mol. Cell Biol. 5:296-304.

Malik, S., and R.G. Roeder. 2005. Dynamic regulation of pol II transcription by the mammalian Mediator complex. Trends Biochem. Sci. 30:256-263.

Margot, J.B., A.E. Ehrenhofer-Murray, and H. Leonhardt. 2003. Interactions within the mammalian DNA methyltransferase family. BMC Mol Biol. 4:7.

Margot, J.B., A.M. Aguirre-Arteta, B.V. Di Giacco, S. Pradhan, R.J. Roberts, M.C. Cardoso, and H. Leonhardt. 2000. Structure and function of the mouse DNA methyltransferase gene: Dnmt1 shows a tripartite structure. J Mol Biol. 297:293-300.

Mayer, W., A. Niveleau, J. Walter, R. Fundele, and T. Haaf. 2000. Demethylation of the zygotic paternal genome. Nature. 403:501-502.

Meilinger, D., K. Fellinger, S. Bultmann, U. Rothbauer, I.M. Bonapace, W.E. Klinkert, F. Spada, and H. Leonhardt. 2009. Np95 interacts with de novo DNA methyltransferases, Dnmt3a and Dnmt3b, and mediates epigenetic silencing of the viral CMV promoter in embryonic stem cells. EMBO Rep. 10:1259-1264.

Meissner, A. 2011. Guiding DNA Methylation. Cell Stem Cell. 9:388-390.

Meissner, A., T.S. Mikkelsen, H. Gu, M. Wernig, J. Hanna, A. Sivachenko, X. Zhang, B.E. Bernstein, C. Nusbaum, D.B. Jaffe, A. Gnirke, R. Jaenisch, and E.S. Lander. 2008. Genome-scale DNA methylation maps of pluripotent and differentiated cells. Nature. 454:766-770.

Mistry, H., L. Tamblyn, H. Butt, D. Sisgoreo, A. Gracias, M. Larin, K. Gopalakrishnan, M.P. Hande, and J.P. McPherson. 2010. UHRF1 is a genome caretaker that facilitates the DNA damage response to gamma-irradiation. Genome Integr. 1:7.

Miura, M., H. Watanabe, T. Sasaki, K. Tatsumi, and M. Muto. 2001. Dynamic changes in subnuclear NP95 location during the cell cycle and its spatial relationship with DNA replication foci. Exp. Cell Res. 263:202-208.

Mohan, K.N., F. Ding, and J.R. Chaillet. 2011. Distinct roles of DMAP1 in mouse development. Mol. Cell. Biol. 31:1861-1869.

Mori, T., D.D. Ikeda, T. Fukushima, S. Takenoshita, and H. Kochi. 2011. NIRF constitutes a nodal point in the cell cycle network and is a candidate tumor suppressor. Cell Cycle. 10:3284-3299.

Mori, T., Y. Li, H. Hata, K. Ono, and H. Kochi. 2002. NIRF, a novel RING finger protein, is involved in cell-cycle regulation. Biochemical and Biophysical Research Communications. 296:530-536.

Mortusewicz, O., L. Schermelleh, J. Walter, M.C. Cardoso, and H. Leonhardt. 2005. Recruitment of DNA methyltransferase I to DNA repair sites. Proc. Natl. Acad. Sci. U.S.A. 102:8905-8909.

Mosca, P.J., P.A. Dijkwel, and J.L. Hamlin. 1992. The plant amino acid mimosine may inhibit initiation at origins of replication in Chinese hamster cells. Molecular and Cellular Biology. 12:4375-4383.

Mousli, M., R. Hopfner, A.-Q. Abbady, D. Monté, M. Jeanblanc, P. Oudet, B. Louis, and C. Bronner. 2003. ICBP90 belongs to a new family of proteins with an expression that is deregulated in cancer cells. Br. J. Cancer. 89:120-127.

Muromoto, R., K. Sugiyama, A. Takachi, S. Imoto, N. Sato, T. Yamamoto, K. Oritani, K. Shimoda, and T. Matsuda. 2004. Physical and functional interactions between Daxx and DNA methyltransferase 1-associated protein, DMAP1. J Immunol. 172:2985-2993.

Muto, M., M. Utsuyama, T. Horiguchi, E. Kubo, T. Sado, and K. Hirokawa. 1995. The characterization of the monoclonal antibody Th-10a, specific for a nuclear protein appearing in the S phase of the cell cycle in normal thymocytes and its unregulated expression in lymphoma cell lines. Cell Prolif. 28:645-657.

Muto, M., Y. Kanari, E. Kubo, T. Takabe, T. Kurihara, A. Fujimori, and K. Tatsumi. 2002. Targeted disruption of Np95 gene renders murine embryonic stem cells hypersensitive to DNA damaging agents and DNA replication blocks. J. Biol. Chem. 277:34549-34555.

Myant, K., and I. Stancheva. 2008. LSH cooperates with DNA methyltransferases to repress transcription. Mol. Cell. Biol. 28:215-226.

Nady, N., A. Lemak, J.R. Walker, G.V. Avvakumov, M.S. Kareta, M. Achour, S. Xue, S. Duan, A. Allali-Hassani, X. Zuo, Y.-X. Wang, C. Bronner, F. Chédin, C.H. Arrowsmith, and S. Dhe-Paganon. 2011. Recognition of multivalent histone states associated with heterochromatin by UHRF1 protein. Journal of Biological Chemistry. 286:24300-24311.

Nakanishi, S., J.S. Lee, K.E. Gardner, J.M. Gardner, Y.H. Takahashi, M.B. Chandrasekharan, Z.W. Sun, M.A. Osley, B.D. Strahl, S.L. Jaspersen, and A. Shilatifard. 2009. Histone H2BK123 monoubiquitination is the critical determinant for H3K4 and H3K79 trimethylation by COMPASS and Dot1. J. Cell Biol. 186:371-377.

Nan, X., H.H. Ng, C.A. Johnson, C.D. Laherty, B.M. Turner, R.N. Eisenman, and A. Bird. 1998. Transcriptional repression by the methyl-CpG-binding protein MeCP2 involves a histone deacetylase complex. Nature. 393:386-389.

Nan, X., R.R. Meehan, and A. Bird. 1993. Dissection of the methyl-CpG binding domain

from the chromosomal protein MeCP2. Nucleic Acids Research. 21:4886-4892.

Nathan, D., D.E. Sterner, and S.L. Berger. 2003. Histone modifications: Now summoning sumoylation. Proc. Natl. Acad. Sci. U.S.A. 100:13118-13120.

Naumann, K., A. Fischer, I. Hofmann, V. Krauss, S. Phalke, K. Irmler, G. Hause, A.-C. Aurich, R. Dorn, T. Jenuwein, and G. Reuter. 2005. Pivotal role of AtSUVH2 in heterochromatic histone methylation and gene silencing in Arabidopsis. EMBO J. 24:1418-1429.

Nelson, C.J., H. Santos-Rosa, and T. Kouzarides. 2006. Proline isomerization of histone H3 regulates lysine methylation and gene expression. Cell. 126:905-916.

Nowak, S.J., and V.G. Corces. 2004. Phosphorylation of histone H3: a balancing act between chromosome condensation and transcriptional activation. Trends Genet. 20:214-220.

O'Carroll, D., S. Erhardt, M. Pagani, S.C. Barton, M.A. Surani, and T. Jenuwein. 2001. The polycomb-group gene Ezh2 is required for early mouse development. Molecular and Cellular Biology. 21:4330-4336.

O'Gara, M., R.J. Roberts, and X. Cheng. 1996. A structural basis for the preferential binding of hemimethylated DNA by HhaI DNA methyltransferase. J Mol Biol. 263:597-606.

Ohsawa, K., Y. Imai, D. Ito, and S. Kohsaka. 1996. Molecular cloning and characterization of annexin V-binding proteins with highly hydrophilic peptide structure.
J Neurochem. 67:89-97.

Okano, M., D.W. Bell, D.A. Haber, and E. Li. 1999. DNA methyltransferases Dnmt3a and Dnmt3b are essential for de novo methylation and mammalian development. Cell. 99:247-257.

Okano, M., S. Xie, and E. Li. 1998. Cloning and characterization of a family of novel mammalian DNA (cytosine-5) methyltransferases. Nat Genet. 19:219-220.

Okitsu, C.Y., and C.-L. Hsieh. 2007. DNA methylation dictates histone H3K4 methylation. Molecular and Cellular Biology. 27:2746-2757.

Ong, S.-E., B. Blagoev, I. Kratchmarova, D.B. Kristensen, H. Steen, A. Pandey, and M. Mann. 2002. Stable isotope labeling by amino acids in cell culture, SILAC, as a simple and accurate approach to expression proteomics. Mol. Cell Proteomics. 1:376-386.

Ooi, S.K., C. Qiu, E. Bernstein, K. Li, D. Jia, Z. Yang, H. Erdjument-Bromage, P. Tempst, S.P. Lin, C.D. Allis, X. Cheng, and T.H. Bestor. 2007. DNMT3L connects unmethylated lysine 4

of histone H3 to de novo methylation of DNA. Nature. 448:714-717.

Oswald, J., S. Engemann, N. Lane, W. Mayer, A. Olek, R. Fundele, W. Dean, W. Reik, and J. Walter. 2000. Active demethylation of the paternal genome in the mouse zygote. Curr. Biol. 10:475-478.

Otani, J., T. Nankumo, K. Arita, S. Inamoto, M. Ariyoshi, and M. Shirakawa. 2009. Structural basis for recognition of H3K4 methylation status by the DNA methyltransferase 3A ATRX-DNMT3-DNMT3L domain. EMBO Rep. 10:1235-1241.

Papait, R., C. Pistore, D. Negri, D. Pecoraro, L. Cantarini, and I.M. Bonapace. 2007. Np95 is implicated in pericentromeric heterochromatin replication and in major satellite silencing. Mol Biol Cell. 18:1098-1106.

Pasini, D., A.P. Bracken, M.R. Jensen, E. Lazzerini Denchi, and K. Helin. 2004. Suz12 is essential for mouse development and for EZH2 histone methyltransferase activity. EMBO J. 23:4061-4071.

Peters, A.H., S. Kubicek, K. Mechtler, R.J. O'Sullivan, A.A. Derijck, L. Perez-Burgos, A. Kohlmaier, S. Opravil, M. Tachibana, Y. Shinkai, J.H. Martens, and T. Jenuwein. 2003. Partitioning and plasticity of repressive histone methylation states in mammalian chromatin. Mol. Cell. 12:1577-1589.

Pichler, G., P. Wolf, C.S. Schmidt, D. Meilinger, K. Schneider, C. Frauer, K. Fellinger, A. Rottach, and H. Leonhardt. 2011. Cooperative DNA and histone binding by Uhrf2 links the two major repressive epigenetic pathways. J. Cell. Biochem.

Portela, A., and M. Esteller. 2010. Epigenetic modifications and human disease. Nat Biotechnol. 28:1057-1068.

Pradhan, S., A. Bacolla, R.D. Wells, and R.J. Roberts. 1999. Recombinant human DNA (cytosine-5) methyltransferase. I. Expression, purification, and comparison of de novo and maintenance methylation. J. Biol. Chem. 274:33002-33010.

Pradhan, S., and G.D. Kim. 2002. The retinoblastoma gene product interacts with maintenance human DNA (cytosine-5) methyltransferase and modulates its activity. EMBO J. 21:779-788.

Pradhan, S., and R.J. Roberts. 2000. Hybrid mouse-prokaryotic DNA (cytosine-5) methyltransferases retain the specificity of the parental C-terminal domain. EMBO J. 19:2103-2114.

Qian, C., S. Li, J. Jakoncic, L. Zeng, M.J. Walsh, and M.M. Zhou. 2008. Structure and

hemimethylated CpG binding of the SRA domain from human UHRF1. J. Biol. Chem. 283:34490-34494.

Qin, W., H. Leonhardt, and F. Spada. 2011a. Usp7 and Uhrf1 control ubiquitination and stability of the maintenance DNA methyltransferase Dnmt1. J. Cell. Biochem. 112:439-444.

Qin, W., H. Leonhardt, and G. Pichler. 2011b. Regulation of DNA methyltransferase 1 by interactions and modifications. Nucleus. 2:392-402.

Quenneville, S., G. Verde, A. Corsinotti, A. Kapopoulou, J. Jakobsson, S. Offner, I. Baglivo, P.V. Pedone, G. Grimaldi, A. Riccio, and D. Trono. 2011. In Embryonic Stem Cells, ZFP57/KAP1 Recognize a Methylated Hexanucleotide to Affect Chromatin and DNA Methylation of Imprinting Control Regions. Mol. Cell. 44:361-372.

Radman-Livaja, M., and O.J. Rando. 2010. Nucleosome positioning: how is it established, and why does it matter? Dev. Biol. 339:258-266.

Rai, K., L.D. Nadauld, S. Chidester, E.J. Manos, S.R. James, A.R. Karpf, B.R. Cairns, and D.A. Jones. 2006. Zebra fish Dnmt1 and Suv39h1 regulate organ-specific terminal differentiation during development. Molecular and Cellular Biology. 26:7077-7085.

Rajakumara, E., Z. Wang, H. Ma, L. Hu, H. Chen, Y. Lin, R. Guo, F. Wu, H. Li, F. Lan, Y.G. Shi, Y. Xu, D.J. Patel, and Y. Shi. 2011. PHD finger recognition of unmodified histone H3R2 links UHRF1 to regulation of euchromatic gene expression. Mol. Cell. 43:275-284.

Reale, A., G.D. Matteis, G. Galleazzi, M. Zampieri, and P. Caiafa. 2005. Modulation of DNMT1 activity by ADP-ribose polymers. Oncogene. 24:13-19.

Reik, W. 2007. Stability and flexibility of epigenetic gene regulation in mammalian development. Nature. 447:425-432.

Reik, W., and A. Lewis. 2005. Co-evolution of X-chromosome inactivation and imprinting in mammals. Nat Rev Genet. 6:403-410.

Rhee, I., K.E. Bachman, B.H. Park, K.W. Jair, R.W. Yen, K.E. Schuebel, H. Cui, A.P. Feinberg, C. Lengauer, K.W. Kinzler, S.B. Baylin, and B. Vogelstein. 2002. DNMT1 and DNMT3b cooperate to silence genes in human cancer cells. Nature. 416:552-556.

Rideout, W.M., K. Eggan, and R. Jaenisch. 2001. Nuclear cloning and epigenetic reprogramming of the genome. Science. 293:1093-1098.

Robertson, A.K., T.M. Geiman, U.T. Sankpal, G.L. Hager, and K.D. Robertson. 2004. Effects of chromatin structure on the enzymatic and DNA binding functions of DNA

methyltransferases DNMT1 and Dnmt3a in vitro. Biochem. Biophys. Res. Commun. 322:110-118.

Robertson, K.D., S. Ait-Si-Ali, T. Yokochi, P.A. Wade, P.L. Jones, and A.P. Wolffe. 2000. DNMT1 forms a complex with Rb, E2F1 and HDAC1 and represses transcription from E2F-responsive promoters. Nat Genet. 25:338-342.

Rothbauer, U., K. Zolghadr, S. Muyldermans, A. Schepers, M.C. Cardoso, and H. Leonhardt. 2008. A versatile nanotrap for biochemical and functional studies with fluorescent fusion proteins. Mol. Cell Proteomics. 7:282-289.

Rothbauer, U., K. Zolghadr, S. Tillib, D. Nowak, L. Schermelleh, A. Gahl, N. Backmann, K. Conrath, S. Muyldermans, M.C. Cardoso, and H. Leonhardt. 2006. Targeting and tracing antigens in live cells with fluorescent nanobodies. Nat. Methods. 3:887-889.

Rottach, A., E. Kremmer, D. Nowak, H. Leonhardt, and M.C. Cardoso. 2008. Generation and characterization of a rat monoclonal antibody specific for multiple red fluorescent proteins. Hybridoma. 27:337-343.

Rottach, A., H. Leonhardt, and F. Spada. 2009. DNA methylation-mediated epigenetic control. J. Cell. Biochem. 108:43-51.

Rountree, M.R., K.E. Bachman, and S.B. Baylin. 2000. DNMT1 binds HDAC2 and a new co-repressor, DMAP1, to form a complex at replication foci. Nat Genet. 25:269-277.

Ruthenburg, A.J., H. Li, D.J. Patel, and C.D. Allis. 2007. Multivalent engagement of chromatin modifications by linked binding modules. Nat. Rev. Mol. Cell Biol. 8:983-994.

Ruthenburg, A.J., W. Wang, D.M. Graybosch, H. Li, C.D. Allis, D.J. Patel, and G.L. Verdine. 2006. Histone H3 recognition and presentation by the WDR5 module of the MLL1 complex. Nature Publishing Group. 13:704-712.

Ruzov, A., B. Shorning, O. Mortusewicz, D.S. Dunican, H. Leonhardt, and R.R. Meehan. 2009. MBD4 and MLH1 are required for apoptotic induction in xDNMT1-depleted embryos. Development. 136:2277-2286. Sadler, K.C., K.N. Krahn, N.A. Gaur, and C. Ukomadu. 2007. Liver growth in the embryo and during liver regeneration in zebrafish requires the cell cycle regulator, uhrf1. Proc. Natl. Acad. Sci. U.S.A. 104:1570-1575.

Santos-Rosa, H., A. Kirmizis, C. Nelson, T. Bartke, N. Saksouk, J. Cote, and T. Kouzarides. 2009. Histone H3 tail clipping regulates gene expression. Nature Publishing Group. 16:17-22.

Schermelleh, L., A. Haemmer, F. Spada, N. Rosing, D. Meilinger, U. Rothbauer, M.C.

Cardoso, and H. Leonhardt. 2007. Dynamics of Dnmt1 interaction with the replication machinery and its role in postreplicative maintenance of DNA methylation. Nucleic Acids Research. 35:4301-4312.

Schones, D.E., K. Cui, S. Cuddapah, T.-Y. Roh, A. Barski, Z. Wang, G. Wei, and K. Zhao. 2008. Dynamic regulation of nucleosome positioning in the human genome. Cell. 132:887-898.

Sharif, J., M. Muto, S. Takebayashi, I. Suetake, A. Iwamatsu, T.A. Endo, J. Shinga, Y. Mizutani-Koseki, T. Toyoda, K. Okamura, S. Tajima, K. Mitsuya, M. Okano, and H. Koseki. 2007. The SRA protein Np95 mediates epigenetic inheritance by recruiting Dnmt1 to methylated DNA. Nature. 450:908-912.

Shilatifard, A. 2006. Chromatin modifications by methylation and ubiquitination: implications in the regulation of gene expression. Annu. Rev. Biochem. 75:243-269.

Smith, G.P. 1985. Filamentous fusion phage: novel expression vectors that display cloned antigens on the virion surface. Science. 228:1315-1317.

So, A.Y., J.W. Jung, S. Lee, H.S. Kim, and K.S. Kang. 2011. DNA methyltransferase controls stem cell aging by regulating BMI1 and EZH2 through microRNAs. PLoS ONE. 6:e19503.

Song, C.-X., M. Yu, Q. Dai, and C. He. 2011a. Detection of 5-hydroxymethylcytosine in a combined glycosylation restriction analysis (CGRA) using restriction enzyme Taq( )I. Bioorg. Med. Chem. Lett. 21:5075-5077.

Song, J., O. Rechkoblit, T.H. Bestor, and D.J. Patel. 2011b. Structure of DNMT1-DNA complex reveals a role for autoinhibition in maintenance DNA methylation. Science. 331:1036-1040.

Spada, F., A. Haemmer, D. Kuch, U. Rothbauer, L. Schermelleh, E. Kremmer, T. Carell, G. Langst, and H. Leonhardt. 2007. DNMT1 but not its interaction with the replication machinery is required for maintenance of DNA methylation in human cells. J. Cell Biol. 176:565-571.

Sterner, D.E., and S.L. Berger. 2000. Acetylation of histones and transcription-related factors. Microbiol. Mol. Biol. Rev. 64:435-459.

Strahl, B.D., and C.D. Allis. 2000. The language of covalent histone modifications. Nature. 403:41-45. Straussman, R., D. Nejman, D. Roberts, I. Steinfeld, B. Blum, N. Benvenisty, I. Simon, Z. Yakhini, and H. Cedar. 2009. Developmental programming of CpG island methylation profiles in the human genome. Nature Publishing Group. 16:564-571.

Stucki, M., J.A. Clapperton, D. Mohammad, M.B. Yaffe, S.J. Smerdon, and S.P. Jackson. 2005. MDC1 directly binds phosphorylated histone H2AX to regulate cellular responses to DNA double-strand breaks. Cell. 123:1213-1226.

Suetake, I., F. Shinozaki, J. Miyagawa, H. Takeshima, and S. Tajima. 2004. DNMT3L stimulates the DNA methylation activity of Dnmt3a and Dnmt3b through a direct interaction. J. Biol. Chem. 279:27816-27823.

Sugiyama, Y., N. Hatano, N. Sueyoshi, I. Suetake, S. Tajima, E. Kinoshita, E. Kinoshita-Kikuta, T. Koike, and I. Kameshita. 2010. The DNA-binding activity of mouse DNA methyltransferase 1 is regulated by phosphorylation with casein kinase 1delta/epsilon. Biochem J. 427:489-497.

Syeda, F., R.L. Fagan, M. Wean, G.V. Avvakumov, J.R. Walker, S. Xue, S. Dhe-Paganon, and C. Brenner. 2011. The RFTS domain is a DNA-competitive inhibitor of Dnmt1. J. Biol. Chem.

Szwagierczak, A., S. Bultmann, C.S. Schmidt, F. Spada, and H. Leonhardt. 2010. Sensitive enzymatic quantification of 5-hydroxymethylcytosine in genomic DNA. Nucleic Acids Research. 38:e181.

Tachibana, M., K. Sugimoto, M. Nozaki, J. Ueda, T. Ohta, M. Ohki, M. Fukuda, N. Takeda, H. Niida, H. Kato, and Y. Shinkai. 2002. G9a histone methyltransferase plays a dominant role in euchromatic histone H3 lysine 9 methylation and is essential for early embryogenesis. Genes & Development. 16:1779-1791.

Tahiliani, M., K.P. Koh, Y. Shen, W.A. Pastor, H. Bandukwala, Y. Brudno, S. Agarwal, L.M. Iyer, D.R. Liu, L. Aravind, and A. Rao. 2009. Conversion of 5-methylcytosine to 5-hydroxymethylcytosine in mammalian DNA by MLL partner TET1. Science. 324:930-935.

Takeshita, K., I. Suetake, E. Yamashita, M. Suga, H. Narita, A. Nakagawa, and S. Tajima. 2011. Structural insight into maintenance methylation by mouse DNA methyltransferase 1 (Dnmt1). Proc. Natl. Acad. Sci. U.S.A. 108:9055-9059.

Tamaru, H., and E.U. Selker. 2001. A histone H3 methyltransferase controls DNA methylation in Neurospora crassa. Nature. 414:277-283.

Tan, M., H. Luo, S. Lee, F. Jin, J.S. Yang, E. Montellier, T. Buchou, Z. Cheng, S. Rousseaux, N. Rajagopal, Z. Lu, Z. Ye, Q. Zhu, J. Wysocka, Y. Ye, S. Khochbin, B. Ren, and Y. Zhao. 2011. Identification of 67 histone marks and histone lysine crotonylation as a new type of histone modification. Cell. 146:1016-1028.

Tatematsu, K.I., T. Yamazaki, and F. Ishikawa. 2000. MBD2-MBD3 complex binds to hemi-

methylated DNA and forms a complex containing DNMT1 at the replication foci in late S phase. Genes Cells. 5:677-688.

Taverna, S.D., H. Li, A.J. Ruthenburg, C.D. Allis, and D.J. Patel. 2007. How chromatin-binding modules interpret histone modifications: lessons from professional pocket pickers. Nature Publishing Group. 14:1025-1040.

Tien, A.L., S. Senbanerjee, A. Kulkarni, R. Mudbhary, B. Goudreau, S. Ganesan, K.C. Sadler, and C. Ukomadu. 2011. UHRF1 depletion causes a G2/M arrest, activation of DNA damage response and apoptosis. Biochem J. 435:175-185.

Tittle, R.K., R. Sze, A. Ng, R.J. Nuckels, M.E. Swartz, R.M. Anderson, J. Bosch, D.Y.R. Stainier, J.K. Eberhart, and J.M. Gross. 2011. Uhrf1 and Dnmt1 are required for development and maintenance of the zebrafish lens. Dev. Biol. 350:50-63.

Trinkle-Mulcahy, L., S. Boulon, Y.W. Lam, R. Urcia, F.M. Boisvert, F. Vandermoere, N.A. Morrice, S. Swift, U. Rothbauer, H. Leonhardt, and A. Lamond. 2008. Identifying specific protein interaction partners using quantitative mass spectrometry and bead proteomes. J. Cell Biol. 183:223-239.

Uemura, T., E. Kubo, Y. Kanari, T. Ikemura, K. Tatsumi, and M. Muto. 2000. Temporal and spatial localization of novel nuclear protein NP95 in mitotic and meiotic cells. Cell Struct Funct. 25:149-159.

Unoki, M., T. Nishidate, and Y. Nakamura. 2004. ICBP90, an E2F-1 target, recruits HDAC1 and binds to methyl-CpG through its SRA domain. Oncogene. 23:7601-7610.

Vire, E., C. Brenner, R. Deplus, L. Blanchon, M. Fraga, C. Didelot, L. Morey, A. Van Eynde, D. Bernard, J.M. Vanderwinden, M. Bollen, M. Esteller, L. Di Croce, Y. de Launoit, and F. Fuks. 2006. The Polycomb group protein EZH2 directly controls DNA methylation. Nature. 439:871-874.

Wade, P.A. 2001. Methyl CpG-binding proteins and transcriptional repression. Bioessays. 23:1131-1137.

Wang, C., J. Shen, Z. Yang, P. Chen, B. Zhao, W. Hu, W. Lan, X. Tong, H. Wu, G. Li, and C. Cao. 2011. Structural basis for site-specific reading of unmodified R2 of histone H3 tail by UHRF1 PHD finger. Cell Res. 21:1379-1382.

Wang, H., L. Zhai, J. Xu, H.Y. Joo, S. Jackson, H. Erdjument-Bromage, P. Tempst, Y. Xiong, and Y. Zhang. 2006. Histone H3 and H4 ubiquitylation by the CUL4-DDB-ROC1 ubiquitin ligase facilitates cellular response to DNA damage. Mol. Cell. 22:383-394.

Wang, J., S. Hevi, J.K. Kurash, H. Lei, F. Gay, J. Bajko, H. Su, W. Sun, H. Chang, G. Xu, F. Gaudet, E. Li, and T. Chen. 2009. The lysine demethylase LSD1 (KDM1) is required for maintenance of global DNA methylation. Nat Genet. 41:125-129.

Wang, Z., C. Zang, J.A. Rosenfeld, D.E. Schones, A. Barski, S. Cuddapah, K. Cui, T.-Y. Roh, W. Peng, M.Q. Zhang, and K. Zhao. 2008. Combinatorial patterns of histone acetylations and methylations in the human genome. Nat Genet. 40:897-903.

Watanabe, D., I. Suetake, T. Tada, and S. Tajima. 2002. Stage- and cell-specific expression of Dnmt3a and Dnmt3b during embryogenesis. Mech. Dev. 118:187-190.

Weber, M., I. Hellmann, M.B. Stadler, L. Ramos, S. P¨a¨abo, M. Rebhan, and D. Sch¨ubeler. 2007. Distribution, silencing potential and evolutionary impact of promoter DNA methylation in the human genome. Nat Genet. 39:457-466.

Wiedemann, S.M., S.N. Mildner, C. B¨onisch, L. Israel, A. Maiser, S. Matheisl, T. Straub, R. Merkl, H. Leonhardt, E. Kremmer, L. Schermelleh, and S.B. Hake. 2010. Identification and characterization of two novel primate-specific histone H3 variants, H3.X and H3.Y. J. Cell Biol. 190:777-791.

Wysocka, J., T. Swigut, H. Xiao, T.A. Milne, S.Y. Kwon, J. Landry, M. Kauer, A.J. Tackett, B.T. Chait, P. Badenhorst, C. Wu, and C.D. Allis. 2006. A PHD finger of NURF couples histone H3 lysine 4 trimethylation with chromatin remodelling. Nature. 442:86-90.

Xiao, W., K.D. Custard, R.C. Brown, B.E. Lemmon, J.J. Harada, R.B. Goldberg, and R.L. Fischer. 2006. DNA methylation is critical for Arabidopsis embryogenesis and seed viability. Plant Cell. 18:805-814.

Xie, S., J. Jean, and C. Qian. 2011. UHRF1 Double Tudor Domain and the Adjacent PHD Finger Act Together to Recognize K9me3-Containing Histone H3 Tail. J Mol Biol.

Xu, B., D.Q. Zeng, Y. Wu, R. Zheng, L. Gu, X. Lin, X. Hua, and G.H. Jin. 2011. Tumor suppressor menin represses paired box gene 2 expression via Wilms tumor suppressor protein-polycomb group complex. J. Biol. Chem. 286:13937-13944.

Zampieri, M., C. Passananti, R. Calabrese, M. Perilli, N. Corbi, F. De Cave, T. Guastafierro, M.G. Bacalini, A. Reale, G. Amicosante, L. Calabrese, J. Zlatanova, and P. Caiafa. 2009. Parp1 localizes within the Dnmt1 promoter and protects its unmethylated state by its enzymatic activity. PLoS ONE. 4:e4717.

Zhang, J., Q. Gao, P. Li, X. Liu, Y. Jia, W. Wu, J. Li, S. Dong, H. Koseki, and J. Wong. 2011. S phase-dependent interaction with DNMT1 dictates the role of UHRF1 but not UHRF2 in DNA methylation maintenance. Cell Res. 21:1723-1739.

Zhang, Q., H.Y. Wang, M. Marzec, P.N. Raghunath, T. Nagasawa, and M.A. Wasik. 2005. STAT3- and DNA methyltransferase 1-mediated epigenetic silencing of SHP-1 tyrosine phosphatase tumor suppressor gene in malignant T lymphocytes. Proc. Natl. Acad. Sci. U.S.A. 102:6948-6953.

Zhang, Y., and D. Reinberg. 2001. Transcription regulation by histone methylation: interplay between different covalent modifications of the core histone tails. Genes & Development. 15:2343-2360.

Zhou, Y., and I. Grummt. 2005. The PHD finger/bromodomain of NoRC interacts with acetylated histone H4K16 and is sufficient for rDNA silencing. Curr. Biol. 15:1434-1438.

Zhu, B., Y. Zheng, H. Angliker, S. Schwarz, S. Thiry, M. Siegmann, and J.P. Jost. 2000. 5-Methylcytosine DNA glycosylase activity is also present in the human MBD4 (G/T mismatch glycosylase) and in a related avian sequence. Nucleic Acids Research. 28:4157-4165.

Zhu, W., J.W. Smith, and C.-M. Huang. 2010. Mass spectrometry-based label-free quantitative proteomics. J. Biomed. Biotechnol. 2010:840518.

Zilberman, D., D. Coleman-Derr, T. Ballinger, and S. Henikoff. 2008. Histone H2A.Z and DNA methylation are mutually antagonistic chromatin marks. Nature. 456:125-129.

Zimmermann, C., E. Guhl, and A. Graessmann. 1997. Mouse DNA methyltransferase (MTase) deletion mutants that retain the catalytic domain display neither de novo nor maintenance methylation activity in vivo. Biol Chem. 378:393-405.

5.2 Abbreviations

5caC: 5-carboxylcytosine
5fc: 5-formylcytosine
5hmC: 5-hydroxymethylcytosine
5mC: 5-methylcytosine
aa: amino acid
Ac: acetylation
ADD: ATRX-Dnmt-Dnmt3L
ATP: adenosine-5′-triphosphate
BAH: Bromo Adjacent Homology domain
BER: base excision repair
bp: base pair
BRCT: BRCA1 C Terminus
CMT: Chromomethylase
CpG: cytosine-phosphatidyl-guanine
cpm: counts per minute
CTD: catalytic domain
Da: Dalton
DBP: Dnmt1 binding protein
DMAP: Dnmt1 association protein
DNA: deoxyribonucleic acid
Dnmt: DNA methyltransferase
ELISA: enzyme linked immunosorbent assay
ESC: embryonic stem cell
FDR: false discovery rate
FRAP: fluorescence recovery after photobleaching
G phase: gap phase
GFP: green fluorescent protein
h: hours
H3K9MT:H3K9 methyltransferases
HDAC: histone deacetylase
HEK293T: human embryonic kidney cells
HeLa: cervical cancer cells taken from Henrietta Lacks
HP1: heterochromatin-associated protein 1
ICBP90: inverted CCAAT box binding protein of 90 kDa
ITC: isothermal titration calorimetry
MBD: methyl-CpG binding domain protein
MBT: malignant brain tumor

MDS: myelodysplastic syndrome
Me: methylation
MEF: mouse embryonic fibroblast
MET: methyltransferase
min: minutes
NFR: nucleosome free region
NHEJ: non-homologous end joining
nm: nanometre
Np95: nuclear protein of 95 kDa
NURF: nucleosomal remodelling factor
p: phosphorylation
P/CAF: p300/CBP-associated factor
PBD: PCNA binding domain
PBS: phosphate buffered saline
PcG: polycomb group
PCNA: proliferating cell nuclear antigen
PCNP: PEST-containing nuclear protein
PDB: protein data bank
PHD: Plant Homeo Domain
PI: propidium iodide
Prc: polycomb repressive complex
PWWP: proline-tryptophan-proline motif
RFP: red fluorescent protein
Ring: really interesting new gene
S phase: synthesis phase
SAM: S-Adenosyl-L-Methionine
SD: standard deviation
SEM: standard error of the mean
SILAC: stable isotope labelling with amino acids in cell culture
SLE: systemic lupus erythematosus
SPR: surface plasmon resonance
SRA: SET and Ring associated
SUMO: sumoylation
TCA: trichloroacetic acid
TDG: thymidine deglycosylase
TRD: transcription repression domain
trxG: trithorax group
TS: targeting sequence
TSS: transcription start site

Ub: ubiquitination
Ubl: ubiquitin-like
Uhrf: Ubiquitin-like-containing PHD and RING finger domains protein
wt: wild type
ZnF: zinc finger
m: micrometre
M: micromolar

5.3 Contributions

Declaration of contributions to "Fluorescent protein speci c Nanotraps to study protein-protein interactions and histone-tail peptide binding"
I wrote the manuscript and corresponding protocols together with Ulrich Rothbauer, performed *in vitro* histone-tail peptide binding assays and prepared figures 2 and 3.

Declaration of contributions to "Versatile Toolbox for High-throughput Biochemical and Functional Studies of Fluorescent Fusion Proteins"
I conceived this project (together with the company ChromoTek). I established and performed the *in vitro* histone-tail binding assay, the DNA binding assay and the ELISA-based assays with the PCNA antibody and Cbx1. I collected and organized the additional data and material from all co-workers, prepared all figures and wrote the manuscript with the help of Sandra Hake.

Declaration of contributions to"The multi-domain protein Np95 connects DNA methylation and histone modi cation"
I established a new *in vitro* histone-tail peptide binding assays and used this assay to determine all *in vitro* histone-tail peptide binding specificities for this project. Based on the *in vitro* data and available structural information, I prepared and contributed figure 3, as well as supplementary figures 7 and 8A. I wrote the corresponding figure legends as well as the corresponding material and methods parts.

Declaration of contributions to "Cooperative DNA and histone binding by Uhrf2 links the two major repressive epigenetic pathways"
Heinrich Leonhardt and I conceived this project. I performed the *in vitro* histone-tail peptide binding and DNA binding assays, and cloned all constructs with help of Patricia Wolf. In addition, I collected and organized the additional data and material from all co-workers, prepared all figures and wrote the manuscript with the help of Heinrich Leonhardt.

Declaration of contributions to "DNMT1 regulation by interactions and modi cations"
I wrote this review with the help of Weihua Qin and Heinrich Leonhardt and prepared all figures. Parts of the manuscript were used for parts of the introduction (Chapter 1.2)

Declaration of contributions to "Cell cycle-dependent regulation of Dnmt1"
Heinrich Leonhardt and I conceived this project. Initially, I tested Dnmt1 binding proteins, provided by ChromoTek (Germany), and performed activity assays and immunoprecipitations. I prepared all samples for SILAC (cell culture, cell cycle synchronization,

FACS analyses and immunoprecipitations). FACS analyses were performed by Sebastian Bultmann. All mass spectrometry analyses were performed by the Core Facilty of the MPI of Biochemistry. Finally, I evaluated the data and prepared all figures.

5.4 Declaration

Declaration according to the "Promotionsordnung der LMU München für die Fakultät Biologie"

Betreuung

Hiermit erkläre ich, dass die vorgelegte Arbeit an der LMU von Herrn Prof. Dr. Heinrich Leonhardt betreut wurde.

Anfertigung

Ich versichere hiermit an Eides statt, dass die vorgelegte Dissertation von mir selbständig und ohne unerlaubte Hilfsmittel angefertigt wurde. Über Beiträge, die im Rahmen der kumulativen Dissertation in Form von Manuskripten in der Dissertation enthalten sind, wurde im Kapitel 5.3 Rechenschaft abgelegt und die eigenen Leistungen wurden aufgelistet.

Prüfung

Hiermit erkläre ich, dass die Dissertation weder als ganzes noch in Teilen an einem anderen Ort einer Prüfungskommission vorgelegt wurde. Weiterhin habe ich weder an einem anderen Ort eine Promotion angestrebt noch angemeldet noch versucht eine Doktorprüfung abzulegen.

München, den 5. März 2012

Garwin Pichler

5.5 Acknowledgement

First of all, I would like to thank my doctor father and direct supervisor Prof. Dr. Heinrich Leonhardt. I am very grateful for the unique opportunity to conduct my PhD thesis in your group. Thank you for your support, your brilliant ideas, motivating discussions and for the appreciation of my work. Also, I want to thank you for offering me new creative scope to start collaborations and try every technique that came in my mind. Also, I want to thank you for your "encouraging" words after the weekend FC Bayern was defeated again. For sure, the experiences during this PhD time have been very influential for my scientific and personal development.
I would like to thank the members of my thesis advisory committee, Prof. Dr. Elena Conti and Prof. Dr. Patrick Cramer, for their interest in my work, the fruitful discussions and advises during our meetings.
I would like to thank Dr. Hans-Jörg Schäffer, Maxi Reif and Dr. Ingrid Wolf from the IMPRS coordination office for continuous support in any situation and for the financial support. Thank you for your help, the great soft-skill workshops and to give me the opportunity using the Core Facility of the MPI.
I thank the IDK-NBT for the financial support and the organization of the interesting scientific and soft-skills workshops. I am grateful to Marie-Christine Blüm and Marilena Pinto from the coordination office.
I would like to thank Dr. Ulrich Rothbauer. I am very grateful for all your support and for constantly providing me with cooperation, contacts and projects.
I would like to thank all my cooperation partners including Dr. Sandra Hake, Antonia Jack, Teresa Barth, Dr. Axel Imhof and Dr. Oliver Poetz. Also, I want to thank Nils for explaining me MaxQuant and Cyril for MassSpec analyses.
I would like to thank all members of Heinrich's group for the friendly and supportive atmosphere. I thank Anja and Susanne taking care of all the administrative stuff keeping the lab running. Special thanks to the members of my office: Carina, Ola and Kamila; Thanks for the nice atmosphere!
Special thanks to Carina for "tolerating" me my whole PhD, sitting next to you. Thank you for the nice time, all the help, and scientific and more important non-scientific discussions and for the tea. Also, special thanks to Christine! Thank you for the nice times drinking coffee discussing about all the "important" things bothering during the PhD thesis. I will really miss you two!
I would like to thank Sebastian for all his help with FACS sorting and the InCell and for the fruitful discussions (and trashtalk). Also, I really want to thank Patricia. Thank you for all your help in the many projects we were both part of.
Furthermore, I would like to thank all lab members. Fabio, Weihua, Udo, Andreas, Irina, Jacqueline, Jonas, JuÃàrgen, Katrin, Daniel, Nan, Congdi, Andrea, Danni, Kamila,

Katharina, Lothar, Mengxi, Tina, Boris, Kourosh and Oliver. Only teamwork makes work successful.
Especially, I would like to thank all my friends: Jan, Roli, Basti, Yuri, Niko, Passi, Andi and Sandi. Ihr seid die Besten! I definitely would be pushed over the edge without all of them. I hope we will someday all live again in the same city after spreading all over the whole worlds doing postdocs.
Special thanks to my family for all the support and love. Mama und Papa, danke, dass ihr immer für mich da wart! Thanks to my little brother Philip (aka Pipo) for the nice time we spend watching soccer, playing soccer and just talking.
Last but not least, I would like to thank my girlfriend, who was not uninvolved in the decision to do my PhD in this group and fundamentally contributed to this work with her love and support. Tina, ich danke dir für alles. Ich wüsste nicht was ich ohne dich machen würde!

5.6 Publications

Garwin Pichler*, Antonia Jack, Patricia Wolf and Sandra B. Hake. (2012). Versatile Toolbox for High Throughput Biochemical and Functional Studies with Fluorescent Fusion Proteins.**PLOSone**, 7(5): e36967.
*** Corresponding author**

Qin, W., Leonhardt, H., & **Pichler, G**. (2011). Regulation of DNA methyltransferase 1 by interactions and modifications. **Nucleus**, 2(5), 392-402.

Pichler, G., Wolf, P., Schmidt, C. S., Meilinger, D., Schneider, K., Frauer, C., Fellinger, K., et al. (2011). Cooperative DNA and histone binding by Uhrf2 links the two major repressive epigenetic pathways. **J Cell Biochem**. 112(9), 2585-93

Pichler G, Leonhardt H, Rothbauer U. (2011) Fluorescent protein specific Nanotraps to study protein-protein interactions and histone-tail peptide binding.
Methods in Molecular Biology (in press)

Rottach, A., Frauer, C., **Pichler, G.**, Bonapace, I. M., Spada, F., & Leonhardt, H. (2010). The multi-domain protein Np95 connects DNA methylation and histone modification. **Nucleic Acids Res**, 38(6), 1796-1804